Emergence of cancer stem cells in the early stages of hepatic carcinogenesis and development of innovative models of hepatocellular carcinoma

Elena Patricia Gifu

N°d'ordre NNT : 2017LYSE1319

THESE de DOCTORAT DE L'UNIVERSITE DE LYON

opérée au sein de

l'Université Claude Bernard Lyon 1

ECOLE DOCTORALE BIOLOGIE MOLECULAIRE INTEGRATIVE ET CELLULAIRE

ED BMIC 340

Spécialité de doctorat : CANCEROLOGIE

Soutenue publiquement le 14/12/2017, par :

Patricia Gifu

STUDY OF THE EMERGENCE OF CANCER STEM CELLS IN HEPATOCELLULAR CARCINOMA AND DEVELOPMENT OF INNOVATIVE MODELS

Devant le jury composé de :

M^{me} Dr Anne CORLU (Université de Rennes)	Rapporteure
M^{me} Dr Françoise PRAZ (Saint Antoine)	Rapporteure
M. Dr Pascal PINEAU (Institut Pasteur)	Examinateur
M. Pr Philippe MERLE (Universite de Lyon)	Examinateur
M. Pr Massimo LEVRERO (Universite de Lyon)	Examinateur
M^{me} Dr Claude CARON de FROMENTEL (CRCL)	Directrice de thèse

UNIVERSITE CLAUDE BERNARD - LYON 1

Président de l'Université	**M. le Professeur Frédéric FLEURY**
Président du Conseil Académique	M. le Professeur Hamda BEN HADID
Vice-président du Conseil d'Administration	M. le Professeur Didier REVEL
Vice-président du Conseil Formation et Vie Universitaire	M. le Professeur Philippe CHEVALIER
Vice-président de la Commission Recherche	M. Fabrice VALLÉE
Directrice Générale des Services	Mme Dominique MARCHAND

COMPOSANTES SANTE

Faculté de Médecine Lyon Est – Claude Bernard	Directeur : M. le Professeur G.RODE
Faculté de Médecine et de Maïeutique Lyon Sud – Charles Mérieux	Directeur : Mme la Professeure C. BURILLON
Faculté d'Odontologie	Directeur : M. le Professeur D. BOURGEOIS
Institut des Sciences Pharmaceutiques et Biologiques	Directeur : Mme la Professeure C. VINCIGUERRA
Institut des Sciences et Techniques de la Réadaptation	Directeur : M. X. PERROT
Département de formation et Centre de Recherche en Biologie Humaine	Directeur : Mme la Professeure A-M. SCHOTT

COMPOSANTES ET DEPARTEMENTS DE SCIENCES ET TECHNOLOGIE

Faculté des Sciences et Technologies	Directeur : M. F. DE MARCHI
Département Biologie	Directeur : M. le Professeur F. THEVENARD
Département Chimie Biochimie	Directeur : Mme C. FELIX
Département GEP	Directeur : M. Hassan HAMMOURI
Département Informatique	Directeur : M. le Professeur S. AKKOUCHE
Département Mathématiques	Directeur : M. le Professeur G. TOMANOV
Département Mécanique	Directeur : M. le Professeur H. BEN HADID
Département Physique	Directeur : M. le Professeur J-C PLENET
UFR Sciences et Techniques des Activités Physiques et Sportives	Directeur : M. Y.VANPOULLE
Observatoire des Sciences de l'Univers de Lyon	Directeur : M. B. GUIDERDONI
Polytech Lyon	Directeur : M. le Professeur E.PERRIN
Ecole Supérieure de Chimie Physique Electronique	Directeur : M. G. PIGNAULT
Institut Universitaire de Technologie de Lyon 1	Directeur : M. le Professeur C. VITON
Ecole Supérieure du Professorat et de l'Education	Directeur : M. le Professeur A. MOUGNIOTTE
Institut de Science Financière et d'Assurances	Directeur : M. N. LEBOISNE

Luminaires pages

Remerciements

Je souhaiterais remercier Dr. Anne Corlu et Dr. Françoise Praz d'avoir accepté d'être rapporteures de mon manuscrit de thèse de doctorat ainsi que Pr Massimo Levrero et Dr Pascal Pineau d'avoir accepté de faire partie de mon jury de soutenance de thèse.

Réaliser une thèse de doctorat est une véritable épreuve. La réussite n'est pas uniquement conditionnée par le travail personnel et la motivation, mais c'est également le résultat des collaborations fructueuses avec des personnes très impliquées ainsi qu'un encadrement constant et de qualité. Ainsi, je souhaiterais remercier dans les paragraphes ci-dessous les personnes avec qui j'ai pu travailler pendant mes trois années de thèse ainsi que ceux qui m'ont soutenue en dehors du labo.

Je remercie la **Dr. Claude Caron de Fromentel** et le **Pr. Philippe Merle** pour leur encadrement pendant les trois années de thèse ainsi que leur amitié et la confiance qu'ils m'ont accordée. Claude, merci pour le savoir-faire que vous m'avez transmis avec beaucoup de patience sur la culture cellulaire. Merci pour avoir partagé avec moi toutes vos connaissances sur la biologie des cancers, en général et sur les membres de la famille p53, en particulier. Merci également pour votre aide pour les démarches administratives (personnelles et liés à mon travail) ainsi que les nombreuses attentions envers moi pendant ces quatre années passées au labo. Philippe, je te remercie pour m'avoir soutenue pendant ma thèse et pour toutes les opportunités que tu m'as offertes. Merci pour ton aide sur le travail lié au recrutement des patients ainsi que l'analyse des données liées aux données clinico-pathologiques des patients. Ton soutien m'a redonné plus de confiance en moi et de motivation. Merci également à tous les deux pour la révision de mes nombreux abstracts et posters et pour vos efforts pour obtenir les financements nécessaires afin de soutenir ces travaux. J'espère que cette thèse sera suivie par d'autres opportunités de collaborations avec vous. Merci à **Isabelle Chemin** pour m'avoir 'co-accueillie' dans l'équipe, pour sa gentillesse, les discussions scientifiques constructives pendant les réunions d'équipe ainsi que son aide à la préparation des congres.

Ce travail n'aurait pas été possible sans l'aide de **Paule** et **Joanna** du Centre de Recherche Clinique de l'Hôpital de la Croix Rousse. Merci à toutes les deux de m'avoir aidé à démarrer le projet Imodi et appris à organiser mon travail auprès des patients. Paule je te remercie également pour ton soutien et mots d'encouragement. Merci également aux médecins chirurgiens et assistantes du bloc opératoire de l'Hôpital de la Croix Rousse pour leur coopération dans le prélèvement des tissus hépatiques.

Merci à **Philippe Halfon**, **Sonia Brun** et **Firas Bassissi** avec qui j'ai eu l'occasion de collaborer pour le développement préclinique du composé GNS561. J'espère que votre initiative permettra avec le temps l'émergence des nouvelles thérapies contre plusieurs types de cancer. Merci à **Lydie L** pour son aide dans la préparation des manips. Cela a été un plaisir de travailler et rigoler avec toi. Merci aux étudiants (**Amelie**, **Lei**, **Wang** et **Marylise**) qui ont travaillé sur les projets présentés dans ce manuscrit pendant leur stage de BTS ou master. Merci à **Janet** d'avoir relu mon manuscrit et pour vos commentaires très pertinents. Merci à **Françoise B** pour m'avoir aidée pour la réalisation des PCR HBV et HCV. Merci à **Olivier Hanz** pour son aide sur les tests d'infection *in vitro* ainsi que ses conseils pour la congélation des hépatocytes et le développement des lignées primaires de CHCs. Merci à **Floriane Fusil** pour son aide pour

l'humanisation des foies de souris ainsi que la réalisation d'une partie des greffes des tumeurs. Merci à **Séverine**, **Isabelle Goddard** et toute l'équipe du Laboratoire des Modèles Tumoraux du Centre Léon Berard pour la réalisation des greffes sur souris. Merci à **Olivier** et **Grégoire**, les deux chefs de projet Imodi pour avoir soutenu le Run Foie malgré les modèles qui se sont fait attendre. Merci aux membres de l'équipe « Biologie et traitement des tumeurs hépatobiliaires » de l'Hôpital de Saint Antoine qui ont participé à la caractérisation du modèle PDX de CHC. Merci à **Nadim** pour avoir participé à la constitution des cohortes des échantillons de CHC humain. Merci au Pr. Michel Rivoire du Centre Léon Berard pour nous avoir fourni les pièce hépatiques qui ont servi à l'isolement des hépatocytes primaires.

Merci à toutes les personnes du labo que je considère comme des amis. Merci à ma très bonne amie **Natali** pour nos « lunch dates » où nous avons pu discuter de plein de choses et partager les galères de la thèse comme des manips qui ne veulent pas marcher, des cellules qui ne poussent pas ou qui ne veulent pas fluorescer. Merci à toi pour toujours avoir un mot gentil et d'avoir apporté 'de l'énergie positive' à mon temps passé au labo. Merci à **Laetitia** qui m'a initiée à plein d'activités hors labo, surtout pendant la première année. Nos petites sorties shopping, piscine, ski et autres m'ont bien aidé à me sortir un peu les idées des manips. Merci à **Suzanne** et **Maelle** pour leur gentillesse et pour avoir facilité mon intégration au sein du labo. Cela a été un grand plaisir de découvrir New York et la côte est de l'US avec vous. Susu je te remercie également de m'avoir accueille dans ta famille toulousaine pour ne pas me laisser passer Noel à Lyon. Merci également aux anciens thèsards avec qui c'était un grand plaisir d'intéragir (**Clément G.**, **Nathalie I.**, **Thomas L.**, **Dulce A.**, **Pierre L.**).

Merci à mes professeurs du lycée qui m'ont ouvert l'esprit vers le monde de la science, en particulier **Mme Gîrju** et **Mme Spînu** pour m'avoir appris tant de choses et m'avoir fait aimer la biologie et la chimie ainsi que pour leur amitié. Merci à mes professeurs de l'INSA pour la qualité de l'enseignement qui a beaucoup enrichi mes connaissances d'une manière très cartésienne.

Merci à mes amis, plus ou moins loin physiquement, pour leur bonne humeur et envie de vivre. Un grand merci particulièrement à ma très bonne amie **Oana** que le destin nous rapproche de plus en plus depuis 24 ans. Je te remercie de toujours avoir été à mes cotés, particulièrement dans les moments les plus compliqués et pleins de doutes et ton attitude maternelle.

Merci à ma famille pour leur soutien tout au long de mes longues études. Merci à mon papi qui a toujours été tellement fier de moi mais que malheureusement cette terrible maladie qui est le cancer l'a emporté beaucoup trop vite. Merci à **mes parents** de toujours m'avoir poussée d'aller plus loin et de mener les choses jusqu'au bout sans ne rien lâcher. Je remercie ma mère de m'avoir donné confiance en moi dans les moments les plus durs et les plus importants et de m'avoir transmis le goût pour le travail et l'espoir qu'on peut accomplir beaucoup de choses en travaillant. Merci à **mon frère** d'exister (car cela m'a appris ce que c'est que le partage et s'amuser ensemble pendant les vacances) et pour nos discussions « profondes » où chaque phrase commence par 'Patri, tu savais que …'.

Last but not least, merci à mon ami **Ludovic** qui partage mon quotidien avec enthousiasme et persévérance. Merci de toujours trouver fabuleux mon travail et de m'insuffler l'espoir que

finalement tout cela pourrait représenter une goutte dans la mer que représente la connaissance du cancer et un pas plus proche vers le traitement de la maladie.

Resumé

Mots clés : Carcinome hépatocellulaire, cellules souches cancéreuses, modèles innovants de maladie, PDX, développement des lignées cellulaires cancéreuses, humanisation des foies de souris, protéines de la famille p53, p73, nouvelles molécules contre le CHC, autophagie.

Le carcinome hépatocellulaire est un problème majeur de santé publique, étant le deuxième cancer le plus mortel au monde, avec une incidence globale croissante. Le seul traitement systémique approuvé est l'inhibiteur des multikinases Sorafenib, qui prolonge la survie globale des patients avec une durée moyenne d'uniquement trois mois. Le CHC est réfractaire aux médicaments chimio-thérapeutiques connus, et après ablation de la tumeur par voie chirurgicale, plus de 50% des patients rechutent. Il a été suggeré que ces phénomènes sont dus à l'existence d'une sous-population de cellules cancéreuses peu différenciées, largement connues sous le nom de cellules souches cancéreuses (CSCs) hépatiques. La compréhension des mécanismes propres aux CSC hépatiques pourrait permettre le développement de médicaments innovants, dotés d'un mécanisme d'action original. Cependant, le développement des nouvelles thérapies contre le CHC est pénalisé par le nombre limité de modèles expérimentaux. Compte tenu de ses défis actuels dans le domaine de la recherche sur le CHC, mon projet de thèse couvre trois axes principaux :

Role of p73 isoforms in the maintenance of liver CSC

Les membres de la famille p53 (*TP53*, *TP63* et *TP73*) codent pour des isoformes longues (TA) agissant comme suppresseurs de tumeurs et des isoformes tronqués (ΔTA) agissant comme des dominants négatifs de formes TA. Les isoformes ΔTA sont obtenus par l'activation d'un promoteur interne ou par un épissage alternatif, et des études antérieures ont démontré leur implication dans le maintien du pool de cellules souches dans les tissus normaux et tumoraux. Dans une cohorte de 180 échantillons de CHC (tumeur et non-tumeur), nous avons analysé l'expression de *TP73*, en particulier l'isoforme longue TAp73, l'isoforme issu du promoteur interne ΔNp73 et les isoformes issus de l'épissage alternatif ΔEx2p73 et ΔEx2/3p73. Nous avons constaté que ces isoformes sont surexprimés dans les tumeurs par rapport au tissu non tumoral apparié. De plus, la surexpression de l'isoforme ΔNp73 est fortement corrélée avec les facteurs de dédifférenciation Oct4, Nanog et Sox2. Les expériences *in vitro* suggèrent que l'expression de ΔNp73 est plus élevée dans les cellules progénitrices du foie par rapport aux cellules différenciées et que son expression dans les lignées cellulaires HCC conduit à une dédifférenciation de la population cellulaire totale.

Development of novel models of disease.

Le consortium IMODI (*Innovative Models of Disease*) est principalement dédié au développement de modèles expérimentaux innovants pour 8 types de cancer différents. Notre participation au projet concerne 3 objectifs principaux : i) le développement de xénogreffes dérivées des tumeurs de CHC humaines (*PDX* en anglais pour ***P**atient **D**erived **X**enograft*) ; ii) le développement de nouvelles lignées cellulaires de CHC ; et iii) la mise au point d'une méthode de cryoconservation des hépatocytes humains primaires (*PHH* en anglais pour ***P**rimary **H**uman **H**epatocytes*) dans le but de les utiliser pour l'humanisation des foies de souris. Trente patients prévus pour une résection de CHC ont été recrutés et des fragments de tumeur fraîche ont été prélevés. Les échantillons tumoraux ont été xénogreffés par voie sous-cutanée chez des souris immunodéficientes ou dissociés pour la mise en culture *in vitro* dans le but de développer des nouvelles lignées cellulaires. Dans un des cas, cela a conduit au développement d'un modèle PDX de CHC moyennement différencié et avec des caractéristiques histologiques similaires à la tumeur humaine initiale. Plusieurs études ont montré l'importance des modèles PDX dans le domaine bio-médical car ils récapitulent les profils de sensibilité aux médicaments observés chez les patients dont ils dérivent. Néanmoins, très peu de modèles ont été décrits dans la littérature pour le CHC. *In vitro*, les cellules primaires de CHC ont pu être maintenues en culture pendant une période de temps limitée, en moyenne 30 jours. Plusieurs lots de PHHs cryoconservés provenant de différents donneurs ont été obtenus. La fonctionnalité des hépatocytes cryoconservés a été évaluée *in vitro* et *in vivo*.

Le premier modèle de transformation *in vitro* d'hépatocytes humains a été précédemment établi au laboratoire. Les hépatocytes ont été d'abord immortalisés avec les onco-protéines de SV40 et ensuite transformés par la forme mutée H-Ras^{G12V}. J'ai pu démontrer que les CSCs CD90+ apparaissent au cours des étapes précoces du processus d'immortalisation alors que la transformation par SV40 et H-Ras^{G12V} conduit à l'apparition de CSC formant des hépatosphères.

New anticancerous drugs targeting liver cancer progenitor cells

GNS561 est un nouvel inhibiteur des transporteurs SLC (pour ***S**olute **C**arier* en anglais), capable d'induire la mort cellulaire par apoptose et d'induire la perméabilisation du la membrane lysosomale. Des travaux antérieurs ont montré que le GNS561 possède un fort hépatotropisme, ce qui justifie sa potentielle utilisation dans le traitement des tumeurs hépatiques. Nous avons montré que le composé GNS561 a une activité antitumorale *in vitro* puissante contre des lignées cellulaires de CHC, et il est également efficace contre la sous- population des CSCs. Nos données suggèrent que le GNS561 induit la baisse de l'ARNm codant pour un transporteur SLC spécifique, précédemment identifié comme étant une de ses potentielles cibles cellulaires. Le soluté transporté par ce transporteur a été montré agir comme un facteur indispensable pour les facteurs de transcription impliqués dans le caractère souche des cellules. Nous avons analysé l'expression de ce transporteur dans une cohorte de 180 échantillons de CHC (tumeur et non-tumeur) et des tissus hépatiques sains. Nous avons constaté qu'il est surexprimé dans les tumeurs et les tissus adjacents non tumoraux par rapport aux tissus sains. Sa surexpression dans les tumeurs de carcinome

hépatocellulaire est corrélée à celles des facteurs de dédifférenciation Oct4 et Sox2, ainsi que du marqueur CD133 des CSC. Comme le montre l'analyse univariée de la survie, la surexpression du transporteur dans les tumeurs des patients est un facteur de mauvais pronostic concernant la survie globale et la survie sans récurrence.

En conclusion, mon projet de thèse a conduit au développement d'un modèle PDX de HCC viro-induit, a partiellement permis d'éclaircir l'implication des isoformes tronqués de p73 dans les caractéristiques de dédifférenciation des tumeurs de CHC et décrit également le développement préclinique d'un nouveau médicament contre le HCC efficace contre les CSCs hépatiques.

Abstract

Keywords : Hepatocellular carcinoma, cancer stem cells, innovative models of disease, PDX, cancer cell lines developement, mouse liver humanization, p53 family, p73, novel molecules against HCC, autophagy.

Hepatocellular carcinoma (HCC) is a major public health problem, being the second most lethal cancer with an increasing incidence around the world. The only approved systemic drug is the multikinase inhibitor Sorafenib, which prolongs patients overall survival with a median time of three months only. HCC is refractory to known chemotherapeutic drugs and more than 50% of patients relapse after surgical tumour removal. These phenomena are thought to be due to the existence of a population of poorly differentiated cancer cells, widely known as liver cancer stem cells (CSCs). The understanding of mechanisms proper to liver CSCs should allow the development of innovative drugs with original mechanism of action against liver CSC, likely to improve patients' outcome. However, the development of new therapies against HCC is penalized by the limited number of experimental models. According to these current challenges in the field of HCC research, my PhD thesis project covers three main axes:

Role of p73 isoforms in the maintenance of liver CSC

The p53 family members (*TP53*, *TP63* and *TP73*) encode full-length isoforms (TA) acting as tumour suppressors and truncated isoforms (ΔTA) which are dominant negative of TAs and promote cell stemness. ΔTA isoforms are obtained by activation of an internal promoter or by alternative splicing and previous studies demonstrated their implication in the maintenance of the stem cells pool in normal tissues and tumours. In a cohort of 180 HCC patients we analyzed the expression of *TP73*, especially the full length isoform (TAp73), the isoform from the internal promoter (ΔNp73) and the alternative splicing isoforms (ΔEx2p73 and ΔEx2/3p73). We found that these isoforms are overexpressed in tumours compared to the matching non-tumoural tissue. Moreover, the overexpression of the ΔNp73 isoform is strongly correlated with the stemness factors Oct4, Nanog and Sox2. *In vitro* data suggested that ΔNp73 expression is higher in liver progenitor cells compared to differentiated cells and that its expression in HCC cell lines leads to dedifferentiation of the entire population.

Development of novel models of disease.

The **I**nnovative **Mo**dels of **Di**sease (IMODI) consortium is mainly dedicated to the development of innovative experimental models for 8 different types of cancer. Our participation to the project concerned 3 main objectives i) development of HCC patient-derived xenografts (PDX) ii) development of new HCC cell lines and iii) set up a cryoconservation method of primary human hepatocytes (PHHs) in the aim to employ them in humanizing murine livers. 30 patients planned for HCC resection were recruited and fresh tumour specimens were subcutaneously xenografted in immune-deficient mice or dissociated for *in-vitro* tumour cell culture. One tumour led to the

development of a moderately differentiated HCC PDX model, as confirmed by histological characterization. Several studies showed the importance of PDX models in the drug discovery field as they recapitulate the drug-sensitivity patterns seen in patients from which they were derived but very few models have been described in the literature for HCC. *In vitro*, primary HCC cells could be maintained in culture for a limited period of time, in average 30 days. Several batches of cryopreserved PHHs were obtained, originating from different donors. The functionality of cryopreserved hepatocytes was assessed *in vitro* and *in vivo*.The first model of *in vitro* transformation of human hepatocyte has been previously established in the lab. Hepatocytes are first immortalized with SV40 and further transformed by mutant H-Ras^{G12V}. I showed that CD90 positive CSCs appear during the early stages of the immortalization process whereas fully transformation by SV40 and H-Ras^{G12V} leads to the appearance of hepatospheres-forming CSCs.

New anticancerous drugs targeting liver cancer progenitor cells

GNS561 is a new small molecule first-in-class SLC (solute carrier) Transporter Inhibitor able to induce apoptotic cell death through inhibition of autophagy. Previous work showed that GNS561 has high hepatotropism, justifying its potential use against HCC. We showed that GNS561 has potent *in vitro* anti-tumour activity against both the tumour bulk and the CSCs population. Our data suggest that the anti-tumoural activity of GNS561 is mediated by down-regulation of a specific SLC transporter expression, previously identified as a potential cellular target of GNS561. The substrate transported by the SLC transporter has been shown to act as a cofactor for transcription factors involved in cell stemness. We analyzed the expression of this transporter in a cohort of 180 HCC patients and found that it is overexpressed in tumours and adjacent non-tumour tissues compared to healthy tissues. Its overexpression in HCC samples is correlated to that of the stemness factors Oct4 and Sox2, as well as the CSCs marker CD133. As shown by univariate survival analysis, the transporter's overexpression in patients' tumour is a factor of poor prognosis regarding the overall survival and the recurrence free survival.

In conclusion, my PhD thesis project led to the development of a PDX model of viral-induced HCC, shed light on the involvement of p73 isoforms in HCC with stem features and describes the pre-clinical development of a new drug against HCC targeting liver CSCs.

Figures

Figure 27. Cellular processes regulated by TA and ΔNp73 isoforms determining cancer outcome. **A.** Upon cellular stress, TAp73 expression and activity increases to regulate biological processes suppressing tumour growth and development. **B.** Amino-terminal truncated ΔTAp73 variants drive tumour progression and confer chemoresistance, stemness and invasiveness through inhibition, de-repression or activation of target genes and EMT activation. **(Engelmann et al., 2015)**

Figure 28. p73 mouse models. The tp73 knockout mouse shows severe developmental defects. TAp73 and ΔNp73 knockout mice show less severe developmental phenotype, but, importantly, depletion of TAp73 predisposes the animal to spontaneous tumourigenesis. **(Rufini et al., 2011)**

Figure 29. ΔTAp73 isoforms act as dominant negatives due to the sequestration of TAp73 (top), the formation of non-functional TAp73– ΔTAp73 heterotetramers (middle) or the competition with TAp73 homotetramers or p53 for binding of the same p53 DNA responsive elements (middle and bottom). **(Melino et al., 2002).**

Figure 30 Combined mechanism(s) whereby the ΔNp73 variant increases cancer stem cell function. The dashed line connecting c-jun to inhibition of ΔNp73 reflects the speculative nature of this particular regulation. **(Basu and Murphy, 2016)**

Figure 31. Role of p73 in neurogenesis. Functional neurons are generated from neural stem cells and then after maturation, are integrated in neuronal circuits. TAp73 is essential for neuronal differentiation and maintenance of neural stem cells. ΔNp73 plays a major role as a survival factor. Question marks indicate that molecular mechanisms have not been fully investigated yet. **(Killick et al., 2011)**

Figure 32. Regulatome balancing TA/ΔTAp73 activity. Coordination of TAp73 and ΔTAp73 activity underlies a complex network of regulatory proteins. In this regard, pharmacological treatment of cancer should consider both TAp73 and ΔTAp73 activities. **(Engelmann et al., 2015)**

Figure 33. TP73 expression changes during the course of in vitro experimental transformation.

Figure 34. Survival curves results for patients with acute promyelocytic leukemia (APL) according to the ΔNp73/TAp73 ratio. Probability of **A.** Overall survival and **B.** Disease Free Survival. **(Lucena-Araujo et al., 2015)**

Figure 35. p73 expression in HCC. A. p73 mRNA transcripts (brown reaction product) within a hepatocellular carcinoma (HCC) nodule (right) and non-neoplastic surrounding hepatocytes and fibrous tissue without transcripts (original magnification×10). **B.** Overall survival in patients with p73-positive and p73-negative tumours (immunohistochemistry detection. **(Tannapfel et al., 1999)**

Table of Contents

I. Cancer

Cancer is the second cause of death in the world, after cardiovascular diseases. Globally, nearly 1 in 6 deaths are due to cancer. First observations depicted cancer as an abnormal proliferation of cells, without knowing what the causes were. In the 20th century, scientific studies deepened our knowledge about the biology of this disease and identified several aetiological factors leading to its development. However, cancer development was revealed to be a very complex process, sometimes lasting over several years, with patients' outcome and responses to treatment varying greatly. To better treat the disease, we have to know more about its characteristics and what makes a normal tissue become a cancerous tissue. All the observations cumulated until the 21 century, were synthesised in a ground breaking review called "Hallmarks of cancer", (Hanahan and Weinberg, 2000)published in 2000 by D. Hanahan and R. Weinberg and updated in 2011 (Hanahan and Weinberg, 2011). According to this second publication, cancer is characterised by 8 hallmarks and 2 emerging characteristics that characterise this disease **(Figure 1)**.

However, depending on the organ of origin, tumours develop differently and do not respond in the same manner when the same cancer hallmark is inhibited. Therefore, a better understanding the biology of each type of cancer could lead to the development of more efficient therapies.

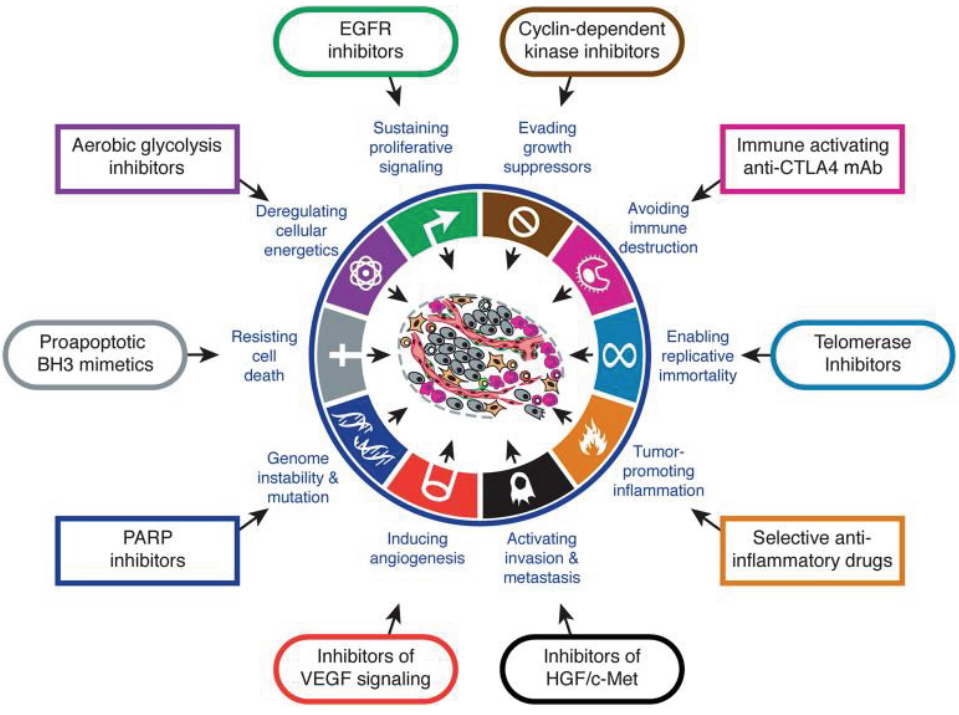

Figure 1. Therapeutic targeting of the hallmarks of cancer. (Hanahan and Weinberg, 2011)

II. Hepatocellular carcinoma

Liver cancer is the sixth most common type of cancer worldwide and second most common cause of cancer death (Ferlay et al., 2010) **(Figure 1)**.

Hepatocellular carcinoma (HCC) is the main type of primary liver cancer (85-90% of cases) and its incidence is constantly increasing. Its pathology is associated with the abnormal proliferation of hepatocytes. The disease has a poor prognosis as in most cases it is diagnosed at an advanced stage and no curative treatments are available as HCC is refractory to most conventional chemotherapeutic drugs. Hepatocellular carcinoma represents therefore a major public health problem.

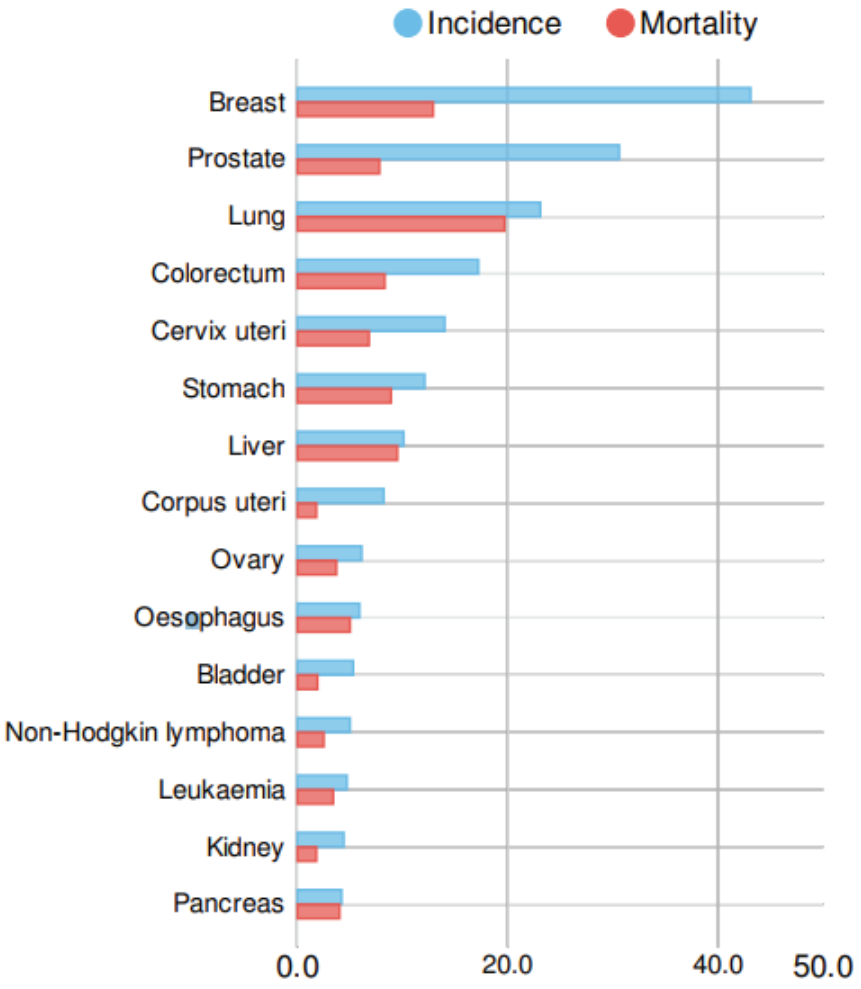

Figure 1. Estimated age-standardised incidence rates and mortality across the world (both sexes). Population weighted average of the area-specific rates applied to the 2012 area population. (Globocan 2012)

In most cases (80%-85%), HCC develops on a cirrhotic liver in which there is a continuous proliferation of hepatic cells. Cirrhosis can be caused by chronic infection with hepatitis B virus (HBV) and hepatitis C virus (HCV), abusive alcohol consumption, aflatoxin intoxication as well as metabolic diseases.

The remaining cases of primary liver cancer mainly consist of cholangiocarcinomas, the second most common sub-class, as well as combined hepatocholangiocarcinomas.

2.1. Liver architecture

The liver is an essential organ located in the right side of the abdominal cavity. It participates in glucose control, lipid and protein metabolism, elimination of xenobiotics, storage of vitamins and iron as well as bile production.

In humans, the liver is structurally divided into 8 segments organised in microscopic units, **lobules**, which arethe functional unit of the liver (**Figure 2**). Hepatic lobules have hexagonal shapes and a portal triad is located at each edge, formed by a hepatic artery, a portal vein and a bile duct. At the centre of each lobule, the central vein collects the blood that has swept the lobule. Lobules are constituted of hepatic cords (sinusoids) arranged radially in a circle. The arterial blood, charged with oxygen, and the venous blood, bringing the nutriments from the intestine, mix inside the sinusoids. The blood flow is directed towards the centre of lobules and collected by the hepatic vein.

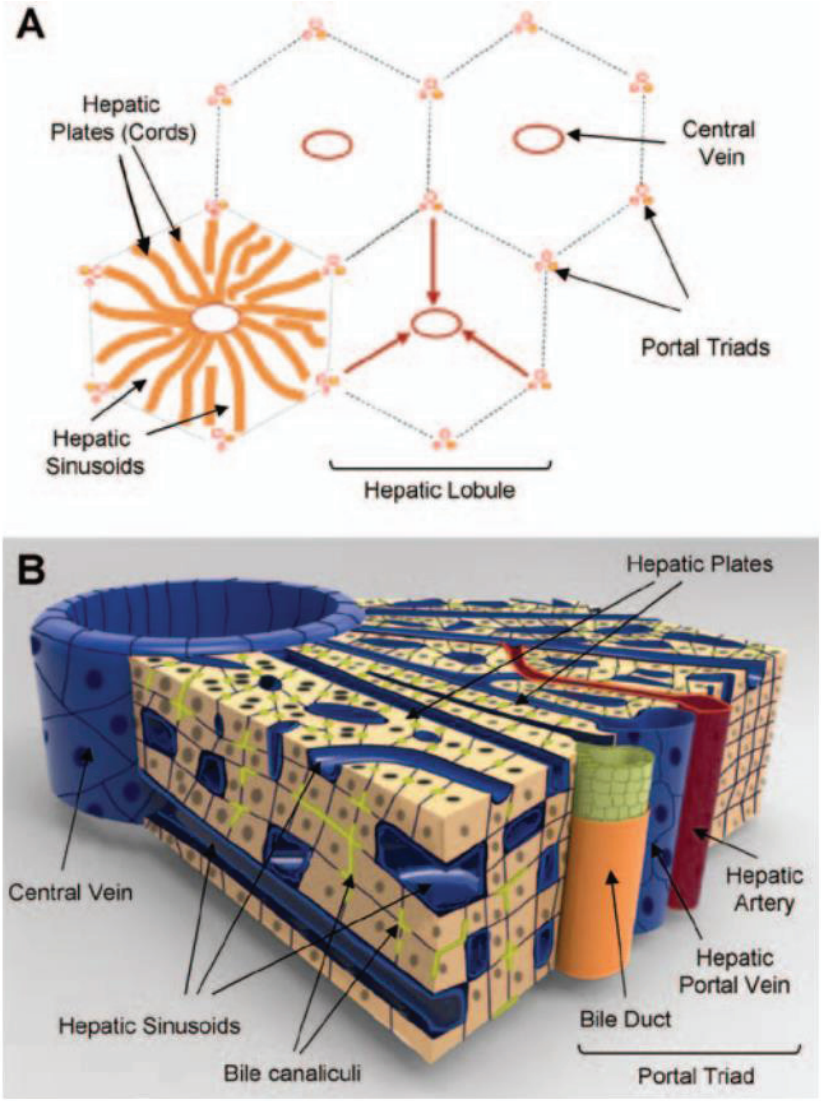

Figure 2. Liver architecture. **A.** Lobule substructure with the relative position of the portal triad directing the blood flow towards the central vein (red arrows). **B.** Schematic representation of the lobule tri-dimensional structure. Bile canaliculi networks (yellow-green) run parallel to the blood flow through the sinusoids.

Hepatocytes are the main type of hepatic cells, representing 80 to 90% of the total cell population. Under physiological conditions, they are quiescent (non-dividing) and have a very long life span compared to other types of epithelial cells. Hepatocytes are polarised cells, with the apical ciliated pole towards the sinusoid space, where the bile is produced, and the basal pole towards the blood flow. Hepatic sinusoids are coated with endothelial cells. Between the endothelial cells and the hepatocyte layer, a small space, called the Disse space, shelters the immune cells and nonparenchymal liver cells that include the Kupffer cells (hepatic macrophages), neutrophils, stellate cells etc.

Towards the outer extremity of the lobules, cholangiocytes (the second most abundant type of epithelial hepatic cells) are arranged in a monolayer forming the bile ducts that collect the bile. Between the cholangiocytes and hepatocytes cords, a small population of liver progenitor cells form the Hering canal. By lineage specific differentiation, hepatic progenitor cells can regenerate both the cholangiocyte and the hepatocyte cell pool.

Indeed the liver has an excellent capacity of regeneration, superior to other organs. In the case of a partial hepatectomy, the lost liver mass will be restored in less than 3 weeks. Hepatocytes as well as liver progenitor cells will become active and start to proliferate. Experimental manipulations by serial transplantation have shown that hepatocytes can undergo as many as 69 proliferation cycles before arriving to complete replicative senescence.

The liver is the site of numerous diseases, called hepatopathies, among which are non-alcoholic fatty liver disease (NAFLD) evolving into non-alcoholic steatohepatitis (NASH), hepatitis (viral or autoimmune associated), cirrhosis and finally liver cancer.

2.2. HCC aetiological factors

The major etiological factors associated with HCC are liver cirrhosis, chronic HBV and HCV infections, alcohol or aflatoxin B1 intoxication. These risk factors induce HCC by direct and indirect mechanisms (**Figure 3**).

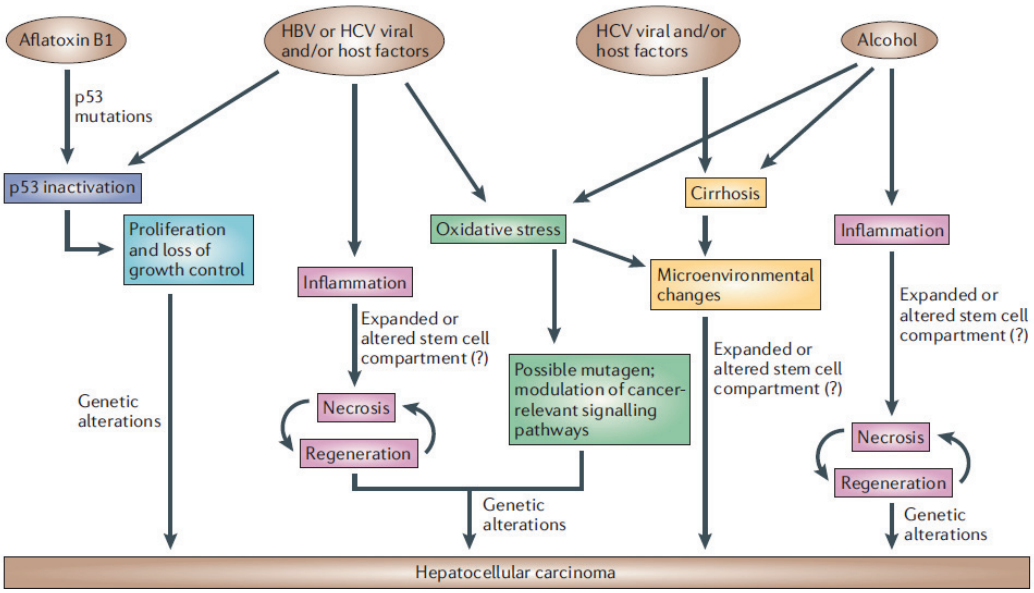

Figure 3. Mechanisms of hepatocarcinogenesis. Common mechanisms between several risk factors are indicated using the same colour. In addition HBV can integrate the host genome. NASH, not represented here, is another HCC risk factor whose contribution to HCC is increasing worldwide **(Farazi and DePinho, 2006)**.

2.2.1 Hepatitis B virus (HBV)

HBV is an enveloped hepatotropic DNA virus belonging to the hepadnaviridae class with a 3.2kb genome size (**Figure 4**). More than 2 billion people are infected by HBV while 240 million are chronic carriers. Globally, HBV chronic infection represents the main risk factor of HCC.

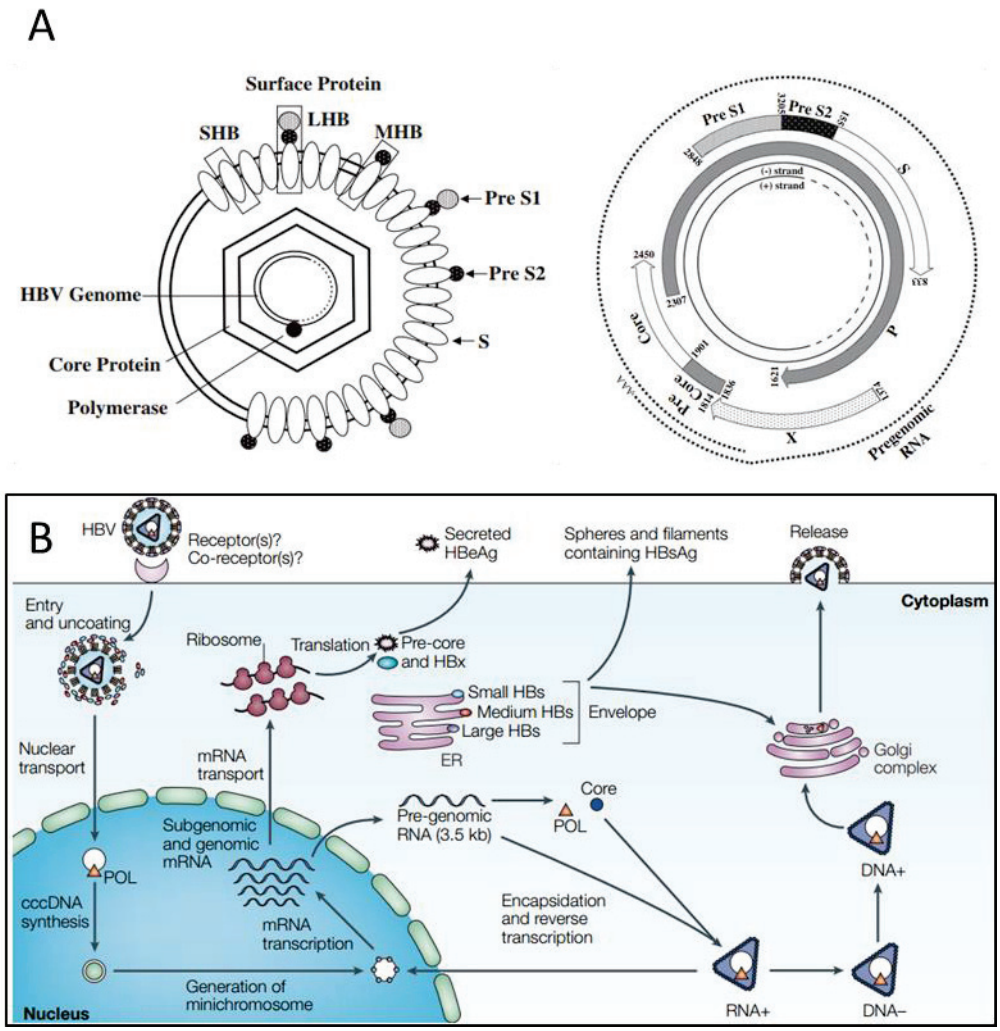

Figure 4. Hepatitis B virus A. The infectious virion (called the Dane particle) is a 42 nm spherical particle containing an envelope and a nucleocapsid. The genome of HBV is a circular partially double-stranded DNA molecule and has four overlapping ORFs encoding for surface (S), core (C), polymerase (P) and X proteins (HBx). **(Yokosuka and Arai, 2006) B.** HBV cell cycle. After entry into the cell, HBV genomic DNA is transported to the nucleus, where the relaxed circular DNA is converted into covalently closed circular (ccc) DNA. The cccDNA functions as the template for the transcription of four viral RNAs, corresponding to the HBV proteins. The longest (pre-genomic) RNA also functions as the template for replication, which occurs within nucleocapsids in the cytoplasm. Nucleocapsids are enveloped during their passage through the endoplasmic reticulum (ER) and/or Golgi complex and are then secreted out from the cell. **(Rehermann and Nascimbeni, 2005)**.

Chronic infection by HBV participates in hepatocellular carcinoma development. In Southeast Asia and sub-Saharan Africa, this pathology is responsible for 70% of HCC cases (Bosetti et al., 2008; El-Serag, 2011; Forner et al., 2012). HBV is classified into 9 genotypes (A to I). In regions where HBV is endemic, genotypes B,C and E are the most commonly encountered and thought to present the greatest risk of HCC development (Chan et al., 2003; Orito and Mizokami, 2003). HBV carriers are 100-fold more likely to develop HCC. In general, the HBV viral load in the blood of chronic carriers is associated with higher incidence of HCC (Chen et al., 2006).

The development of the HBV vaccine in the 1980s participated to the reduction of the prevalence of HBV thanks to governmental HBV immunisation programs. However, the disease remains a major public health problem, especially in low income countries.

Cirrhosis is the main consequence of HBV infection. It has been proposed that HBV induces HCC by direct and indirect functions. Two mechanisms have been proposed for **HBV direct-associated hepatocarcinogenesis**. First, HBV can directly induce HCC because of the capacity of the viral genome to integrate into the host genome, also named the '*cis* effect'. Even though no consistent integration sites have been found, whole genome sequencing studies identified several "*hot site*" breakpoints as the predilection integration regions such as within or upstream the sequence of telomerase reverse transcriptase (*TERT*), the epigenetic regulator *MLL4* or the cell cycle gene *CCNE1* (Fujimoto et al., 2012; Jiang et al., 2012; Sung et al., 2012). The number of integration sites varies from 1 to 12 and the HBV integration sequences can be either complete genome or rearranged sub-genomic fragments. However, it has been reported that HBV integration is mostly partial and it mainly concerns the *S* and the *X* genes. Viral integration interrupts one or more viral genes and as a result, not all viral genes are expressed in HCC. Viral genome insertion leads to HCC development probably due to the cis/trans-activation of oncogenes, deletions and inactivation of tumour suppressors, translocations, production of fusion transcriptions and disruption of chromosome stability. This direct oncogenic effect of HBV could explain the cases of non-cirrhotic HCC when patients are HBV carriers. HBV integration has been reported to occur in the majority of HBV-related HCC, in the tumour and the surrounding non-tumour cells (Bréchot et al., 2000; Tsai and Chung, 2010).

A second mechanism of HBV directly-induced HCC is associated with the viral proteins that can act as putative onco-proteins, which is called the '*trans*' effect. The development of powerful *in vitro* techniques and transgenic animals expressing the viral transgenes have allowed researchers to gain a little more insight into the oncogenic potential of viral proteins and their involvement in cellular damage. Several sets of data suggest that mainly two viral proteins, HBx and HBs have the potential to transform hepatic cells. HBx plays an important role in the

regulation of the viral cell cycle, acting as a transcriptional activator and also directly interacting with host proteins (Bouchard and Schneider, 2004). Transgenic mice expressing the entire coding sequence of HBx with its own regulatory elements develop HCC. The transcriptional activity of HBx in human hepatocytes alters the expression of oncogenic genes *c-myc* and *c-myb*, as well as the tumour suppressors *APC*, *TP53*, *p21waf/cip* and *WT1* (2001). Furthermore, HBx is capable of directly interacting and sequestering p53, leading to the inhibition of p53-mediated apoptosis. This is thought to be one of the main mechanisms responsible for HBX-induced hepatocarcinogenesis. During the hepatocarcinogenesis process, HBx induces epigenetic modifications by interacting with histone deacetylase 1 and DNA methyltransferase (Park et al., 2007). The HBV *S* gene has three translation starting sites leading to the synthesis of three surface proteins (HBs): large (L) obtained from the PreS1 region, middle (M) obtained from the PreS2 region and small (S) encoded by the PreS region. Transgenic mice obtained by the insertion of the PreS/S region develop HCC, indicating a direct oncogenic potential of the S viral proteins.

The **indirect oncogenic activity of HBV** is thought to be due to the stimulation of the host immunity and interaction with host proteins. Host immunological responses may lead to HCC development by inducing oxidative stress and DNA damage in the hepatic cells.

Furthermore, several recent studies have reported that the presence of HBV in liver cells is tightly linked to the emergence of cancer stem cells (CSCs) but little is known about the effect that the virus has on the biology of liver CSCs. When the HBV viral protein HBx is over-expressed in hepatic cells, an EpCAM+ cell population emerges and these cells express the pluripotent stem cell transcription factors Oct4, Nanog and Klf4 (Arzumanyan et al., 2011). Furthermore, HBX-expressing cells have a higher migration potential, cell growth in soft agar and spheroid formation capacities. Clinical data suggested that in HBV positive HCC, high expression of HBx is correlated with the expansion of EpCAM+ cells, aggressive clinicopathological features and the activation of the Wnt/β-catenin pathway. Recently published data suggests that HBX induces the expression of EpCAM through DNA demethylation in hepatocytes, increasing the transcription rate of the encoding gene (Fan et al., 2016).

2.2.2 Hepatitis C virus (HCV)

HCV is a RNA virus belonging to the flaviviridae family, deficient in the reverse transcriptase polymerase and has no integration capacity into the host genome. The viral genome is 9.6kb and encodes for the structural proteins core, E1 and E2 and non-structural proteins p7, NS2, NS3, NS4A, NS4B, NS5A and NS5B **(Figure 5)** (Shlomai et al., 2014). 170 million people are chronic HCV carriers worldwide.

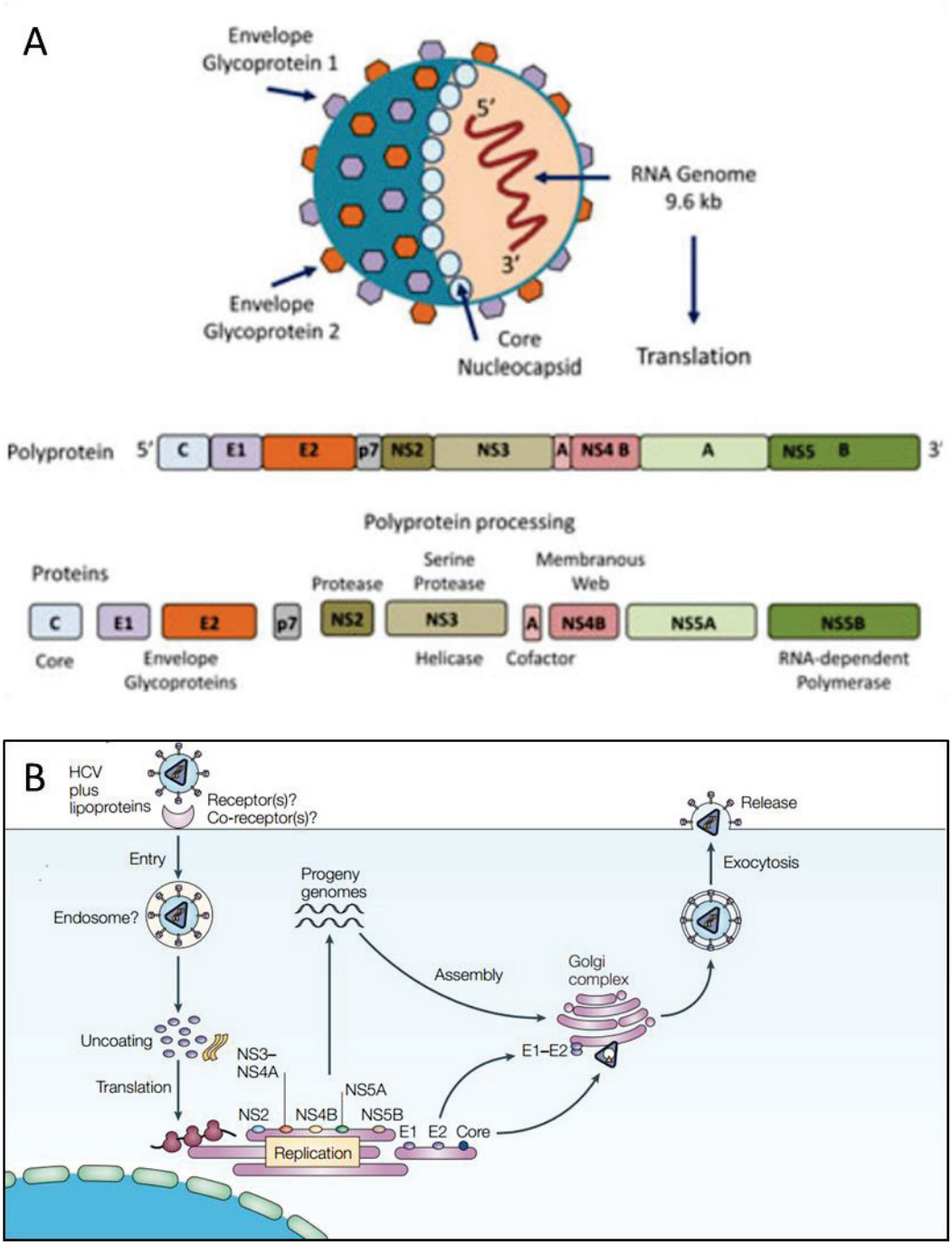

Figure 5. Hepatitis C virus. A. HCV viral particle is an enveloped, positive stranded RNA virus. **B. HCV life cycle**. After entry into the cell, hepatitis C virus (HCV) nucleocapsids are delivered to the cytoplasm,

where the viral RNA functions directly as an mRNA for translation of a long polyprotein precursor of approximately 3000 amino acids. Cleavage of the polyprotein by viral and host-cell proteases yields structural viral proteins (core protein and envelope proteins E1 and E2) and non-structural viral proteins (NS2 through NS5B), with a number of putative activities and functions. Replication occurs within cytoplasm membrane-associated replication complexes in a perinuclear membrane. Genomic RNA is encapsulated into cytoplasmic vesicles, which fuse with the plasma membrane. **(Rehermann and Nascimbeni, 2005)**.

In Europe and North America countries, HCV infection is responsible for about 50-70% of HCC cases (Bosetti et al., 2008), generally presenting with underlying liver fibrosis and/or cirrhosis. No vaccine has been developed yet against HCV but new generation direct-acting anti-viral molecules are associated with a radical decline in the number of HCV infected persons. HCV carriers are thought to be 17-fold more prone to develop HCC, HCV cirrhotic patients having a risk of about 1-4% each year (Degos et al., 2000; Gordon et al., 1998).

HCV has been classified into seven genotypes (1 to 7). HCV genotypes have been associated to different therapy responses (mainly in the case of interferon-based therapies) as well as different capacities to provoke HCC. Studies reported that genotypes 1b and 3 present the highest risks. However, until now, no consensus has been found concerning which genotype has the highest oncogenic potential (Bruno et al., 2007; Raimondi et al., 2009).

Since the HCV viral genome does not integrate into the host genome, it has been suggested that *i)* several HCV proteins could have transformation potential and/or *ii)* the virus could indirectly provoke liver cancer *via* chronic inflammation and oxidative stress. Oxidative stress is the consequence of the imbalance between the production and the clearance of reactive oxygen species (ROS) and has two major consequences. First, by directly reacting with the DNA and forming DNA adducts, ROS produce DNA damage. On the other hand, ROS molecules can act as second messengers in cellular signalling and trigger the activation of oncogenic signalling pathways (Arzumanyan et al., 2013; Higgs et al., 2014). HCV carriers express aberrantly high levels of oxidative stress markers such as 8-hydroxydeoxyguanosine (8-OHdG), malondialdehyde, and thioredoxin in both sera and liver biopsy samples (Farinati et al., 1999; Sumida et al., 2000). The HCV oxidative stress has mainly been attributed to the viral core protein which has been shown *in vitro* and *in vivo* to induce alteration of mitochondrial function and increased intrahepatic lipid peroxidation (Korenaga et al., 2005; Moriya et al., 2001; Okuda et al., 2002). Concerning the ROS activity as a second messenger, it has been reported that increased ROS activate p38, MAPK, JNK, NF-kB and STAT3 pathways, which promote cell survival (Gong et al., 2001; Qadri et al., 2004; Waris et al., 2005). The activation of these pathways further activates TGF-β1. TGF-β1 is an activating factor of hepatic stellate cells

and therefore a profibrogenic factor (Friedman, 2008; Lin et al., 2010). Activated stellate cells further produce TGF-β1 and pro-inflammatory cytokines, the latter inducing cell death and further contributing to oxidative stress (Kang et al., 2009; Kisseleva and Brenner, 2008; Nomura-Takigawa et al., 2006). HCV-induced ROS molecules generate genomic DNA damage, including highly toxic double strand DNA (dsDNA) breaks (Higgs et al., 2014; Machida et al., 2004) and mitochondrial DNA (mtDNA) damage, mitochondria DNA being particularly susceptible since it is not associated with histone proteins (Koike and Miyoshi, 2006).

The HCV viral replication cycle involves the endoplasmic reticulum (ER) and interferes with ER functions involved in protein synthesis and post-translational modifications. Consequently, it leads to ER stress and triggers the activation of the unfolded protein response (UPR) pathway. The expression of HCV proteins has been described to activate the UPR pathway and affect the ER calcium pool. Decrease of the calcium levels, a second messenger transducer, results in mitochondrial membrane depolarization and triggers cell apoptosis.

The direct transforming potential of HCV viral proteins has been described both *in vitro* and *in vivo* in transgenic mice (Lemon and McGivern, 2012). Core proteins have been reported to deregulate the tumour suppressor p53 pathway, but multiple studies have shown contradictory effects regarding the effect of the viral protein on the expression level of p53 target genes (McGivern and Lemon, 2011). The core protein has also been reported to activate the Wnt/β-catenin pathway, by regulating several important actors upstream of β-catenin and probably promoting cell proliferation (Liu et al., 2011b). The NS5A protein phosphorylates and inactivates GSK3β, leading to the stabilisation and accumulation of β-catenin. Both HCV NS5B and core proteins inhibit the tumour suppressor RB function and the DNA damage response (Hassan et al., 2004; Hernando et al., 2004; Munakata et al., 2005). NS3/4A and core interfere with the DNA damage response by impairing the function of the ataxia telangiectasia mutated kinase (ATM), a tumour suppressor that detects dsDNA breaks. This favours the accumulation of DNA damage and promotes chromosome instability and subsequent malignant transformation. Furthermore, it has been described that the presence of HCV virus increases the expression of the proto-oncogene c-Myc *in vivo* and in infected human livers probably due to the activation of the Wnt/β-catenin pathway *via* the Akt pathway (Higgs et al., 2013).

Similar to HBV, HCV has also been described to favour the emergence of CSCs populations. The expression of part of the HCV genome in cultured cells increased the expression of progenitor markers such as Lgr5, CD133, AFP or CK19. The same observations have been made in liver tissues from HCV-carriers (Ali et al., 2011).

2.2.3 Aflatoxin B1

Aflatoxins are mycotoxins produced by two species of molds, *Aspergillus flavus* and *Aspergillus parasiticus*. In Southeast Asia and sub-Saharan Africa, they contaminate nuts and grains that are stored in hot and humid atmospheres. Aflatoxin B1 induces HCC by a mechanism involving its interaction with DNA after its conversion into the AFB1-8,9-epoxide within the human hepatocytes and this leads to DNA mutations. This carcinogenic compound targets the tumour suppressor gene *TP53,* and induces mutations, in particular on its 249 codon. This hotspot mutation leads to the conversion of Arginine into Serine (Hsu et al., 1991; Puisieux et al., 1991; Smela et al., 2001). Aflatoxin B1 synergises with HBV and increases the risk of HCC by 6-fold (73% both agents present vs 11.3% HBV only or 6.4% AFB1 only (Liu et al., 2012b).

2.2.4 Alcohol abuse

Alcoholism is an important risk factor for HCC because it causes fatty liver, necro-inflammation, fibrosis and liver cirrhosis. The association between alcohol abuse and HCV or HBV infection enhances patients' predisposition to develop HCC (McKillop and Schrum, 2005; Stickel et al., 2002; Voigt, 2005). Alcohol abuse is the most important risk factor for HCC in North America and Northern Europe. In Europe and North America, it is responsible for about 20% of HCC cases and most of these patients present with underlying alcohol steatohepatitis (ASH) (Bosetti et al., 2008; Forner et al., 2012). Despite the knowledge that pathologists have on the consequences of ethanol induced liver injury, the exact mechanism of alcohol-induced HCC is still not clear. Several lines of evidence suggest that it is the metabolism of ethanol rather than the ethanol *per se* that is an oncogenic event. Ethanol metabolites produced by hepatocytes generate ROS molecules and thus an oxidative stress. These metabolites are able to form DNA adducts and induce mutations. When high levels of ethanol are present in the liver, the expression of CYP2E1 is induced in order to increase the levels of ethanol that can be metabolised. However, it has been suggested that CYP2E1 can have detrimental effects on cells that are associated with cellular transformation due to activation of protooncogenes and changes in the cell cycle duration (Albano et al., 1999; McKillop and Schrum, 2005). Independently of the effects of ethanol metabolism, alcohol abuse depletes the stock of the antioxidant glutathione and leaves cells unprotected against the deleterious effects of ROS (Fernández-Checa et al., 1998; Lu, 2000).

2.2.5 Non-alcoholic steatohepatitis and other risk factors

Non-alcoholic steatohepatitis (NASH) is an advanced stage of non-alcoholic fatty liver disease (NAFLD) and has been recognised as being an increasing risk factor for HCC across the world. NAFLD affects 1.0 billion individuals worldwide, representing more than 10% in developed countries (Noureddin et al., 2015; Rozman, 2014). It is characterised by chronic changes in fatty acid metabolism and hepatic inflammation. The main causes leading to the development of this pathology are high fat and glucides content in the diet. Until now, the exact mechanisms contributing to hepatocarcinogenesis are not known. NAFLD patients are prone to fibrosis or cytogenic cirrhosis development. Once cirrhosis is installed, the rate of HCC development has been shown to be over 10% (Oda et al., 2015; White et al., 2012). Genetical predispositions have been described in NASH-related HCC patients, such as the PNPLA3 rs738409 C > G polymorphism, but this result has not been fully confirmed (Liu et al., 2014). Another possible link has been described between NASH development and the gut microbiota. This last factor has been described to impact on the level and quality of bile acid metabolites, for example increasing the levels of deoxycholic acid, which is toxic for hepatocytes and which provokes the senescence of hepatic stellate cells. *In vivo*, in mice, murine senescent hepatic stellate cells release tumourigenic factors, such as platelet derived growth factor (PDGF) and vascular endothelial growth factor (VEGF) contributing to hepatocellular transformation (Hara, 2015; Lade et al., 2014; Yoshimoto et al., 2013).

Several other conditions have been described as risk factors for HCC such as α1-antitrypsin deficiency, Wilson disease, diabetes or hemochromatosis. Hemochromatosis is the most common genetic defect (1/200 prevalence) and leads to the accumulation of iron in the liver. Type 2 diabetes is associated with hyperinsulinemia and increased production of IGF-1, which is also thought to contribute to HCC development (Smedile and Bugianesi, 2005).

2.3. Epidemiology

The geographical distribution of HCC prevalence follows the global repartition of its main risk factors (**Figure 6**). Because this tumour is often detected at late stages, the estimated annual rate of deaths related to liver cancer is close to the rate of newly diagnosed cases. Therefore, HCC is the second most frequent cause of cancer-related death after lung cancer. In 2012, 782

000 HCC cases were diagnosed and HCC was associated with 746 000 deaths (Ferlay et al., 2010; Kabbach et al., 2015; Wang et al., 2015; Zuo et al., 2015).

Since the first epidemiological studies in the 1970s, important geographical differences in HCC incidence rates have been noted (Szmuness, 1978). The highest rates occur in Eastern Asia whereas the lowest rates are in Northern Europe and North America. The majority of HCC cases (84%) affect developing countries, especially where infection by hepatitis B virus (HBV) is endemic and contributes to 70-80% of HCC cases. Owing to national vaccination programs against hepatitis B, the incidence of HCC in these areas has started to decline. Another etiological factor encountered in developing countries is aflatoxin intoxication. In Western countries and Japan, the most common etiological factors are HCV infection, excessive alcohol intake, diabetes and obesity associated with NASH (El-Serag, 2011).

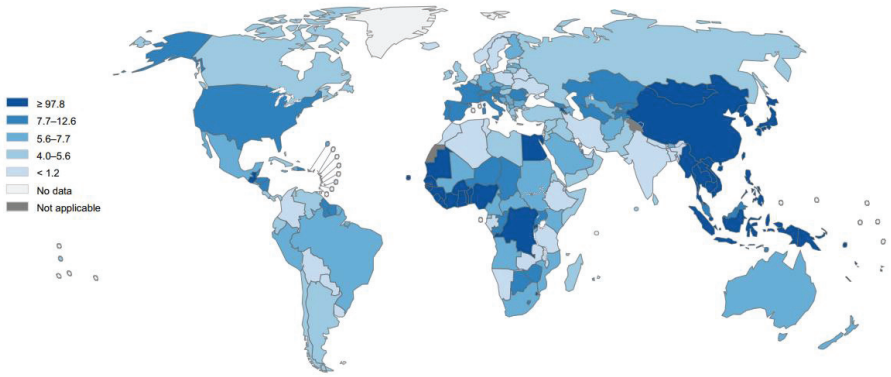

Figure 6. HCC epidemiology. Estimated age-standardized rates (World) of incidence cases, males, liver cancer, worldwide in 2012. (Globocan 2012)

Primary liver cancer is more common among males than in females as globally, rates are more than twice as high in males than in females (Jemal et al., 2011). The incidence increases with age, reaching a peak in the 30–50 year age group.

According to recent data, the global incidence of HCC is still increasing, although it varies throughout the world. Its increase in Western countries is related to the hepatitis C virus and non-alcoholic steatohepatitis (NASH) (El-Serag, 2011).

2.4. Diagnosis of HCC

As is the case for most solid tumours, HCC is asymptomatic for several months and sometimes for years. For this reason, screening for HCC should be carried out in all known chronic liver disease patients at regular time intervals. The population of patients at high risk is composed of those with chronic cirrhosis or chronic infection by hepatitis B or C virus. When HCC develops on the background of a healthy liver, the disease is found by chance following ultrasound scan and/or computerized tomography carried out for other reasons, and usually is at an advanced stage at the time of diagnosis.

When manifested, the most frequently observed symptoms are: chronic hepatitis with pain in the right side of the abdomen, increased volume of the liver, fatigue, change in mood, edema in the legs, swollen abdomen due to ascite fluid accumulation and/or rapid occurrence or deterioration of portal hypertension (sometimes accompanied by oesophageal varices).

The diagnosis of HCC patients is based on imaging techniques (ultrasound, CT, nuclear magnetic resonance (NMR)), but the diagnosis can only be confirmed by histology. Generally, ultrasound is the first tool recommended for detecting HCC nodules in the population at risk. The effectiveness of ultrasound in detecting any form of HCC is quite good (94%), but its sensitivity drops to 63% for small nodules (Singal et al., 2009; Trevisani et al., 2007). Contrast-enhanced ultrasound does not increase the sensitivity for small HCC but it helps in differentiating some lesions (Terzi et al., 2016). The threshold for detecting HCC by imaging techniques is 1cm. However, lesions less than 1cm are relatively common in patients at risk. These lesions are difficult to diagnose even when using biopsy because of the complexity of the sampling procedure and therefore the occurrence of false-positive or false-negative results.

Most scientific societies for the study of liver diseases agree that patients at risk should be checked every 6 months for the development of HCC. It is considered that the doubling period of an HCC nodule is 6 months. In the case of patients with detected lesions inferior to 1 cm or undergoing follow-up post-treatment, tumours should be checked at shorter interval times of around 3 months.

Blood tests are not very useful at diagnosis but may help in patient follow-up. No blood marker has been found for the diagnosis of HCC, except the observation that in some HCC patients the alpha-fetoprotein (AFP) is aberrantly elevated and a proportion of these patients tend to have a worse prognosis (Nagasue et al., 1977; Tangkijvanich et al., 2000). Since HCC is often

accompanied by an underlying hepatopathy, several serum liver enzymes, such as alanine aminotransferase (ALT) and aspartate aminotransferase (AST), are quantified in order to appreciate the degree of underlying liver disease.

Prognosis. Patients with HCC usually have a poor prognosis. Previous estimations suggest that close to 70% of patients will relapse within 5 years following surgery. Typically, recurrence rate of HCC follows a 2 peaks distribution (Imamura et al., 2003). The first group of patients usually develop new hepatocellular tumours within 2 years after resection and this is clinically recognised as 'early' recurrence. This is mainly related to the metastatic spread of cells originating from the primary tumour. The second group of patients develop *de novo* tumours more than 2 years after tumour resection and are clinically labelled as 'late' recurrence. Patients representing the second peak of HCC relapse, develop additional tumours as a consequence of the carcinogenic cirrhotic tissue. Predictive factors for relapse are vascular invasion of the primary tumour (both macroscopic and microscopic), tumour size, the number of nodules, alpha-fetoprotein (AFP) levels, the degree of differentiation and the presence of satellites nodules. Early stage HCC are more likely curable, with a lower relapse probability while advanced HCCs are more prone to develop early recurrence.

Unfortunately, microvascular invasion and satellites can only be assessed on liver biopsies, once the tumour has been removed. This eliminates the possibility to predict relapse before surgery and adjust the treatment. Besides cancer, another life-threatening condition (i.e., cirrhosis) is present in more than 80% of patients with HCC, which renders prognosis prediction a major challenge.

2.5. Histopathological characteristics

In the initial phase, HCC develops as a well differentiated nodule. In the case of cirrhotic patients, the cancerous nodule develops inside a dysplastic regenerative nodule. The initial cancerous nodule grows until it exits the regenerative nodule and progresses to moderate and than towards a poorly differentiated tumour. In advanced stages, the tumour will develop satellite nodules, resembling to small nodules exiting the primary tumour while in the final stage the tumour will evolve into a multinodular structure spread across the liver.

The **macroscopic** aspect of hepatocellular tumours depends on the natural history of the disease. If the tumour develops in a cirrhotic environment, it is commonly surrounded by a fibrous capsule. HCC nodules that develop on a healthy liver tend to be invasive into the

adjacent liver tissue, without a visible capsule. In some cirrhotic cases, numerous small tumours can occur throughout the liver but are not distinguishable from regenerative nodules. Micro- and macrovascular invasion is a common feature of HCC, in particular when involving the portal veins. In advanced HCC, more than 70% of cases have tumour thrombi in the portal vein and are a cause of intrahepatic metastases due to tumour spread through the portal vein.

The main target organ for **extrahepatic metastasis** is the lung.

HCC is formed of cells resembling hepatocytes. Generally, cells maintain their organisation in sinusoid-like shapes lined by a single-cell sheet of endothelial cells while the microscopic architecture of lobules is generally lost, especially in cirrhotic patients. HCC exhibits different architectural patterns and cytological variants.

Depending on the organisation of cancerous hepatocytes, the resulting sinusoids can have **trabecular** (tumour cells grow in cords and are commonly encountered in well and moderately differentiated HCC), **pseudoglandular and acinar** (the tissue has a glandular aspect, with cells forming a bile canaliculi-like structure, smaller in well differentiated tumours than in moderately differentiated), **compact** (no apparent organisation, cells have a solidarious appearance) or **scirrhous pattern** (marked by accentuated fibrosis) (illustrated in **Figure 7**).

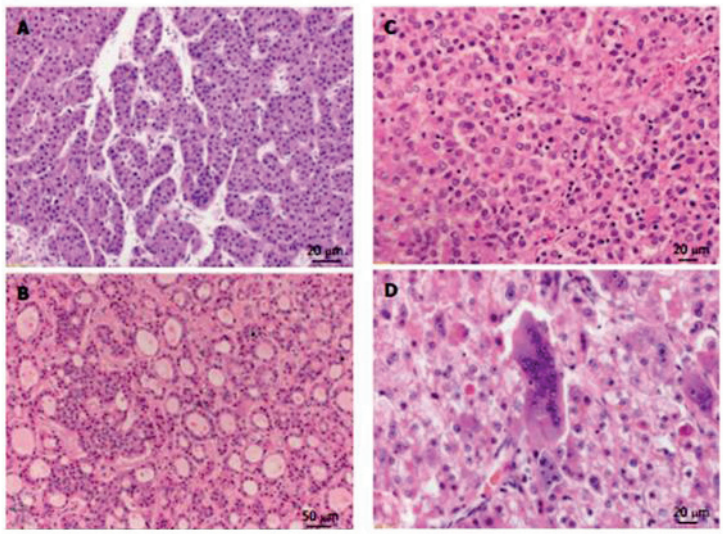

Figure 7. Growth patterns of progressed hepatocellular carcinoma. A. Trabecular [hematoxylin and eosin (HE), × 300]; **B.** pseudoglandular (HE, × 100); **C.** solid/compact (HE, × 200); **D.** giant cells formation (HE, × 200). **(Schlageter et al., 2014)**

Several **cytological variants** are encountered depending on the cell appearance, such as pleomorphic or clear cells with glycogen storage, evidence of sarcomatous or fatty change, bile production (the tumour colour turns to green after formalin fixation) or presence of mallory hyaline bodies (aggregated intermediate filaments), globular hyaline bodies, pale bodies (accumulation of amorphous materials in cystically dilated endoplasmic reticulum) or ground glass inclusions.

According to the **histological grade**, hepatocellular tumours are classified following the Edmonson classification. They can be **well differentiated** (common in small tumours less than 2 cm in diameter with frequent pseudoglandular or acinal pattern), **moderately differentiated** (the most common form in tumours more than 3 cm in diameter accompanied by trabecular pattern), **poorly differentiated** (associated with a compact patterns, with no visible sinusoid-like shapes) or **undifferentiated**.

However, HCC neoplastic nodules are known to be highly heterogeneous and vary histologically even at the level of a single nodule. When smaller than 1 cm, HCC nodules are uniformly well differentiated but when surpassing this size, they usually contain more than two types of tissue with varying histological grades. The tissue at the centre of the tumour is generally less differentiated than at the exterior. In general, the well differentiated area diminishes and is replaced by less differentiated during tumour growth. Otherwise, if the two cellular contingents grow and expand in the same time, the nodule often has a 'nodule-in-nodule' appearance.

Benign precursor HCC lesions can originate from cirrhotic nodules (dysplastic nodules) or on the healthy liver in the case of hepatocellular adenoma. Dysplastic nodules evolve by expansion of cirrhotic nodules and show variable cellular atypia without clear malignancy. To the naked eye, they resemble both cirrhotic regenerative nodules and to cancerous ones. They present no invasion into the portal tracts and many of them have been shown to evolve into HCC in follow-up studies, being therefore considered as precancerous lesions.

2.6. Hepatocarcinogenesis

Hepatocarcinogenesis is a multi-step process, generally developing in an altered hepatic microenvironment, typically on a background of chronic liver damage and rarely on healthy liver. Chronic liver injury is accompanied by fibrosis and massive inflammation responsible for the deregulation of several signalling pathways and accumulation of genetic alterations in normal hepatocytes. Hepatic lesions first present as dysplastic nodules evolving into early carcinoma which finally progresses to HCC (

Figure 8).

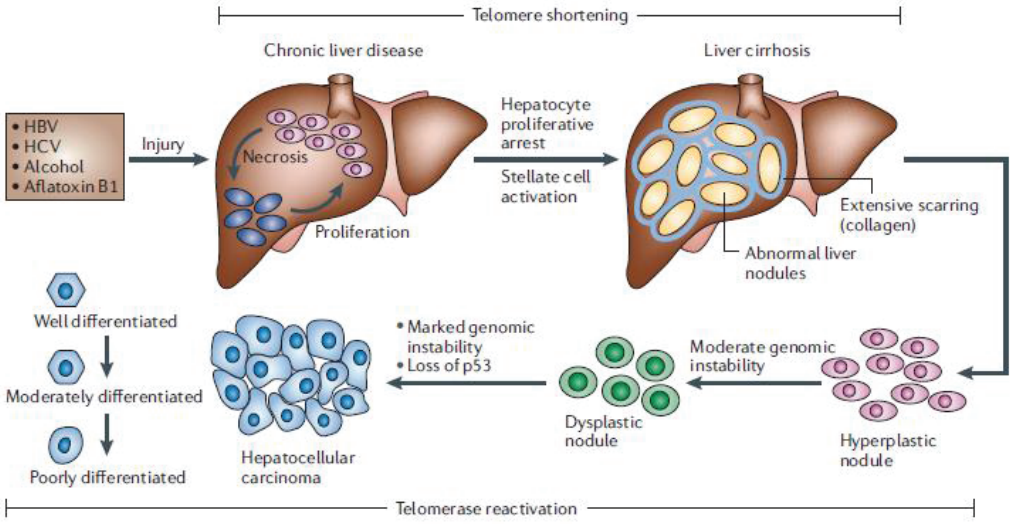

Figure 8. Histopathological progression and molecular features of HCC. After hepatic injury, necrosis followed by hepatocyte proliferation fosters a chronic liver disease condition that culminates in liver cirrhosis. Cirrhosis is characterized by abnormal liver nodule formation surrounded by collagen deposition and scarring of the liver. Subsequently, hyperplastic nodules are observed, followed by dysplastic nodules and ultimately hepatocellular carcinoma (HCC), which can be further classified into well differentiated, moderately differentiated and poorly differentiated tumours — the last of which represents the most malignant form of primary HCC. Telomere shortening is a feature of chronic liver disease and cirrhosis. Telomerase reactivation has been associated with hepatocarcinogenesis. (Farazi and DePinho, 2006)

The process that transforms normal hepatic cells into neoplastic cells is not known, but it is thought to be the combination between changes in normal liver histology associated to cellular alterations due to hepatic viruses, oxygen derived free radicals and toxic compounds, and changes in the host immune system. All these factors induce liver cancer over a period of time long enough to cause an irreversible phenomenon.

Recent data published on colon cancer suggest that the main risk factor of cancer is bad luck (Tomasetti and Vogelstein, 2015). The liver is a good example of the model proposed by Tomasetti and Vogelstein. Liver cells are quiescent but in response to cell death due to chronic liver injury, they show intense replicative activity. Since the greater the replication rate, the higher the risk that one or more daughter cells have mutations in their DNA, it makes sense that the risk of acquiring HCC is higher in the presence of risk factors, such as HBV or HCV infection, alcoholism, aging, excessive iron, and smoking.

In general cell transformation is mostly governed by an intertwined relationship between abnormal cell proliferation and resistance to apoptosis. However, in liver cancer the process is a bit more complicated because hepatic cells have a very specific metabolic activity, which when deregulated seems to participate to the carcinogenic process.

Several molecular alterations have been described to be common to most small HCC, encountered independently of the associated risk factor, are thought to constitute the early stages of hepatocarcinogenesis. Hepatocarcinogenesis is accompanied by dedifferentiation, loss of cell adhesion, degradation of the extracellular matrix and constitutive activation of the survival and growth-promoting pathways. Analysis of liver biopsies coming from patients with cirrhosis suggests that HCC is often multiclonal. On the other hand, the natural progression of intermediate and advanced HCC is considered to be highly heterogeneous.

It is widely accepted that carcinogenesis is a multistep process triggered by the accumulation of genetic alterations that activate different signal transduction pathways and drive the progressive transformation of normal cells into malignant cells (Fantini et al., 2015; Hai et al., 2014; Merle and Trepo, 2009). The phenotypic (morphological and microscopic) and genetic heterogeneity of HCCs also adds an additional level of complexity to our understanding of hepatocarcinogenesis. However, despite many remaining challenges, substantial progress has been made in this field. As in other solid cancers, numerous genetic alterations accumulate during the process of hepatocarcinogenesis. Genetic alterations affect a limited number of genes and chromosomal loci during the early preneoplastic stage and accelerate throughout dysplasia and HCC development (Takai et al., 2014). Previous studies have shown that the incidence of genetic alterations in HCC is relatively rare and limited to a subset of a few cancer-specific genes (Nishida and Goel, 2011).

Liver cirrhosis is accompanied by a significant rate of hepatocellular senescence and characterized by considerably short hepatocyte telomeres (Wiemann et al., 2002). The molecular mechanisms leading to the development of HCC are extremely complicated and consist of prominent genetic and epigenetic alterations (Facciorusso et al., 2016).

2.6.1 Epigenetic alterations

Epigenetics refers to mechanisms modulating gene expression without the modification of the DNA sequence itself. In cancer, in general, and in HCC in particular, several epigenetic changes have been reported including DNA hyper- and hypomethylation, histone modifications, chromatin remodelling and aberrant expression of micro-RNA and long noncoding RNAs (lncRNAs) (Liu et al., 2012a; Nishida and Goel, 2011; Zhang, 2015).

Hereafter follows a non exhaustive summary of a few of these epigenetic alterations reported to be present in HCC.

DNA methylation. Like in other types of cancer, HCC presents a higher hypermethylation status of the tumour DNA compared to the surrounding non-tumour tissue. Hypermethylation contributes to the regulation of gene expression and mainly affects CpG islands situated in close proximity to gene promoters. Specific promoter hypermethylation and global hypomethylation affect the expression of tumour-suppressors leading to downregulation of their expression and favouring genomic instability. It has been described that differential DNA aberrant hypermethylation of *FZD7*, *CDKN2A*, *RASSF1A* and *APC* allows HCC nodules and the surrounding tissue to be discriminated. Several other genes have been reported to be aberrantly methylated such as *CDKN2A* (Liu et al., 2012a; Nishida and Goel, 2011), *NFATC1*, *GSTP1*, *BMP4* and *GABRA5* (Lambert et al., 2015) and recently reviewed by Wahid et al. (Wahid et al., 2017).

Histone modifications. Histone levels and biochemical modifications affect gene expression and chromatin structure. Modifications include ubiquitinations, phosphorylation, methylation and acetylation at the histones' N-terminal tails, affecting the turn-over of these proteins, as well as their affinity for their target DNA sequence. These modifications have consequences on cellular processes, such as DNA repair, DNA replication and gene transcription. It has been reported that in HCC patients, histone-encoding genes are either over-expressed (H3K4diMe, SETDB1) (Magerl et al., 2010; Wong et al., 2016; Zhang et al., 2016), downregulated (Patt1) (Shon et al., 2009), or that mutations can affect the methyltransferase enzymes (SMYD3) (He et al., 2012a). Some histone modifications act as a signature for risk factor exposure, such as the PP2Ac phosphatase whose expression is increased in HCV chronic infection and is considered as an important event in viral hepatitis associated hepatocarcinogenesis, partly responsible for the inhibition of the DNA damage repair (Gong et al., 2015).

Chromatin remodelling is mainly the result of nucleosomes recruitment at DNA sites by ATP-dependent chromatin remodelling complexes and covalent enzymatic modifications of histones. Chromosome remodelers are thought to have tumour suppressor roles, as inactivated mutations have been reported in cancer (Wilson and Roberts, 2011). Whole exome sequencing of hepatocellular tumours revealed that chromatin remodellers are the third more frequently mutated genes (Guichard et al., 2012). Mutations of *ARID1A*, *ARID1B* and *ARID2*, components of the SWI/SNF chromatin remodelling complex are mutated in HCC at frequency of 16.8%, 6.7%, and 5.6%, respectively (Li et al., 2011).

Noncoding RNAs are divided in several sub-groups based on their length. Of these, the most studied are short miRNAs with less than 200 nucleotides and long noncoding RNAs (lncRNA) exceeding this length threshold. miRNAs regulate the stability of mRNA and therefore impact on the quantity of the synthesised proteins. The level of several miRNAs such as miRNA 122, miRNA 125b, miRNA-26, miRNA-101, miRNA-221 and miRNA-1180 are perturbed in HCC leading to cell cycle progression, tumour invasion and proliferation of HCC cells (Liu et al., 2016b, 2016b; Nassirpour et al., 2013; Wu et al., 2016; Yang et al., 2013; Zhao and Wang, 2015; Zhou et al., 2016b). LncRNAs have been shown to act as scaffold, signal, guide and decoy in cancer in general and in HCC in particular. For example, HOTAIR is associated with progression of HCC *via* activation of the Wnt/β-catenin pathway and autophagy while HOTTIP is associated with metastasis in HCC patients (Gao et al., 2016; Yang et al., 2016a). These lncRNAs could be a good option as therapeutic targets, as well as decision making biomarkers. However, the molecular mechanism of noncoding RNAs in cancer is still an emerging area of study which will eventually lead to the development of next generation drugs.

2.6.2 Genetic alterations

As in other solid tumours, a large number of genetic alterations accumulate during the carcinogenic process. Compared to other types of cancer such as melanoma and lung cancer, HCC possesses a low rate of mutations/tumour (90 in average) (**Figure 9**).

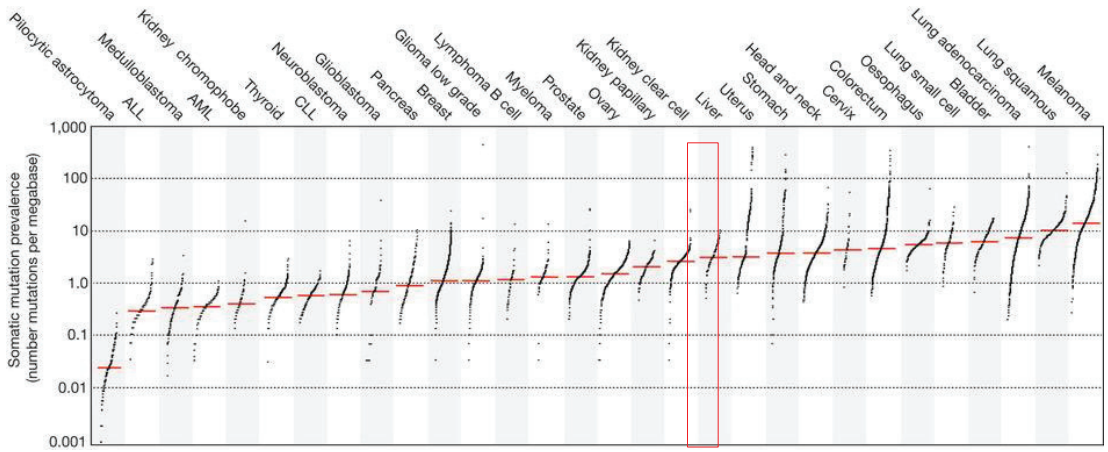

Figure 9. The prevalence of somatic mutations across human cancer types. Every dot represents a sample whereas the red horizontal lines are the median numbers of mutations in the respective cancer types. The vertical axis (log scaled) shows the number of mutations per megabase whereas the different cancer types are ordered on the horizontal axis based on their median numbers of somatic mutations. The red rectangle highlights the frequency of mutations affecting liver tumours. **(Alexandrov et al., 2013)**

Over the past decade, great progress has been made in elucidating the molecular mechanisms underlying hepatocarcinogenesis. In particular, recent advances in next-generation sequencing technologies have revealed numerous types of genetic alterations, including recurrent mutated genes and dysregulated signalling pathways in HCC.

Genomic instability (also known as "genetic instability" or "genome instability") consists of mutations, including changes in nucleic acid sequences, chromosomal rearrangements, or aneuploidy (Zhang, 2015). However, it remains unclear whether genomic instability is a cause or a consequence of tumourigenesis. In neoplasms, genomic instability can be broadly classified based on its origin as **chromosomal instability (CIN)** or, less commonly, **microsatellite instability (MSI)** (Chan, 2011).

1. *Chromosomal instability*

In cancer, chromosomal instability is a consequence of increased rate of chromosome missegregation during mitosis. CIN is a hallmark of human cancer and is believed to contribute to tumourigenesis, tumour progression, and development of therapy resistance (Bastians, 2015). In addition, it has been widely accepted that CIN is associated with clinical and pathological parameters in solid tumours. CIN is one of the most frequent abnormalities in HCC.

CIN usually involves both **numerical changes** (DNA copy number alterations [CNAs] or aneuploidy) and **structural chromosomal changes** (gain or loss of chromosome fragments,

translocations, inversions, amplifications, deletions and allelic loss [loss of heterozygosity (LOH)]) (Martin et al., 2010; McGranahan et al., 2012).

DNA copy number alterations (CNAs) is an important subclass of somatic mutations. Aberrant amplifications of chromosomal regions and deletions are commonly associated with overexpressed oncogenes or the loss of tumour suppressor genes (TSGs) (Pinkel and Albertson, 2005).

Although the distribution of aberrant chromosomal arms differs among HCCs, numerous studies have shown that certain regions are frequently affected in HCC, including **gains** in chromosomes 1q, 5p, 6p, 7q, 8q, 17q, and 20q and **losses** in 1p, 4q, 6q, 8p, 9p, 13q, 14q, 16p-q, 17p, 21p-q, and 22q (Fernandez-Banet et al., 2014; Homayounfar et al., 2013; Kan et al., 2013; Nishida et al., 2013a; Roessler et al., 2012; Wang et al., 2013a). These findings reflect a high degree of CIN in HCC, contributing to hepatocarcinogenesis (Wilkens et al., 2004). Some of these regions contain CNA-associated oncogenes or tumour suppressor genes (TSGs), such as *c-myelocytomatosis viral oncogene* (*C-MYC*) (8q), *cyclin A2* (*CCNA2*) (4q), *cyclin D1* (*CCND1*) (11q), *retinoblastoma 1* (*RB1*) (13q), *axis inhibition protein 1* (*AXIN1*) (16p), *TP53* (17p), *mannose-6-phosphate receptor* (*IGFRII/M6PR*) (6q), *p16Ink4A* (9p), E-cadherin (*CDH1*) (16q), *suppressor of cytokine signalling* (*SOCS*) (16p), and *phosphatase and tensin homolog* (*PTEN*) (10q), which have been identified to be associated with HCC (Bertino et al., 2014; Mínguez et al., 2009).

Loss of heterozygosity (LOH) refers to loss of one of the two alleles at one or more *loci* and is the main mechanism for the inactivation of tumour suppressor genes (TSGs). In HCC patients, LOH is frequently observed on chromosomes 1p, 4q, 6q, 8p, 9p, 10q, 11p, 13q, 14q, 16q, and 17p (Midorikawa et al., 2009; Okuno et al., 2009). Of these, losses on 4q and 8p are the most frequent chromosomal alterations in HCC. The LOH at 4q has been reported to be strongly correlated with increased in alpha-fetoprotein (AFP) levels in HCC (Zhang et al., 2010), and is significantly more frequent found in poorly differentiated HCCs (Moinzadeh et al., 2005). These results suggest that the inactivation of TSGs on chromosome 4q might be a late event occuring after malignant transformation. Two hotspot regions are located on chromosome 4q encoding for several TSGs including *neil endonuclease VIII-like 3* (*NEIL3*), *interferon regulatory factor 2* (*IRF2*) and *inhibitor of growth family member 2* (*ING2*). Chromosome 8p is rich in candidates and validated TSGs, with a cluster of six genes, including *deleted in liver cancer 1* (*DLC1*), *coiled-coil domain-containing protein 25* (*CCDC25*), *elongator complex protein 3* (*ELP3*), *proline synthetase co-transcribed bacterial homolog* (*PROSC*), *SH2 domain-containing protein 4A* (*SH2D4A*), and *sorbin and SH3 domain containing 3* (*SORBS3*).

Chromothripsis is a new class of complex catastrophic chromosomal rearrangements. It occurs as a single cellular crisis during which a chromosome is broken and reassembled by DNA repair mechanisms, resulting in a large number of rearrangements clustered in a chromosomal region (Stephens et al., 2011). The process is considered as extremely rare, but can affect cancer-related genes and has a major impact on the tumour progression, prognosis and therapeutic response. To date, only one study reported the implication of chromothripsis in HCC affecting chromosomal arms 1q and 8q and favouring gene amplifications (Fernandez-Banet et al., 2014).

Somatic mutations in the open reading frame can lead to loss-of-function of tumour suppressors or gain-of-function of oncogenes. Mutations can also occur in the regulatory regions of genes affecting transcription, translation and stability of the gene product and impacting on individual's cancer risk and progression. Whole genome sequencing of HCC in/or the surrounding tissue has evidenced that several genes present recurrent mutations. Mutations in genes such as *TP53*, *CTNNB1* (the β-catenin coding gene) and *Axin1* were identified more than 10 years ago (El-Din et al., 2010; Wang et al., 2013b), but recent studies employing deep-sequencing techniques have identified additional recurrent mutations affecting chromatin remodelling (*ARID1A* and *ARID2*), oxidative stress (*NFE2L2* and *KEAP1*), the RAS/MAPK (*RPS6KA3*) and the JAK/STAT pathways (*JAK1*) (Fujimoto et al., 2012; Guichard et al., 2012; Kan et al., 2013; Kawai-Kitahata et al., 2016; Nault et al., 2013, 2014). *TERT*, *TP53* and *CTNNB1* mutations are the most frequent genetic alterations and play a major role in HCC pathogenesis, generally independent of the etiological background, except for the association between the codon 249 *TP53* mutation and HBV chronic infection and aflatoxin intoxication.

TERT mutations are observed in 90% of human cancers, and enable cells to bypass cell senescence and escape apoptosis, a major step towards the initiation of malignant transformation (Bell et al., 2015; Makowski et al., 2016). The *TERT* gene encodes for the catalytic subunit of the reverse transcriptase telomerase which maintains the length of telomeric DNA and chromosomal stability. In HCC, *TERT* mutations mainly affect the promoter region, leading to over-expression of the coding sequence. Even though the functional role of this genetic alteration is not known, DNA sequencing studies showed that it occurs early during the hepatocarcinogenesis process (Chen et al., 2014b; Schulze et al., 2015). The *TERT* mutation frequency varies around the world being found in between 20% to 60% of cases but is considered to be the most frequent somatic genetic alteration regardless of patients' geographical origin (Cevik et al., 2015; Chen et al., 2014b; Huang et al., 2015; Killela et al., 2013; Quaas et al., 2014; Yang et al., 2016c). *TERT* promoter mutations have been found to be

associated with *CTNNB1* mutations suggesting an interaction between the telomere's activity and the activation of the Wnt/β-catenin pathway (Nault et al., 2013; Pezzuto et al., 2016; Schulze et al., 2015; Totoki et al., 2014).

TP53 mutations. The p53 protein is responsible for cell cycle arrest and apoptosis in response to cellular stress signals and its inactivation leads to uncontrolled proliferation of abnormal cells. TP53 mutations rates vary among different geographical regions depending on the prevalence of risk factors. The reported mutations lead to the inactivation of p53 proteins (Loss of function, LOF) or to p53 acquiring new functions (gain of function, GOF). *TP53* mutations favour the initiation or the progression of HCC, depending on the etiological factor. For example, the *TP53* mutation at codon 249 is almost exclusively induced by AFB1 and appears to be an early event in hepatocarcinogenesis (Hussain et al., 2007). In contrast, in AFB1-non related HCC, *TP53* mutations are generally found in advanced tumours, suggesting in these tumours that p53 inactivation is only required for progression. Mutant p53 represents an interesting target for HCC therapy (Parrales and Iwakuma, 2015). Nevertheless, p53 protein inactivation without mutation has been observed in several pre-tumoural tissues (Piccinin et al., 2012). For HCC, in the case of aetiologies involving cell regeneration, inactivated p53 could facilitate continued proliferation, but could also favour the emergence of abnormal pre-cancerous cells.

CTNNB1 mutations lead to β-catenin stabilisation, which will translocate into the nucleus. It acts as a transcriptional co-factor and activates target genes such as *MYC*, *CCND1*, *COX2* and *matrix metalloproteinase 7* (*MMP7*) (Gregorieff and Clevers, 2005). In some studies, *CTNNB1* mutations have been related to early-stage HCCs while in others to HCC progression (An et al., 2001; Peng et al., 2004; Thorgeirsson and Grisham, 2002). In HCV-induced HCC, *CTNNB1* mutations have been described to be more frequent that in HBV-related HCC (Hsu et al., 2000; Huang et al., 1999). Finally, some studies in HCC biopsies showed that *CTNNB1* and *TP73* mutations are mutually exclusive, as has already been described for *CTNNB1* and *TP53* mutations (Boyault et al., 2007).

ARID1A **and** ***ARID2*** inactivating mutations affect the functionality of the chromatin remodelling complex SWI/SNF and have been identified in about 10% of HCC cases (Fujimoto et al., 2012; Huang et al., 2012; Schulze et al., 2015; Totoki et al., 2014; Zhu et al., 2016). Some studies suggested that *ARID1A* mutations are more frequent in patients with an HCC related to alcohol intake while *ARID2* mutations would occur in HCV-associated HCC but these findings have not been confirmed in other studies (Abe et al., 2015; Guichard et al., 2012; Huang et al., 2012; Li et al., 2011; Zhao et al., 2011). Most of the mutations affecting these two proteins are

inactivating mutations, suggesting that *ARID1A* and *ARID2* could act as tumour suppressors. *ARID1A* and *ARID2* mutations are able to initiate HCC in combination with active PI3K/AKT, but not *per se*.

NRF2* and *KEAP1 mutations lead to the activation of an oxidative stress pathway in about 12% of HCC cases (Schulze et al., 2015). The NRF2-KEAP1 pathway regulates the cytoprotective response to cellular stress, widely caused by ROS molecules. NRF2 acts as a transcription factor with KEAP1 being a negative regulator of its activity. These mutations could represent late events in hepatocarcinogenesis in humans, since they have been observed only in advanced HCC. The NRF2/KEAP1 pathway seems to lead to HCC *via* epigenetic instability, abnormal methylation of tumour suppressor genes or by favouring the accumulation of additional genetic alterations (Geismann et al., 2014; Karin and Dhar, 2016; Nishida and Kudo, 2013; Nishida et al., 2013b). Furthermore, somatic mutations of *NRF2* or *KEAP1* would correlate with *CTNNB1* or *AXIN1* mutations that activate the Wnt pathway (i.e. the two types of alterations are found in the same tumour sample) (Amaddeo et al., 2012; Guichard et al., 2012).

JAK1 gene mutations occur at a low frequency (about 9%) in HCC. Nevertheless JAK/STAT signalling pathway has been reported as a hepatocarcinogenesis promoter and altered in about 45% of HCC (Kan et al., 2013).

2. *Microsatellite instability*

MSI is the result of defects in mismatch repair genes that impacts on the stability of microsatellites, which are tandem repeats that are present at millions of loci in the human genome. MSI plays an important role in carcinogenesis as it can result in the inactivation of TSGs or can disrupt other noncoding regulatory sequences (Kim and Park, 2014). Data suggest that MSI is present in cirrhotic liver, mainly induced by HBV infection and is associated with more aggressive tumour features and shorter median delays before recurrence (Dore et al., 2001; Kawai et al., 2000). The degree of MSI was significantly correlated with poor differentiation and portal vein invasion (Kondo et al., 2000; Togni et al., 2009). These studies suggest that MSI could play a minor role in hepatocarcinogenesis but might be associated with the progression of HCC in patients with a background of chronic hepatitis and/or cirrhosis (GOUMARD et al., 2017).

2.6.3 Deregulated pathways

The pathways commonly altered by genetic alterations (somatic mutations or homozygous deletions) in hepatocellular carcinoma include the Wnt/β-catenin pathway, phosphatidylinositol 3-kinase (PI3K)/Ras signalling pathways, oxidative and endoplasmic reticulum stress modulators and processes responsible for chromatin remodelling **(Figure 10)**.

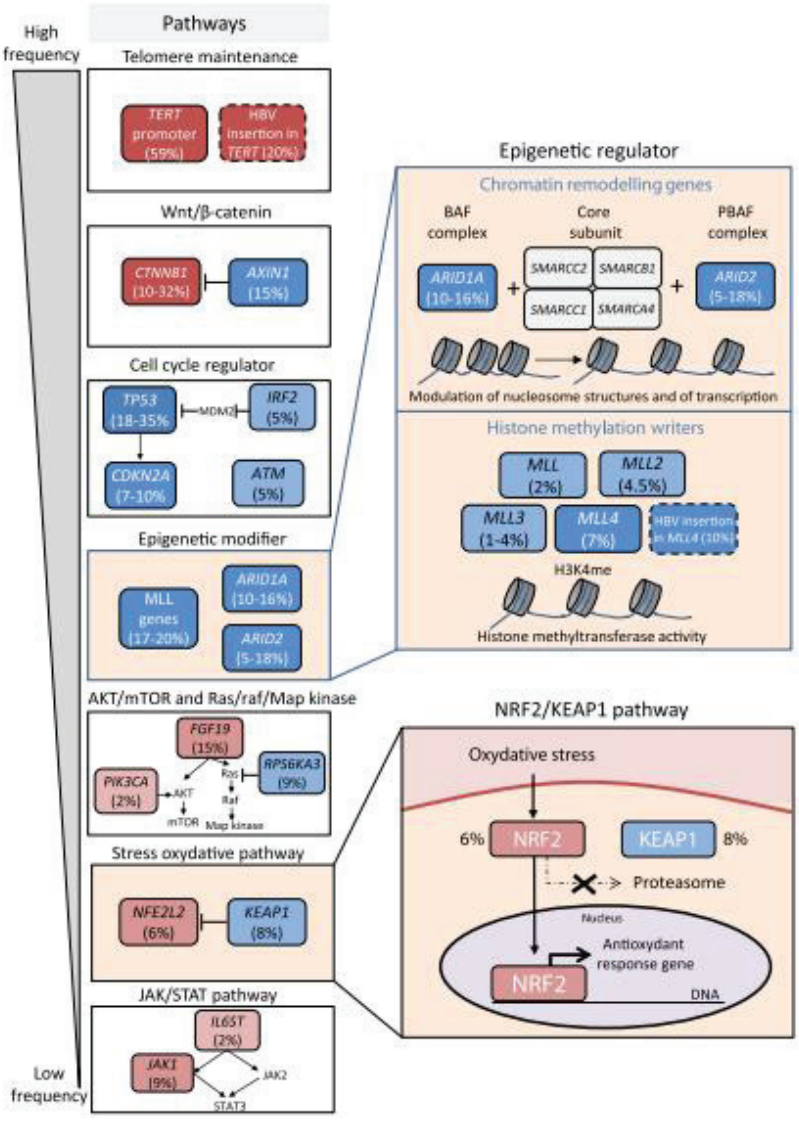

Figure 10. Major pathways altered in hepatocellular carcinoma. Signalling pathways frequently mutated in HCC are shown in the left panel, oncogenes are indicated in red and tumour-suppressor genes in blue. The percentage of alterations found in HCC is noted in brakets. **(Nault and Zucman-Rossi, 2014)**

The Wnt pathway plays a major role in the pathogenesis of HCC and has been described to be aberrantly activated in 40% to 70% of HCC samples (Yang et al., 2016b). The central Wnt pathway effector is β-catenin. When the pathway is inactivated, β-catenin is degraded by the proteasome, after phosphorylation by casein kinase 1 (CK1) and glycogen synthase kinase 3β (GSK-3β), in the presence of the axis inhibition protein (AXIN) and the adenomatous polyposis coli (APC) proteins (Cervello et al., 2012). In contrast, the activation of Wnt pathway, triggered by interaction between Wnt ligands and their frizzled (Fzd) receptors, prevents β-catenin phosphorylation and degradation. Consequently, β-catenin accumulates in the cytosol and in part translocates into the nucleus. By interacting with the transcription factors T-cell factor (TCF)/lymphoid enhancer factor (LEF), it initiates the transcription of target genes (Pez et al., 2013).

In HCC, mutations in *CTNNB1* exon 3 are the main cause of Wnt pathway aberrant activation, followed by inactivating mutations in *AXIN1* and *APC*, over-expression of Frizzled-7 (*FZD-7*) and inactivation of GSK-3β (Kim et al., 2008; Merle et al., 2005; Oishi and Wang, 2011; Takigawa and Brown, 2008). In these cases, hepatocytes display abnormal cellular proliferation and the resulting tumours are associated with metastatic behaviour and cancer stem cells (Herencia et al., 2012). The canonical Wnt pathway contributes to angiogenesis, tumour infiltration and metastasis through the regulation of factors involved in the execution of these processes such as MMP-2, MMP-9, VEGF and bFGF. In HBV-related HCC, β-catenin mutations have been found to occur at a lower frequency compared to alcohol and HCV-related HCCs which show a higher incidence of these mutations (Fujimoto et al., 2012; Guichard et al., 2012; Kawai-Kitahata et al., 2016; Levrero and Zucman-Rossi, 2016; Li et al., 2011; Shin and Chung, 2013; Waly Raphael et al., 2012).

The PI3K/Akt/mTOR pathway is a major intracellular signalling cascade that is involved in the regulation of cell proliferation, growth and survival, through the activation of tyrosine kinase receptors, such as VEGFR, EGFR, PDGFR, and IGFR. When a ligand binds to one of these receptors, phosphoinositide-3-kinase (PI3K) and AKT become activated (Fruman and Rommel, 2014). Akt can activate mTOR by inhibition of the TSC1/2 complex. The mTOR pathway is implicated in cellular metabolism and inhibition of autophagy. Nearly 50% of patients with HCC exhibit activation of the mTOR pathway, which may be partially attributable to activation signals from receptor tyrosine kinases such as IGFR and/or EGFR pathways. mTOR pathway activation is associated with aggressive HCC and decreased survival of patients (Matter et al., 2014; Zhou et al., 2010). Despite promising results with the new drugs targeting mTOR, a substantial benefit in HCC patients has not yet been shown in clinical practice.

The Ras/Raf/MEK/ERK signalling cascade is another important intracellular pathway altered in HCC (Lavoie and Therrien, 2015). Activation of Ras and Raf results in the phosphorylation and activation of MEK1/2 and than ERK1/2. This leads to apoptosis inhibition and cell proliferation. The pathway has a negative feedback loop as ERK1/2 is capable of phosphorylating and activating the RSK2 member (encoded by *RSP6KA3*) which inhibits MEK1/2. In 2-9% of HCC cases, inactivating mutations of *RSP6KA3* occur, suppressing the inhibition control of the pathways and therefore favouring non-controlled activation of the pathway. *KRAS* activating mutations have been reported to be very rare, being found only in about 1% of cases (Guichard et al., 2012).

JAK-STAT activation has been reported due to activating mutations of *JAK1* (9.1%), in a series of HBV-related HCC (Kan et al., 2013). However, these results have not been confirmed in western countries. *IL6ST* has been reported to be rarely mutated in HCC originating from France (2%) (Guichard et al., 2012).

2.6.4 Molecular classification of HCC and patient prognosis

Hepatocellular carcinomas (HCCs) are a heterogeneous group of tumours with regard to risk factors and genetic alterations. A second level of heterogeneity is identified at the individual level with differences found between different tumour nodules in the same patient and even in the same nodule itself (Bruix et al., 2014; Tao et al., 2011). These two sources of heterogeneity have a strong impact on the molecular classification of hepatocellular tumours. HCC patients have a highly variable clinical course, indicating that HCC comprises several biologically distinctive entities (Llovet et al., 1999a, 2003).

Several groups have performed studies to quantifiate the expression profile of large panels of genes, in order to define gene expression patterns in HCC and better understand the underlying hepatocarcinogenesis. These have led to the description of subgroups of HCC (between two and six) that differ according to aetiological factors, mutations in tumour suppressor genes, rate of recurrence and intrahepatic metastases, as well as the disease stage (Boyault et al., 2007; Chen et al., 2002; Chiang et al., 2008; Hoshida et al., 2009; Iizuka et al., 2003; Lee et al., 2004b; Makowska et al., 2016; Nam et al., 2005; Okabe et al., 2001; Ye et al., 2003). However, genomic molecular information of the tumour is not robustly associated with prognosis, as patient outcome greatly depends on the recurrence probability post-resection (Hoshida et al., 2008).

Despite plausible distinct mechanisms of carcinogenesis according to the clinical background, several alterations are observed across different aetiologies, patient race (i.e., host genetic variations) and environmental factors, suggesting that the same molecular pathways are deregulated irrespective of aetiology (Totoki et al., 2014).

Laurent-Puig and collaborators proposed in 2001 a classification of HCC based on the incidence of chromosomal aberrations and the status of the three genes known at the time to be the most frequently mutated in HCC: *TP53*, *AXIN1* and *CTNNB1* (Laurent-Puig et al., 2001). Two groups of patients were identified, based on the chromosome stability status: the first group comprises *CTNNB1* mutations, with chromosome stability except for 8p loses, and are characterised by large tumours and negative hepatitis B virus status; the second group demonstrates higher chromosome instability, mutations of *AXIN1* and *TP53*, and are poorly differentiated tumours, often associated with HBV chronic infection **(Figure 11).**

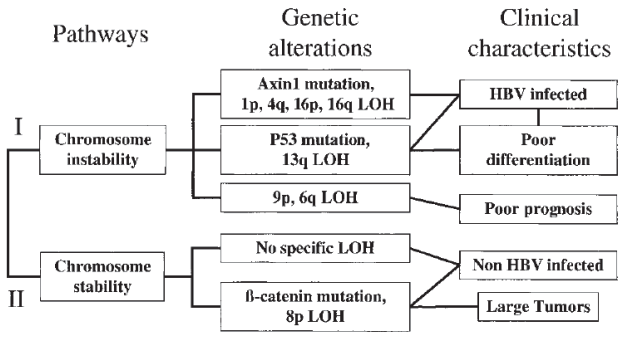

Figure 11. Classification of HCC as proposed by Laurent-Puig and collaborators. Two classes are clearly distinct: Those characterised by chromosome instability with *TP53* mutations (I) and those characterised by chromosome stability and *CTNNB1* mutations (II). **(Laurent-Puig et al., 2001)**

The first classification based on a large gene expression profile was proposed by Breuhahn and collaborators in 2004 (Breuhahn et al., 2004). By analysing the mRNA expression pattern of 43 different human HCC samples and by comparing them with normal adult liver, two main groups have been characterised based on the most highly varying gene expression profiles. The group A (65% of cases) showed an induction of the IFN pathway, whereas group B was characterised mainly by down-regulation of apoptosis-related genes and inactivation of the IFN pathway. Based on the expression pattern of insulin-like growth factor type 2 (IGF-II), the group B could be further classified into two groups, B1 (14% of cases) with high expression of IGF-II and B2 (21% of cases) without differential expression. In HCC, IFN-pathway and overexpression of IGF-II are mutually exclusive (**Figure 12)**. However, no association analysis has been performed with respect to patient prognosis.

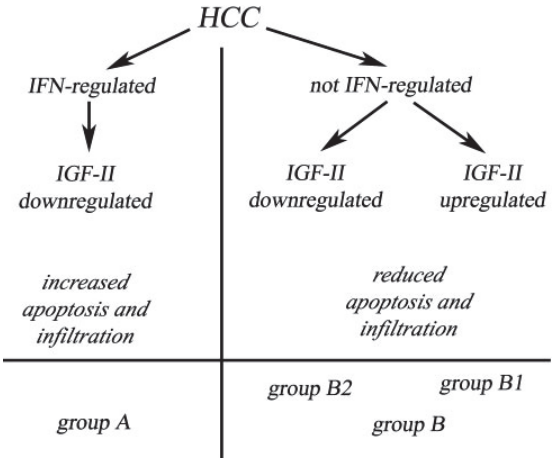

Figure 12. Schematic display of HCC subtyping according to Breuhahn *et al*, 2004.

Lee and collaborators proposed in 2004 another classification of HCC based on gene expression profile but in relation to patient prognosis (Lee et al., 2004b). The gene expression profile was established in 91 human primary HCC and matching non-tumour surrounding tissue. The authors showed that differential gene expression clustering defined 2 groups of patients with poor and good survival. The over-expressed genes in the poor prognosis group are enriched with genes involved in cell growth and maintenance, suggesting that these tumours grow faster. Many of the genes with lower expression in the cell proliferation group were liver-specific, which is consistent with the observation that poorly differentiated HCC have less favourable clinical outcomes.

The first most comprehensive molecular classification is the **6-group classification** proposed by J Zucmann Rossi's group in 2007, based on a detailed analysis at the clinical, genetic, and transcriptomic level (Boyault et al., 2007). Gene expression profile of 57 hepatocellular tumours allowed the identification of 6 groups of tumours (G1 to G6) **(Figure 13)**. The association of genetic and clinical data to each one of the 6 groups allowed the identification of two larger clusters, with a relatively better or worse prognosis:

- the first cluster (G1-G3) is characterised by chromosome instability, mutations in the *TP53* and *AXIN1* genes, expression of genes involved in cell cycle and cell proliferation, presence of cancer stem cells markers and activation of the Akt pathway; this group is frequently encountered in patients with HBV infection. Patients in this group have a poor prognosis.

- the second cluster (G4-G6) is characterised by chromosome stability and activation of the Wnt pathway with frequent mutations of the *TCF1* and *CTNNB1* genes. Patients in this group have a better prognosis than those of the first cluster.

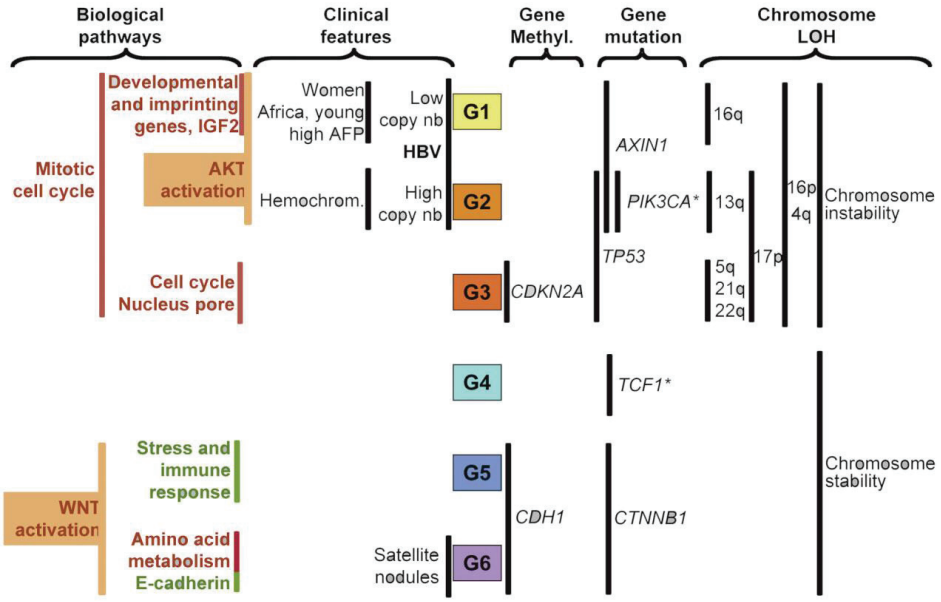

Figure 13. HCC subgroups defined by transcriptome analysis with their related clinical and genetic characteristics. Vertical lines indicate significantly associated features. Red and green primarily indicate over- and underexpressed genes, respectively, in that particular functional category. (Boyault *et al*, 2007)

Of important note, *TP53* mutations and *CTNNB1* mutations, the two first discovered and most common gene mutations, are mutually exclusive and each define a distinct cluster of patients. A 16-gene signature has been validated to efficiently define a tumour as belonging to one of the 6 groups.

Ten years later, a study originating from the same group, completed this 6-group classification in relation to clinical and histological features **(Figure 14)** (Calderaro et al., 2017). The G1, G2, G3 proliferative groups enriched in *TP53* mutations are poor differentiated tumours, with macro- and micro-vascular invasion, high AFP serum levels and activation of PI3K/AKT pathway. In addition, the G1 subtype showed progenitor subtype with positive CK19 and EpCAM staining. Tumours belonging to the second cluster with *CTNNB1* mutations have been shown to be cholestatic (bile production), well-differentiated with intact tumour capsule, lack of inflammatory infiltrates, maintenance of various markers of hepatic differentiation and function (APOB, several isoforms of Cyp450, HNF1A, HNF4A), low AFP expression and low cell proliferation.

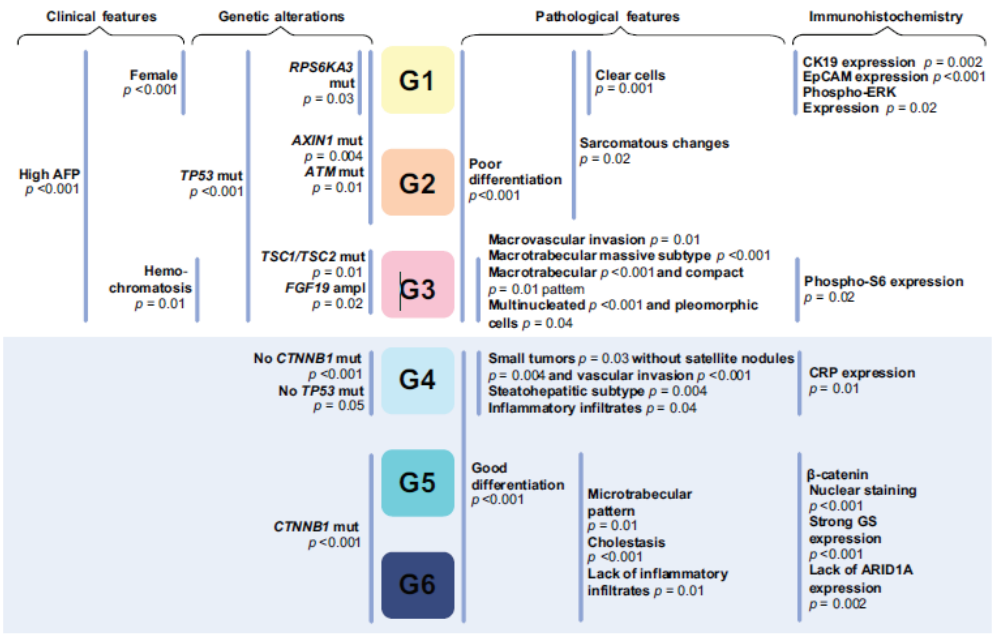

Figure 14. Integration of clinical, pathological and molecular features into HCC 6-group molecular classification. (Calderaro et al., 2017)

In 2010, Hoshida and collaborators proposed another classification based on a meta-analysis of previous gene expression analyses **(Figure 15)** (Hoshida et al., 2010). Hepatocellular tumours fall in 3 groups based on the expression of differentially expressed genes.

- The first group, **S1** is clinically characterised by greater risk of early recurrence with more vascular invasion and satellite nodules, poor survival with more advanced HCC, expression of genes associated with epithelial-to-mesenchymal transition and activation of the Wnt pathway. This class did not contain *CTNNB1* mutated tumours, but authors identified TGF-β as an activator of the Wnt pathway.
- The second group, **S2** is characterised by bigger tumours, high serum AFP, signature of poor survival with more advanced HCC, suppression of IFN targeted genes, myc-related genes activation, EpCAM+, higher AFP mRNA in the tumours and Akt activation as shown by IHC.
- The third group, **S3** is characterised by smaller tumours, well differentiated and with a good survival signature, related to *CTNNB1* mutations and further named "CTNNB1" class.

The S3 group can be assimilated to the G5-G6 groups from Boyault's classification while the S1-S2 group can be assimilated to the G1-G3 cluster.

For the first time this study, later confirmed by Lachenmayer and collaborators in 2012 (Lachenmayer et al., 2012), identified two different mechanisms of activation of the Wnt pathway leading to two subclasses with activated Wnt. The first one (S3) exhibits *CTNNB1* activating mutations that leads to the constitutive activation of the Wnt pathway thanks to the

stabilisation of β-catenin, and its accumulation in the nucleus. The second one (S1) involves the activation of the TGF-β pathway that favours the translocation of β-catenin from the cell membrane to the cytoplasm, but not to the nucleus. As a consequence, the Wnt-associated differentially expressed genes are different in the two subclasses, called classical Wnt target genes and liver-related Wnt target genes, respectively.

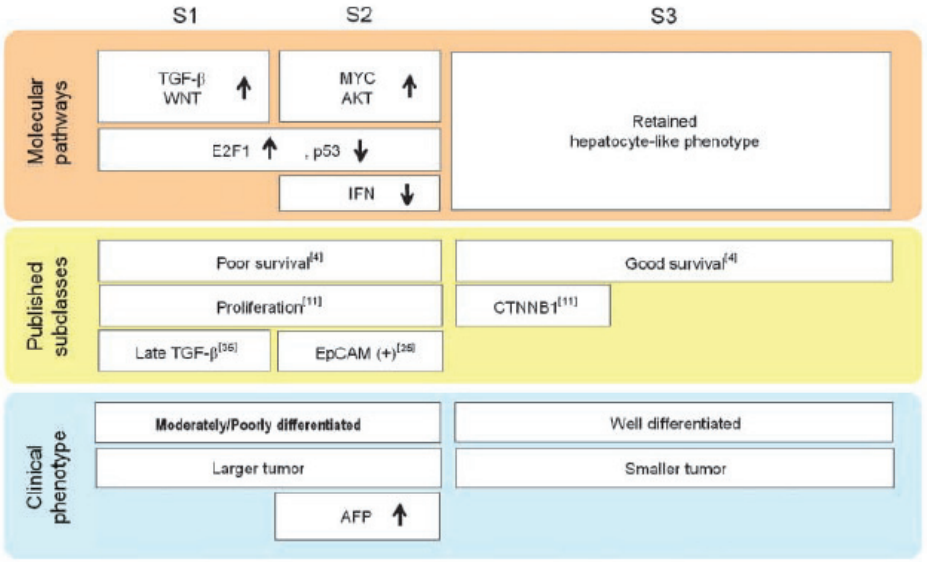

Figure 15. Schematic classification of HCC in 3 groups as proposed by Hoshida et al, 2010.

Tan *et al.* completed the S1-S3 classification by assessing the clinicopathological features for each of the 3 subclasses (Tan et al., 2016). The association of distinct histopathological features to each molecular subclass suggests that the deregulations observed in the molecular pathways are related to morphological features.

- the S1 subclass is characterised by a steatohepatitic-HCC variant with immune cell infiltrate and expression of the hepatocarcinogenesis associated marker *BIRC5*.
- the S2 subclass present features of macrotrabecular/compact pattern (accelerated cell cycle progression and cell proliferation), high serum alpha-fetoprotein, activation of oncogene YAP and stemness markers EpCAM and CK19, vascular invasion, HBV infection as well as expression of the hepatocarcinogenesis associated marker *GPC3*.
- the S3 variant is characterised by a lack of steatohepatitic-HCC, clear cell variants, lower histological grade with a microtrabecular pattern (retained normal hepatocyte functions involved in a variety of metabolic pathways) and expression of the hepatocarcinogenesis associated markers *LYVE1* and *GLUL*.

These results suggest that HCC molecular subclasses can be attributed based on the assessment of the clinicopathological features. However, there was no significant association between HCC molecular subclasses and patient prognosis with respect to survival or recurrence.

Desert and collaborators performed a classification of the non-proliferative, well differentiated class described by Boyault's (G4, G5 and G6 sub-classes) and Hoshida's classification (S3) (Désert et al., 2017). This group of tumours comprises tumours with mutant β-catenin and the rest of well differentiated tumours with wild-type β-catenin. According to Desert's work, gene set enrichment analysis divides non-proliferative HCCs into two distinct subclasses, recapitulating the phenotypes of hepatocytes at the two distinct ends of the zonation program. The wild-type β-catenin group recapitulates the "perivenous" phenotype of hepatocytes, responsible for lipogenesis and glycolysis. The mutant β-catenin group recapitulates the "periportal" phenotype, responsible for gluconeogenesis and urea synthesis. Furthermore, a robust 5-gene signature (*GLUL*, *LRG5, ODAM* positive correlation, *HAL* and *VNN1* negative correlation) has been validated allowing discriminating well differentiated tumours with wild-type β-catenin from tumours with the mutant allele.

The first limitation of all these studies is due to the sampling method. All the expression profiles have been established using resected tumours. This introduces a selection bias towards patients without decompensated liver cirrhosis and with early stage HCC. Secondly, the differentially expressed genes were defined in comparison of the matching non-tumour tissue, which is already a pre-cancerous tissue, since HCC ofter arises in the context of chronic liver disease with cirrhosis.

2.6.5 Tumour microenvironment

It is now known that carcinomas are complex systems consisting of a variety of cells that promote tumour growth and protect it from the immune system (Bissell and Radisky, 2001). The tumour microenvironment includes endothelial cells, fibroblasts, T, B, natural killer (NK) lymphocytes, and antigen presenting cells, such as macrophages and dendritic cells **(Figure 16)** (Albini and Sporn, 2007). The tumour microenvironment defines the behaviour of the tumour, due to interactions with and influences of surrounding cells. It is now clear that the cross-talk between tumours and the tumour microenvironment is crucial for cell survival, growth, proliferation, the epithelial–mesenchymal transition (EMT) and metastasis (Leonardi et al.,

2012; Yang et al., 2011a). Given the complex risk factors and progression of HCC, an understanding of the key players is crucial.

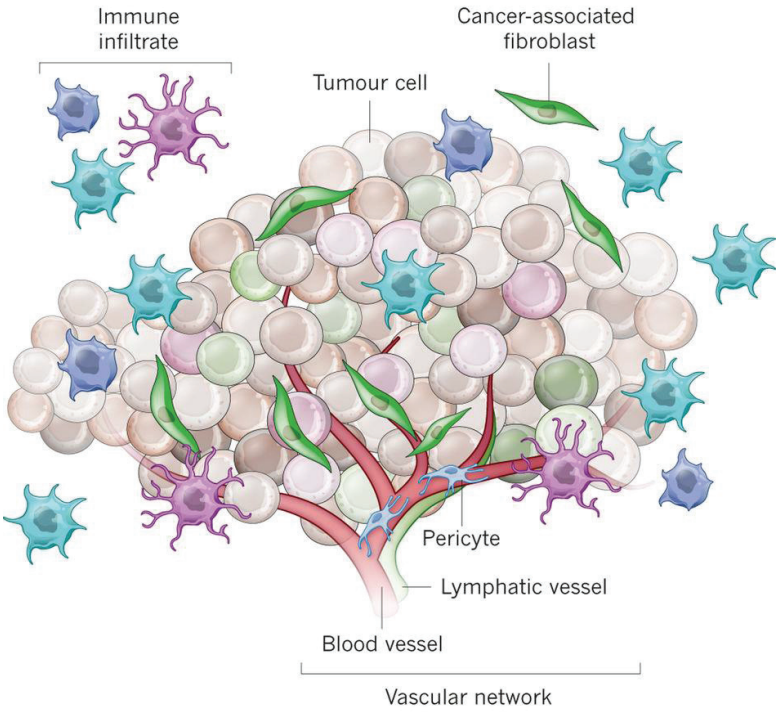

Figure 16. Tumour microenvironment is a dynamic physical topography providing structural support, access to growth factors, vascular supply and immune cell interactions. **(Junttila and de Sauvage, 2013)**

Fibroblasts

Fibroblasts are the non-vascular, non-epithelial, non-inflammatory cells of the connective tissue and are its main component (Kalluri and Zeisberg, 2006; Tarin and Croft, 1969). They are embedded into the extracellular matrix and are responsible for its production. Cancer associated fibroblasts (CAFs) are the most abundant cell type of the tumour stroma and play a critical role in tumour-stroma interactions. They are positive for the following markers: alpha-smooth muscle actin (α-SMA), vimentin, desmin and fibroblast activation protein (FAP) (Garin-Chesa et al., 1990). CAFs promote tumourigenesis and are involved in tumour growth and invasion. They are able to produce a range of inflammatory and tumourigenic mediators such as epidermal growth factor (EGF), fibroblast growth factor (FGF), IL-6, the chemokine ligand 12 (CXCL12), matrix metalloproteinase 3 (MMP3), and 9 (MMP9) (Mueller and Fusenig, 2004).

Hepatic stellate cells

Hepatic stellate cells (HSCs) are a key factor in the development of liver fibrosis (Friedman et al., 1985). HSCs are normally quiescent but in response to chronic liver injury they become activated. During this process, HSCs trans-differentiate into myofibroblast-like cells, a crucial event in the development of liver cirrhosis (Moreira, 2007). Activated HSCs can infiltrate the stroma of the liver and localise around tumour sinusoids, fibrous septa and capsules (Faouzi et al., 1999; Wu et al., 2012). Co-culture of HCC cells with HSCs promotes HCC cell migration and invasion via the FAK-MMP9 signalling pathway (Han et al., 2014).

Tumour-associated macrophages

Tumour associated macrophages (TAMs) are located in the tumour stroma and can be in several polarised activation states. Activated M1 macrophages, which produce type 1 pro-inflammatory cytokines, play an anti-tumourigenic role, while alternatively activated M2 macrophages, which produce type 2 cytokines, promote both anti-inflammatory response and pro-tumourigenic activity (Biswas and Mantovani, 2010).

Alternatively activated M2 macrophages with pro-tumourigenic phenotypes have been well documented in cancers other than HCC. M2 macrophages appear to contribute to poor prognosis in human HCC through CCL2-induced EMT (Yeung et al., 2015). The Kupffer cells, which are liver specific macrophages, are able to impair CD8+ T cell-dependent immune response through the interaction between Programme death 1 (PD1) on CD8+ T cells and PD ligand-1 (PD-L1), causing a deficiency of CD8+ T cell cytotoxic function in HCC (Afreen and Dermime, 2014; Wu et al., 2009).

2.6.6 Experimental hepatocarcinogenesis *in vitro*

To elucidate the initial events and progression of HCC, cellular models of carcinogenesis are extremely important. Several highly characterized HCC cell lines have been developed, leading to a better understanding of pathways and alterations commonly encountered in HCC. However, in order to understand what the processes are occurring in the early stages of hepatocarcinogenesis, there is an absolute requirement for developing models that reflect the sequential neoplastic transformation of normal hepatocytes.

Normal human cultured cells are quite resistant to neoplastic transformation, whereas rodent cultured cells are transformed to neoplastic cells with relative ease (McCormick and Maher, 1988; Namba et al., 1996). This species difference is probably due to the difficulty in

immortalizing normal human cells *in vitro*. Until now, neither spontaneous immortalization nor spontaneous neoplastic transformation of normal human hepatocytes has been reported. No successful malignant transformation of human hepatocytes by chemical agents or ionizing radiation *in vitro* has been reported either despite the fact that exposure to some chemical agents has been associated with an increased risk of HCC in humans.

In contrast to human cells, rodent cells display substantial telomerase activity in several somatic tissues, including the liver. Therefore, *in vitro* they are not sensitive to replicative senescence as it is the case for primary human cells. In humans, telomerase activity in most cell types is repressed early during development. Consequently, telomere DNA in proliferating somatic cells undergoes progressive attrition. Once a critical minimal length is reached, cellular growth is irreversibly arrested, a process known as replicative senescence, which was first described by Hayflick and Moorhead nearly 50 years ago.

In 1985, two transgenic mouse lines expressing the HBV surface proteins were independently established by two different groups using genetically modified transgenic technology (Babinet et al., 1985; Chisari et al., 1985).

Several strategies have been set-up allowing immortalisation of primary human hepatocytes. Immortalized hepatocytes are defined as a population of indefinitely dividing parenchymal cells that retain critical liver functions. Immortalization strategies have been developed based mainly on the transduction or transfection of hepatocytes with well-known immortalizing genes. The most frequently used immortalization methods are (i) overexpression of viral oncogenes (the adenoviral E1A/E1B genes, the simian virus 40 large T antigen (SV40TAg) or the early region (SV40ER, encoding large T and small t Ag) and the human papillomavirus 16 (HPV16) E6/E7) genes, (ii) forced expression of hTERT, or (iii) a combination of both (Cascio, 2001; Reid et al., 2009). As hepatocytes differentiation and proliferation are mutually exclusive *in vitro*, cell growth was associated with deterioration of the differentiated morphology and functional phenotype, a phenomenon already described by others (Chamuleau et al., 2005; Kim et al., 2000). Hepatocytes were successfully immortalized only by introducing the SV40 large T antigen; however, immortalisation is necessary but not sufficient for transformation (Schippers et al., 1997). Furthermore, there is no evidence that SV40 is related to human liver cancer (Strickler et al., 1998). A comprehensive review describing all possible techniques of immortalisation has been published (Ramboer et al., 2014).

2.6.7 Experimental animal models of hepatocarcinogenesis

The multi-factorial and multi-step nature of cancer development makes analysis difficult when using cell cultures, since the interaction between neoplastic cells and the surrounding microenvironment may be lost.

There are three model systems currently used for the study of HCC in mice and rats that allow all these steps to be investigated: chemically induced, genetically engineered and xenograft models. HCC models in use generally combine two or more model types as liver injuries generally synergise.

Mice with a humanised liver also represent a valuable tool for the study of viral infection as well as hepatocarcinogenesis and a brief description of the different models is provided below.

Viral animal models have been used to investigate the different steps of viral induced hepatocarcinogenesis even though mice cannot be naturaly infected with HBV due to the narrow host range of HBV and the absence of a proper cellular receptor and other factors necessary for HBV infection and replication.

Transgenic mouse models carrying the HBV genome have been proposed as an alternative. However, this model is not adapted for studying HBV-induced HCC as no cccDNA has been detected in the animals' liver, the viruses produced by the transgenic liver cannot re-infect hepatocytes and these animals do not develop hepatitis. Nevertheless, viral HBV particles have been detected in the blood of HBV transgenic and resemble those purified from HBV-infected patients. These observations suggest that the molecular mechanisms regulating the synthesis of HBV transcripts and proteins, as well as the viral package and viral secretion, are probably shared in human and mouse hepatocytes and this model could be used to evaluate the therapeutic efficiency of agents against viral replication. Currently the chimpanzee and tupaia are the only animal models that can be infected by HBV.

Transgenic mice expressing the HBV surface protein were the earliest HBV-related transgenic mice to be created (Ng and Lee, 2011; Yamazaki et al., 2008). In the 1980s, Chisari's group developed the first transgenic mouse model expressing the HBsAg. This led to severe chronic injury, accompanied by inflammation and regenerative hyperplasia, finally leading to HCC (Chisari et al., 1989). However, this model may not fully reflect the changes brought about by HBV infection as the phenotype observed could be due to HBsAg accumulating in hepatocytes. A second HBV viral protein, HBx, has also been shown to have carcinogenic potential: HBx transgenic mice develop HCC and HBx expression induces hepatocyte proliferation,

contributing to hepatocarcinogenesis (Kim et al., 1991; Koike et al., 1994, 1998). In this model system, cell proliferation is not the early event preceding HCC, but proliferative nodules are observed before the onset of HCC (Kim et al., 1991). Since HBx has been described to contribute to altered cellular gene regulation, this property could predispose to malignant process.

In contrast to the limitations of HBV mouse models, results obtained with HCV transgenic mice proved to be much more fructuous, notably regarding the HCV- induced fibrosis present in HCV-infected patients. Mice expressing the complete HCV viral genome develop steatosis and finally HCC with immunological reactions (Lerat et al., 2002). HCV core transgenic mice develop steatosis from the age of 3 months and about 25% of them developed HCC in their later life, demonstrating the direct role of HCV core protein in hepatocarcinogenesis, probably due to underlying steatosis (Moriya et al., 1998).

Genetically engineered animal models (GEMs) including transgenic, knock-out and knock-in mice, are valuable tools to elucidate the molecular mechanisms related to pathogenesis, including carcinogenesis in the liver. They have also been shown to be very useful to evaluate potential chemopreventive agents and new therapeutic targets under physiological conditions. GEM models are developed by gene targeting providing knock-out models for genes thought to act as tumour suppressors or *via* loss-of-function studies, as well as knock-in models useful for the study of putative oncogenes. Conditional GEMs obtained by the use of site-specific recombinase systems are useful to control the spatio-temporal gene expression (Frese and Tuveson, 2007). Despite the fact that the precise genetic events contributing to HCC remain elusive, several commonly deregulated pathways have been explored in the development of GEM models such as p53, RB or Wnt/β-catenin (Leenders et al., 2008). The transgenic SV40TAg model has also been widely employed. Large T antigen is responsible for the inactivation of the tumour suppressors p53 and Rb. c-Myc liver-specific expression has also been used to induce HCC in mice, since its deregulation and coexpression with transforming growth factor alpha (TGF-α) are frequent in primary liver tumours (Leenders et al., 2008; Murakami et al., 1993). The synergistic effect of c-myc/TGF- α on neoplastic development has been demonstrated thanks to the development of a transgenic model expressing these two factors (Santoni-Rugiu et al., 1996). The team of Geller and collaborators proposed an *in vivo* mouse model of HCC induced by α1-antitrypsin deficiency (Geller et al., 1994). These animals expressed high levels of the Z mutant of human α1-antitrypsin in hepatocytes. The gene product cannot be efficiently transported outside cells into the serum

thus accumulating in hepatocytes and causing α1-antitrypsin deficiency. The carcinogenesis is due to the toxicity of the accumulated protein.

Chemically-induced models of hepatocarcinogenesis are obtained by exposing animals to carcinogenic compounds. Carcinogens roughly divide into genotoxic (or direct acting) compounds that act as cancer initiators that modify the cells' DNA and non-genotoxic compounds that act as promoting agents, with no direct interaction with DNA and displaying intricate mechanisms favouring carcinogenesis. Several carcinogens have been shown to induce liver tumours in mice, among which the more commonly used will be described here. *DEN (Diethylnitrosamine)* is the most extensively used genotoxic agent for the chemical induction of HCC, causing hepatocyte DNA damage (Ellinger-Ziegelbauer et al., 2009). Generally, liver tumours appear within a year but the younger mice are at the time of exposure, the faster the HCC occurs because of the high hepatocyte proliferation rates of juvenile animals (Anilkumar et al., 1995). Mouse DEN-induced HCC often present with activating mutations of the H-RAS proto-oncogene (Aydinlik et al., 2001; Peraino et al., 1984). *Carbon-tetra-chloride (CCl4)* has been used for over 60 years to induce free radical-induced liver injury in rodents evolving into liver tumours (Avasarala et al., 2006; Recknagel, 1967). The mechanism is related to free radical production, affecting the cell membrane integrity and disturbing cell energy processes and protein synthesis (Avasarala et al., 2006; Heindryckx et al., 2009). In this model, liver inflammatory responses have been described, probably due to activated Kupffer and stellate cells, cytokines and proinflammatory factors release and activation and recruitment of monocytes, neutrophils and lymphocytes. *Phenobarbital (PB)* is used in combination with DEN to induce HCC in two stages. After administration of a genotoxic agent such as DEN, phenobarbital can produce a 5-fold increase in HCC development (McGlynn et al., 2003).

Metabolic injury is another method frequently employed to induce liver cancer in mice. Administration of a choline deficient diet induces steatohepatitis followed by fibrosis and cirrhosis in mice and rats. Animals develop HCC in about 50 weeks. Choline is essential for hepatic beta-oxidation and the production of very low density lipoproteins (VLDL). Deficiency of choline leads to hepatic lipid accumulation and steatohepatitis, representing the pathology of human non-alcoholic steatohepatitis (NASH) (Kang et al., 2008). High Fat Diet (HFD) has also been used to promote HCC in mice, but it seems that this model presents a sex bias since males in overweight have a 4.52-fold increase in HCC risk (Chilakapati et al., 2005). HFD models were developed to mimic fatty liver disease characterised by accumulation of fat inclusions in

liver cells, plus tissue reorganisation leading to fibrotic remodelling. It seems that this is due to ROS accumulation driving liver damage and HCC and it is associated with low grade inflammatory response.

Patient derived xenografts (PDX) are obtained by engraftment of tumour tissue coming directly from patients into immunodeficient animals. This method allows the intra-tumour and inter-tumours heterogeneity barrier observed during the screening of new anticancer drugs and fundamental studies on the biology of the disease to be overcome. To obtain a transplantable model, immunodeficient animals can be used to avoid graft rejection. The most often used mouse strains are nude (*nu/nu*) athymic mice and SCID (*scid/scid*) mice with severe combined immunodeficient mice—that is, T-cell deficient and B + T-cell deficient (Ito et al., 2002; Morton and Houghton, 2007; Shultz et al., 2005). The models are established by the implantation of fragments of human tumours either under the skin (ectopic) or into the organ of tumour origin (orthotopic). The implants consist of small fragments of intact tumour tissue or rough tissue digestions. To reproduce the tumour microenvironment and organ tropism, an orthotopic model is better than the ectopic model but these former models are more technically challenging. Orthotopic implantation is better suited for studying metastases (Fu et al., 1992). For increased orthotopic engraftment efficiency, the initial implantation can be done subcutaneously and once grown, the tumour may then be digested and orthotopically transplanted into subsequent generations of mice. PDX models retain the principal characteristics of donor tumours, including histological patterns of differentiation, microscopic organisation and staining of marker, as well as molecular features such as gene expression and mutational status (Ding et al., 2010; Kresse et al., 2012). Studies have showed a high degree of correlation between clinical response to targeted and conventional chemotherapy in patients with cancer and the responses to the same agent in the PDX models generated from these patients (Fiebig et al., 1985; Houghton et al., 1982; Keysar et al., 2013; Rubio-Viqueira et al., 2006).

In basic research, PDX models are extremely useful to study cancer biology, the cellular processes involved in cancer cell initiation and proliferation including the involvement of cancer stem cells, as well as the metastatic process (Giuliano et al., 2015; Kreso et al., 2013; Lawson et al., 2015; Marusyk et al., 2014; Singh et al., 2004; Torphy et al., 2014; Wang et al., 2007; Williams et al., 2015). In preclinical cancer research PDX models are extremely useful for the identification of novel cancer markers, screening of potential new drugs and drug combinations, antibody testing and for evaluating the anticancer activity of microorganisms (Allen et al., 2013; Berghauser Pont et al., 2015; Chao et al., 2010; Deng et al., 2016; Goel et al.,

2016; Ham et al., 2016; Kurtova et al., 2015; Li et al., 2013; Martin et al., 2016; Prahallad et al., 2012; Siu et al., 2013; Vora et al., 2014; Wang et al., 2016b; Wei et al., 2016; Zhao and Subramanian, 2017).

Unfortunatly, hepatocellular tumours have very low engraftment efficiency in immunodeficient mice and only a few human HCC derived PDX models have been described (Cheung et al., 2016; Gu et al., 2015; Reiberger et al., 2015).

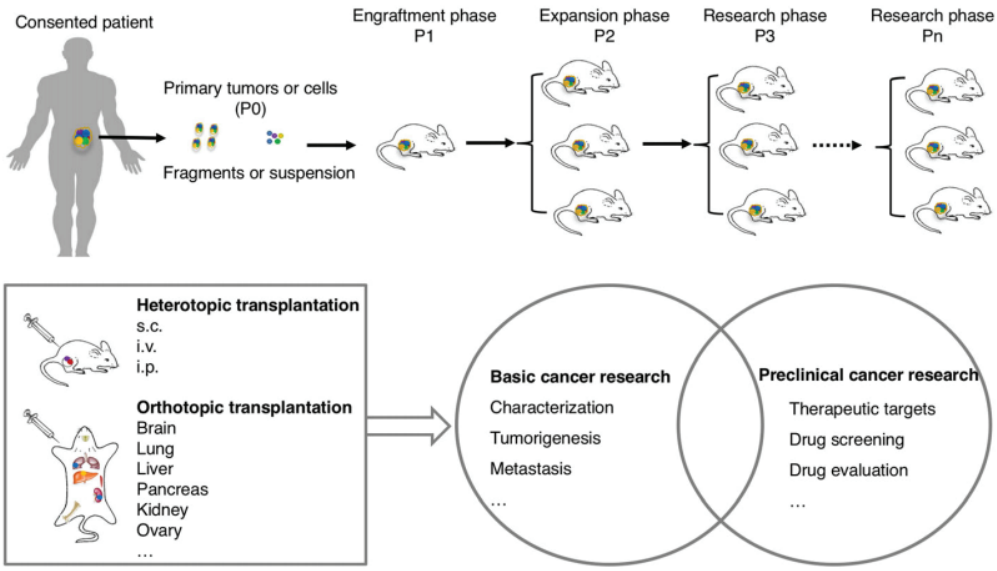

Figure 17 Overview of the methodology to establish PDX models and their uses in cancer research. Tumours from cancer patients (P0) are transplanted into immunodeficient mice (P1) for engraftment. Once grown, tumours are transplanted into secondary recipients (P2) for tumour expansion. The expanded tumours can then be cryopreserved or transplanted into P3 mice for experiments and model characterisation. Tumours can be transplanted in sites other than that the tumours are derived, called heterotopic transplantation or in the corresponding sites of the tumours which is called orthotopic transplantation. The successfully established PDX models are used both in basic and preclinical cancer research. **(Lai et al., 2017)**

Chimeric mice with humanised liver are obtained by partially decellularizing mouse liver and repopulating it with human hepatocytes. A 70% decellularisation of the liver is achieved in immunodeficient mice that overexpress the cytotoxic urokinase-type plasminogen activator (uPA) or alternatively, with a knock-out of the fumarylacetoacetate hydrolase (Fah) gene (Azuma et al., 2007; Dandri et al., 2001; Mercer et al., 2001). The injected hepatocytes commonly consist of differentiated hepatocytes obtained from resected livers or hepatocytes obtained by directed differentiation of induced pluripotent human stem cells. Decellularised murine liver provides the donor-derived hepatocytes a niche for engraftment and the

regenerative stimulus to promote proliferation of the donor cells in the mouse liver. The level of liver humanisation is defined by the level of human serum albumin. These models are particularly useful for the study of viro-induced HCC.

2.7. Hepatic cancer stem cells

Tumours are composed of anarchically proliferating cancer cells displaying high morphological and functional heterogeneity. Two hypotheses have been proposed to explain cancer cell origin and the intratumour heterogeneity **(Figure 18)**. According to the **stochastic theory**, all cells inside a tumour have the same tumourigenic potential, have evolved through hazardous oncogenic events, and have equal tumourigenic capacities. The **hierarchical theory** states that cells follow an established hierarchy depending on their potential to initiate and sustain tumour growth so that cells at the top of the hierarchy, called cancer stem cells (CSCs) or tumour initiating cells (TICs) are the most tumourigenic with stem features. Cells down the hierarchy are more differentiated and less aggressive. The hierarchical model explains the heterogeneity observed within many clonally derived tumours including liver cancer (Bonnet and Dick, 1997; Campbell and Polyak, 2007; Clarke et al., 2006; Nowell, 1976; Reya et al., 2001).

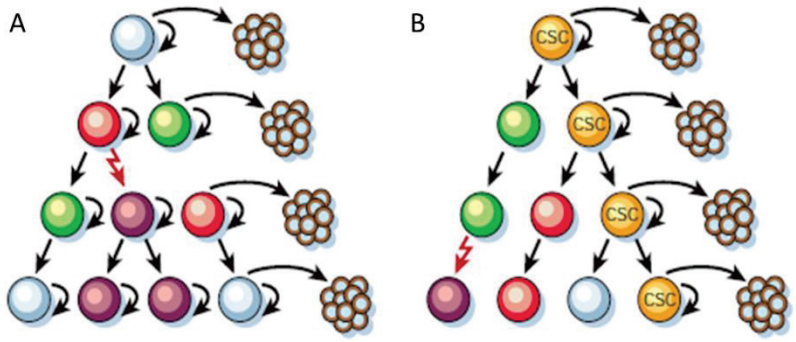

Figure 18. Stochastic and hierarchical theories in cancer. **A.** All cancer cells have the capacity to proliferate extensively and form new tumours. **B.** Only the cancer stem cell subset (CSC; yellow) has the ability to proliferate extensively and form new tumours. **(Reya et al., 2001)**

Similar to normal stem cells, CSCs detain two extraordinary features: self-renewal and generation of heterogeneous cancer cells lineages constituting the tumour. Contrary to cancer

bulk cells, a very small number of CSCs is sufficient to form xenografts in immunodeficient mice.

Cancer stem cells were first identified in hematological cancers and isolated thanks to surface markers. The first CSCs signature described was CD34+CD38- surface markers (Lapidot et al., 1994). In solid tumours, CSCs existence was confirmed a little later and were first isolated in 2003 from breast tumours thanks to a CD44+CD24- signature. Since, CSCs have been isolated from tumours originating from diverse organs.

At present, CSCs can be identified and isolated by surface markers and functional assays. In solid tumours they are positive for several markers such as CD133, EpCAM, CD44, CD90, CD24, ALDH1 enhanced activity (aldehyde dehydrogenase is a metabolic enzyme responsible for cell detoxification) and ABCB5. Also, dye exclusion assays allow the identification of a cell side population corresponding to CSCs (Hermann et al., 2007; Monzani et al., 2007; O'Brien et al., 2007; Singh et al., 2004). Indeed, CSCs possess very efficient efflux pumps that eliminate foreign substances. Functional assays allow the identification of the presence of CSCs in a cancer cell population. Unlike bulk cells, CSCs are able to develop in non-adherent conditions and in absence of nutriments, and after 3 to 15 days they form spheroids. Spheroids are thought to originate from a single cancer stem cell and to contain cancer progenitor cells at several stages of engagement towards cancer lineages. Another functional assay consists of determining the clonogenic potential of cells. This assay, first described by Barrandon and Green for normal skin stem cells, has been translated to CSCs later. It allows the identification of three types of single cell-derived clones when *in vitro* culturing a heterogeneous population of epithelial cells:

- **Holoclones** are formed of cells with the highest proliferative potential. These colonies are big, with a regular shape, almost circular and cells on the borders are small. Holoclones are generated from stem cells.
- **Meroclones** are intermediary clones between holoclones and paraclones. They have an irregular contour suggesting some extent of heterogeneity inside the colony. They are thought to contain cells with a regenerative *in vivo* potential in response to acute injury. They are generated from an early progenitor.
- **Paraclones** are formed of cells with a limited proliferation potential which stop growing after a few replication cycles (not more than 15 cell cycles). These colonies are generally the smallest, with an irregular shape, containing large and flattened cells. They are generated from a late progenitor.

In HCC, CSCs or T-ICs are thought to be responsible for initiation, progression and relapse, resistance to therapy and metastasis formation **(Figure 19)** (Ding and Wu, 2015).

As assessed by dye exclusion, CSCs possess efflux pumps, explaining their multidrug resistance. Another reason explaining their drug resistance is that cancer stem cells are quiescent cells that are dormant when the tumour niche is intact. Several drugs target proliferative cells therefore leaving CSCs untouched. Consequently, only bulk cells are eliminated upon treatment and CSCs are activated in response to tumour cell mass loss. CSCs can rapidly reconstitute the initial tumour leading to relapse post-treatment.

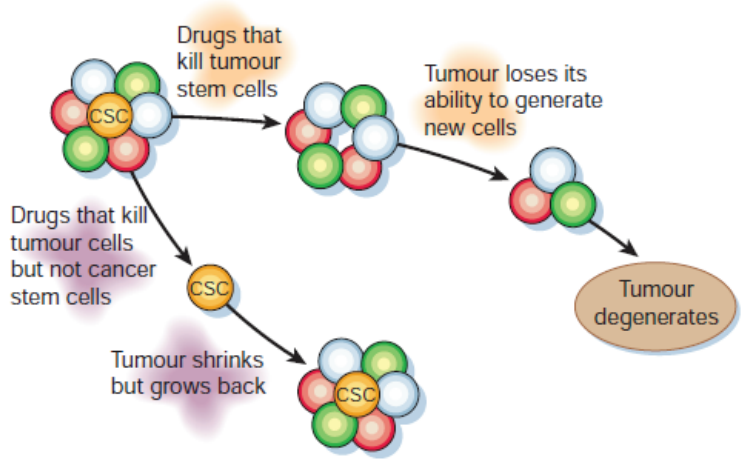

Figure 19. Cancer stem cells (in red) are resistant to conventional therapies and can regenerate the primary tumour. Only the use of drugs targeting CSCs (in orange) could result in the complete eradication of the tumour (Reya et al., 2001)

Numerous publications suggest that CSCs may be involved in liver cancer and participate to the aggressiveness of the disease. Chiba and collaborators first identified identified a small HCC CSCs population called the side population by dye exclusion using Hoechst 33342 and propidium iodide. CSCs markers previously identified in other types of tumour have also been shown to be specific to HCC CSCs, namely CD133, CD90, EpCAM, CD44, OV6 **(Figure 20)** (Ma et al., 2007; Yamashita et al., 2009; Yang et al., 2008b, 2008c; Yin et al., 2007; Zhu et al., 2010, 2010).

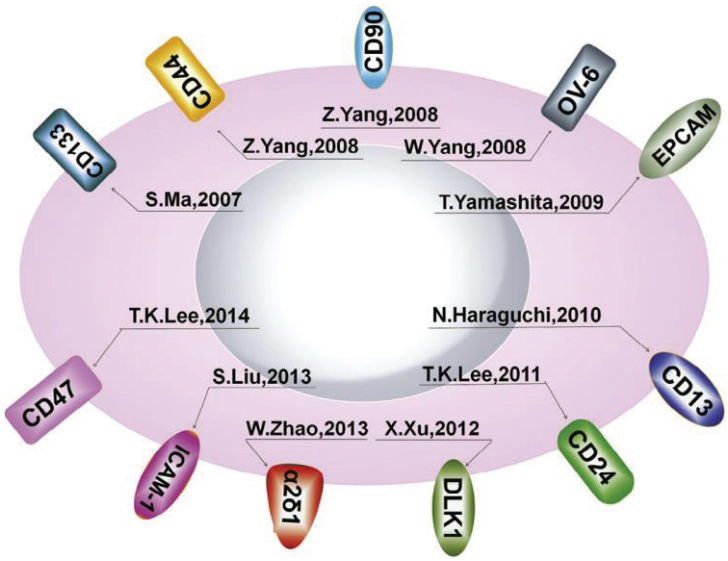

Figure 20. Liver CSC surface markers identified to date. (Cheng et al., 2016)

Until now the origin of these cells has not been elucidated **(Figure 21)**. They could hypothetically derive from stem, progenitor or differentiated hepatic cells. Several studies suggest that normal stem/progenitor cells accumulate transforming events which convert them into cancer stem cells able to generate tumours (Zhu et al., 2009). In a same manner, it has been shown that granulocyte macrophage progenitors can generate leukemic stem cells (Krivtsov et al., 2006).

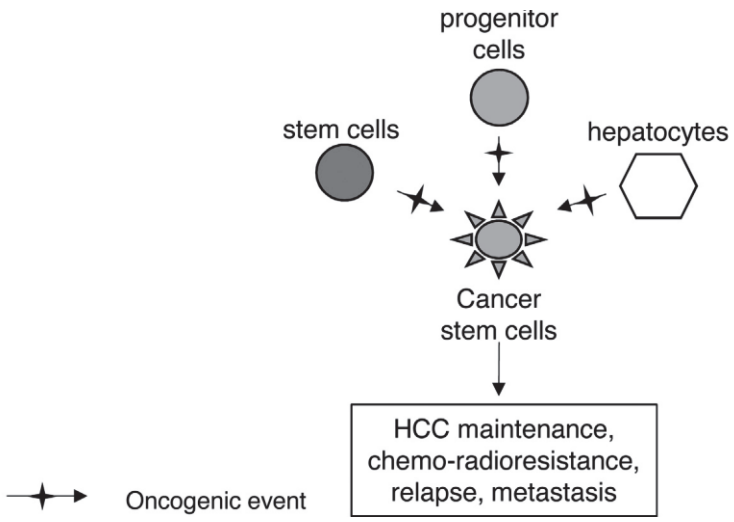

Figure 21. Liver CSCs origin. Oncogenic events in different hepatic cells can induce cancer stem cell phenotype and initiation of liver cancer. **(Anfuso et al., 2015)**

In HCC, the role played by liver progenitor cells (LPCs) during hepatocarcinogenesis is still under debate. It has been described that LPC proliferation is correlated to the severity of the disease and therefore, to the risk of HCC development during chronic liver disease and precancerous conditions such as chronic inflammation (Hsia et al., 1992, 1994; Lowes et al., 1999; Roskams and Desmet, 1998). Several mouse HCC models indicate that CSCs arise from LPC forming tumours with gene expression profiles resembling that of hepatoblasts (precursor of epithelial liver cells) (Becker et al., 1996; Dumble et al., 2002; Fang et al., 2004; Gordon et al., 2000; Knight et al., 2000, 2008; Yaswen et al., 1985). However, in DEN-induced HCC in mice, it is widely accepted that HCC induced by this carcinogen develops from hepatocytes (Scherer et al., 1972). Indeed, LPC proliferation is very rare in this model and does not explain the emergence of liver tumours. A large number of human HCC expresses LPC (CK19, OV6) or embryonic (AFP) markers and are formed of cancer cells with bipotent properties expressing both hepatocyte and biliary markers (albumin, CK7, CK19) (Durnez et al., 2006; Roskams, 2006). The presence of these markers is associated with poor prognosis and suggests a progenitor origin of HCC (Wu et al., 1999).

Pathways contributing to the emergence and maintenance of CSCs are shared by normal stem cells including Bmi-1, Wnt/ β -catenin, Notch and Sonic Hedgehog signalling (Chiba et al., 2007; Dontu et al., 2003; Kasper et al., 2006; Wong et al., 2008, 2008). Bmi-1 has been shown to regulate stem cell renewal in tissue (Iwama et al., 2004). Bmi-1 has been observed to be frequently overexpressed in primary HCC and ectopic expression of Bmi-1 in liver progenitor cells results in the development of poorly differentiated liver tumours *in vivo* (Chiba et al., 2007; Wang et al., 2008).

Wnt/β-catenin has been described to play a critical role on stem cell proliferation during an organ's development as well as during regeneration. Similar to Bmi-1, constitutive activation of the pathway enhances self renewal and promotes cancer initiation (Chiba et al., 2007).

The Notch pathway is important in the regulation of stem cells self-renewal and differentiation but plays a double role in cancer depending on the cell context (Reya et al., 2001). Activation of Notch seems to stop the growth of hepatocellular tumours, whereas cohort studies have shown that it is constitutively activated in this disease (Ning et al., 2009). Activation of the pathway participates to the maintenance of CSCs whereas its inhibition depletes this cell sub-population (Fan et al., 2010).

Recent publications show that Sonic Hedgehog pathway regulates the self-renewal ability of CSCs implicated in several types of cancer, such as breast cancer, glioma and multiple myeloma (Clement et al., 2007; Dierks et al., 2007; Liu et al., 2006a). Although the role of Sonic

HH pathway has not been extensively investigated in liver CSCs, this pathway has been reported to be activated in HCC (Sicklick et al., 2006).

2.8. HCC therapies

Patient's prognosis strongly depends upon the condition of his/her liver at the time of HCC diagnosis.

Staging. As in all patients with cancer, staging is crucial before deciding any treatment. Since more than 90% of HCC patients have an extensive underlying liver disease, careful staging must also be performed to avoid cancer treatment that damages the surrounding liver. In the last 50 years several systems have been proposed to stage liver disease with or without HCC. The Barcelona Clinic Liver Classification (BCLC) system established in 1999, with a few modifications is the most frequently used (Llovet et al., 1999b). This is due to the fact that, besides the tumour burden (size and number of nodules), the stage of liver cirrhosis, the liver function and the physical condition are also taken into consideration for the choice of treatment **(Figure 22)**. Some authors have proposed that the staging system can be improved by introducing tumour biomarkers, such as the level of α-fetoprotein in serum and pathological features like microvascular invasion and tumour differentiation (Forner et al., 2012; Roayaie et al., 2009).

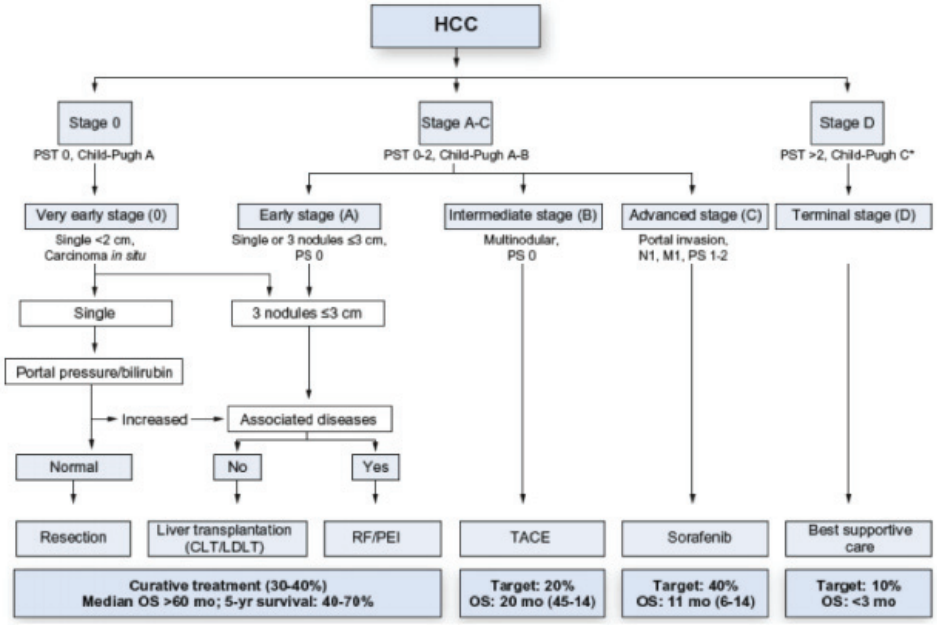

Figure 22. Barcelona-Clinic Liver Cancer (BCLC) staging classification and treatment schedule. (European Association for the Study of the Liver, 2012)

HCC is considered as a chemorefractory tumour. Moreover, underlying cirrhosis and impaired liver function can affect the schedule of administration and efficiency of chemotherapeutic agents. Response rates achieved with single agents and combination chemotherapies do not exceed 10%-20% in most studies, and an encouraging survival benefit has thus far not been shown.

Despite recent advances in therapeutic approaches for treating HCC, this type of cancer is still associated with a poor survival mainly due to late diagnosis, the 5-year overall survival remaining as low as 18% (Kulik and Chokechanachaisakul, 2015).

Patients with good liver functions (Child A or Child B) can benefit from curative treatments, descrbed below, whereas those with bad liver functions (strong cirrhosis, fibrosis steatohepatitis) can only benefit from systemic chemotherapy.

Targeted molecular therapies have significantly improved cancer treatment in general. The only drug that has shown significant benefit in advanced HCC patients is the multikinase inhibitor Sorafenib which prolongs patients overall survival with a median time of three months (SHARP trial) (Llovet et al., 2008). It inhibits BRaf et CRaF serine/threonine kinases, VEGFR (vascular endothelial growth factors receptors)-1/2/3 and PDGFR (platelet-derived growth factor receptors)-α/β. The improved patients survival in the Sorafenib group is mainly linked to tumour growth stabilisation, since patients in this group show an ORR (objective

response rate) of only 2%, compared to 1% in the control group (p=0.05). This year, following the RESORCE trial results, the FDA approved the multikinase inhibitor Regorafenib (STIVARGA, Bayer HealthCare Pharmaceuticals Inc.) as a second line treatment for patients progressing on Sorafenib **(Figure 23)** (Bruix et al., 2017).

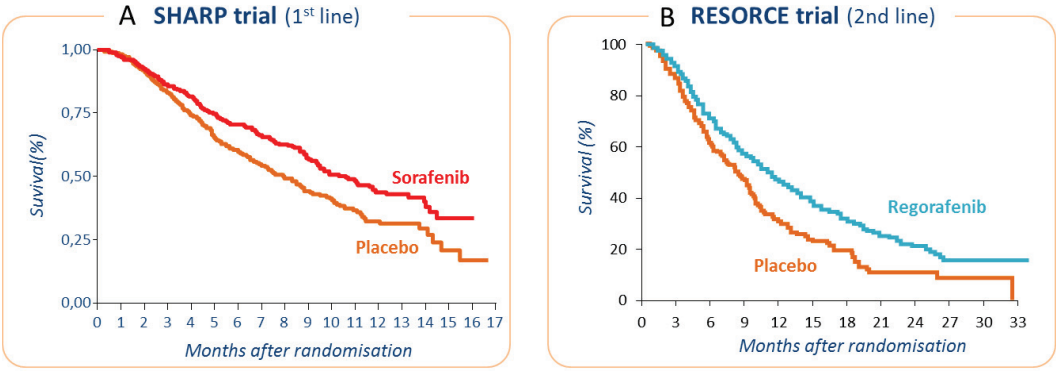

Figure 23. Targeted therapies in HCC treatment. Survival curves of patients enrolled in the SHARP trial for Sorafenib evaluation as a first line treatment (A) and in the RESORCE trial for Regorafenib evaluation a second line treatment (B). **(Llovet et al., 2008, Bruix et al., 2017)**

Contrary to what has been expected initially, clinical trials with other antiangiogenic tyrosine-kinase inhibitors (TKIs) failed to show an equivalent or superior antitumour response to Sorafenib (Llovet and Hernandez-Gea, 2014). Other molecules targeting other signalling pathways are currently under evaluation.

Liver transplantation is widely considered as the only real potentially curative approach that provides treatment of both HCC and the underlying liver cirrhosis. 70% of transplanted patients for HCC are alive after 5 years. Unfortunately, only a minority of patients can undergo liver transplantation even when it is indicated. The number of donors is largely insufficient to cope with the worldwide need and the shortage of organs makes waiting lists longer each day in every country. Many patients become unsuitable for transplantation or die while awaiting transplant. Patients with early or very early unresectable HCC and liver cirrhosis with good liver reserve function (Child Pugh A) (stage 0 or A according to the BCLC system) are excellent candidates for liver transplant. Another problem with liver transplant resides in HBV and HCV chronic infections. HCV infects several sanctuaries of the body and thus, transplanted patients treated with immunosuppressive drugs can develop infection relapse. Moreover, reactivation of HBV infection has been reported in patients upon treatment with these new anti-HCV drugs and the issue is still open to possible surprises (Takayama et al., 2016).

Tumour resection is the other surgical option for HCC treatment (Pang and Lam, 2015; Ramesh, 2014). Recurrence of HCC is quite common (70% to 100% within five years) and patients may develop liver failure after large resection (Llovet, 2005; Schwartz et al., 2007). Liver resection does not treat the underlying cirrhosis that is a pre-neoplastic lesion and this therapeutic option is too risky for patients with advanced HCC and/or liver disease (stage C according to the BCLC). Liver resection has some advantages over transplantation (organ saving, costs, expertise, *etc.*) and in addition leaves open the possibility of later transplantation, thus allowing many patients to gain time.

Tumour ablation performed using different techniques can be used in patients where surgery is not possible or too risky. Percutaneous ethanol injection (PEI) was the first to be used in patients with small HCC lesion(s) (< 3 cm diameter). Excellent results have been observed with a recurrence rate at 5 years similar to that resection. PEI consists in injecting ethanol inside the tumour mass to cause coagulative necrosis of all neoplastic nodules. PEI has been the most successful technique in treating small (less than 3 cm diameter) HCC nodules. It is easy, inexpensive, requires minimal equipment and expertise, and has been shown to prolong survival of these patients to the same extent as surgery. PEI can be used in patients with more than one nodule, usually no more than 3, and because it can easily be repeated on the already treated nodule, offers patients a simple and inexpensive treatment of their disease.

Transarterial embolization (TAE) and transarterial chemoembolization (TACE) are used to embolize the artery feeding the HCC and can be employed in patients where surgery is not an option. Necrosis of the tumour is rarely complete because tumour angiogenesis forms brunches of new small vessels that feed the cancer nodule. In addition, in many cases significant blood supply comes from portal blood and the liver cancer cells are ischemia resistant (Lv et al., 2015; Peng et al., 2006). This procedure is largely used for downstaging patients on the waiting list for liver transplantation because it leads to tumour shrinkage or growth arrest. In the last 10 years, the procedure has been improved thanks to radio-labelled microspheres or embolizing beads that carry anticancer agents such as doxorubicin or cisplatin.

III. The role of the p53 family member p73 in cancer

TP53 gene has been identified in 1979 and until 1997 was considered as an orphan gene. It was only in 1997 that two other paralogues genes, *TP63* and *TP73,* were identified and the notion of a p53 family was proposed (Kaghad et al., 1997; Schmale and Bamberger, 1997). These three genes have a strong sequence homology, suggesting they are derived from the same ancestral gene **(Figure 24)**. The most primitive organisms with paralogs of p53/63/73 family member genes are the single-cell choanoflagellates and the sea anemone. During evolution, the ancestral gene could have undergone successive duplications leading to *TP63* and *TP73,* and to *TP53*. The simultaneous presence of the three paralogs has only been observed in the evolutionary tree since bony fishes (Belyi et al., 2010).

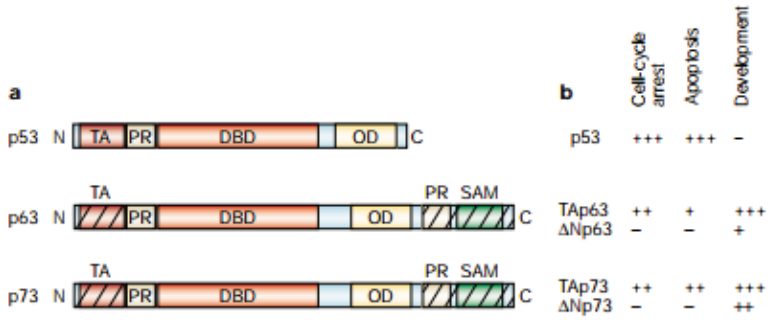

Figure 24. The p53 family. The overall domain structure is conserved between p53, p63 and p73. (Melino et al., 2002).

TP53 encodes for the tumour suppressor p53, also known as the 'guardian of the genome' because of its protecting role against genetic alterations and thus cancer initiation. It is ubiquitously expressed. The p53 protein acts as a transcription factor regulating genes involved in cell cycle arrest, apoptosis, DNA damage response, cell metabolism and several other mechanisms. Pathways associated to p53 are mainly activated in response to an oncogenic stress and the *TP53* gene is frequently inactivated in cancer.

TP63 and *TP73* expression is tissue specific and the encoded proteins play specific roles in response to stress and in the control of specific physiological functions in the nervous tissue and various epithelia.

3.1. TP73 gene

In humans, the *TP73* gene is 80kb long and is composed of 15 exons, sharing more than 60% of sequence homology with *TP53* in the DNA-binding domain (DBD). *TP73* gene is located in the short arm of chromosome 1 (1p36), a region frequently exposed to chromosomal rearrangement in neuroblastoma (Kaghad et al., 1997; Yang et al., 2000). It encodes for multiple transcript isoforms, the longest one containing 636 aminoacids. In relation of the protein structure, the exons 2 and 3 encode for the transactivation domain, exons 4 to 11 encode for the DNA binding domain and the last exons, 12 to 14 encode for the C-terminal domain. *TP73* has two promoters, called P1 and P2, one of which is internal (P2). This second promoter P2 is situated in the exon 3', positioned right after the exon 3 **(Figure 25**Error! eference source not found.**)**.

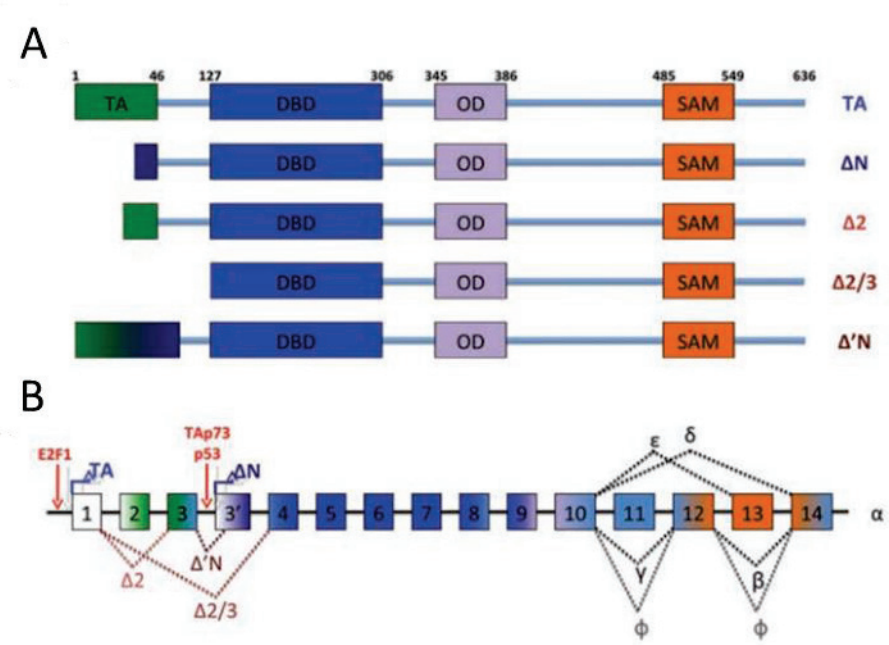

Figure 25. *TP73* gene. The different N-terminal spliced isoforms and protein domains positions are shown in **A**. The structure of the TP73 gene and transcripts is depicted in **B**. The *TP73* gene is composed of 14 exons plus a 15th one, called exon 3', inside the intron 3. Sites of alternative splicing are shown below the concerned exons. Note the binding of E2F on P1 promoter upstream exon 1 and the activation of ΔNp73 expression by binding of p53 or TAp73 on P2 promoter upstream exon3'. **(Rufini et al., 2011)**

TP73 expression is modulated through epigenetic mechanisms as well as promoter activation. *TP73* P1 promoter hypermethylation and consequently loss of gene expression has been

mainly described in haematological malignancies (Zawacka-Pankau et al., 2010). *TP73* P1 promoter contains at least three E2F-binding sites and E2F1-deficient cells have undetectable basal TAp73 expression at both protein and mRNA levels (Urist et al., 2004).

TP73 gene expression is regulated through the activation of both the conventional and internal promoters. The P1 promoter is activated by transcription factors such as E2F1 and c-myc (Irwin et al., 2000; Lissy et al., 2000; Ozaki and Nakagawara, 2005; Stiewe and Pützer, 2000; Zaika et al., 2001). Furthermore, MDM2, the main modulator of the p53 intracellular level, has been reported to synergistically cooperate with E2F1 in P1 transactivation (Kasim et al., 2014). The P2 promoter contains TAp73 and p53 responsive elements (Buhlmann and Pützer, 2008). This generates a negative feedback loop where TAp73 activates the transcription of the ΔNp73 isoform which in turn acts as a dominant negative of TAp73. Post-translational modifications of E2F1 modulate the activity of the P1 promoter. Phosphorylation by Chk1/2 and acetylation by histone acetyl-transferase PCAF (P300/CBP-associated factor) positively modify E2F1 activity while E2F1 deacetylation by NAD-dependent deacetylase sirtuin-1 leads to the inhibition of TAp73 transcription (Bisso et al., 2011). ZEB1 acts as a repressor on the transactivation function of E2F1 of the *TP73* P1 promoter. It binds within the regulatory region located in the first intron of *TP73* and attenuates the activity of E2F1 on the *TP73* promoter (Zawacka-Pankau et al., 2010). Hypermethylation within this particular region decreases ZEB affinity and shows increased expression of TAp73 isoforms (Rufini et al., 2011).

3.2. Protein Biochemistry

TP73 expression leads to the synthesis of several isoforms due to alternative promoter and alternative splicing. Alternative splicing has been described at the 5' terminus, affecting exons encoding for the N-terminal transactivation domain as well as the 3' end encoding for the C-terminal oligomerisation domain. Based on their cell functionality, p73 isoforms can be divided into two categories **(Figure 25)**:

- **full length variants (TAp73)**, synthesised from the entire *TP73* coding sequence. They have an intact fully functional transactivation domain.
- and **N-terminal truncated variants (ΔTAp73)** lacking the transactivation domain. Truncated isoforms originate from differential splicing events at the 5'-end of P1-

derived transcripts (ΔExon2p73, ΔExon2/3p73 and ΔN'p73 isoforms), as well as the activation of the internal promoter within the intron 3', giving rise to ΔNp73 isoform.

The ΔN'p73 isoform is obtained by activation of the P1 promoter but the exon 3'sequence is aberrantly integrated into the mRNA. This inclusion generates a premature 'stop' codon in the open reading frame and the translation begins at the start codon corresponding to the second promoter leading to the synthesis of a protein that is indistinguishable from the ΔNp73 protein generated from the alternative promoter. Therefore, ΔNp73 and ΔN'p73 transcripts encode the same protein and can only be distinguished at the mRNA and not at the protein level.

The organization of the TAp73 functional domains is similar to that of p53: an N-terminal transactivation domain (TA), a central DNA binding domain (DBD) and a C-terminal domain. The DNA binding domain shows the highest degree of homology between p53 and p73 suggesting that they can bind to the same DNA sequence and regulate the same gene promoters. The transactivation domain is responsible for initiating target gene transcription and can bind proteins such as transcriptional adaptors or coactivators. The C-terminal domain contains a C-terminal oligomerisation domain (OD), a sterile alpha motif (SAM), not found on p53, and a transactivation-inhibitory domain (TID).

Generally, truncated isoforms ΔTAp73 do not have a transactivation activity, the exception being the ΔNp73 isoform. In this isoform the N-terminal region is composed of 14 aminoacids, encoded from the 3' exon, upstream of the DNA-binding domain. These 14 aminoacids are specific to ΔNp73 and have been suggested to participate to the gain of function of this isoform (discussed below).

Alternative splicing at the 5' end of *TP73* RNA leads to isoforms with or without a transactivation activity. Alternative splicing at the 3' end generates several C-terminal isoforms, called α, β, γ, δ, ε and ς but little is known about their different activities (De Laurenzi et al., 1999; Kaghad et al., 1997; Laurenzi et al., 1998). C-terminal isoforms with the SAM domain are expected to interact with proteins during the embryonic development, isoforms devoid of the TID to exhibit a better transactivating activity, if they possess the N-terminal TA domain.

In order to exert their activity, p73 proteins form dimers thanks to the C-terminal domain. The dimers bind together to form tetramers. Since they share the same OD, full-length isoforms can bind and tetramerise with the truncated isoforms.

Nuclear localisation is tightly regulated because of the ability of p73 to act as a transcription factor. The nuclear localization signal (NLS) and the nuclear export signal (NES) sequences are present within the p73 C-terminal region.

Post-translational modifications. Numerous post-translational modifications of p73 protein have been described **(Figure 26).** In normal conditions during the cell cycle, TAp73 transcriptional activity is abrogated due to Thr86 phosphorylation by the cyclin A-CDK1/2, cyclin B-CDK1/2 and cyclin E–CDK2 complexes (Gaiddon et al., 2003). Following DNA damage, the cell cycle checkpoint kinases Chk1 and Chk2 phosphorylate TAp73 at Ser-47 which converts it into an active form (Urist et al., 2004). In damaged cells, TAp73 is also phosphorylated at the PxxP motif located in the C-terminus of the OD (Ben-Yehoyada et al., 2003). c-Abl phosphorylates and stabilizes ΔTAp73 isoforms, probably favouring their antiapoptotic roles. Following phosphorylation, TAp73 interacts with PIN1 which changes p73 conformation allowing p300 acetylation (Mantovani et al., 2004). Acetylation of TAp73 at Lys-321, Lys- 327, and Lys-331 is required for full transcriptional activity and is a key event in the decision of p73 to promote apoptosis instead of cell cycle arrest since nonacetylated p73 fails to selectively transactivate proapoptotic target genes (Ozaki et al., 2005). Yes-associated protein (YAP) has also been shown to mediate p73 acetylation and trigger p73-dependent apoptosis in response to DNA damage. However, the impact of acetylation in ΔTAp73 isoforms is complex and the results are not as clear as those for TAp73 (Marabese et al., 2007).

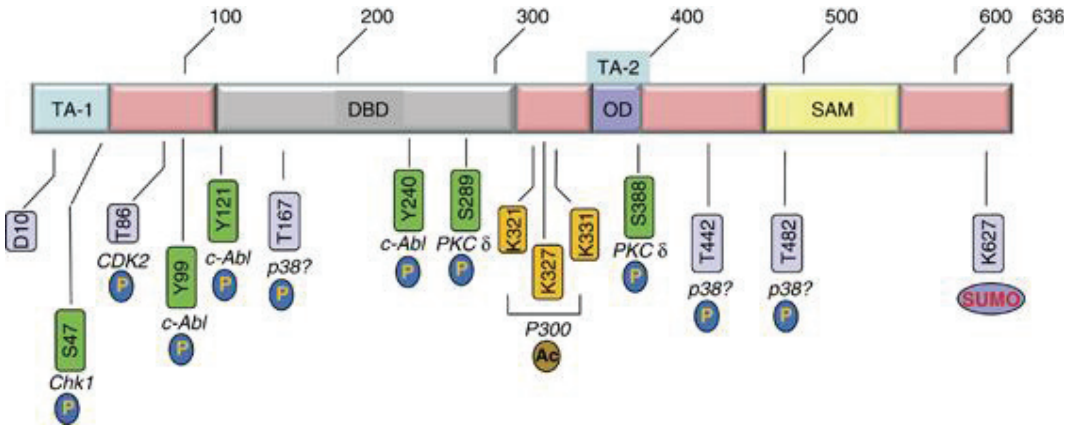

Figure 26. Post translational modifications of p73. (Conforti et al., 2012)

Degradation. Under normal cellular conditions TAp73 undergoes proteasomal degradation by binding with the E3 ubiquitin ligase ITCH. In case of DNA damage, ITCH expression is down-

regulated and non-degraded TAp73 accumulates inside the cell (Rossi et al., 2005). N4BP1 and YAP1, have the same ITCH-binding motif as TAp73 and compete for the occupation of the binding site, increasing the amount of non-ubiquitinated TAp73. Sumoylation of p73 at the C-terminus SAM domain increases the proteasomal degradation efficiency. Sumoylation at Lys-627 by small ubiquitin-like modifier (SUMO) proteins occurs specifically in p73α, but not in p73β, due to the lack of the sumoylation domain and leads to the inability of p73α to transactivate *BAX* and *WAF1* gene promoters.

Contrary to the p53-MDM2 interactions that leads to ubiquitination and proteolytic degradation of both proteins, MDM2-p73 interactions stabilize p73 (Conforti et al., 2012). However, MDM2 is transcriptionally activated by p73 and in turn MDM2 competes with p300/CBP for p73 binding. Thus, overexpression of MDM2 results in the loss of p73 transcriptional activity, generating a negative feedback loop. . The U-box-type E3/E4 ubiquitin ligase UFD2a promotes the ubiquitination-independent proteasomal degradation of p73α, but not of p73β, by interacting with the SAM domain. NQO1 is another regulator of TAp73 ubiquitination-independent degradation. It acts as a gatekeeper of the 20S proteasome and following irradiation, it binds TAp73 in an NADH-dependent manner and protects it from 20S proteasomal degradation (Asher et al., 2005). Another protein that interacts directly with TAp73 protein and stabilises it is the histone deacetylase 1 (HDAC1). After DNA damage, HDAC1 triggers the interaction between Hsp90 and TAp73 and further stabilisation of the protein. Hyperacetylation of Hsp90 disrupts the complex formed with TAp73 and free TAp73 is subsequently degraded (Zhang et al., 2013a).

3.3. p73 functions in cancer

In addition to sharing several similarities with p53, p73 also exhibits specific functions not carried out by other p53 family members. Indeed, several studies have shown that p73 plays a role both in cancer and development **(Figure 27, 28)**. In cancer, *TP73* acts as a tumour suppressor, by sharing several activities with p53, in particular by inducing cell cycle arrest and cell death in response to cellular stress. However, there is accumulating evidence that p73 does not act as a Knudson-type tumour suppressor, *ie* a gene inactivated during tumourigenesis due to genetic alterations in both alleles. In contrast to *TP53* which is one of the most frequently mutated genes in many tumour types, *TP73* is rarely mutated in cancers with such a profile being found in hepatocellular carcinoma. Instead, in many cancers, *TP73*

has been described to be over-expressed compared to the surrounding tissue and be a poor prognosis factor.

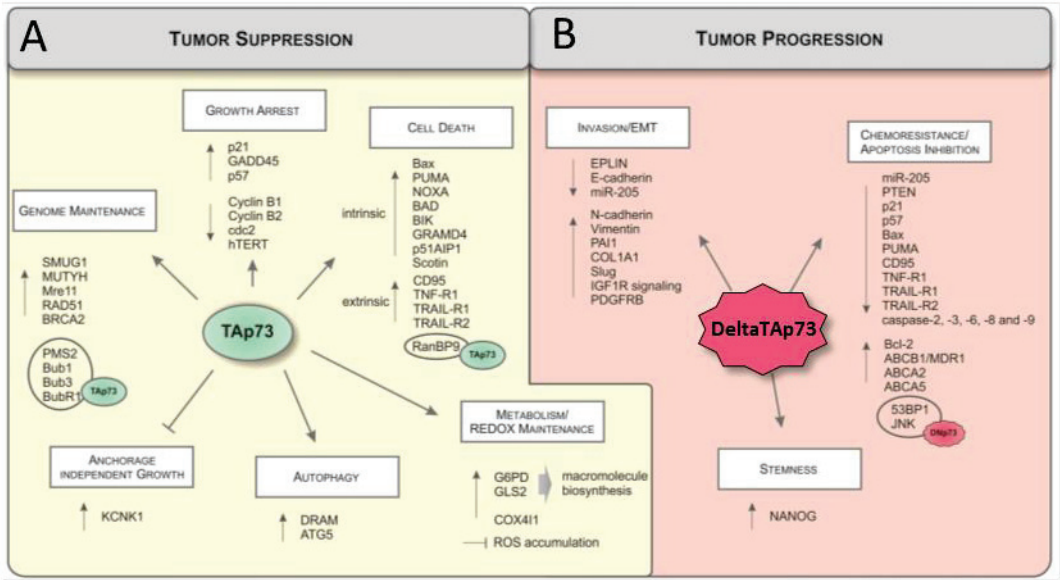

Figure 27. Cellular processes regulated by TA and ΔNp73 isoforms determining cancer outcome. **A.** Upon cellular stress, TAp73 expression and activity increases to regulate biological processes suppressing tumour growth and development. **B.** Amino-terminal truncated ΔTAp73 variants drive tumour progression and confer chemoresistance, stemness and invasiveness through inhibition, de-repression or activation of target genes and EMT activation. **(Engelmann et al., 2015)**

Unlike p53, *tp73* knock-out mice are not particularly prone to spontaneously develop cancer **(Figure 28)** (Yang et al., 2000). On the other hand, $tp73^{+/-}$ mice develop lung adenocarcinomas and thymic lymphomas, whereas $tp53^{+/-}tp73^{+/-}$ mice develop lung adenocarcinomas, acinar pancreatic carcinomas and HCC. Mice specifically lacking the TAp73 isoforms show an intermediate phenotype between p53-/- and p73-/- with development of spontaneous or carcinogenic-induced tumours, infertility, aging and hippocampal dysgenesis. TAp73 knockout mice show enhanced genomic instability and high incidence of spontaneous tumours suggesting its key role in cell-cycle arrest and genomic maintenance (Tomasini et al., 2008). These animals specifically lack the TAp73 isoform but continue to express the ΔTAp73 isoforms therefore provoking an imbalance in the TAp73 and ΔTAp73 ratio. ΔNp73 knockout mice show some signs of neurodegeneration. In addition, cells from these mice are sensitized to DNA damaging agents and show elevated p53-dependent apoptosis (Wilhelm et al., 2010). Finally,

ΔNp73 transgenic mice under the control of Albumin promoter display aberrant cell growth of hepatocytes and develop hepatic carcinomas (Tannapfel et al., 2008).

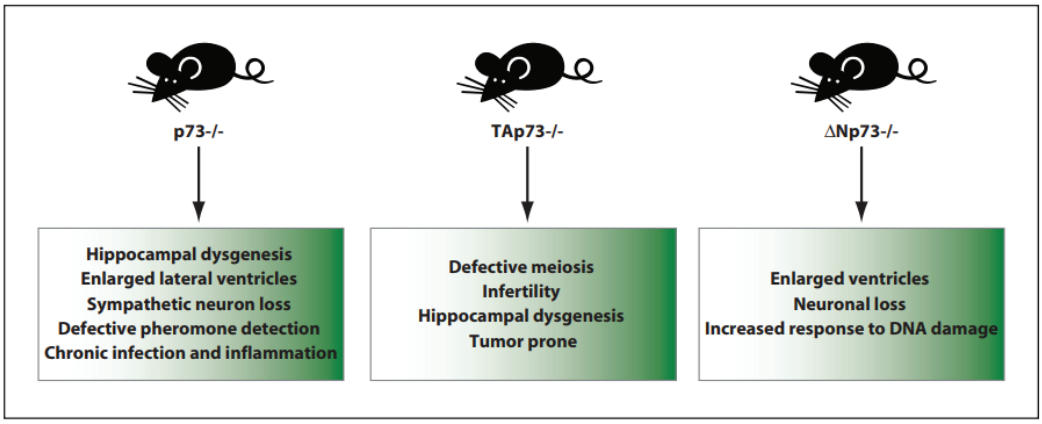

Figure 28. p73 mouse models. The tp73 knockout mouse shows severe developmental defects. TAp73 and ΔNp73 knockout mice show less severe developmental phenotype, but, importantly, depletion of TAp73 predisposes the animal to spontaneous tumourigenesis. **(Rufini et al., 2011)**

3.3.1 Functions of TAp73 isoforms in cancer

TAp73 isoforms act as transcription factors and bind DNA specific sequences *via* their DNA-binding domain. Several TAp73 responsive elements and thus target genes are common with p53. For example, TAp73 regulates genes involved in the response to oncogenic stress, partially compensating for a lack of p53 function in situations where it is inactivated. This is extremely important since *TP53* has been described to be mutated in more than 50% of tumours. But TAp73 can also transactivate its own target genes, especially during development and differentiation (Marqués-García et al., 2009).

The oncosuppressive properties of TAp73 are mediated through the inhibition of cell cycle progression, maintenance of genome stability and promotion of cell death **(Figure 27)**. It contributes therefore to tumour surveillance, cytotoxicity and elimination of genetically altered cells in response to DNA-damaging agents. TAp73 can induce these effects by activating genes classified as p53-target genes, as well as in a p53-independent manner.

Growth arrest. By transactivation of the p53 targets genes *p21 WAF1* and *GADD45*, TAp73 induces cell cycle arrest in G1 and G2/M (Lee and La Thangue, 1999; Strano et al., 2005). Secondly, TAp73 indirectly down-regulates human telomerase reverse transcriptase (*hTERT*). TAp73 forms a complex with Sp1 and prevents Sp1 from binding and activating *hTERT*

promoter (Beitzinger et al., 2006; Racek et al., 2005). TAp73 is essential to control mitotic arrest by interacting with the Spindle Assembly Checkpoint key components Bub1, Bub3 and BubR1 (Tomasini et al., 2009). TAp73 is phosphorylated in a cell-dependent manner and regulates p57 *Kip2* transcription to coordinate mitotic exit (Merlo et al., 2005). TAp73 induces mitotic cell death *via* direct BIM transactivation and suppresses polyploidy and aneuploidy independently of p53 (Talos et al., 2007; Toh et al., 2010).

Genome maintenance. TAp73 regulates the activity of some mismatch repair proteins therefore participating to correcting replication errors. TAp73 transactivates base excision repair genes such as the glycosylases *SMUG1* and *MUTYH* (Zaika et al., 2011). In the absence of TAp73, DNA damage levels increase. In case of double strand breaks it has been shown in several mouse models that TAp73 is required for Mre11, RAD51 and BRCA2 upregulation (Lin et al., 2009).

Cell death. Upon genotoxic or oncogenic stress, TAp73 accumulates and triggers cell death through several pathways and mechanisms. For example, cis-Platin treatment of cells can lead to physical interaction between TAp73 and the mismatch repair protein PMS2, an interaction required for TAp73-dependent apoptosis of damaged cells. Also, YAP1 is the key transcriptional co-activator of the TAp73-dependent transcription of proapoptotic genes in the presence of chemotherapeutic agents (Levy et al., 2007; Strano et al., 2005). In damaged cells, ATM leads to c-Abl-dependent phosphorylation of TAp73 and YAP1, formation of a TAp73-YAP1 complex and finally recruitment at DNA-response elements (Agami et al., 1999; Baskaran et al., 1997; Levy et al., 2008; Shafman et al., 1997; Yoshida et al., 2005).

It directly induces mitochondrial death through several mechanisms:

- By activating p53 target genes such as BCL-2 family members *BAX*, *PUMA*, *NOXA*, *BAD*, *BIK* and the mitochondrial membrane protein *p53AIP1* (Pietsch et al., 2008). PUMA triggers Bax mitochondrial translocation and release of cytochrome c, therefore activating the intrinsic caspase cascade leading to mitochondrial-mediated apoptosis (Melino et al., 2004). TAp73 also regulates several activators and inhibitors of apoptosis, such as the JNK apoptotic signalling pathway *via* the upregulation of GADD45a (Baxter, 2014; Broadhead et al., 2009; Díaz et al., 2008; Harms and Chen, 2005; Ho et al., 2007; Sasaki et al., 2005; Zhang et al., 2012a).

- Secondly, p73 elicits p53-independent mitochondrial-mediated apoptosis through direct transcriptional activation of *GRAMD4* (also known as Death Inducing Protein) (John et al., 2011). GRAMD4 translocates to the mitochondria, physically interacts with Bcl-2, promotes

Bax mitochondrial relocalisation and oligomerization and is highly efficient in inducing mitochondrial membrane permeabilization with release of cytochrome c and Smac.
As described above, TAp73 is able to induce the expression of factors directly involved in apoptosis execution.

- p73 seems to play a structural role in mitochondria-induced death, independent of its transactivation function, consistent with several arguments on those of p53 at the mitochondria (Mihara et al., 2003). The full-length protein TAp73 and some of its products, cleaved by caspases in response to DNA-damaging agents and death-receptor activation, were found localised near the mitochondria suggesting that it might facilitate the progression of apoptosis (Sayan et al., 2008).

The ability to stimulate expression of the death receptors CD95, tumour necrosis factor (TNF)-R1, TRAILR1 and TRAIL-R2 as well as the caspases-3, -6 and -8 suggests that TAp73 is also involved in the **extrinsic apoptosis pathway** (Melino et al., 2002; Müller et al., 2005). Induction of p73-dependent programmed cell death following DNA damage also involves endoplasmic reticulum stress and upregulation of scotin, a putative transmembrane protein able to colocalize with endoplasmic reticulum heat-shock proteins, such as GRP94 (Terrinoni et al., 2004). It was shown that NIS/SLC5A5, a transmembrane glycoprotein that mediates active iodide uptake into thyroid follicular cells, is stimulated after doxorubicin treatment of liver cancer cells in a TAp73-dependent manner (Guerrieri et al., 2013). Upregulation of NIS contributes to DNA-damage-induced apoptosis by yet undetermined mechanisms.
- Finally, several studies have described the role of TAp73 in autophagy-induced cell death. TAp73 induces the transcription of several actors involved in autophagy initiation, such as the damage-regulated autophagy modulator (DRAM), as well as proteins involved in the autophagy process like ATG5, required for the formation of autophagosomes (He et al., 2013).

Redox and metabolism. TAp73 modulates mitochondrial respiration by directly transactivating COX4I1, an essential component of the mitochondrial complex IV, and thereby prevents ROS accumulation (Rufini et al., 2012). Ablation of TAp73 increases oxidative stress that could drive oncogenic mutations in addition to favour genomic instability (Tomasini et al., 2008). TAp73 provides a fail-safe mechanism by inducing ATM (ataxia telangiectasia mutated) - triggered apoptosis in response to persistent accumulation of ROS (Dixit et al., 2014). Cancer cells adapt their metabolism in order to promote rapid cell proliferation and favour cytosolic aerobic glycolysis and lactate fermentation rather than mitochondrial oxidative phosphorylation (Blum and Kloog, 2014). In TAp73 knockout cells, mitochondrial respiration and ROS homeostasis are also affected, with reduced cellular ATP levels, suggesting that TAp73 deletion leads to a

similar switch in energy metabolism (Rufini et al., 2012). TAp73 promotes GLS2 transcription and thus drives serine biosynthesis, a precursor of other amino acids, glutathione, lipids and nucleotides essential for cell survival (Amelio et al., 2014). Importantly, TAp73 ablation interferes with cell proliferation, indicating that TAp73 activity is essential for cancer cells to cope with metabolic/ oxidative stress. These results appear to be in disagreement with the tumour-suppressor role of TAp73, but one can hypothesize that p73, similarly to p53, helps normal and hence cancer cells to face serine starvation, in order to preserve cellular anti-oxidant capacity, in agreement with their role in genomic and cell integrity.

3.3.2 Functions of N-truncated variants in cancer

Truncated isoforms act as dominant negatives of full length TAp73 isoforms and p53. They exert this function by two different structural mechanisms **(Figure 29)** (Bailey et al., 2011; Ishimoto et al., 2002; Rocco et al., 2006; Stiewe et al., 2002; Zaika et al., 2002) :

- Truncated isoforms can form heterotetramers with the full length form because they share the same oligomerisation domain. ΔTAp73-TAp73 heterotetramers do not retain the transactivation activity because they have not a complete transactivation domain. Therefore, ΔTAp73 traps TAp73 isoforms in non-functional complexes.
- Homo- and heterotetramers with truncated isoforms (ΔTAp73-ΔTAp73 and TAp73-ΔTAp73) have a functional DNA-binding domain and compete with the fully functional TAp73 homotetramers to bind DNA-specific sequences.

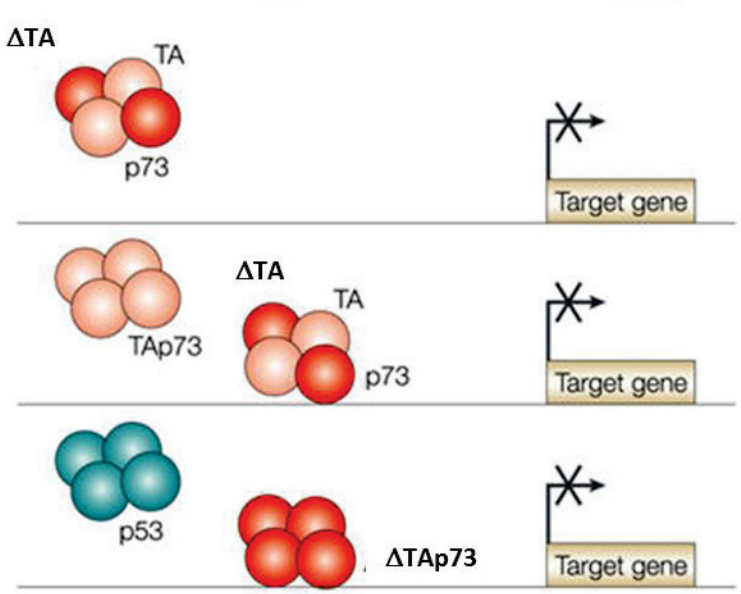

Figure 29. ΔTAp73 isoforms act as dominant negatives due to the sequestration of TAp73 (top), the formation of non-functional TAp73– ΔTAp73 heterotetramers (middle) or the competition with TAp73 homotetramers or p53 for binding of the same p53 DNA responsive elements (middle and bottom). **(Melino et al., 2002)**

Since p73 and p53 have structurally distinct oligomerization domains, they do not form heterotetramers (Joerger et al., 2009). Therefore, ΔTAp73 only inhibits p53 transactivation activity by competition for promoter binding and not by direct protein–protein interaction.

ΔNp73 isoform has also been described as possessing gain of function properties, independent of its dominant negative effect on p53.

The oncogenic activity of the ΔTAp73 isoform has been demonstrated by the classical *in vitro* experiment of oncogenic cooperation. Indeed, over-expression of ΔEx2/3p73 or ΔNp73 in fibroblasts led to malignant cell transformation and tumourigenicity in nude mice in cooperation with the RAS, MYC or E1A oncogenes (Petrenko et al., 2003; Stiewe et al., 2002). Wild-type p53 is likely a major target of ΔNp73 inhibition in primary fibroblasts, since deletion of TP53 or its requisite upstream activator ARF abrogates the growth-promoting effect of ΔNp73. Furthermore it has been described that ΔTAp73 can also act independently of any p53/TAp73 antagonism. By triggering hyperphosphorylation of pRB, ΔNp73 blocks the tumour-suppressor function of this protein. This leads to the activation of cyclin E-cyclin-dependent kinase 2 (Cdk2) and cyclin D-Cdk4/6 kinases and consequently to the enhanced E2F release, together with the downregulation of the cell cycle inhibitors p21 and p57 (Cam et al., 2006; Stiewe et al., 2003; Tannapfel et al., 2008).

Apart from contributing to initiating carcinogenesis through inhibition of classical tumour-suppressor pathways, ΔTAp73 isoforms interfere with several other pathways, thus favouring the aggressive behaviour of several tumour types. Indeed, in neuroblastoma patients, ΔNp73 is a strong independent predictor of poor prognosis. Other reports highlighted that in neuroblastoma, prostate, and cervical cancers, increased level of ΔNp73, without a concomitant increase of TAp73, is a significant risk factor for reduced survival and is associated with resistance to radiotherapy (Buhlmann and Pützer, 2008).

Chemoresistance. In many cancers, ΔTAp73 over-expression in tumours is associated with cell death resistance. In cervical squamous cell carcinomas, TAp73 and ΔNp73 are inverse predictors of sensitivity to therapy (Liu et al., 2004, 2006b). In patient with ovarian cancers and HCC, the presence of ΔTAp73 isoforms predict failure to platinum-based chemotherapy in p53-mutant tumours, as well as shorter survival (Concin et al., 2005; Müller et al., 2005). One of the possible explanations is that ΔTAp73 blocks the transactivation activity on TAp73 and therefore suppresses death-receptor signalling and mitochondrial-mediated apoptosis, making tumours resistant to DNA damaging agents (Schuster et al., 2010; Simões-Wüst et al., 2005). ΔNp73 also contributes to multidrug resistance, by counteracting the inhibitory effect of p53 on ABCB1/MDR1 expression, through its dominant negative effect (Vilgelm et al., 2008). Truncated isoforms indirectly lead to ATP-binding cassette (ABC) transporter activation, by the following mechanism: ΔEx2/3p73 suppresses TAp73-mediated activation of miR-205 in melanoma cells treated with cisplatin. miR-205 is known to suppress ABCA2, ABCA5 and Bcl-2 but, since the suppression is removed, the presence of efflux transporters at the cell membrane generates anti-cancer drug resistance (Alla et al., 2012; Vera et al., 2013). ΔNp73 can also contribute to the evasion from chemotherapy independently of its dominant negative effect. ΔNp73 interacts with the sensor protein 53BP1 at the site of DNA-damage, inhibits signal transduction and prevents ATM activation and consequently p53 stabilization through phosphorylation. Moreover, ΔNp73 directly protects cells from apoptosis by interaction with JNK and down-regulation of the tumour-suppressor PTEN (Lee et al., 2004a; Vella et al., 2009). In agreement with these activities, it has been observed that ΔNp73 knock out cells are sensitive to genotoxic drugs and undergo apoptosis in response to DNA-damage (Wilhelm et al., 2010).

Epithelial-to-mesenchymal transition (EMT), cell invasion and stemness.

EMT is a highly conserved process, essential for organ development and the spreading of cancer cells. The phenotypic changes accompanying EMT include loss of cell–cell junctions, loss of apico-basal polarity, acquisition of migratory and invasive properties, as well as extracellular matrix degradation. EMT hallmarks include E-cadherin loss and up-regulation of N-cadherin, vimentin and/or fibronectin.

Recent studies suggest that ΔTAp73 isoforms enhance the tumourigenic activity of cancer cells beyond their capacity to transform cells. Contrary to normal cells, ΔNp73 ectopic expression in tumour cells does not enhance the proliferation rate suggesting alternative mechanisms for ΔTAp73-mediated invasiveness. ΔNp73 is aberrantly over-expressed in advanced stages of cancer, like in metastases of skin cancer and has been suggested to regulate EMT (Tuve et al., 2004). Specific depletion of endogenous ΔNp73 in highly metastatic melanoma cell lines abolishes the aggressive cell phenotype. On the contrary, tumour xenografts over-expressing this variant possess significantly greater capacity of invasion of the surrounding tissue and higher efficiency of metastatic lesions formation (Steder et al., 2013).

ΔNp73 leads to drastic reorganisation of the cell cytoskeleton, loss of E-cadherin and up-regulation of N-cadherin, as well as of vimentin. ΔNp73 triggers up-regulation of SNAI2 (Slug), leading to transcriptional silencing of E-cadherin. ΔNp73 interferes with TAp73-dependent transcription of the tumour-suppressor LIMA1/EPLIN. EPLIN plays an important role in maintaining cell morphology and tissue integrity, by stabilisation of the actin stress fibres and focal adhesion plaques. ΔNp73 over-expression causes EPLIN depletion at the invasive front of primary melanoma cells, which will break through the basal membrane. This leads to activation of the IGF1R-AKT/STAT3 signalling, increase of Slug transcription and attenuation of E-cadherin expression (Steder et al., 2013). Studies in colon cancer show that TAp73 represses IGF1R expression suggesting a fine tuned balance between the p73 isoforms in the regulation of IGF1R pathway (Nahor et al., 2005). In highly malignant cancer cells, IGF1R signalling has been associated with development of resistance to BRAF inhibitors, suggesting that EMT and therapy resistance are tightly linked (Villanueva et al., 2010).

ΔNp73 seems to deregulate the apico-basal polarisation of mammary epithelial cells that are capable of forming three-dimensional acini *in vitro*. When knocking down TAp73 and leaving ΔTAp73 expression unaltered, the structure of the acini is altered due to loss of apico-basal polarity accompanied by E-cadherin ablation, nuclear accumulation of β-catenin and increased expression of laminin V, and of the EMT factors Snail, Slug and Twist (Zhang et al., 2012b). ΔNp73 cooperates with TGF-β to increase the metastatic potential of cancer cells. In the

cytosol, ΔNp73 binds and forms protein complexes with Smad3/4. Following TGF-β stimulation, Smad-ΔNp73 complexes translocate into the nucleus, bind on Smad Binding Elements and enhance the transactivation of TGF-β signalling targets.

3.3.3 ΔTAp73 role in stem cells

As for ΔNp63, accumulating data suggest that ΔTAp73 isoforms play a role in the maintenance of the stem cell pool in several tissues and could also favour the emergence of cancer stem cells. In view of the implication of ΔTAp73 in EMT, a biological process that can appear during the acquisition of cancer stem cell-like phenotypes, several lines of evidence support the implication of DeltaTAp73 forms in cell stemness **(Figure 30)** (Thiery et al., 2009).

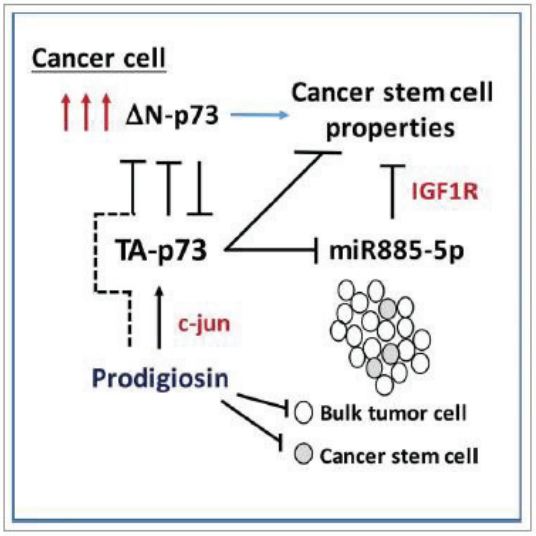

Figure 30 Combined mechanism(s) whereby the ΔNp73 variant increases cancer stem cell function. The dashed line connecting c-jun to inhibition of ΔNp73 reflects the speculative nature of this particular regulation. **(Basu and Murphy, 2016)**

Nanog is a transcription factor involved in cell immaturity and regulating pluripotency in mammalian cells. It is expressed at high levels in embryonic stem cells. ΔNp73 directly stimulates the expression of NANOG and participates to the generation of induced pluripotent cells by reprogramming human fibroblast (Lin et al., 2012). Induced pluripotent stem cells by ectopic expression of ΔNp73 express higher levels of embryonic factors c-Myc, KLF4, OCT4 and *in-vivo* generate less differentiated teratomas. In Acute Myeloid Leukemia, our team showed

that ΔNp73 transactivates NANOG expression, is preferentially overexpressed in very immature leukemic cells and is associated with an increased rate of early relapse (Voëtzel *et al*., Leukemia, submitted). In addition, it has been shown ΔNp73 triggers IGF1R signalling, important in preserving cancer stem cell traits (Chen et al., 2014a). Therefore all these data suggest that ΔNp73 could potentially be involved in cancer stem cell generation.

Two independent studies showed that ΔNp73 silencing decreases the expression of stem cell markers, impairs anchorage-independent growth (a hallmark of cancer stem cell function) and decreases the engraftment efficiency *in vivo* (Meier et al., 2016; Prabhu et al., 2016). Consistent with these observations, the overexpression of ΔNp73 in the melanoma cell line Sk-Mel-29 leads to increased expression of CD133, Nanog and Oct4 (Meier et al., 2016). Mechanistically, ΔNp73 confers cancer cells with stem-like properties by attenuating the expression of miR885-5p, a negative regulator of IGF expression. Similar results have been found by another group in colorectal cancer (Prabhu et al., 2016). Through pharmacological indirect inhibition of ΔNp73, cells exhibited a decreased capacity to form colonospheres, down-regulated the expression of stemness markers ALDH, CD44, ID3 and E-cadherin, and showed a decreased capacity to initiate tumours *in vivo*.

3.3.4 p73 Role in development

It became evident that ΔTAp73 isoforms play an essential role in development when *tp73-/-* mice were described to have several developmental pathologies (Yang et al., 2000). p63 has been described to be implicated in the maintenance of epithelial stem cells from stratified and glandular epithelia (Mills et al., 1999; Yang et al., 1999). *tp73-/-* mice present hippocampal dysgenesis due to massive apoptosis of sympathetic neurons, hypersecretion of cerebrospinal fluid resulting in hydrocephalus and runting, immunological defects causing chronic infections and inflammation, as well as altered reproductive behaviour due to pheromone weakness.

Aberrations of *TP73* expression pattern have mainly been described to affect the nervous system. ΔNp73 is essential in neuron differentiation and in the nervous system, it blocks neuronal terminal differentiation and thus prevents tissue maturation (Cam et al., 2006; Hüttinger-Kirchhof et al., 2006) **(Figure 31)**. Pozniac et al (2000) demonstrated that ΔNp73 is present in developing neurones and has antiapoptotic functions (Pozniak et al., 2000). In the absence of ΔNp73, neurons undergo cell death during the development of the nervous system but ΔNp73 rescue by ectopic expression protects neurons from apoptosis. TAp73 has also

been implicated in the differentiation of neuroblastoma cells (Billon et al., 2004; Laurenzi et al., 2000). Endogenous TAp73 levels rise in neuroblastoma cells induced to differentiate and TAp73 may support differentiation by antagonizing Notch signalling in neuroblastoma cells and in primary neurons (Hooper et al., 2006).

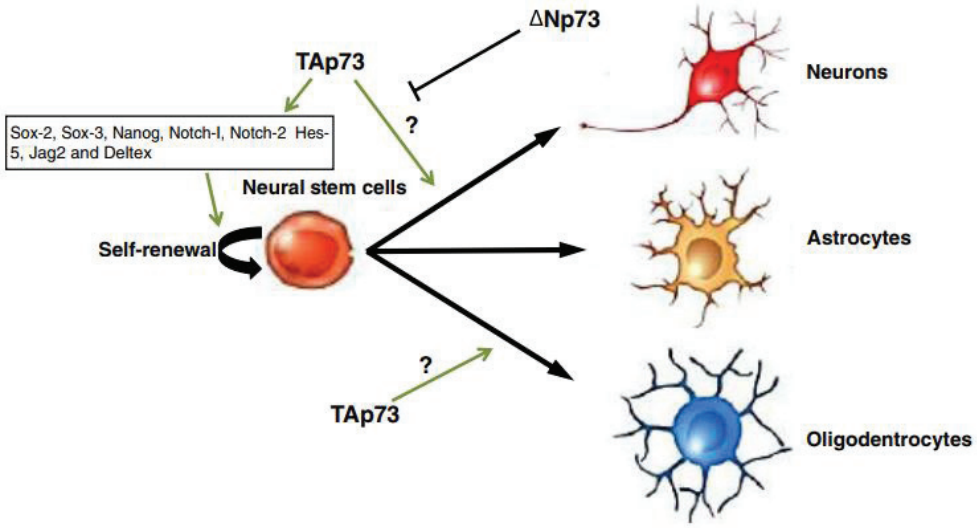

Figure 31. Role of p73 in neurogenesis. Functional neurons are generated from neural stem cells and then after maturation, are integrated in neuronal circuits. TAp73 is essential for neuronal differentiation and maintenance of neural stem cells. ΔNp73 plays a major role as a survival factor. Question marks indicate that molecular mechanisms have not been fully investigated yet. **(Killick et al., 2011)**

Whereas TAp73 enhances terminal differentiation of oligodendrocyte precursors, ΔNp73 inhibits this process (Billon et al., 2004). Similarly, during nephrogenesis, ΔNp73 is preferentially expressed in proliferating nephron precursors, whereas TAp73 is rather expressed in the differentiated region of the renal cortex (Saifudeen et al., 2005). This spatiotemporal switch from ΔNp73 to TAp73 may play an important role not only in the regulation of terminal differentiation in the developing nephrons, but suggests general antagonistic roles in differentiation control for the different p53 family proteins.

TAp73-/- mice mate normally but they are sterile and it has been found that TAp73-/-oocytes reveal a striking increase in spindle organization abnormalities leading to impaired preimplantation embryonic development (Tomasini et al., 2008).

3.3.5 TAp73 – ΔNp73 balance

Increasing evidence suggest that p73's effects on tumour progression do not rely on total p73 levels but rather on the ratio between the TA and ΔTA isoforms expression.

TAp73 and ΔTAp73 isoforms have dominant negative opposing roles, as well as independent cellular functions. In cancer, the balance between the intracellular levels of the TAp73 and ΔTAp73 isoforms determines cell fate with respect to survival or death. Expression and activity of *TP73* products are tightly regulated by a large number of molecular mechanisms including promoter activation, transcriptional control, alternative splicing, post-translational modifications, isoform-specific degradation and protein-protein interactions (summarised in **Figure 32**).

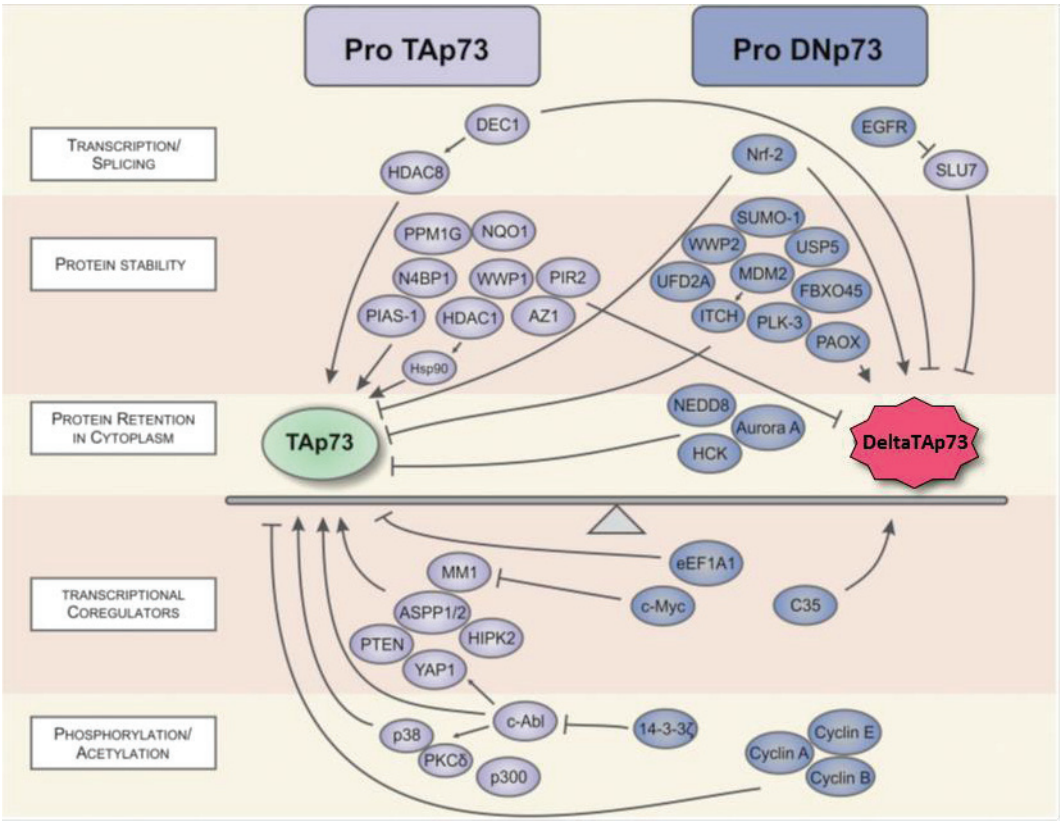

Figure 32. Regulatome balancing TA/ΔTAp73 activity. Coordination of TAp73 and ΔTAp73 activity underlies a complex network of regulatory proteins. In this regard, pharmacological treatment of cancer should consider both TAp73 and ΔTAp73 activities. **(Engelmann et al., 2015)**

At a given time-point, cells express both TAp73 and ΔTAp73 isoforms at levels that vary depending on the cell context. In cancer cells, the balance between these isoforms favours a

pro-oncogenic or a tumour-suppressor environment. In premalignant stages, the level of the transactivation competent TAp73 isoform increases in order to promote cell cycle arrest and apoptosis. However, during the progression towards cell transformation, TAp73 expression starts to decrease whereas ΔTAp73 increases as demonstrated in an *in vitro* model of cell transformation by oncogenic Ras **(Figure 33)** (Beitzinger et al., 2008). In patients, the switch of the TAp73/ΔNp73 ratio in favour of ΔNp73 has been frequently observed in many different cancer types and has been shown to correlate with advanced tumour stage, lymph node metastasis, vascular invasion, weak response to chemo- and radiotherapy, and poor overall patient survival (Casciano et al., 2002a; Concin et al., 2005; Domínguez et al., 2006; Müller et al., 2005; Stiewe et al., 2004). Whether the poor prognosis of patients with an altered TAp73/ΔNp73 ratio is caused by ΔNp73 overexpression, loss of TAp73 expression or both, remains to be investigated.

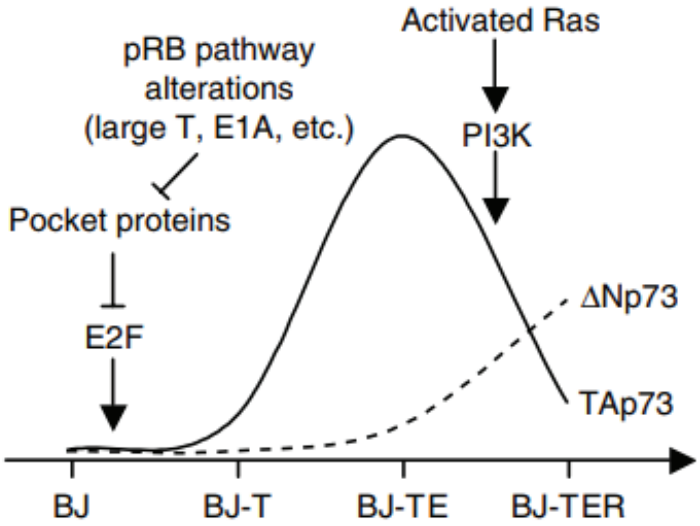

Figure 33. *TP73* expression changes during the course of *in vitro* experimental transformation. During the early stages of cell transformation, the expression of both TAp73 and ΔNp73 increases while during the fully transformed stage, TAp73 decreases and ΔNp73 continues increasing. Therefore, while in the early stages TAp73 level is higher than ΔNp73, in the advanced stages, the balance between the two isoforms changes. **(Beitzinger et al., 2008)**

Epigenetic regulation of the P1 and P2 promoters is one of the mechanisms accounting for ΔNp73 accumulation. P2 hypomethylation-associated over-expression of ΔNp73 has been reported to be a common mechanism in lung cancer and neuroblastoma while in breast cancer promoter methylation redirects the transcription factor Nrf-2 from P1 to P2 (Casciano et al., 2002b; Daskalos et al., 2011; Lai et al., 2014). In tumours, hypermethylation affects more

intensely the P1 promoter than the P2 promoter, as the former one contains three CpG islands while P2 has only one.

Alternative splicing phenomenon affecting P1 transcripts also influence the balance switch. However, only one study has explored the deregulation of splicing factors participating to the generation of truncated isoforms. Amphiregulin activates the EGF receptor in an autocrine manner, inducing phosphorylation of the transcriptional repressor Elk1, which down-regulates the splicing factor SLU7. SLU7 suppression causes alternative splicing of the p73 pre-mRNA and synthesis of the ΔEx2p73 isoform (Castillo et al., 2009).

Apart from the control of the TAp73 and ΔTAp73 synthesis, the balance is also affected by factors involved in the stabilisation and activity of these proteins. The C35 protein, which has been described to be involved in cancer progression and metastasis, specifically interacts with ΔNp73 isoform *via* the 13 aminoacids N-terminal sequence that is only present in this isoform. The ΔNp73-C35 complex activates AKT signalling and the expression of nuclear factor-kB (NF-kB), especially in response to genotoxic drugsn thus conferring chemoresistance in cancer cells (Leung et al., 2013).

Chaudhary and collaborators described a specific degradation mechanism of ΔNp73 coupled with the stabilisation of TAp73. WWP2 is an E3 ligase that ubiquitinates and degrades all p73 isoforms. In contrast, when WWP2 heterodimerizes with another E3 ligase, WWP1, the complex specifically ubiquitinates and degrades ΔNp73. PPM1G is a functional switch that controls the balance between monomeric WWP2 and the heterodimeric WWP2/WWP1 state. During cellular stress, WWP2 monomers are absent and p73 accumulates, whereas WWP2-WWP1 heterodimers are functional and degrade ΔNp73, thus shifting the balance TAp73/ΔNp73 in favour of the full length TAp73(Chaudhary and Maddika, 2014).

Carastro and colleagues suggested that the rs1801173 dinucleotide polymorphism located in exon 2 of the *TP73* gene negatively impacts the TAp73/ΔNp73 ratio in cancer cells. In patients with prostate cancer, this specific polymorphism is associated with poor overall survival (Carastro et al., 2014). A previous meta-analysis study showed that this polymorphism is correlated with an increased risk for patients to develop colorectal and head and neck cancers (Liu et al., 2011a).

In addition, ΔTAp73 isoforms have a longer half-life than TAp73, implying that even with a similar transcription rate, ΔTAp73 intracellular protein levels are higher than TAp73 due to its higher stability (Stiewe et al., 2002).

Two studies showed the impact of the balance between TAp73 and ΔNp73 on prognosis of patients with leukemias. In acute promyelocytic leukemia (APL), both isoforms are expressed, and high ΔNp73/TAp73 expression ratio is associated with low overall survival, low disease-free survival, and high risk of relapse in APL patients treated with chemotherapy **(Figure 34)** (Lucena-Araujo et al., 2015). Hamdy and collaborators showed that in chronic lymphocytic leukemia (CLL) and acute lymphocytic leukemia (ALL) both type of isoforms are over-expressed compared to normal peripheral blood lymphocytes : 27-fold for TAp73 and 233-fold for ΔNp73 in CLL, 9-fold for TAp73 and 386-fold for ΔNp73 in ALL. In both cases patients show an over-expression of TAp73 in tumour cells, but a resulting ΔNp73/TAp73 ratio in favour of ΔNp73 (Hamdy et al., 2016).

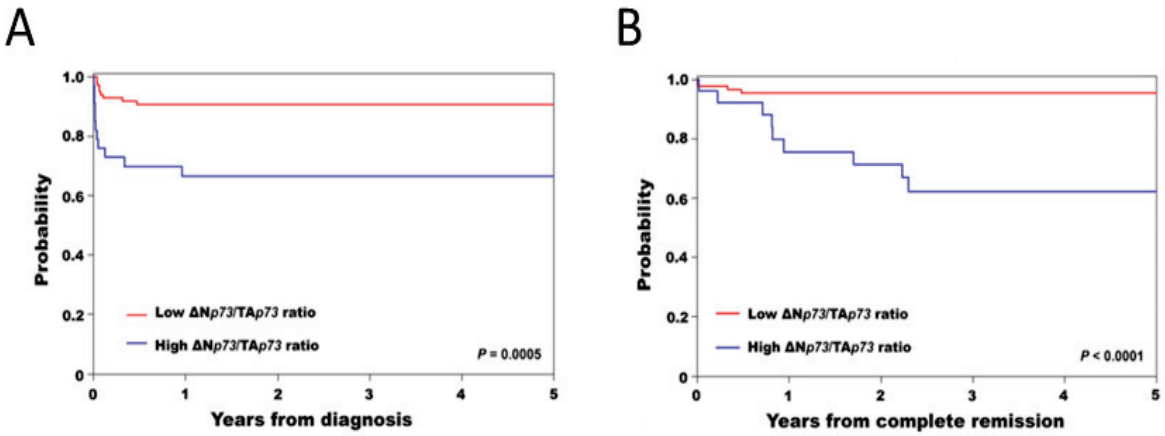

Figure 34. Survival curves results for patients with acute promyelocytic leukemia (APL) according to the ΔNp73/TAp73 ratio. Probability of **A.** Overall survival and **B.** Disease Free Survival. **(Lucena-Araujo et al., 2015)**

3.4. p73 in HCC

Since the discovery of p73 in 1997, several studies showed that p73 is aberrantly over-expressed in liver tumours and contributes to the development of primary liver cancer independently on other genetic or environmental factors.

Tannapfel and colleagues observed that *TP73* is over-expressed in 32% of HCC nodules (Tannapfel et al., 1999). Survival analysis showed that it is an independent poor prognosis factor with respect to overall survival **(Figure 35)**. Patients positive for p73 protein in the

tumours were twice more likely to die within the same period of time than negative patients. In this study, the surrounding non-neoplastic tissue was negative for p73 (mRNA and protein) and the antibody used for the immunostaining did not allow discriminating between the different p73 isoforms.

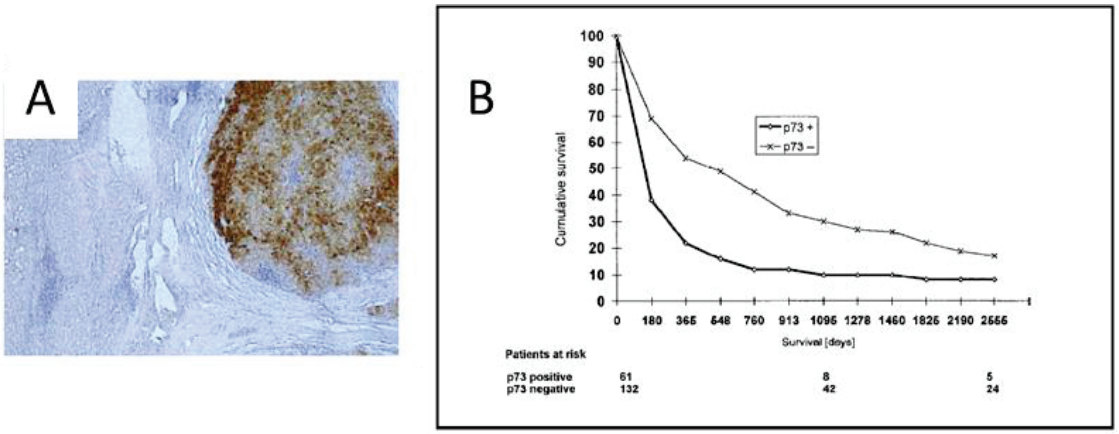

Figure 35. p73 expression in HCC. **A.** p73 mRNA transcripts (brown reaction product) within a hepatocellular carcinoma (HCC) nodule (right) and non-neoplastic surrounding hepatocytes and fibrous tissue without transcripts (original magnification×10). **B.** Overall survival in patients with p73-positive and p73-negative tumours (immunohistochemistry detection. **(Tannapfel et al., 1999)**

Sayan and colleagues investigated the differential expression of the p73 isoforms ΔNp73 and Δ'Np73, originating from the P1 and the P2 promoter, respectively. They described that only the ΔNp73 truncated isoform, originating from the P2 promoter, is expressed in normal murine hepatocytes while TAp73 and ΔNp73 coexpression is present in human HCC (Sayan et al., 2001). To investigate the contribution of the activation of the internal promoter and aberrant splice processes leading to p73 truncated isoforms in HCC, one study investigated the relative expression of ΔNp73 and ΔN'p73 by using specific primers against these two isoforms (Pützer et al., 2003). Authors showed that in HCC, ΔN'p73 isoforms are more abundant than ΔNp73 and that their expression is differently regulated by p53 and E2F suggesting that the two promoter are not regulated through the same mechanisms. These data suggested that P1 promoter-derived transcripts are the predominant source of potentially oncogenic p73. Stiewe and colleagues further analysed the expression of p73 isoforms, by analysing of the expression of all p73 truncated isoforms (ΔNp73, ΔN'p73, ΔEx2p73, ΔEx2/3p73) (Stiewe et al., 2004). Authors found that in tumour cells, the main source of N-terminal truncated isoforms are alternative splicing events and to a lesser extent the activation of the second promoter, in relation to what has been described before. Overall enhanced activity of the conventional P1

promoter compared to the internal P2 promoter could explain the increase in both full length TAp73 and the truncated isoforms.

Regarding the action of p73 isoforms in HCC, it has also been confirmed that TAp73 and ΔTAp73 isoforms have opposite roles in apoptosis regulation (Müller et al., 2005). TAp73 is induced in response to DNA damaged induced by chemotherapy. TAp73 cooperates with drugs to induce apoptosis by inducing the expression of the pro-apoptotic Bcl-members and subsequently mitochondrial apoptosis as well as by transactivating the death receptor CD95. When ΔNp73 is coexpressed, tumour cells are less responsive to chemotherapy showing inhibition of the TAp73- mediated transactivation of CD95 mediated by and p53 and interfere with the mitochondrial apoptosis. In HCC patients, ΔNp73 correlates with low survival. The expression of N-terminal isoforms selects against both the expression of death receptors and TAp73-mediated mitochondrial apoptotic activity **(Figure 36)**. Schuster and collaborators highlighted the ΔNp73-direct effect on the transcription activity of TAp73 in HCC cells. The inhibition concerns apoptotic factors acting at several levels of the apoptotic signalling. ΔNp73 down-regulates both the expression of death receptors as well as mitochondrial factors effectuating the apoptosis (Schuster et al., 2010).

Gonzales et al showed in a cohort study that increased ΔNp63 and ΔNp73 expression, as well as reduction of TAp63, TAp73 and cell death receptor expression are associated with reduced survival of patients due to tumour recurrence following orthotopic liver transplantation (González et al., 2017). The *in vitro* approach showed that truncated isoforms have more potent anti-apoptotic and proliferative activities in WT p53 HCC cell lines than in null p53 cells. These results would suggest that ΔNp73's effect is mainly due to its dominant negative function on p53.

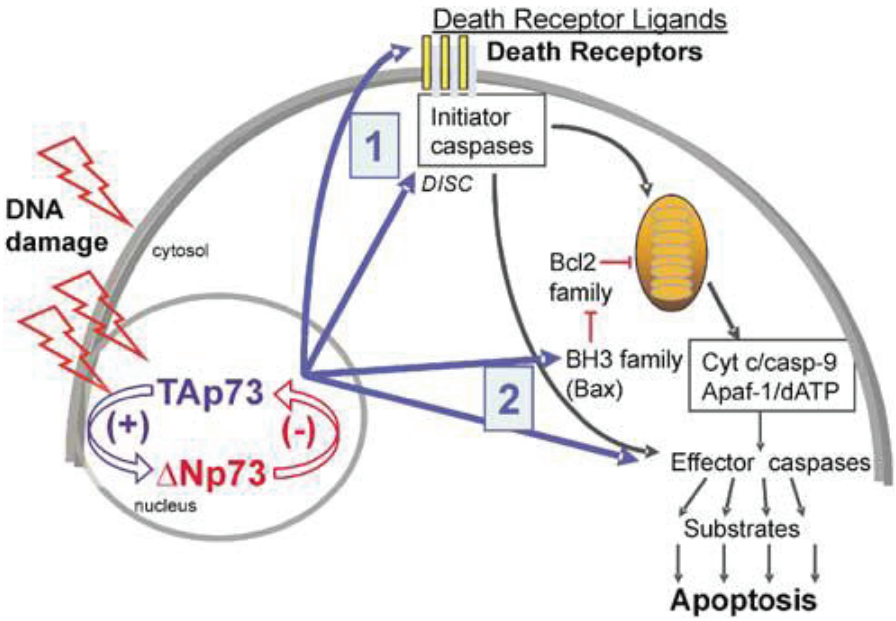

Figure 36. Model of TAp73/ΔNp73-regulated apoptosis. Upon DNA damage, TAp73 activates both, the death receptor- (pathway 1) and the mitochondrial-(pathway 2) apoptosis pathway. ΔNp73 is a strong inhibitor of both pathways. **(Müller et al., 2005)**

In order to understand what are the hepato-specific consequences of the expression of p73 truncated isoform, Tannapfel and collaborators studied the effect of the liver-specific expression of ΔEx2/3p73 isoform, originating from the P1 promoter, under the control of the albumin promoter (Tannapfel et al., 2008). After 3-4 months, it was observed that mice developed preneoplastic lesions, with high hepatocyte proliferation. After 12- to 20-months 83% of the animals developed hepatic carcinoma. These lesions were characterised by phosphorylating inactivation of RB as well as down-regulation of cell cycle inhibitors controlled by p53. These results confirm previous findings that p73 is over-expressed in human HCC nodules and it acts as an oncogene since it is capable alone to drive HCC development. HCC nodules were characterised by high penetrance into the adjacent tissue without visible capsule, well differentiation and tumour formation occurred gender independent. Whereas transgenic p73 was equally detected in HCC nodules and in the adjacent tissue, phosphorylated Rb responsible for ΔTAp73-mediated proliferation was highly detected in HCC nodules, at a lower intensity in preneoplastic lesions and barely detected in normal liver. This provides an explanation for the selective advantage of p73 overexpressing cells during human tumourigenesis. E2F targets cyclin E and cyclin D1 are present in normal liver tissue in transgenic mice suggesting that E2F activity is enhanced in normal hepatocytes. In HCC, the 2 target genes are expressed at a higher level suggesting that p73 truncated isoforms favour the development and progression of HCC in a stepwise manner.

Both p53 and p73 regulate AFP production in the liver by binding to the p53 responsive elements in the promoter of the gene. By targeting corepressor proteins and inducing repressive histone modification, the two transcription factors decrease the AFP transcription within 2 to 3 weeks of age (Cui et al., 2005).

Since HBV chronic infection is one of the major causes of HCC in the world, *Knoll et al* (2011) studied the diverse effects of the interaction between p73 and the HBV viral protein HBx concerning HBV-induced HCC **(Figure 37)** (Knoll et al., 2011). Both p73 and HBx play dual roles in the regulation of apoptosis. While p73's dual role is due to isoforms with opposing effect, HBx's effect on apoptosis depends on the cells context. In normal cells, HBx induces apoptosis while in transformed cells it has an inhibitory effect. In normal cells HBx inhibits apoptosis by binding p53 and p73 and retaining them in the cytoplasm. HBx prevents both factors from going to the nucleus and binding to the DNA. In HCC cell lines but not in normal hepatocytes, HBx induces ATM activation by phosphorylation which further phosphorylates p53, stabilising it and inhibiting its degradation by MDM2. In NIH3T3 transformed cells, HBx interacts with E2F1 and enhances its transactivation activity, favouring therefore the E2F1-reactive P1

promoter activation and showing synthesis of truncated isoforms originating from this promoter. The overexpression occurs concomitantly with the rise of TAp73, suggesting once again that the ratio between the pro- and the anti-oncogenic forms of p73 is determinant for the liver cell fate.

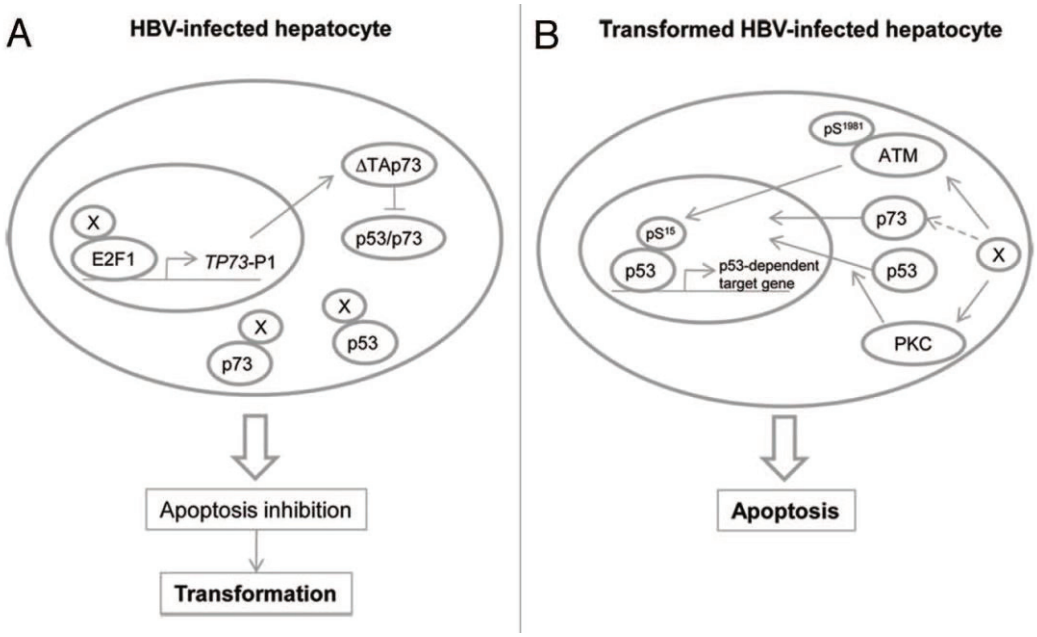

Figure 37. Model for cell context-dependent regulation of apoptosis by HBx. A. In normal HBV-infected hepatocytes, HBx is anti-apoptotic, raising the level of N-terminally truncated p73 isoforms that act as transdominant inhibitors of wild-type p53/ p73. (B) The apoptotic function of HBx in cancer cells is due to enforced p53/p73 nuclear translocation and upregulation of p53-dependent target genes. **(Knoll et al., 2011)**

Kurinna and collaborators investigated the epigenetic effect of p73 in the liver tissue (Kurinna et al., 2010). Foxo2 was identified as the transcription factor whose expression is the most deregulated during liver regeneration. The authors identified p53 binding elements in the promoter of this gene suggesting that both p53 and TAp73 could regulate its expression. During liver regeneration, p53 and TAp73 bind to the promoter of Foxo3, recruits the acetyltransferase p300 and the active chromatin structure of the gene is disturbed leading to loss of Foxo3 expression. After mice partial hepatectomy, authors observed decrease of histone activation marks at the site of p53 binding. Foxo3 is a tumour suppressor that regulated the expression of genes inhibiting the cell cycle and activating apoptosis (Yang et al., 2008a).

3.5. Drugable actions of the p73 axis

Several studies explored the usefulness of using pharmacological approaches to re-equilibrate the aberrantly regulated balance between TAp73 and ΔNp73. Targeting this mechanism is particularly attractive since it is a distinguishing feature of tumour cells.

The small molecule **prodigiosin** has been recently found as targeting the ΔNp73 isoform and abolishes its oncogenic effect both on tumour bulk cells and also on cancer stem cells (Prabhu et al., 2016). Indeed, Prodigiosin prevents the formation of cancer spheroids in *vitro*, independently of the p53 status and is effective against ALDH+ cancer stem cells. *In vivo*, Prodigiosin inhibits the growth of tumour xenografts derived from ALDH+ cancer cells. Prodigiosin is therefore capable of restoring the p53 pathway otherwise disturbed by ΔNp73. The inhibition of ΔNp73 by prodigiosin is mediated by the c-Jun pathway.

Bunjobpol and colleagues demonstrated that **acetylpolyamine oxidase (PAOX) inhibitors** could be used to modulate the stability of ΔNp73. PAOX up-regulates ΔNp73 levels by suppressing its degradation *via* the ubiquitin-independent antizyme (Az) pathway (Bunjobpol et al., 2014). Down-regulation of PAOX activity by siRNA or chemical inhibition leads to ΔNp73 degradation in an Az-dependent manner and reversed the resistant phenotype of ΔNp73-over-expressing cancer cells to genotoxic drugs.

The **cyclooxygenase inhibitor Celecoxib** was reported to reduce the expression of ΔNp73 isoforms in primary and immortalized neuroblastoma cell lines (Lau et al., 2009). Low doses of Celecoxib negatively affect E2F1, the main regulator of *TP73* P1 promoter. Reduced E2F1-dependent transactivation of the *TP73* P1 promoter down-regulates the expression of both the full length and the truncated isoforms. However, at the same time, Celecoxib stabilises the pro-apoptotic TAp73β isoform at the protein level, through still unknown mechanisms, thus leading to apoptosis. Therefore combining cyclooxygenase inhibitors with chemotherapy could be an excellent therapeutic strategy in cancer treatment. This original approach is now in clinical trials. In particular, the trial "p73 as a Pharmaceutical Target for Cancer Therapy Current Pharmaceutical Design, 2011, Vol. 17, No. 6 583 clinical trial NCT00346801", aimed at testing the efficacy of combined treatment with Celecoxib and cisplatin in non-small cell lung cancer.

The altered balance between ΔTA- and TAp73 isoforms has been also shown to be important in acute promyelocytic leukemia (APL). APL is characterized by the t(15;17)(q22;q12) translocation, that generates the oncogenic PML-RAR chimeric protein. Treatment with arsenic

trioxide (ATO) in combination with two **MEK1** (mitogenactivated protein kinase kinase 1) **inhibitors** (PD98059 and PD184352) greatly enhanced apoptosis of primary cells from APL patients, and of immortalized APL and erythroleukemia cell lines (Lunghi et al., 2004, 2006, 2008). This effect is p53-independent and relies mainly in the modulation of ΔTAp73/TAp73 ratio. While ATO treatment alone stimulates the expression of both TAp73 and ΔNp73 isoforms, the co-administration of MEK1 inhibitors results in preferential induction of TAp73, thus increasing p73-dependent apoptosis both *in vivo* and *in vitro*.

RNA-based strategy targeting all ΔTAp73 isoforms seems to be very promising. Locked nucleic acid (LNA) antisense oligonucleotide gapmers coupled to magnetic nano-bead polyethyleneimine (MNB/PEI) carriers selectively target ΔTAp73 transcripts and can be efficiently delivered to tumour cells both *in vitro* and *in vivo*. These molecules induce the selective degradation of ΔTAp73 mRNA variants. Down-regulation of aberrantly expressed truncated isoforms in neoplastic cells, as well in rapidly growing tumour xenografts, resulted in inhibition of tumour growth and sensitization to chemotherapy, supporting the further development of specific ΔTAp73 inhibitors as potentially new anticancer agents (Emmrich et al., 2009).

IV. Autophagy in cancer

Autophagy (from the ancient Greek αυτο + φagos/φagεῖν = self-eating) is a physiologic degradation process assuring both the turnover of biomolecules that are dangerous for cells (misfolded proteins or damaged organelles), as well as the recycling of cellular components in conditions of nutriment deficiency (Hara et al., 2006). The process is useful both for *de novo* synthesis and energy production. Autophagy is constitutively active at low basal levels but can be further triggered in response to stress conditions, allowing cells to survive on their own resources. Autophagy occurs in non-pathological conditions, assuring homeostasis, but also in specific cases, like aging and cancer.

4.1 Autophagy – a process of degradation

Autophagy takes place at the level of the lysosome which contains degradation proteins and provides a favourable environment for them to function.

According to the delivery mode of substrate to the lysosome, three different types of autophagy have been described in mammalian cells: macroautophagy, chaperone-mediated autophagy (CMA) and microautophagy. The **macroautophagy** is the mechanism most commonly employed by cells and the most studied. During macroautophagy, the material to degrade is surrounded by a double membrane forming the autophagosome. Macroautophagy can be considered as a process occurring in 4 stages: elongation, maturation, fusion and degradation **(Figure 38)**. Several cellular compartments participate to the formation of the double membrane including the endoplasmic reticulum, the Golgi apparatus and the plasma membrane. The autophagosome fuses with the lysosome and forms the autophagolysosome. The proteases, lipases, nucleases and glycases contained inside the lysosome degrade the material under the coordination of 37 ATG proteins. **Chaperone-mediated autophagy** is mediated by cytosolic chaperones that recognise specific peptide motifs on the proteins to degrade. Chaperones such as HSC70 are specifically recognised by lysosome-associated membrane protein, direct the substrate towards the lysosome where is degraded. Finally, in **microautophagy**, the material to degrade, associated or not with chaperones, is directly engulfed by the lysosome *via* membrane rearrangements.

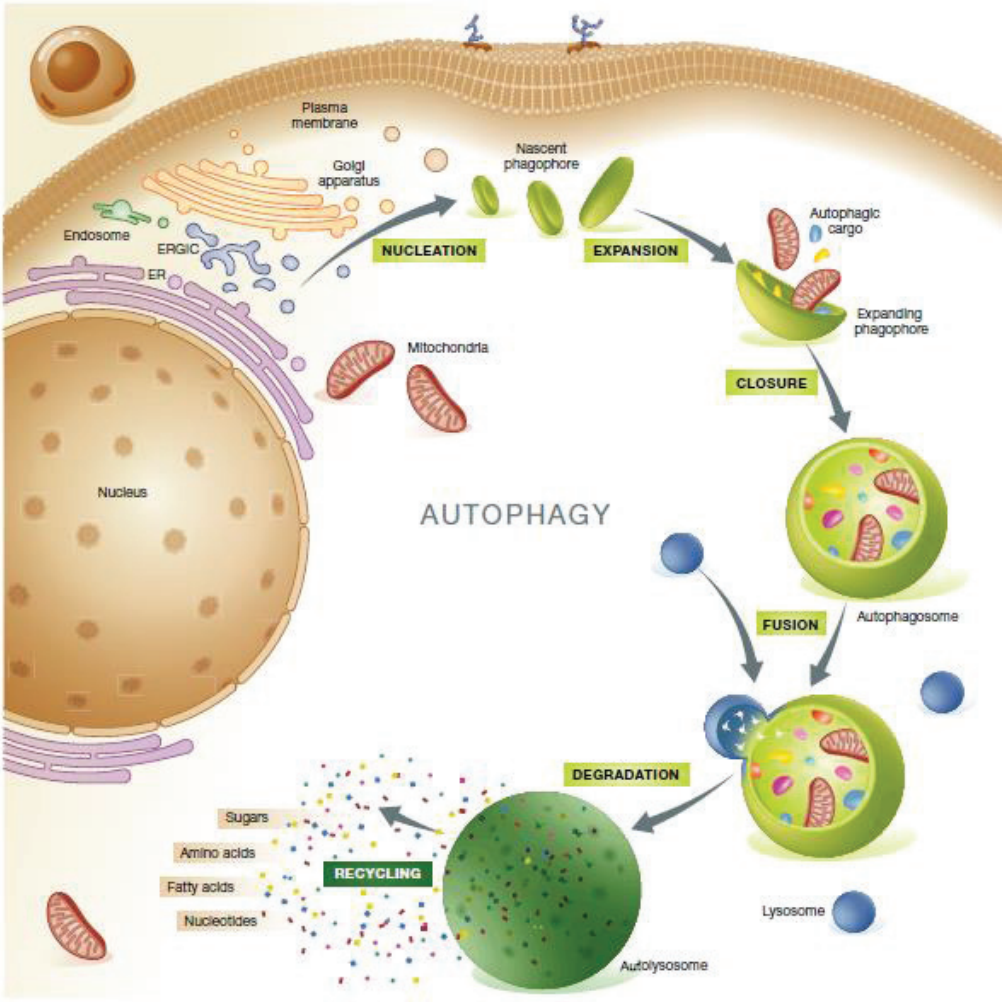

Figure 38. The macroautophagic process. (Galluzzi et al., 2015)

The initiation and termination of autophagy is controlled by nutrient-sensing mechanism. Low energy state of the cells as well as depletion of amino acids levels in the cytoplasm inhibit the mTOR pathway and initiate autophagy. On the contrary, high energy states activate mTOR and inhibit cellular autophagy.

Autophagy is a highly complex mechanism that is finely regulated depending on cell's needs. The main regulator of the pathway is the mTOR pathway, sensitive to the availability of amino acids in the cytoplasm (Laplante and Sabatini, 2012). A major inhibitor of the mTOR pathway is AMPK protein (protein kinase, AMP-activated), sensitive to declining ATP/AMP ratios (Mihaylova and Shaw, 2011). The level of autophagy is also regulated by post-translational modifications of autophagy proteins (ATG) such as phosphorylation, leading to their activation or inhibition. Besides its role on mTOR regulation, AMPK stimulates autophagy by phosphorylating ULK1, phosphatidylinositol 3-kinase catalytic subunit type 3 (PIK3C3) and Beclin 1 (the mammalian ortholog of yeast Atg6). PIK3C3 and Beclin 1 are essential for the

production of phosphatidylinositol 3-phosphate, an essential component for autophagosomes biogenesis (Egan et al., 2011; Kim et al., 2013; Zhao and Klionsky, 2011). Two ubiquitin-like conjugation systems involving ATG7 are indispensable for autophagy (Mizushima, 2007). A detailed discussion of additional factors that are involved in the control and execution of autophagic responses can be found here (Boya et al., 2013).

Sustained autophagy leads to cell death, being considered the second type of programmed cell death, right after apoptosis.

4.2 Autophagy in cancer

Autophagy plays a dual role in cancer **(Figure 39)**. First observations regarding this process suggested that it prevents malignant transformation through mediating oncosuppressive effects due to its key role in the preservation of intracellular homeostasis.

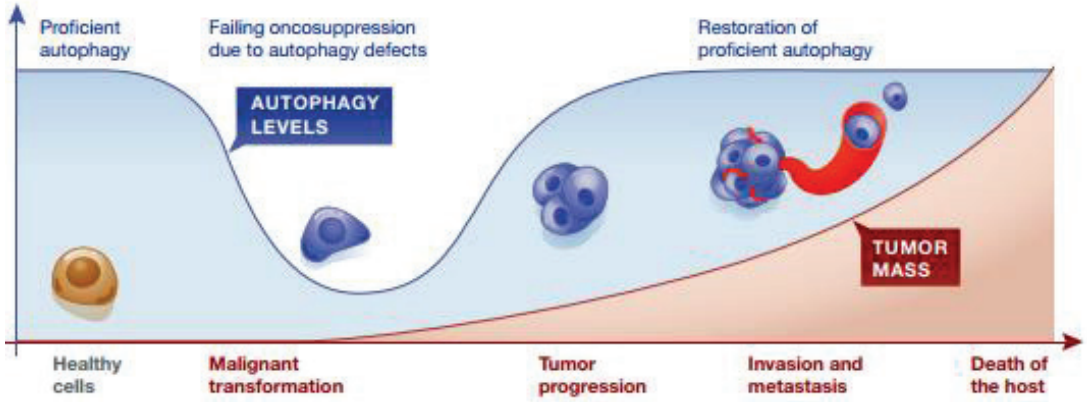

Figure 39. Autophagy in malignant transformation and tumour progression. Proficient autophagic response appears to protect healthy cells from malignant transformation. Conversely, autophagy promotes tumour progression and therapy resistance in a variety of models. Thus, the transition of a healthy cell toward a metastatic and therapy-insensitive neoplasm may involve a temporary (but not a stable) loss in autophagy competence. **(Galluzzi et al., 2015)**

Oncosuppressive role. It has been shown that inactivation of autophagy predisposes to development of spontaneous tumours. As such, several factors involved in autophagy are considered as tumour suppressors (Beclin 1), since it has been found that in several tumour types, cancer cells have lost the corresponding genes. Some studies suggest that oncogenes inhibit autophagy, while proteins preventing malignant transformation stimulate autophagic

responses (Morselli et al., 2011). Basal autophagy prevents the formation of tumours as it promotes genomic stability in normal cells and obviated cancer initiation. Proficient autophagy suppresses the accumulation of genetic and genomic defects that occur during malignant transformation, through a variety of mechanisms. Autophagy prevents ROS overproduction by removing dysfunctional mitochondria as well as redox-active aggregates of ubiquitinated proteins (Green et al., 2011; Komatsu et al., 2007; Mathew et al., 2009; Takahashi et al., 2013); maintains the physiological metabolic homeostasis (Galluzzi et al., 2014; Kenific and Debnath, 2015); contributes to oncosuppressive mechanisms such as oncogene induced cell death or oncogene-induced senescence (Elgendy et al., 2011); is involved in the degradation of oncogenic proteins, including mutant (but not wild-type) p53 (Choudhury et al., 2013; Garufi et al., 2014; Rodriguez et al., 2012); mediates oncosuppressive immune responses and potent anti-inflammatory effects (Ma et al., 2013); and represents a first line defense against viral and bacterial infection **(Figure 40)** (Deretic et al., 2013).

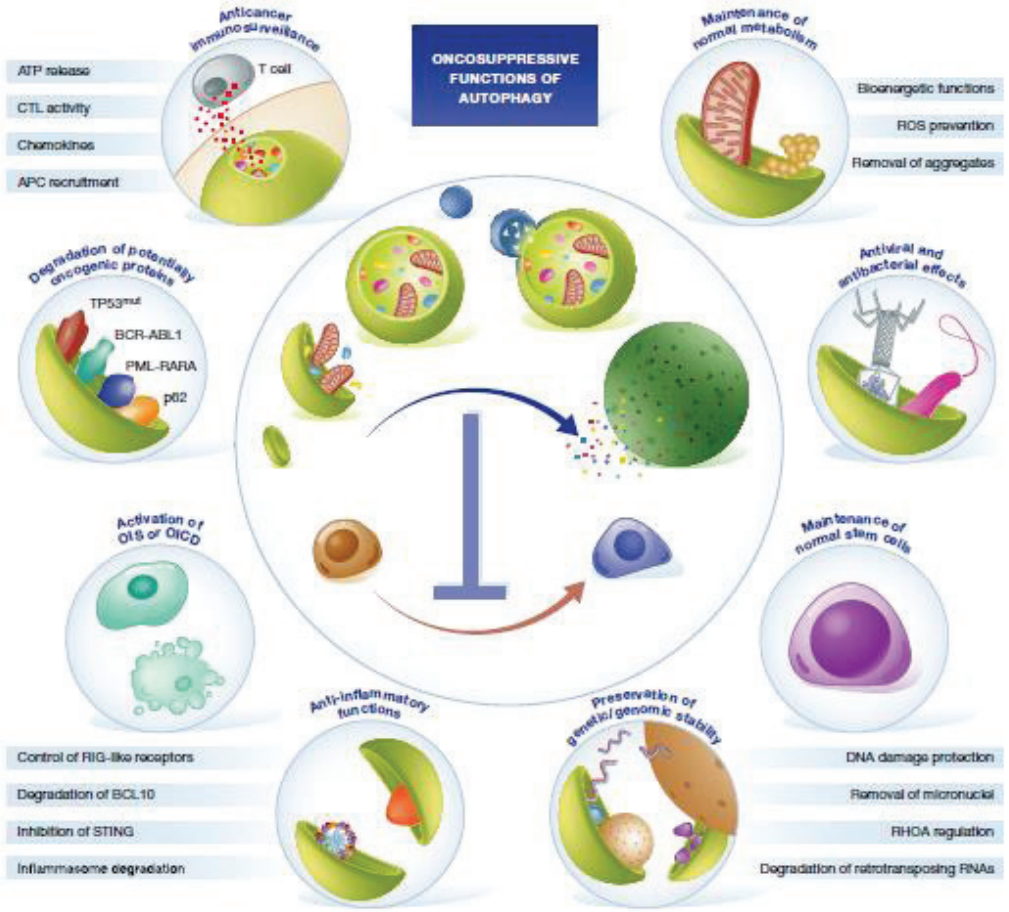

Figure 40. Oncosuppressive functions of autophagy. (Galluzzi et al., 2015)

Pro-oncogenic role. However, several studies sustain the hypothesis that cancer cells increase the autophagic flux in order to promote their survival and favour tumour cell growth (Amaravadi et al., 2016; White, 2012). Autophagy supports the growth and progression of established tumours by reducing their sensitivity to cell-intrinsic and microenvironmental stimuli that would normally promote their elimination (Avivar-Valderas et al., 2013; Cai et al., 2015; Kroemer et al., 2010). Defects in the autophagic machinery often restrain the proliferation, dissemination and metastatic potential of malignant cells (Lazova et al., 2012; Mikhaylova et al., 2012). In this context, autophagy participates to the maintenance of the cancer stem cell pool, survival of senescent cancer cells and resistance to EMT, starvation, hypoxia and chemotherapy **(Figure 41)** (Galluzzi et al., 2015; Viale et al., 2014).

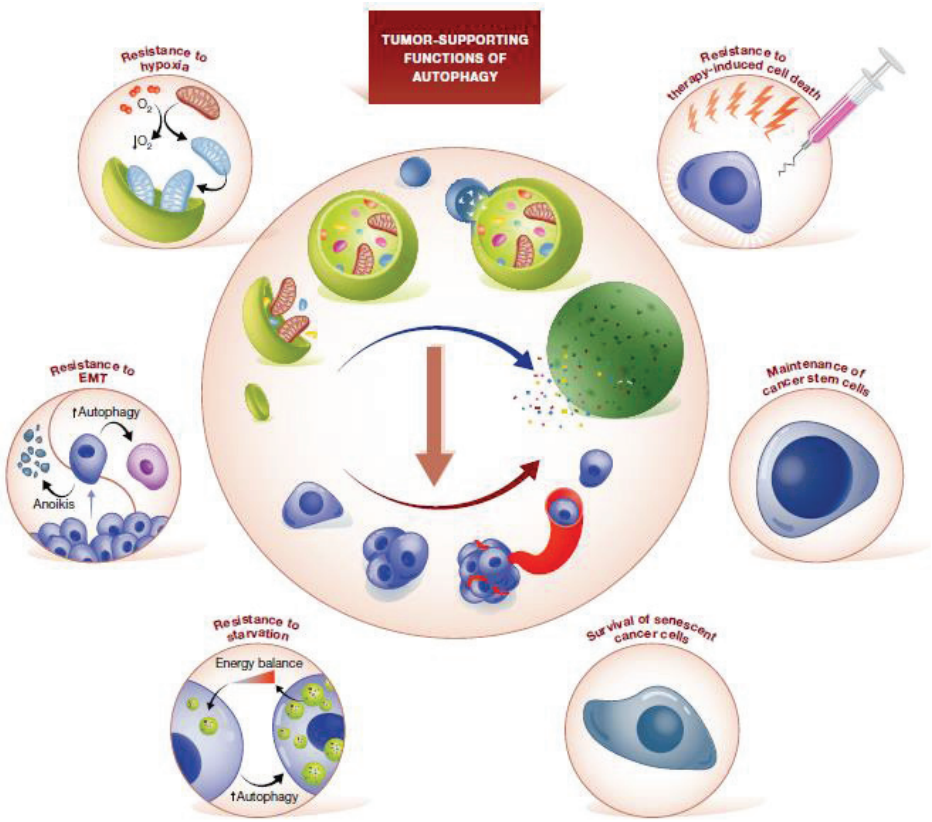

Figure 41. Tumour-supporting functions of autophagy. (Galluzzi et al., 2015)

4.3 Role of autophagy in HCC

Autophagy plays an important, still poorly understood role in hepatocellular carcinoma and the balance between its activation or inhibition is easily affected **(Figure 42)** (Chang et al., 2012a). Mice deficient for essential autophagy factors develop hepatomegaly and hepatic failure, indicating the essential role played by this mechanism in liver metabolism (Komatsu et al., 2005). Deletion of *Beclin1*, *ATG5* or *ATG7* key autophagic genes in mice leads to development of HCC besides other types of malignancies, showing the primordial protective role of autophagy against the development of liver tumours (Qu et al., 2003; Yue et al., 2003).

In dysplastic nodules, autophagy plays a **protective role against HCC** development by eliminating newly damaged cells and cells accumulating mutations. However, once the tumour is established, deregulation of autophagy contributes to tumour growth by favouring cancer cell survival (Sun et al., 2013). According to this observation, autophagy inhibitors favour the transition of dysplastic nodules into malignant tumours. Autophagy deficiency has also been shown to increase the accumulation of damaged mitochondria, to cause oxidative stress and to allow damaged DNA accumulation and genome mutations in hepatic progenitor cells (White, 2012; Xue et al., 2016).

Furthermore, p62 is a substrate of autophagy that accumulates into hepatocytes in case of inactivation of this process and contributes to hepatic tumour formation. Indeed, autophagy-deficiency in absence of p62 shows HCC nodules with smaller size (Kessler et al., 2015).

IFN-γ, known to inhibit HCC growth, has been found to be mediated by autophagy cell death. IFN-γ stimulates autophagosome formation. Inhibition of autophagy abolishes the anti-tumour effect of IFN- γ on HCC, suggesting that this process is essential for the IFN-γ inhibition of tumour growth.

The PI3K/Akt/mTOR pathway regulates cell growth, survival, metabolism and apoptosis. This pathway that is often activated in cancer is able to inhibit autophagy. On the other hand, PTEN activates autophagy, both by inhibiting the PI3K/Akt/mTOR pathway through decrease of PI3K activity and by initiating the formation of the autophagosome. PTEN is often mutated or downregulated in hepatocellular tumours. Thus, in HCC, the repression of PI3K/AKT/mTOR pathway and the activation of autophagy with small molecules restrict the cancer cells' growth.

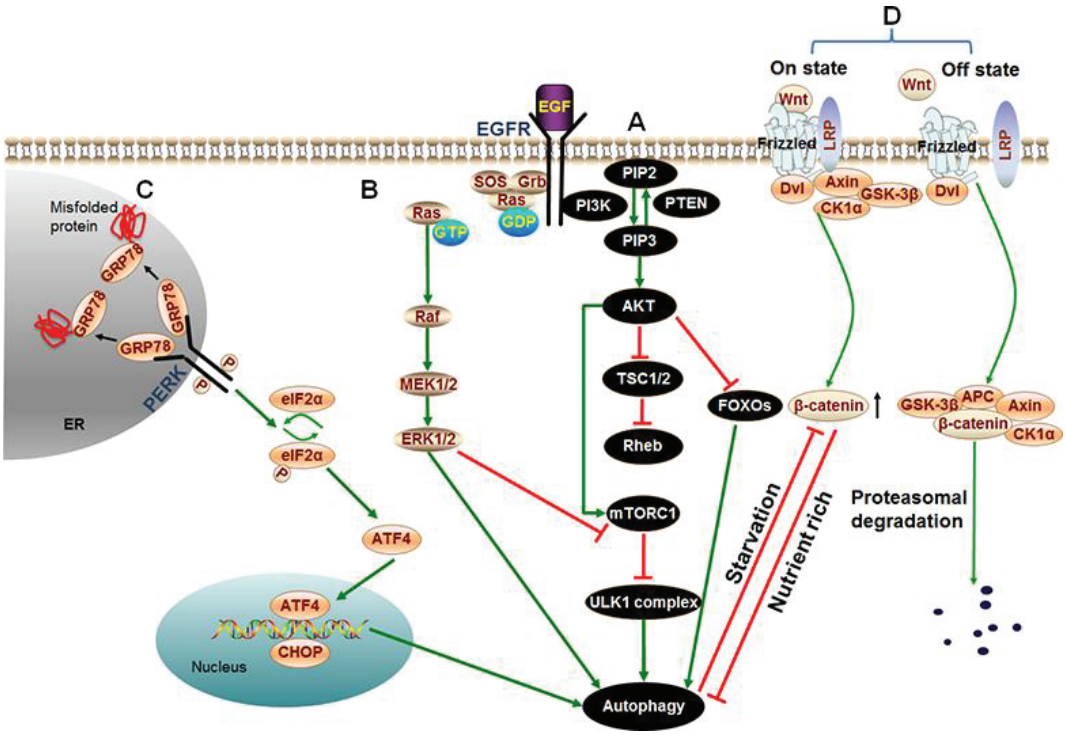

Figure 42. Signalling cascades of autophagy in HCC. (A) PI3K/AKT/mTOR pathway: Binding of growth factors to the corresponding receptors such as EGFR activates the signalling pathway, leading to repression of autophagy. In addition to activating mTORC1 directly or indirectly, active AKT can also directly regulate transcription factors FOXOs resulting in inhibition of autophagy. (B) ERK/MAPK pathway: binding of ligands on EGFR or IGFR receptors stimulates Ras signalling cascade, resulting in activation of autophagy. (C) PERK pathway: Under conditions of accumulation of misfolded or unfolded proteins, GRP78 binds to these proteins, permitting the release and the activation of PERK and the subsequent phosphorylation of eIF2α. PERK-eIF2α activation, by increasing the intracellular level of ATF4 and CHOP, induce autophagy. (D) Wnt/β-catenin pathway: In the presence of Wnt ligand (On state), GSK-3β is displaced from the APC/Axin/GSK-3β complex which prevents β-catenin phosphorylation and subsequent proteasomal degradation. Thus, the concentration of β-catenin is increased in cytoplasm. A growing number of β-catenin limits autophagy in nutrient rich condition, while β-catenin itself is specifically targeted for degradation by autophagy upon starvation stress **(Liu et al., 2017)**.

However, autophagy can play a **protective role in hepatocellular carcinoma,** by detoxifying cells and supporting cancer cell survival in low nutriment conditions, hypoxia and even metabolic stress (White, 2015). In HCC patients, the activation of autophagy, as assessed by overexpression of LC3-II in tumours compared to adjacent tissue, is positively correlated with poor overall survival (White, 2015). On the other hand, it has been shown that Beclin 1 is downregulated in hepatocellular tumours compared to the adjacent tissue (72.8 vs 89.5%) and its overexpression is an independent indicator of poor prognosis (Qiu et al., 2014). These contradicting results are probably due to the complexity of the autophagy. Analysis of individual markers cannot provide the full picture regarding the level of autophagy at a given

time point. In other studies it has been shown that autophagy is related to malignant transformation and low survival rate (Lazova et al., 2012; Mikhaylova et al., 2012).

It has been shown that miR-375, one of the most strongly down-regulated miRNA in HCC impacts the autophagy balance in HCC cells. In hypoxic conditions, miR-375 decreases viability of HCC cells and inhibits autophagy through down-regulation of Atg7 and blocking the conversion of LC3-I into LC3-II. By down-regulating miR-375, established HCC cells use autophagy to promote survival (Chang et al., 2012b; He et al., 2012b).

Several body of evidence has shown that autophagy impairment during HCC development activates tumour suppressors such as p53, p16, p21 and p27 (Tian et al., 2015). That means that during cancer progression, autophagy contributes to the inactivation of tumour suppressors and that inhibition of this mechanism could restore the oncosuppressive activity of these proteins. In the same manner autophagy seems to increase the transformation potential of activated Ras (Guo et al., 2011, 2013; Song et al., 2009).

It has been shown that autophagy also contributes to chemoresistance in HCC. In hypoxic conditions, autophagy decreases the sensitivity of cells to apoptosis. Sorafenib was shown to partially act by inducing autophagy (Llovet et al., 2008; Yuan et al., 2014). The acquired resistance to Sorafenib, currently encountered in clinic, seems to be mediated by the induction of autophagy and the inhibition of autophagy in resistant cells renders them sensitive again to the drug.

The ERK/MAPK pathway promotes cell growth, proliferation, survival and differentiation, partially by inducing autophagy (Yoon and Seger, 2006; Maddodi et al., 2010). In a cohort study of 46 HCC, it has been observed that the ERK pathway members MEK1/2 and ERK1/2 are activated/up-regulated in 69% to 100% of the cases, but whether the role of ERK on HCC promotion is solely mediated by activation of autophagy has not been demonstrated until now.

The Wnt/β-catenin pathway, often activated in HCC, inhibits autophagy through the β-catenin (Petherick et al., 2013). When stabilised, β-catenin acts as a co-repressor and down-regulates the expression of p62 in nutrient-rich conditions and therefore limits autophagy. On the other hand, in starvation conditions, β-catenin directly interacts with LC3, being itself a substrate of degradation by autophagy.

In conclusion, autophagy seems to have a dual effect in hepatocarcinogenesis. It appears to exert a protective role in normal liver cells, to eliminate damaged/preneoplastic cells, but also to favour survival of liver tumour cells. Considering the discrepancies observed between the

different reports, extensive studies are required to better characterise the mechanisms by which autophagy exerts different functions at different stages of HCC. Indeed, regulators of autophagy could represent promising anti-cancer molecules, in particular for HCC.

4.4 Autophagy and cancer stem cells

Stem cells reside for very long periods of time inside an organ and are the main source of somatic cells. Several observations suggest that autophagy plays a crucial role in the maintenance and function of normal stem cells and is therefore thought to ensure their quality control (Guan et al., 2013; Phadwal et al., 2013; Vessoni et al., 2012). However, the exact contribution of autophagy to stem cell function has not been studied in detail (Lin et al., 2015). Given the analogy between CSCs and normal stem cells, it has been suggested that autophagy also plays a cytoprotective role in CSCs. Autophagy is thought to be able to drive cell survival and evasion of death after cancer therapy.

Several key components of the autophagy process have been shown to be involved in CSCs biology. ATG4A inactivation (through shRNA technology) in breast cancer cells was shown to inhibit mammospheres formation (Wolf et al., 2013). Strikingly, Beclin 1, considered as a tumour suppressor, promotes the survival of CSCs (but not of bulk cells) and contributes to their *in vivo* tumourigenicity. This suggests a dual role for Beclin-1 in tumourigenesis. The expression of Beclin 1 is higher in CSCs than in the total cancer cell population (Gong et al., 2013). DRAM1 and p62, two regulators of autophagy were shown to be involved in bioenergetic metabolism, migration and invasion of glioblastoma CSCs (Galavotti et al., 2013). Downregulation by shRNA of LC3 and ATG12 decreases the CD44+ breast CSCSs population (Cufí et al., 2011).

In triple negative breast carcinoma (TNBC), cells that are able to form mammospheres have a more intense autophagy flux compared to parental cells (Rao et al., 2012). Preclinical and clinical studies have been conducted with the autophagy inhibitor, chloroquine (CQ), and demonstrated that CQ is able to deplete the CD44+ CSCs population in TNBC (Choi et al., 2014). Also, in breast ductal carcinoma *in situ*, CQ treatment reduces propagation, invasion and growth potential of cancer stem/progenitor cells forming mammospheres (Espina et al., 2010).

Autophagy is important for CSCs not only in solid cancers, which are confined inside the tumour mass, but also in haematological cancers. In these latter, the survival of cancer cells and cancer stem cells have been shown to rely mainly on autophagy, since the impairment of autophagy by knock-down experiments is lethal for these cells (Altman et al., 2011; Rothe et al., 2014).

One of the most widely expressed markers of CSCs is CD133. It has been shown that $CD133^{+}$ cells show a high level of autophagy (Song et al., 2013). In fact, CD133 is a regulator of autophagy. In starvation conditions, CD133 is translocated to the cytoplasm and stimutates phagosome formation as well as glucose uptake and thus, enhances CSCs survival under conditions of stress or nutrient restriction within tumours (Chen et al., 2013a, 2013b). According to this, CD133 depletion favours cell death by inhibition of autophagy and induction of necrotic cell death and leads to diminished tumourigenicity of CSCs in several tumour types (Wei et al., 2013). In particular, it has been shown that CD133-blocking antibody inhibited hepatocellular carcinoma CSCs to develop *in vitro* into spheroids and to form *in vivo* tumours in NOD/SCID mice.

Autophagy is activated in CSCs in response to environmental stress stimuli such as hypoxia, metabolic or oxidative stress which promote self-renewal and plasticity. In poorly vascularized tumours, hypoxia stimulates autophagy and activation of stem cell markers and factors (Degenhardt et al., 2006; Heddleston et al., 2009; Lin and Yun, 2010; Ma et al., 2011; Mathieu et al., 2011; Qiang et al., 2012). In one study, hypoxia has been described to enhance the metastatic capacity of CD133+ pancreatic cancer stem cells (Zhu et al., 2014a). If considering that autophagy helps CSCs to adapt to hostile environmental conditions, it has been shown that interfering with autophagy in hypoxic conditions specifically eliminates pancreatic cancer stem cells (Rausch et al., 2012; Song et al., 2013).

Autophagy also impacts on CSC plasticity. Activation of autophagy blocks differentiation and leads to conversion of CD133 negative cells into CD133 positive cells (Yang et al., 2011b; Zhu et al., 2013). On the other hand, CD133 translocation into the cytoplasm enhances autophagic process, thus creating a positive feedback loop that results in the increased survival of CSCs in stress conditions (Jang et al., 2017 for review).

4.5 Modulation of autophagy in anti-cancerous treatments

Given the dual role of autophagy in cancer, should we try to enhance autophagy or should we try to inhibit it for the treatment of cancer? In pre-malignant lesions, enhancers of autophagy might prevent cancer development and conversely, in advanced cancers, both enhancing autophagy and inhibiting it have been suggested as therapeutic strategies (Amaravadi et al., 2016; Galluzzi et al., 2015; Levy and Thorburn, 2011; Towers and Thorburn, 2016). The protumoural role of autophagy opens the hope that the inhibition of autophagy by new drugs could improve the prognosis of HCC patients (Guo et al., 2013; White, 2015).

Autophagy can be blocked at several key levels: inhibition of the lysosome functionality, inhibition of autophagosome formation, inhibition of the fusion between the autophagosome and the lysosome or post-translational inactivating modifications of ATG proteins (Gozuacik and Kimchi, 2004; Xie et al., 2015).

HCQ (hydroxychloroquine) is a derivative of the natural compound CQ (chloroquine) and the most famous molecule inhibiting autophagy through suppression of lysosome functions. HCQ has been approved by the FDA for the treatment of malaria. However, the dosage needed for cancer treatment exceeds the threshold of toxicity of this drug and for this reason its anti-cancer effect has only been explored in preclinical studies (Maclean et al., 2008). These studies showed that inhibition of autophagy enhances the death-promoting activity of tumour suppressor pathways (White and DiPaola, 2009).

Anti-autophagic agents can be associated to other commonly used therapies in order to enhance their efficiency or preventing acquired resistance. It has been shown that 3-MA (3-methyladenine) which blocks the fusion between the autophagosome and the lysosome, can enhance the pro-apoptotic effect of meloxicam, a selective inhibitor of Cox2, effective in several types of cancer (Maclean et al., 2008; Zhong et al., 2015).

However, further studies need to be conducted in order to determine whether cancer cells are more sensitive to autophagy inhibitors that normal cells. Since autophagy is a physiological process indispensable at basal level in normal cells, the ideal treatment would spare non-malignant cells while being deleterious to cancer cells (Karsli-Uzunbas et al., 2014; White, 2015). In particular, such a treatlent should eliminate CSCs with a limited toxicity for normal stem cells.

The inhibition of autophagy in HCC cells could be one of the reasons that Sorafenib significantly improves HCC patients' outcome (Shimizu et al., 2012). When associated to specific autophagy repressors, Sorafenib shows an increased efficiency against HCC. Several body of evidence raises the possibility that autophagy control may be used to avoid cellular resistance to Sorafenib or other anticancerous agents (Liu et al., 2016a; Zhai et al., 2014).

AIM

In view of the current state of the art regarding hepatocellular carcinoma pathogenesis, I have focused during my PhD thesis on the development of innovative models of study of this disease, as well as investigating the role of p73 isoforms in the acquisition of stemness characteristics of these tumours. Furthermore, I have contributed to the preclinical development of a new potential drug against HCC that inhibits autophagy and is efficient against cancer stem cells. The aim was to combine several approaches that together would lead to a better management of hepatocellular carcinoma as well as a deeper understanding of its pathogenesis.

Study 1

In vitro and *in vivo* models of hepatocarcinogenesis

The IMODI initiative (**I**nnovative **Mo**dels of **Di**sease) is a consortium including public laboratories, biotechnology and bio-pharma companies sustained by the French Public Investments Bank (BPI). The aim of IMODI is to develop novel models of eight human tumour types: prostate, breast, ovary, liver, pancreas, lung, myeloma and lymphoma. The main objective is the development of three types of models: patients derived xenografts (PDX), patient-derived cancer cell lines and PDX models in mice with humanised liver or immune system. In addition, several other deliverable products should be the result of this collaboration (not discussed here).

Our research group "Hepatocarcinogenesis and Viral Infection" from the Cancer Research Centre in Lyon participated to this project by contributing to the development of PDX and patient-derived cell lines of HCC. We acted as a collection centre for fresh HCC samples from La Croix Rousse Hospital (Lyon) and we also provided our research expertise by performing *in vitro* culture of primary HCC cells. A second collection centre was situated at Pitié-Salpetrière Hospital and Saint Antoine Hospital in Paris. I will only describe here the experience of our team in this project.

Secondly, we also contributed to the mouse liver humanisation part of the project. Mice livers were repopulated using a conventional source of cells namely primary human hepatocytes (PHHs) (studies reported that iPS reprogrammed hepatocytes can also be used (Zhu et al., 2014b)). The goal was to set up a cryoconservation/thawing method of PHHs, in order to use them at any time after isolation from human liver fragments. PHHs were isolated from human liver fragments obtained after liver resection for colorectal carcinoma metastases.

***

The team initiated a study regarding the capacity of PHHs to be transformed *in vitro*. I contributed to this study by evaluating the emergence of the cancer stem cell pool during immortalisation and transformation of hepatocytes. The corresponding manuscript of this article is presented after the results of the IMODI project.

Innovative models of cancer disease

Introduction

Hepatocellular carcinoma is a disease with very few treatment options. Until now, most of the clinical trials showed negative results due to the limited knowledge of the pathogenesis of HCC, the high radio- and chemoresistance of tumour hepatic cells and the absence of therapeutic strategies specific to this type of cancer. Only a limited number of preclinical models are available for this disease. These models are extremely useful for the identification of new targets for therapies (not only intrinsic to tumour cells but also related to the microenvironment and to the modulation of the immune system), for the screening of novel drugs, as well as for assessing their toxicity. At the preclinical stage, cancer cell line models are extremely important because they are less expensive and less time consuming than *in vivo* models. They are employed both for screening new libraries of molecules and for searching for new potential targets of interest. *In vivo* models are complementary to *in vitro* models, because they better model the physiological conditions encountered in patients. During this last decade, a new type of *in vivo* models of cancer has emerged, the PDX models. These transplantable models are obtained by implanting patient's tumour specimens in immunodeficient mice, subcutaneously (ectopically) or in the organ of origin of the tumour (orthotopically). PDX tumours were shown to retain most of the characteristics of the original tumour and be highly predictive for the clinical outcome (Bertotti et al., 2011; Damhofer et al., 2015; Fichtner et al., 2008; Gao et al., 2015; Garrido-Laguna et al., 2011; Julien et al., 2012; Keysar et al., 2013; Marangoni et al., 2007; Michelhaugh et al., 2015; Migliardi et al., 2012; Siolas and Hannon, 2013; Sivanand et al., 2012; Tentler et al., 2012; Zhang et al., 2013b). PDX models are extremely useful in the study of the interaction between cancer cells with the tumour microenvironment and the host immune system as well as performing pharmacokinetics and pharmacodynamics studies.

Besides the tumour models described here above, *in vitro* and *in vivo* biological systems using PHHs are extremely useful. PHHs cultured *in vitro* are used to study infection by hepatitis B (HBV) and C virus (HCV), cell transformation, as well as drug metabolism. Of note, HBV and HCV viruses have a very narrow host range and only PHHs and the HepaRG cell line can be infected *in vitro* (Galle et al., 1994; Gripon et al., 1988, 1993, 2002; Ochiya et al., 1989).

Mice with humanised livers are extremely useful in virology, oncology as well as drug discovery for performing studies at the level of an organism. However, the biggest limit of these models is that, contrary to cancer-related models, they are not transplantable. Therefore, there is a constant need for sources of PHHs which do not replicate *in vitro*. These cells are isolated from human liver fragments but since the number of donors is extremely low, primary hepatocytes need to be stored frozen to be used at different times after isolation. However, as for many other primary human cell types, PHHs are very sensitive to the freezing process due to intracellular ice formation. Current protocols involve the use of cryoprotectants (*e.g.* DMSO, glycerol, antifreeze glycoproteins) and a controlled freezing rate in order to promote vitrification or dehydration and thus limit intracellular ice formation (Stéphenne et al., 2010). Until now, no method of cryoconservation of PHHs has been described that could be easily employed in the laboratory. Other than fresh PHHs, another source of cells are those commercialised by biotechnology companies.

The aim of this project was both the development of HCC patient-derived cell lines and PDX models, as well as setting up of a less expensive cryopreservative method of hepatocytes that could be easily adapted in any laboratory.

Results

In vitro functionality of cryoconserved PHH

PHHs were isolated from human liver resections with a viability rate close to 100%. Immediately after isolation, hepatic cells were cryoconserved in one-step manner by resuspension in the CS10 solution and then were frozen at -80°C (details are provided below). Hepatocytes were stored in liquid nitrogen for at least 1 week prior to thawing and functional assays. In total, 15 liver fragments were collected from different donors and for each of them a separate batch of hepatocytes was prepared.

Three million viable cells were obtained after thawing each vial and the cell viability was close to 100%. However, since five million cells were initially distributed per vial, it means that the cryoconservation and thawing steps are fatal for about 40% of cells. Dead cells were eliminated during the washing step prior to cell counting and plating. Plated cryopreserved and fresh hepatocytes had the same morphology (**Figure 1A**).

The functionality of PHHs was investigated *in vitro* by using different assays: human albumin production and secretion, leakage of lactate dehydrogenase (LDH) and infection by HBV.

Albumin is the most abundant protein produced by hepatic cells and albumin synthesis is a classical assay for the study of liver-specific function. The level of this protein was measured by ELISA in the supernatant of fresh and cryopreserved hepatocytes cultures, obtained from the same donor. It was found that cryopreserved and thawed PHHs secrete similar quantities of albumin as compared to fresh hepatocytes, for example 213 ng/mL and 138 ng/mL, respectively for one of the batches. High level of albumin in the supernatant is indicative of a functional metabolic circuit and secretory system of hepatocytes.

Membrane integrity was assessed by LDH dosage in the cell medium. When the cell membrane is damaged, the LDH is leaking out of the cell. LDH dosage in the cell supernatant is commonly employed as a cell death assay. As for the albumin, the levels of released LDH was compared between freshly isolated and cryoconserved hepatocytes. The quantification method of the released LDH is relative to the intracellular pool of this enzyme. The cryoconserved hepatocytes did not release a higher quantity of LDH than fresh hepatocytes. We found that the supernatant of cryoconserved hepatocytes contained less than 1% of LDH compared to the intracellular level, while the supernatant of the fresh hepatocytes contained the equivalent of 30% of the intracellular pool. The high levels of LDH observed to be released by fresh hepatocytes cultured right after isolation from liver resections suggests that the perfusion method of the liver fragments endangers the cells membrane. This is probably a consequence of perfusing the liver resections with buffers containing proteases, namely the collagenase in this case. The use of collagenase is intended to dissociate cells from the extracellular matrix and from each other. However, the collagenase is a fast-acting enzyme and probably it creates holes in the hepatocytes' membrane that are not repaired fast enough after cell plating. Since LDH leakage was not observed for cryoconserved hepatocytes, it is possible that freezing and thawing the cells would affect the dynamics of the cell membrane in a way that would allow the redistribution of lipids and proteins and thus repair of the membrane damage. Alternatively, cryopreserved hepatocytes with membrane damage have perhaps been destroyed during thawing, since 40% of frozen hepatocytes are lost during this process. These results could be confirmed by electron microscopy of freshly isolated and cryopreserved hepatocytes.

Thirdly, the capacity of cryoconserved hepatocytes to be infected by HBV was investigated in collaboration with the HBV infection group in our team. Infectivity by HBV is of major importance, since PHHs are the cells that best sustain *in-vitro* infection by HBV. Cryoconserved hepatocytes and fresh hepatocytes were infected with HBV virions three days post-plating. The efficiency of infectivity was assessed by measuring the levels of HBe and HBs antigens in the

supernatant by ELISA. HBsAg represents the protein at the surface of both genome-containing HBV virions and empty HBV particles released from the host hepatocytes. The viral HBeAg is an indicator of active viral replication. For both HBe and HBs proteins, the quantity released by the fresh infected hepatocytes and cryoconserved hepatocytes were similar (**Figure 1B**). These results remain to be confirmed on more samples, but they suggest that cryopreserved hepatocytes sustain infection and replication of HBV *in vitro* with an efficiency similar to freshly isolated hepatocytes.

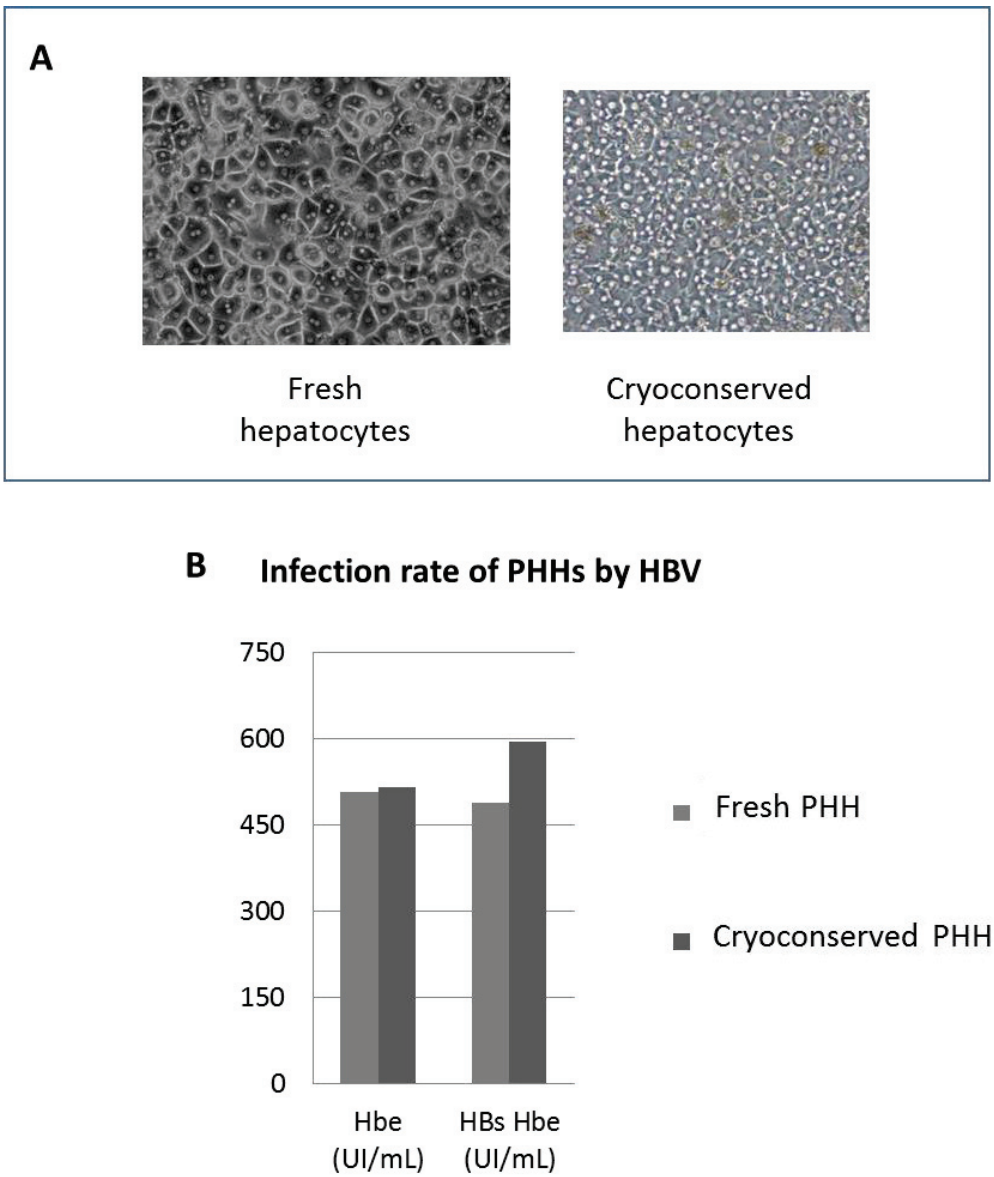

Figure 1. Comparison between fresh and cryopreserved hepatocytes. A. Contrast microscopy of hepatocytes monolayer before and after cryopreservation (200X). Photos were taken two days post-plating. **B.** Levels of the viral proteins HBeAg and HBsAg in cell culture supernatant, after HBV infection of fresh (light grey) and cryopreserved hepatocytes (dark grey). HBV virions were obtained by concentration of HepG2 2.2.15 cell culture supernatants. Infection was pursued for 6 days and quantification of the viral antigens was done by ELISA.

PHH for *in vivo* humanisation

After testing *in vitro* the quality of cryopreserved hepatocytes, their *in vivo* functionality was investigated with respect to their capacity to repopulate FRG mouse livers after liver injury, thus leading to chimeric mice with a humanised liverd.

Seven batches of cryopreserved PHHs were tested. Briefly, cells were thawed, counted and 500 000 viable hepatocytes were injected intrasplenically in two FRG mice with chemically-induced liver destruction. Two vials of each batch were tested. A commercial batch of cryoconserved hepatocytes was used as a positive control for which the humanization efficacy was found to be excellent. Humanization was assessed by measuring the level of human serum albumin in the mice sera every 3 weeks. It was considered that albumin levels exceeding 10-12mg/mL, reflect a mouse liver fully humanized *i.e.* when the human hepatocytes replaced around 90% of murine hepatocytes and took over the animal's hepatic functions. For cryopreserved hepatocytes as well as for the commercial hepatocytes, we observed a progressive increase in the level of human serum albumin that reached more than 10mg/mL at week 14 (**Figure 2**). After 14 weeks following humanization with both cryopreserved and commercial hepatocytes, the level of albumin diminished, probably related to the degradation of the animal general condition. At the end of the study, mice were sacrificed, and the morphology of the liver was analyzed by histology with H&E staining. Human hepatocytes were found to represent more than 80% of the volume of the liver (data not shown).

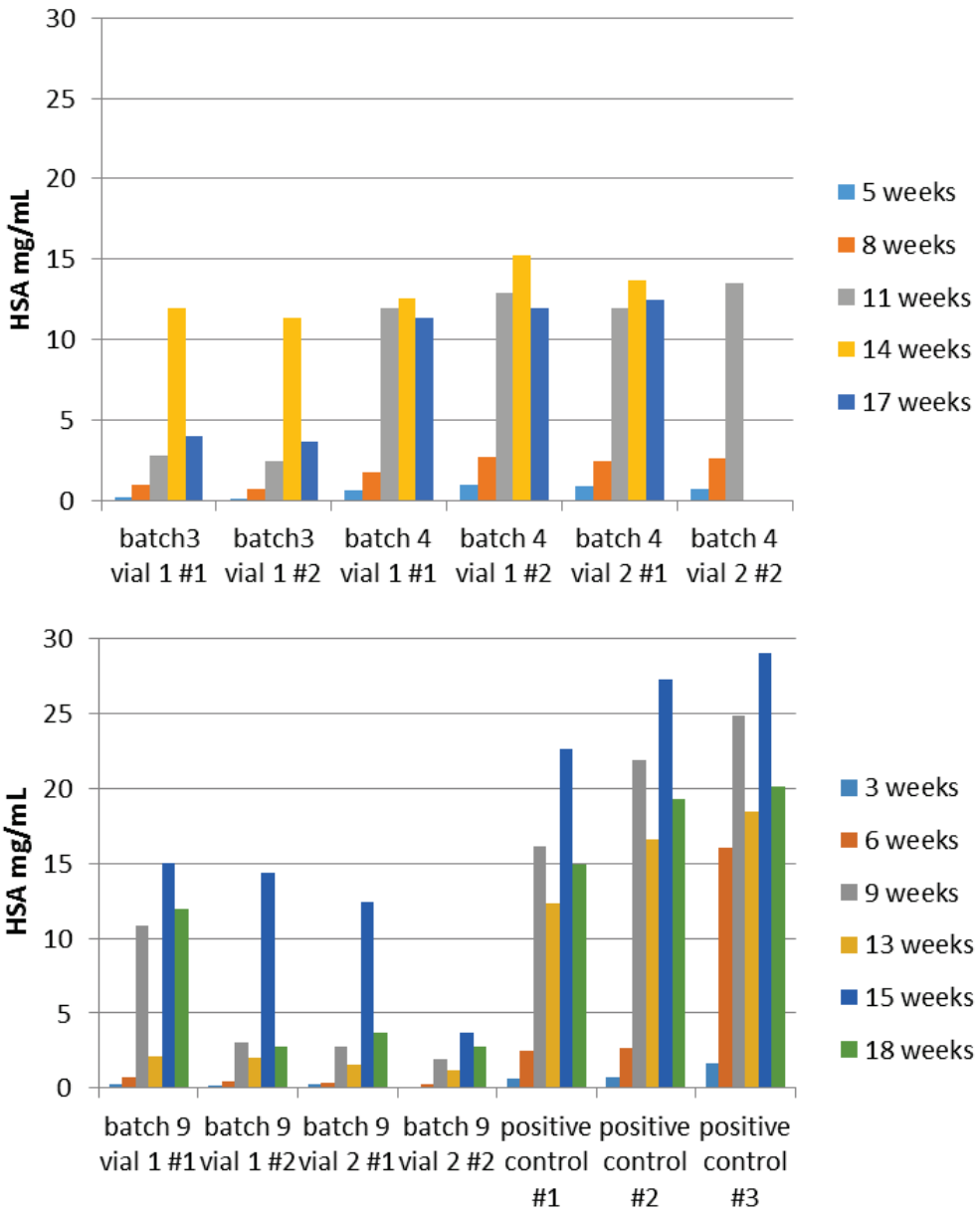

Figure 2. Human serum albumin (HSA) concentration in the sera of FRG mice with humanized livers. For each of the three batches of cryopreserved hepatocytes, two vials (vial 1 and vial 2) were tested, and for each vial two recipient mice were injected (#1 and #2). HSA concentration after liver humanisation with home-made hepatocytes was less high than using commercial hepatocytes, but sufficiently high to consider mice livers as fully humanised. A commercial batch of cryoconserved hepatocytes was used as a positive control for which the humanization efficacy was found to be excellent.

Patient recruitment for tumour specimens' collection

Thirty patients were included in the preclinical study aimed at developing preclinical models of HCC. The clinical features of our series were common for Western patients with HCC treated by liver resection. The prevalence of viral factors was 27% and 10% for HCV and HBV infection, respectively (**Figure 3**). For the other patients, the main risk factor was alcohol abuse but for some of them no risk was identified. Mixed aetiologies were observed in 1 patient (3%) that was HCV positive and HBV spontaneously cured (anti-HBs and anti-HBc positive). There was a strong male predominance (97%). Since the tumour fragments were obtained from patients for whom surgery was prescribed, we can assume that only patients with early stages HCC were included (Child A and B).

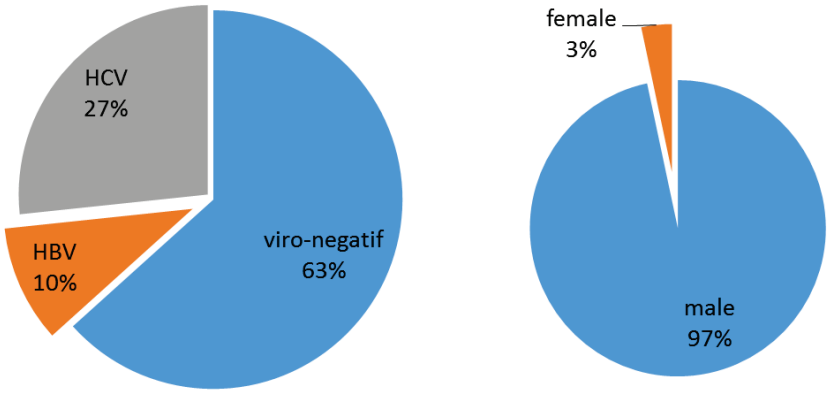

Figure 3. Prevalence of HCC aetiologies and patients gender in the IMODI cohort. Tumours were classified according to their HCC aetiology: 8 patients (28%) were HCV positive, 3 (10%) were HBV positive and 19(63%) were viro-negative; 29 patients were male (97%) and 1 patient was female (3%).

***In vitro* cell culture**

Three types of cell culture systems were tested with the aim of developing HCC cell lines from patients' tumour fragments (**Figure 4A**).

At first, HCC fragments were digested with the Tumour Dissociation Kit from Miltenyi Biotec. Most probably, this technique was extremely aggressive for HCC cells which seem to be quite sensitive to mechanical as well as enzymatic methods. Twenty-four hours after plating the cell mixture obtained by tissue digestion on collagen-coated plates, all cells were found floating in the media. A collagenase-based digestion technique was therefore preferred for tumour cell isolation. Contrary to the commercial kit, where the composition of the enzymatic cocktail is unknown and the concentrations of the enzymes cannot be adapted during the experiment, the classical digestion with collagenase is a protocol much more flexible that can be adjusted depending on the texture of the tissue. Indeed, big differences in tissue stiffness have been observed for HCC coming from individual patients.

The explant technique on collagen matrix yielded good results. For most of the tumour fragments, colonies of epithelial-like cells were observed circling the explant. These colonies were surrounded by fibroblast-like cells and the two cell types did not mix. Once the two cell populations arrived at confluency, cells would stop proliferating. At this point, cells were gently trypsinated or detached with enzyme-free dissociating buffers in order to try to amplify the epithelial-like cell population. However, cells did not survive to any of the dissociation attempts and no cell line was derived by this method. Probably explant culture conditions previous to cell dissociation could be improved so that cells would better tolerate cell detachment from the support. Additionally, other dissociation methods could be tested that would be less harmful to cells.

Regarding the 2D single cell culture technique following digestion with the collagenase, a primary cell monolayer was established with a good efficiency after plating (**Figure 4B**). For some HCC specimens, cell monolayers at 70% to 90% of confluency were observed as early as 24 hours after plating. This was probably due to cell attachment with a good efficiency rather than cell division, in view of such a short period of time after tissue digestion. Unfortunately, these primocultures would start to degrade after 1 week. Cells would become less and less numerous and those remaining would increase in size. By one month of culture, individualized cells were observed, with a big ratio cytoplasm/nucleus, typical for senescent cells. For some of these cells, several nuclei per cell were observed. Replicative senescence is a physiological process that appears in all cells except immortalised/ tumour cells, suggesting that the cells

observed in our cultures were not true tumour cells. The senescent phenotype could be confirmed by performing a staining of the senescence-associated β-galactosidase (SA-β-gal) marker as previously described (Dimri et al., 1995). In some cases, attempts were done to amplify these cells before they would go into replicative senescence. Following gentle trypsination, cells adhered again but after about one week they continued their natural course towards cell senescence. 2D culture was performed for the 30 HCC specimens but no cell line was derived.

Attempts to amplify the cancer stem cell population from the digestion mix have proven quite successful (**Figure 4C**). In most of the cases, we observed that spheres would form after 1 week of cell culture in low-adherence conditions. Once spheres were formed, they did not increase in size over time and they could not be amplified by trypsination and re-seeding in the same conditions.

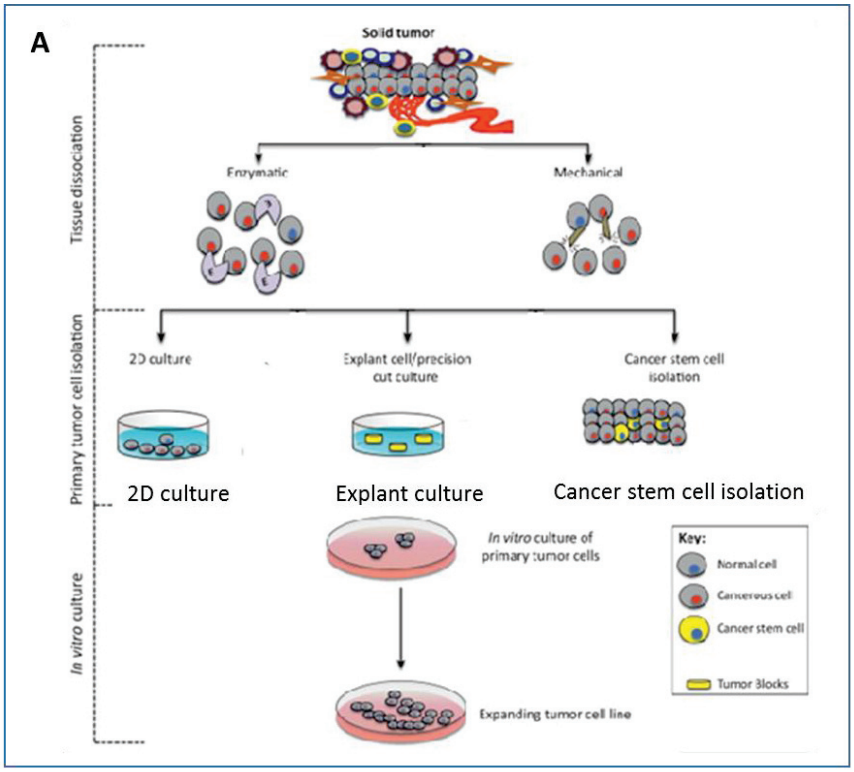

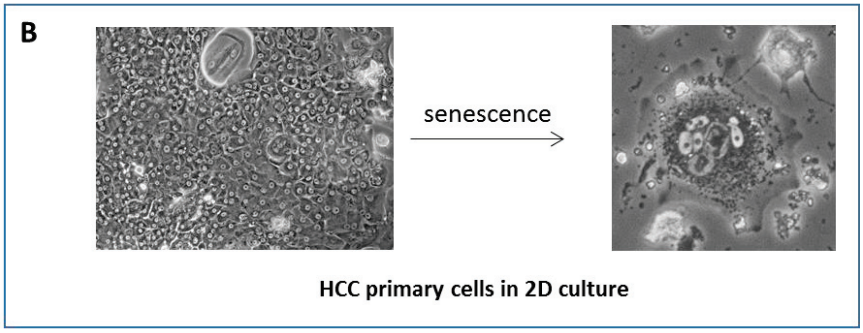

HCC primary cells in 2D culture

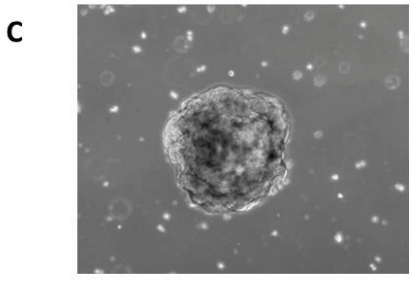

HCC primary sphere

Figure 4. *In vitro* culture of primary HCC cells coming from patient included in the IMODI cohort. A. Three culture systems were tested : explant fragments as well as monolayer and sphere conditions after tissue dissociation by chemical and enzymatic means. **B.** Monolayer cultures were obtained from primary HCC cells but over the time cells became senescent and could not be amplified (40x and 400x). **C.** Primary HCC sphere obtained after culturing primary HCC cells in low-adherence and in absence of serum (200x). The photos presented in this figure are representative of the results.

One model of HCC PDX

Twenty-eight of the thirty tumour samples were engrafted in immunodeficient mice for PDX development. The first 16 specimens were engrafted in BALB/c nude mice. Since no tumour growth was observed for these tumours, it was possible that the tumour fragment was eliminated by the mouse's remaining immune system. Therefore the following engraftments assays were performed on a more immunodeficient mouse strain, the NSG mouse strain. While nude mice are devoid of T cells, the NSG strain is even more immunodeficient since it does not possess T, B, and natural killer (NK) cells. Unfortunately, the efficacy of engraftment on NSG mice was not better.

Of the 28 specimens, only one gave rise to a PDX model called IM-LIV-516 (**Figure 5A**). The tumour originated from a 53 years old male patient. The patient was HCV positive and HBV spontaneously cured. He had a high AFP serum concentration of 542 ng/mL.

The primoengraftment of the tumour fragment was performed on a BALB/c nude mouse and the second passage as well as the amplification step of the model was done on the NSG strain in the hope to ensure better engraftment efficiency. The second passage was done three months after the primograft.

In order to confirm that the IM-LIV-516 model indeed originated from the human hepatocellular carcinoma fragment implanted, and that it retained the pathological features of the original tumour, the histology of the PDX tumours was performed and compared to that of the original tumour tissue collected from the patient. Tissue morphology was assessed by counterstaining with H&E as well as the tumour markers HepPar 1, Arginase 1, and Glypican 3. The histopathological staining as well as the analysis of these experiments was performed by Pr Dominique Wendum in Paris (Saint Antoine Hospital). Results showed that the IM-LIV-516 PDX tumours preserved similar histological, differentiation and immune-histochemical characteristics as the original tumour (**Figure 5B**). The original tumour as well as the transplanted PDX showed strong and homogenous staining for the Glypican 3 marker as well as focal staining for HepPar 1 and Arginase 1. In summary, the HCC PDX model IM-LIV-516 is moderately differentiated, positive for Glypican 3 and focally positive for Arginase 1 and HepPar 1, in the same manner as the original tumour.

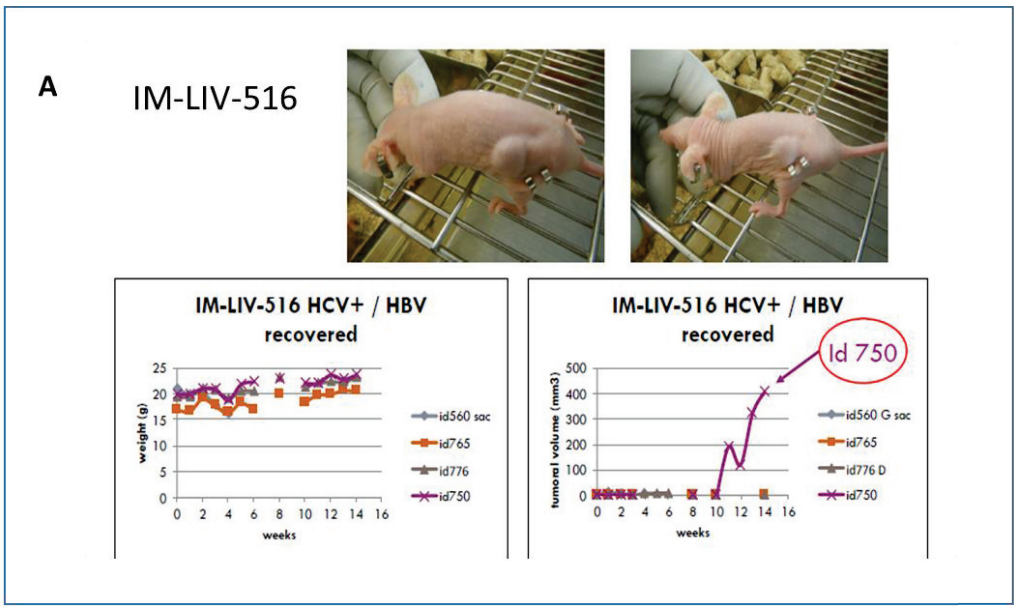

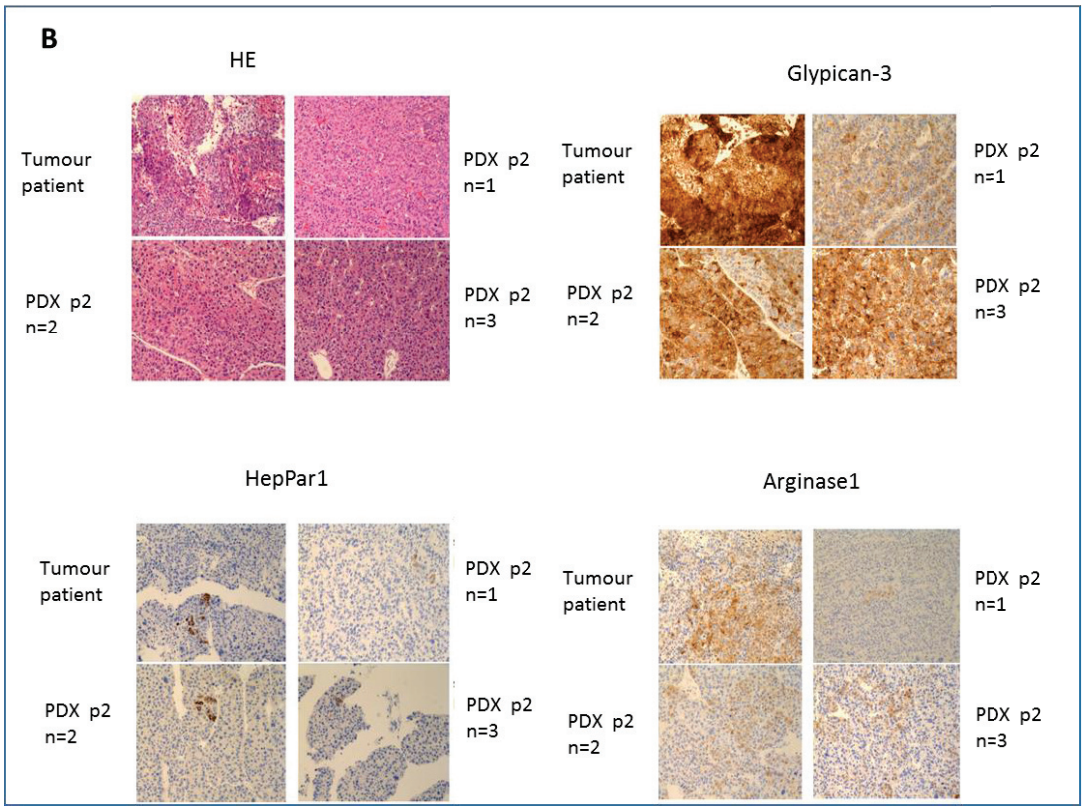

Figure 5. Development and characterization of the PDX model IM-LIV-516. A. IM-LIV-516 was derived from the HCC of a patient spontaneously cured from HBV and HCV positive. The tumour engraftment was not found to have cachexic properties as the animal's weight was constant (left panel). Tumour growth was observed 10 weeks after engraftment in one of the four xenografted immunodeficient mice (right panel). **B.** Histology of patient's tumour and xenografts of IM-LIV-516 from passages 1, 2 and 3 (p1, p2 and p3). H&E staining confirmed the moderate differentiation of the primary and xenografted tumours. Tumour markers Glypican-3, HepPar 1 and Arginase 1 confirmed the human HCC origin of the PDX tumour as well as the maintenance of the main histological features.

HBV replication could be reactivated in the tumour

Since the PDX model IM-LIV-516 was derived from a patient previously infected with HBV and HCV, it was possible that tumour cells allow the replication of the virus. As no other PDX model has been described for viral-induced HCC, it is not known whether the sub-cutaneous xenografted tumour itself can produce HBV and/or HCV virions. In patients it could be very difficult to assess whether tumour cells are able of sustain the replication of the HBV and/or HCV virus in the context of an infected liver.

The presence of viral genomic DNA and RNA was tested both inside IM-LIV-516 mice tumours as well as in sera. The quantification of HBV and HCV genomes was performed by RT-qPCR, a technique already described before, both for HBV as well as for HCV (El-Shamy et al., 2016; Lucifora et al., 2008). The analysis was performed on several passages of the PDX in order to determine whether proliferation of HCC cells would finally lead to loss of replication or, on the contrary, to its reactivation. Serum samples were collected at passages 1, 3 and 5 while tumour samples were collected at passages 2, 3 and 5.

Neither HBV DNA nor HCV RNA has been detected inside the PDX tumours at either of the investigated passages. On the contrary, we found HBV circulating DNA even though at relatively very low levels (**Table 1**).

Sample	qPCR VHB copies /ml	qPCR VHC copies/ml
Serum IM-LIV-5156 passage 1	**N=1 139** **N=2 33**	**NEGATIVE**
Serum IM-LIV-516 passage 3	**N=1 922** **N=2 811**	**NEGATIVE**
Serum IM-LIV-516 passage 5	**N=1 190** **N=2 NEGATIF**	**NEGATIVE**
Tumour IM-LIV-516 passage 2	**NEGATIVE**	**NEGATIVE**
Tumour IM-LIV-516 passage 3	**NEGATIVE**	**NEGATIVE**
Tumour IM-LIV-516 passage 5	**NEGATIVE**	**NEGATIVE**

Table 1. Virological parameters of the PDX model IM-LIV-516. The genomes of HBV and HCV were quantified in the sera and tumours of mice by RT-qPCR. The detection threshold was 160 copies/mL for HBV and 1200copies/mL for HCV. Viral HBV genome was found in the sera of 5 out of 6 animals, while HCV viral genome was undetected.

Discussion

Despite the fact that numerous efforts are done worldwide to improve HCC treatment and cancer in general, HCC still remains a disease difficult to treat. This is tightly linked to the heterogeneity of the disease, explained by the patient's clinical history and the natural history of the tumour. Knowing that at the moment there are only few experimental tools reflecting this patient variability, it becomes extremely difficult to develop targeted and efficient therapies against this type of cancer.

Clinical trials are the time-limiting step in the development of new therapies as they require large number of patients, are expensive and they can expose patients to fatal outcomes. However, only very few clinical trials lead to the commercialisation of efficient antitumour compounds with an acceptable toxicity.

Experimental models of human cancers are thus a very valuable tool that could be used to select the most effective molecules to enter clinical trials as they closely mimic clinical situations observed in patients.

The aim of the IMODI project is to develop and characterise new experimental models of human cancer. The project is focused on the development of primary models *i.e.* models developed directly from fresh human samples. Primary models were shown to be most suited for testing new drug candidates, very useful in the process of biomarker validation, help to predict patients' response to therapies and leads to a better selection and stratification of patients in clinical trials.

More precisely, these models consist of *in vivo* amplification of tumours in immunodeficient mice, called PDX models as well as establishment of new cancer cell lines. These two models are extremely useful both for the bio-medical industry and in the academic research.

Maintaining *in vivo* a human tumour by implanting it in immunodeficient mice provides a renewable tissue resource. It has been shown that from a biological point of view, PDX models resemble the original human tumours regarding their cytogenetic, genetic or phenotypic characteristics. PDX models can also be useful to study synergisms in combined therapies, to predict their toxicity or efficacy or detect antagonistic effects. Coupled to imaging techniques, it is possible to observe treatment effects at the vascular level or at the tumour's metabolic level.

In this context, we have recruited 30 patients with resectable HCC for the development of PDX models and HCC cell lines. One PDX model was established, named IM-LIV-516 and significant progress was done in performing *in vitro* culture of primary human HCC cells. Another PDX

model has been derived from a cholangiocarcinoma collected at La Pitié-Salpétrière Hospital (IM-LIV-019). Its histological characterisation is currently under progress.

The PDX model IM-LIV516 was established from a patient with HCC on HBV and HCV infection background. The model was shown to recapitulate the features of the original tumour in terms of histopathology. The original and the PDX tumour were found positive for the markers Arginase 1, Glypican 3 and HepPar 1. The HepPar 1 antigen is employed as a positive marker for histopathologically differentiating HCC from metastatic carcinoma (Hanif and Mansoor, 2014). The use of this marker is particularly useful for poorly differentiated HCC where tumour cells lose the hepatocyte-specific morphology. Glypican-3 has been described as a highly reliable marker in differentiating benign hepatocellular lesions (such as hepatocellular adenoma) from HCC (Capurro et al., 2003; Hsu et al., 1997; Midorikawa et al., 2003; Nakatsura et al., 2003; Zhu et al., 2001).

From the 30 patients that have been included, this was the only case with a double infection by HBV and HCV. No previous studies reported whether tumour aetiology is correlated with the engraftment efficiency in immunodeficient mice. In the present case, it is possible that the original tumour was more aggressive due to the synergy between cellular mechanisms that the two viruses trigger to induce cell transformation. One of these mechanisms (but probably not the only one) could be linked to the emergence of cancer stem cells, described in the case of both HBV and HCV infection (Arzumanyan et al., 2011; Fan et al., 2016; Ali et al., 2011).

Cancer stem cells have high tumourigenic potential and possess tumour-initiating properties. Regarding the contributions of cancer stem cells to the efficiency of generating PDX models, it should be noted that the patient had an abnormally high level of AFP of 542 ng/mL at the time the surgery was performed. High levels of AFP together with EpCAM positivity were described as poor prognosis factors in HCC patients thus associated with tumour aggressiveness (Yamashita et al., 2008). The presence of cancer stem cells could be investigated in the PDX tumours by performing staining against EpCAM and CD133 markers.

The virological status of HBV and HCV was assessed in both IM-LIV-516 mice sera as well as inside the tumours. It confirmed the presence of HBV viral genome in the blood of the mice but not inside the PDX tumours while HCV was negative both in the blood and the tumours. It should be noticed that the patient was considered as viro-suppressed for HBV, but still infected by HCV. This result raised several questions such as: Where is the HBV in the blood coming from? Is it linked to HBV replication or HBV integration in the genome of the HCC cells? Why was HBV detected but not HCV?

One of the major differences between HBV and HCV is that HBV viral DNA can integrate into the host genome. In our case, it is indeed possible that HBV had partially integrated into the genome of the HCC host cells. Thus, the viral sequence is transcribed by the transcriptional machinery of HCC cells. However, in that case, the mRNA level within the tumour tissue should be in a greater amount than the free RNA circulating in the animal's blood and more easily detectable.

The most probable source of HBV in the blood is the replication of the virus by the tumour cells. However, in this case, it is surprising that HBV was not detected inside the tumours. One of the explanations could be that our detection method is not sensitive enough to detect very low levels of HBV. In the literature, reports concerning the replication of HBV in HCC cells are contradictory. As such, in HCC patients with chronic HBV infection, it has been described that at the time the HCC appears, cancerous hepatocytes no longer allow viral DNA replication and do not express HBcAg, although HBsAg can be detected in approximately 20% of cases (Wang et al., 1991). The core protein, which is required for replication, is detected in only 15% of HCC cases but only in a minor fraction of tumour cells (Hsu et al., 1989). On the contrary, other reports demonstrated the persistence of intermediates of replication in tumour liver cells from patients with HCC and suggested that they may not normally be encapsidated (Raimondo et al., 1988). Finally, it has been recently reported that cccDNA can be found both in tumour or non-neoplastic liver tissue of patients with HCC and that cccDNA copy number correlates with the level of circulating HBs (Wang et al., 2016a). Thus, in our case, additional analysis by quantification of the HBV viral proteins both in the tumour and serum, could shed some light on the question regarding HBV replication in tumour-bearing mice. Quantification of HBsAg viral protein by ELISA in the serum is a very good method for assessing active infection. In addition, measurement of HBeAg in the serum is considered as a strong reliable test for HBV replication.

Another explanation for the presence of HBV DNA in the blood of mice could be due to the release of dying or viable HCC cells in the bloodstream. An abundant literature describes the use of circulating tumour DNA, called liquid biopsy, and its huge potential to serve as a biomarker for early detection, real-time monitoring of treatment response and prediction of tumour metastasis/recurrence, especially for HCC (Tang et al., 2016; Zhou et al., 2016a).

Regarding the replication of HCV inside the liver tumoural tissue, although some previous investigations have shown no difference in the presence and levels of HCV RNA between the tumour and nontumour liver tissues from HCV-associated HCC patients, others have reported low to undetectable levels of HCV RNA within the tumour (Dash et al., 2000; Gerber et al.,

1992; Harouaka et al., 2016; Haruna et al., 1994; Horiike et al., 1993; Kobayashi et al., 1994; Sobesky et al., 2007). On the basis of these observations, three hypotheses rise regarding the absence of detection of HCV in the tumour and serum of our PDX IM-LIV-516 model: (i) the tumour cells from the patient do not contain the HCV virus; (ii) the tumour cells from the patient do not allow the replication of the HCV RNA-genome; (iii) our detection method is not sensitive enough.

Very few studies have described the development of PDX models from human HCC and none of them from a viro-positive tumour (Cheung et al., 2016; Gu et al., 2015). The reason for the absence of a large panel of PDX models is probably linked to the low efficiency of engraftment. In our case, this issue represented the main limit in the development of a panel of PDX models of HCC. HCC is not the only tumour type for which the IMODI consortium had difficulties to obtain PDXs. At present, only one PDX from multiple myeloma, 2 from lymphoma and 0 from prostate carcinoma were established, whereas many PDXs were obtained for breast, lung, ovarian and pancreatic carcinomas. The absence of tumour growth in mice can be linked both to the viability of the tumour cells at the time of engraftment, as well as the graft intake rate by the mice. One of the adjustements that could be done is to try to improve the transport procedure of the tumour fragments from patients to the animal facility, by testing other transport media as well as transporting the samples in temperature-controlled conditions. Secondly, the low intake rate of tumours in the recipient organism could be related to the mouse strain used and/or the engraftment site. Another axis of the project, not discussed here, tested the efficiency engraftment when performed subcutaneously or orthotopically. No better results were obtained for the orthotopic engraftment.

In order to validate the HCC PDX model IM-LIV-516, a more profound characterisation could be considered. Apart for the three markers that were assessed, several others are interesting of testing. Several reports identified subgroups of patients positive for the stem-cell like markers CK19, EpCAM and AFP. They suggested that these HCC are enriched in CSCs and were associated with poor prognosis (Kim et al., 2011; Yamashita et al., 2008). EpCAM is strongly expressed in several types of human cancers from epithelial origin. The function and the regulation of EpCAM are not clearly elucidated to date. In the adult liver, hepatocytes are negative for EpCAM. On the contrary, in the embryonic liver, most of hepatocytes express EpCAM. In the cirrhotic liver, EpCAM is expressed in the proliferative region next biliary canaliculi, considered as the place where hepatic progenitor cells reside. The same pattern of expression has been described for CK19 and AFP, while a small difference that CK19 is also a marker for cholangiocytes, the hepatic epithelial subtype forming the bile canaliculi. The

reason why some patients have a very poor prognosis is mainly related to primary or secondary resistance of cancer to treatment as well as relapse post-surgery, both attributed to CSCs. CSCs have a high tumourigenic capacity and are capable by themselves to initiate tumour growth. Histological assessment of the expression of these three markers would allow determining whether the PDX model IM-LIV-516 is enriched in CSCs, in which case it would represent an excellent model predicting the response to treatment for a sub-group of HCC patients with poor prognosis.

A second axis of characterisation is the immune infiltrate in these tumours. A new emerging field in oncology is the immune response to tumour formation. Tumour cells were shown to modulate the host immune system in order to stop their elimination, by expressing immune-checkpoint molecules. The better example in this case is the couple PD1 & PD-L1. PD-L1 (*programmed cell death 1*) expressed by some tumour cells is the ligand of the PD1 receptor present at the membrane of cytotoxic T cells, B cells and myeloid cells. The coupling PD1 – PD-L1 inhibits the proliferation of T cells and can induce immune cells' death (Topalian et al., 2016).

Thirdly, genetic characterisation of the model would allow classifying it according to the molecular classification previously established (see Fig. 14 of introduction). We expect that IM-LIV-516 will be close to human HCC that are poorly differentiated, with an HBV aetiology, genetic instability, *TP53* mutation and expression of stemness markers, thus, belonging to the G1-G3 subgroup of HCCs.

A cryoconservation method for primary human hepatocytes was established and can be easily adapted in any lab performing isolation of PHHs. Regarding the humanisation capacity of the cryopreserved hepatocytes, we observed a lower level of human albumin in the sera of mice humanised with these cells compared to the commercial batch of hepatocytes used as a positive control. The difference could be due to the young age of this particular donor (8 years). Nevertheless, most commercial batches of cryopreserved hepatocytes tested were found to yield comparable results to what was found for the cryopreserved hepatocytes in the lab (F. Fusil personal communication).

The efficiency of cryoconservation is not reproducible between liver donors. This could be in part due to the health condition of the donor. Indeed, liver fragments originated from patients suffering of a colorectal carcinoma with liver metastases and might exhibit impaired liver function linked to treatment as well as steatohepatitis, fibrosis or mild cirrhosis. Moreover, the perfusion procedure is very much dependent on the morphology of the liver fragment. When the entry points for the perfusion are large, the digestion buffer will be easily and uniformly

distributed inside the tissue. This will require a shorter perfusion and lead to preservation of cells' quality.

In perspective, we plan to perform orthotopical HCC engraftment in mice with humanised liver which could strongly increase the engraftment efficiency and represent a more adapted model for the preclinical studies.

Materials and Methods

Primary human hepatocytes isolation and culture

Primary human hepatocytes (PHHs) were isolated from liver resections obtained from patients undergoing surgery for colorectal metastases in the liver at the Center Léon Berard. Only the liver parenchyma surrounding the metastasis was used for hepatocyte isolation, which would have otherwise been disposed of. Appropriate consent was obtained from all patients. Hepatocytes were isolated by a two-step collagenase perfusion technique as previously described (LeCluyse et al., 2005). Cell viability was assessed by trypan blue exclusion and hepatocytes were sedimented by centrifugation for 1min at 170g. The hepatocyte suspension was adjusted to 1 million viable cells per millilitre of complete medium (William's medium supplemented with 5µg/mL bovine insulin, $5*10^{-5}$ M hydrocortisone hemisuccinate (Roche Diagnostics), 50 U/mL penicillin/ 50µg/mL streptomycin (Invitrogen), and 10% fetal calf serum (FCS, Fetal Clone II, Hyclone)). Cells were plated in cell culture dishes previously coated with collagen at a seeding density of 150 000 cells/cm^2. After incubation for 16h at 37°C, 5%CO_2 and 95% humidity, cell medium was replaced with fresh cell medium without serum in order to eliminate non-attached cells and limit the proliferation of fibroblasts. Twenty-four hours later and then every 2 or 3 days, medium was changed with fresh complete culture medium containing 10% FCS.

Primary human hepatocytes cryoconservation and thawing

Primary human hepatocytes were prepared for cryopreservation immediately after liver perfusion. No additional step of cell purification was performed. Cells were washed once with PBS and suspended in pre-cooled cryoconservaton medium CS10 (Sigma) at a final cell density of $5*10^6$ /mL. One mL of the cell suspension was distributed in each cryovial. Vials were put into a pre-cooled isopropanol freezing chamber, incubated for 10min at +4°C and then stored at -80°C. After 24 hours, the vials were removed from the isopropanol freezing chamber and left at -80°C in a storage box. For storage longer than 1 week, cells were transferred in liquid nitrogen.

For functional assays, hepatocytes were thawed at least 1 week later after freezing. Hepatocytes were thawed by putting the cryovial into a water bath at 37°C immediately after taking it out of the liquid nitrogen container. The vial was removed from the water bath when a small ice cube still remained inside. Five hundred microliters of complete cell medium was added into the vial in order to dilute the DMSO-containing freezing media that is toxic for cells

at room temperature. The suspension of hepatocytes was diluted in 6mL of complete medium and centrifuged for 1min at 170g in order to eliminate the DMSO and dead cells. Hepatocytes were suspended in complete medium and plated in the same manner as fresh hepatocytes.

***In vitro* LDH dosage**

Cell death was assessed by lactate dehydrogenase (LDH) release. The level of LDH release was measured in hepatocytes culture supernatants with the Lactate Dehydrogenase Activity Assay Kit (Sigma) according to the manufacturer's instructions. Cell supernatants were collected every 3 days starting from day 4 post-plating.

***In vitro* albumin dosage**

The level of human albumin secreted by hepatocytes cultured *in-vitro* was measured in culture supernatant. Continuous secretion of albumin from hepatocytes is an indicator of well-being. Human albumin was measured by enzyme-linked immunosorbent assay (ELISA) with the kit Human Serum Albumin DuoSet ELISA (R&D Systems) according to the manufacturer's instructions. Cell supernatants were collected every 3 days starting from day 4 post-plating.

In vitro infection of hepatocytes by HBV

The *in-vitro* infection assay of primary human hepatocytes by HBV was performed with the expertise of Dr Olivier Hanz and Dr Laetitia Gerossier, two members of our team. Concentrated culture supernatant of HepG2 2.2.15 cell was used to inoculate cells as previously described (Glebe et al., 2001; Luangsay et al., 2015). Cells were infected with the concentrated infectious supernatant, 1000-fold diluted in the culture medium supplemented with 4% PEG and 0.42mg/mL hydrocortisone. The infection was pursued for 16h at 37°C. At the end of the incubation, cells were washed three times with culture medium and complete medium was added (see composition above). The level of infection was assessed by measuring the level of the viral antigens HBeAg and HBsAg in the supernatants 9 days post infection. HBsAg and HBeAg were quantified in the medium by ELISA kit (Autobio Diagnostics Co., China) following manufacturer's instructions.

Humanization of mice liver with cryoconserved hepatocytes

The functionality of cryopreserved hepatocytes was assessed *in vivo* by investigating their capacity to repopulate mice livers partially depleted in murine hepatocytes. The liver humanisation experiments were performed in the laboratory of Floriane Fusil and Francois Loic Cosset at the International Center for Infectiology Research (CIRI) in Lyon. The FRG (Rag2−/− Il2rg−/− Fah−/−) mouse strain was employed where immunodeficient mice (for innate and

adaptive immunity) are depleted of the fumarylacetoacetate hydrolase (Fah) gene (Azuma et al., 2007). Since accumulation of the toxic metabolite fumarylacetoacetate could induce liver damage, mice were treated with NTBC in order to prevent it. Previous to the humanization process, administration of NTBC was stopped, leading to liver damage. PHHs were then injected in order to restore the population of the hepatic cells. A selection pressure operates between human and remaining mouse damaged hepatocytes because of fumarylacetoacetate accumulation. Cryopreserved PHHs were thawed as described above and one million cells in suspension were injected in the mice spleen. Human hepatocytes localized in the liver and repopulate the empty spaces left by the murine hepatocytes. The damaged liver will provide physical support for the implantation of human hepatocytes as well as liberating stimulatory signals favoring proliferation. The repopulation of liver was assessed every three weeks by quantification of the human albumin in the serum. At the end of the study, mice were euthanized for liver examination. Liver fragments were collected, fixed in 4% formaldehyde, embedded in paraffin and stained with H&E in order to assess their morphology.

HCC samples specimens

Fresh tumour samples were collected from patients undergoing surgery for removal of HCC at the Hopital de la Croix Rousse, Lyon, France. Appropriate consent was obtained from patients. Thirty patients were recruited for the study over a period of time of two-years. The clinical history of these patients was collected in an eCRF database. Patients were recruited independently of their virological status (HBV and/or HCV) and patients positive for HIV or HTLV1&2 were excluded. All experimental procedures were conducted in accordance with French laws and regulations and were approved by the Ethics Committee. Tumours were collected within 15 minutes following tumour resection in order to preserve tumour cell viability. Two fragments were collected in the core of the HCC nodule and placed in two separate jars, containing pre-cooled sterile 'transport medium' AXIQ (Life Science Production) and transported on ice. One fresh fragment was dedicated to the development of PDX and the other to HCC patients-derived cell lines. A third fragment was collected at the site adjacent to the fragment intended to xenograft and placed in 4% formol for the histological characterization of the tumour. A fourth fragment was collected in the same manner as the third one and frozen in dry ice for later genetic analysis.

***In vivo* xenograft**

Six to eight weeks-old female Balb/c nude or NSG mice (Charles River) were used for implantation of patient tumour fragments. Two animal facilities performed the engraftment of

the fresh tumour sample. Non-viral HCC (negative for HBV, HCV, HIV and HTLV 1&2) were engrafted in a pathogen-free animal facility at "Laboratoire des Modèles Tumoraux", Centre Léon Berard in Lyon. Tumours that were HBV and/or HCV positive were engrafted in an A3 animal facility belonging to the CIRI. The engraftment was performed subcutaneously, in both sides of the flanks of mice. Mice were monitored for tumour growth for at least 6 months after tumour implantation. The histopathology of these tumours and the immunohistochemistry characterization were performed by Pr Dominique Wendum and Dr Francoise Praz in order to confirm the human origin as well as the maintainance of the original tumour characteristics.

Viremia in tumours

PDX models developed from patients HBV and/or HCV positive were tested for the presence of HBV and HCV genomes in the serum and in the tumour grafts. In both cases, nucleic acids were extracted with the MasterPure RNA purification kit from Epicentre. Nucleic acids were extracted following manufacture's instructions from 50 µL of serum or a small tumour fragment of about $1mm^3$.

HBV DNA was quantified as previously described by real-time PCR using the primers 5'-GCTGACGCAACCCCCACT-3' (forward) and 5'-AGGAGTTCCGCAGTATGG-3' (reverse) (Lucifora et al., 2008). An iCycler MyiO thermocycler (96-well format; Bio-Rad) was used with an iQ SYBR Green Supermix kit.

For the quantification of the HCV genome, HCV RNA was reverse transcribed (RT) using MMLV Reverse Transcriptase (Invitrogen) on 10µL of the extracted nucleic acid mixture (for the serum samples) or on 1000ng of RNA (for the tissue samples). The RT reaction was performed at 25°c for 10mn, followed by 37°c for 50mn, and finally 70°c for 15mn. Amplification was performed by RT-qPCR on 5µL of the cDNA by using the following primers: forward 5'-GTCTAGCCATGGCGTTAGTA-3' and reverse 5'-CTCCCGGGGCACTCGCAAGC-3'. The following amplification programme was used: preincubation at 95°C for 180 seconds; 30 cycles of amplification at 95°C for 15 seconds, at 60°C for 30 seconds, at 72°C for 30 seconds; melting at 95°C for 60 seconds, at 65°C for 60 seconds and at 97°C for 1 seconds; cooling at 37°C for 60 seconds.

Primary HCC cell isolation and *in vitro* culture

Primary HCC cells were cultured *in vitro* after isolation from fresh human tumour samples collected as described above. At first, the commercial tissue digestion kit *Tumor Dissociation Kit* (Miltenyi Biotec) was tested. Since the results were not satisfactory, the protocol was changed and three *in vitro* culture systems were tested: conventional 2D culture, culture as

explants and culture in non-adherent conditions. Tumour samples weighting approximately one gram were washed with PBS buffer and then minced into small pieces with a sterile scalpel. For the tumour explant culture, several tiny fragments inferior to $1mm^3$ were taken and put in cell culture dishes coated with collagen. After a brief dried up incubation at 37°C, 5% CO_2 and 95% humidity, complete culture medium was added (several culture media were tested, the same as for the 2D culture described below). The rest of the tumour sample was digested with 0.025% collagenase (Sigma) diluted in Hepes buffer containing 0.075% CaCl2 and 0.5mg/mL Deoxyribonuclease I from bovine pancreas (Sigma). The tumour homogenate was incubated for 10min at 37°C and mixed every 3min by shaking the jar up and down. The single-cell suspension was diluted with complete cell culture medium containing 10% heat-decomplemented FCS to neutralize the collagenase. Cells were washed twice with the same medium. Viable cells were separated from dead cells and cell debris by a gradient centrifugation on Percoll 1/12 (GE Healthcare) and washed again with PBS to eliminate silica traces from Percoll. Cells were resuspended in 100µl of PBS buffer. 10µL of the cell suspension were taken and added into 12mL of tumorospheres medium (William's medium supplemented with 2mM GlutaMAX (Invitrogen), 5µg/ml bovine insulin, $5*10^{-5}$ M hydrocortisone hemisuccinate (Roche Diagnostics), B27 (Life Technologies), 20ng/mL EGF (R&D Systems), 20ng/mL bFGF (StemCell Technologies) and 4µg/mL heparin) and equally distributed in ultra-low adherence 6-well plates (Corning). The rest of the tumour cell suspension (90µL) was added into 12mL of complete cell culture media and distributed in cell culture dishes coated with collagen. Several cell media were tested in order to optimize cell platting and proliferation: IMDM (Sigma)(supplemented with 10% heat-decomplemented FCS), EMEM (ATCC) (supplemented with 10% heat-decomplemented FCS), DMEM (supplemented with 10% heat-decomplemented FCS) and William's (supplemented with 10% heat decomplemented FCS, 2mM GlutaMAX (Invitrogen), 5µg/mL bovine insulin and $5*10^{-5}$ M hydrocortisone hemisuccinate (Roche Diagnostics)). Culture medium was changed the next day to eliminate dead cells and then replaced with fresh medium twice a week. Epithelial cell colonies were observed and passaged by gentle trypsination or with enzyme free cell removal buffer. Cells were observed via inverted phase-contrast microscope.

ARTICLE

Differentiated human hepatocytes can be transformed *in vitro* and gain epigenetic changes and cancer stem cell properties

Floriane PEZ [1, 2, 3], Patricia GIFU [1, 2, 3], Davide DEGLI ESPOSTI [4], Nadim FARES[1, 2, 3], Anaïs LOPEZ [1, 2, 3], Lydie LEFRANCOIS [1, 2, 3], Maud MICHELET [1, 2, 3], Michel RIVOIRE [5], Brigitte BANCEL [6], Bakary S. SYLLA [7], Zdenko HERCEG [4], Claude CARON DE FROMENTEL [1, 2, 3*], Philippe MERLE [1, 2, 3, 8*]

[1] INSERM U1052 CNRS UMR5286, Centre de Recherche en Cancérologie de Lyon, France

[2] Université Lyon-1, France

[3] Centre Léon Bérard, Lyon, France

[4] Epigenetics Group, International Agency for Research on Cancer (IARC), Lyon, France.

[5] Département de Chirurgie et Institut de Chirurgie Expérimentale, Centre Léon Bérard, Lyon, France

[6] Hospices Civils de Lyon, Service d'Anatomopathologie, Groupement Hospitalier Lyon Nord, France

[7] Molecular Biology Group, International Agency for Research on Cancer (IARC), Lyon, France.

[8] Hospices Civils de Lyon, Service d'Hépatologie et Gastroentérologie, Groupement Hospitalier Lyon Nord, France

[*] co-last authors.

Running Title: Paradigm for primary human hepatocyte transformation.

Key words: hepatocellular carcinoma, transformation, primary human hepatocytes, epigenetic

Financial Support: This work was supported by French grants: PAIR-CHC 2009 (contract #2009-143, project ENELIVI) from Institut National du Cancer (INCa), and the Ligue Nationale Contre le Cancer (LNCC). F Pez and N Fares are supported by the French National Institute of Cancer (INCA), A Lopez by the French Ligue Nationale Contre le Cancer (LNCC). P Gifu was supported by the IMODI consortium.

Corresponding author: Pr Philippe Merle, UMR Inserm U1052 CNRS5286, Centre de Recherche en Cancérologie de Lyon, 151 cours Albert Thomas, 69424 Lyon cedex 03, France.

Phone: (+33) 472681954; Fax: (+33) 472681971; E-mail: philippe.merle@inserm.fr

Conflicts of Interest: No conflict of interest to declare.

Word count: ***3819***, excluding Title page, Abstract, References and Figures legends.

Number of figures and tables: 6 figures, 1 table.

Supplementary material: one supplementary "Materials and Methods" and 7 supplementary figures.

List of abbreviations in the order of appearance

PHH, primary human hepatocytes; $SV40^{LT}$, SV40 large T antigen; $SV40^{ST}$, SV40 small T antigen; $HRAS^{V12}$, oncogenic RAS; hTERT, human telomerase reverse transcriptase subunit; lncRNA, long non coding RNA; RT-qPCR, Reverse transcription-quantitative real-time RT-PCR; FACS, Fluorescence-activated cell sorting; HCC, Hepatocellular carcinoma; FCS, foetal calf serum; DMSO, dimethyl sulfoxide; MMLV-RT, Moloney murine leukemia virus reverse transcriptase; MTT, 3-(4,5-Dimethylthiazol-2-yl)-2,5-diphenyltetrazolium bromide; PBS, phosphate buffer saline; RT, room temperature; PI, propidium iodide; FACS, fluorescence activated cell sorting; BSA, bovine serum albumin; DAPI, 4',6-diamidino-2-phénylindole; HE, hematoxylin and eosin; EV, empty vector; AAT, Alpha-1 antitrypsin; CYP3A4, CYP2B6, cytochrome P450 3A4, 2B6; HNF4, hepatocyte nuclear factor-4; TAT, tyrosine aminotransferase, TDO, tryptophan 2,3-dioxygenase; DLK1, delta-like homolog 1; EpCAM, Epithelial cell adhesion

molecule; HCV, hepatitis C virus; EMT, epithelial-mesenchymal transition; pRb, retinoblastoma protein; CSC, cancer stem cell; DEGs, differentially expressed genes; RT, room temperature.

ABSTRACT ***word count: 244***

Human hepatocarcinogenesis is a complex process in which the early changes initiating transformation and the liver cells most permissive to this process are poorly identified. In order to address these issues, we have made use of an innovative model based on primary human hepatocytes (PHH) lentivirus-transduced with SV40, $HRAS^{V12}$ and hTERT genes. The differentiation program of these transduced-PHHs was characterized by total RNA sequencing including lncRNAs, and the expression of hepatocyte and stemness markers confirmed by RT-qPCR and immunofluorescence. In addition, their ability to cycle was monitored by FACS and transformation capacity assessed by colony formation in soft agar and tumorigenicity in immunodeficient mice. $HRAS^{V12}$ triggered senescence in the PHHs whereas co-expression with SV40 antigens, in association or not with hTERT, led to the cancerous transformation of some clones. These latter clones were characterized by a poorly differentiated phenotype with expression of stemness and mesenchymal-epithelial transition markers and gave rise to cancer stem cells. *In vivo*, they resulted in poorly differentiated hepatocellular carcinoma with a reactivation of endogenous hTERT. These proof-of-principle experiments have demonstrated for the first time that non-cycling human mature hepatocytes can be permissive to *in vitro* cancerous transformation through a dedifferentiation process. This tool provides a means to identify the role and impact of genetic/epigenetic changes associated with the initiation of hepatocarcinogenesis, as well as to explore the potential role of liver progenitors and stem cells as a first step to set up a comprehensive *in vitro* paradigm for human hepatocarcinogenesis.

INTRODUCTION

Hepatocellular carcinoma (HCC) is a poor prognosis tumor ranking third in terms of the most frequent cause of cancer death worldwide (1). Hepatocarcinogenesis is a complex process combining the accumulation of widely heterogenous genetic and epigenetic changes that occur during the initiation, promotion, and progression of the disease. Common alterations have been identified, such as the deregulation of p53, the Wnt pathway, ErbB receptor family members and $p16^{(INK4a)}$ (2). Nevertheless, the early changes leading to the initiation of transformation and the identity of the liver cells most permissive to this process are poorly characterised. The Weinberg oncogene combination, *i.e.* SV40 large T antigen ($SV40^{LT}$), SV40 small T antigen ($SV40^{ST}$), oncogenic RAS ($HRAS^{V12}$), and human telomerase reverse transcriptase subunit (hTERT) (3, 4), has been used in many human primary cell types including fibroblasts, mammary and bronchial cells, in order to better characterize the initiation of the transformation steps during *in vitro* transformation (5). In rodents, numerous cell types, including primary hepatocytes, have been successfully transformed *in vitro* by the $SV40^{LT+ST}$ and $HRAS^{V12}$ combination and recently, it has been demonstrated that such a strategy leads to primary mouse hepatocyte transformation regardless of the cell differentiation state. These results indicate that any cell type in the mouse hepatic lineage can initiate HCC (6-8). However to date, little is known about the transformation of primary human hepatocytes (PHH), since only immortalized hepatocyte cell lines seem to be permissive (9). In order to address this, we have set up the first model of *in vitro* cancerous transformation of PHH.

MATERIALS AND METHODS

Cell culture and transduction

PHHs were isolated from freshly resected normal liver tissue from three individuals undergoing surgery for colorectal adenocarcinoma liver metastasis (Centre Léon Bérard Resource Biological Centre, ministerial agreements #AC-2013-1871 and DC-2013-1870). Signed informed written consent was obtained from patients before surgery. Histological analysis was performed to ensure the absence of microscopic tumour invasion. The two-step collagenase (0.05%, Sigma-Aldrich C5138) perfusion method was used and cells were seeded at confluence in collagen-coated plates (10). They were maintained for 3 days in William's medium devoid of foetal calf serum (FCS), supplemented with 100UI/mL penicillin-G, 100µg/mL streptomycin, 5µg/mL insulin, and 5.10^{-5}M hydrocortisone hemisuccinate, and then grown in complete William's medium containing 10% FCS and 1.8% DMSO. The HuH7 cell line, used as control in tumorigenicity experiments, was cultured in RPMI1640 medium supplemented with 10% FCS, 100UI/mL penicillin G, 100µg/mL streptomycin, 1% non-essential amino acids and 0.01M Hepes buffer.

The pLenti6-RASV12 vector was obtained by inserting the RAS^{V12} gene from pBabe-puro Ras^{V12} (Addgene) into the pLenti6 lentiviral vector (Invitrogen), by using the Gateway technology (Invitrogen). The same strategy was used to transfer hTERT from pBabe-hygro hTERT (Addgene) into the plenti6 vector. pLenti CMV/TO SV40 small + Large T (Addgene) was also used. Virions from lentiviral constructs encoding human $HRAS^{V12}$, $SV40^{ST+LT}$ or hTERT were produced in 293FT cells (Invitrogen), and PHHs were transduced at a multiplicity of infection of one (MOI-1) in a medium with 6µg/mL polybrene. Cells were then selected with 300µg/mL geneticin ($SV40^{ST+LT}$) and/or 3µg/mL blasticidin ($HRAS^{V12}$) and/or 200µg/mL zeocin (hTERT). Lentiviral particles containing empty vector (EV) were used as controls.

RNA extraction, RNA sequencing and real-time quantitative PCR (RT-qPCR)

Total RNA was extracted using Extract-all (Eurobio) from two independent experiments, according to the manufacturer's instructions. About 3.5 µg of total RNA was ribodepleted using the Ribozero kit (Epicentre) and then cDNA libraries for PHH-EV, PHH-$SV40^{LT+ST}$ and PHH-$SV40^{LT+ST}$/$HRAS^{V12}$ samples were prepared following the Illumina protocol. Libraries were single-end 50 bp sequenced on an Illumina HiSeq

2500 sequencer. Fastq files underwent a first quality control to assess the quality of sequencing data. Raw reads were aligned on the human genome GRCh38. After filtering not aligned reads or reads with multiple alignments, sequencing depth ranged from 26 to 40 million of aligned reads.

Immunofluorescence

Cells were plated on glass coverslips in a 12-well plate. Twenty four hours later, cells were fixed in 4% paraformaldehyde and then permeabilized in PBS-0.1% saponin (30min at room temperature (RT)). After saturation in PBS-3% BSA-0.1% saponin, cells were incubated (1hour at RT) with a primary antibody against either vimentin (EP21), CK19 (EP72), CK18 (EP30) (Epitomics), albumin (15C7; AbCam), or N-Cadherin (13A9; Upstate). After washing with PBS-0.1% saponin an alexaFluor488 or 555-conjugated secondary antibody against mouse or rabbit IgG (Dako) was added (30min/ RT). Finally, coverslips were washed with PBS-0.1% saponin, incubated (5min/ RT) with 0.25µg/mL DAPI prior to mounting in Vectashield medium (Vector Laboratories) and analyzed using a Nikon fluorescence microscope.

Cell growth determination

Growth curves of PHH-SV40^{ST+LT}, PHH- SV40^{ST+LT}/HRAS^{12V} and PHH-SV40^{ST+LT}/ HRAS^{12V}/hTERT were compared using cell counting and 3-(4,5-Dimethylthiazol-2-yl)-2,5-diphenyltetrazolium bromide (MTT). Cells were seeded at a density of $1.5x10^4$/cm² in complete medium with 10% FCS. For the 1% FCS cell growth assay, after overnight plating, cells were washed twice in PBS-1X, and complete medium with 1% FCS added to the flasks. MTS assay (Promega) was done every day according to the manufacturer's instructions. Two independent experiments were conducted in triplicate.

Flow cytometry

For cell cycle analysis, cells were harvested in a citrate/sucrose/DMSO buffer 48h after seeding. Then, RNA was digested and DNA content was stained with propidium iodide (PI) (CycleTest Plus kit, Becton Dickinson). The cell cycle distribution was determined using a FACScan flow cytometer (Becton Dickinson), according to the manufacturer's instructions.

Soft agar assay and soft agar colonies isolation

About 5.10^3 cells were seeded in 6-cm dishes with culture medium containing 0.35% noble agar, overlaid on culture medium containing 0.7% noble agar. Liquid medium was refreshed every 5 days and cultures were maintained for 4 weeks when colonies (> 0.15 mm) were then counted. For soft agar colonies isolation, macroscopic colonies formed in the semi-solid medium were isolated, trypsinized and re-plated for sub-culture.

Hepatospheres formation

Cells were collected after trypsinization in 15mL tubes containing 8mL of complete medium and centrifuged for 5min at 200g. The supernatant was discarded and the pellets were resuspended in PBS 1X buffer at 10^6cells/mL. For each cell line, cells were then diluted to 1.6 10^4 cells/mL in 2mL of serum-free hepatosphere medium (William's media supplemented with 100UI/mL penicillin G, 100µg/mL streptomycin, 1% non-essential amino acids, 0.01M Hepes buffer, B27 1/50, EGF 10µg/mL, bFGF 20µg/mL, heparin 4µg/mL). 0.5mL of this dilution was dispensed in two wells of a 24-well ultra-low adherence plate (BD). Photos of spheres were taken 4 days after seeding. Each condition was performed in duplicate.

Nude mice tumorigenicity

BALB/c nude mice (Charles River) were maintained in accordance with Rhone-Alpes ethics committee for animal experimentation and institutional and national guidelines. Transduced-PHHs ($1x10^6$) were implanted subcutaneously into the flanks of 5-week-old females. Food and water were given ad libitum. Mice were sacrificed when the tumor size reached 1 cm^2 following ethical committee recommendations, or systematically after 6 months post-injection. Immediately after sacrifice, the tumors were removed and divided into two parts: one piece for freezing in liquid nitrogen, and the second for fixation in 4% buffered formalin and paraffin embedded. Sections were cut from the paraffin block and stained with hematoxylin and eosin (H&E).

Statistical Analysis

Continuous variables and proportions were compared using the Mann-Whitney (Wilcoxon for paired samples), *t*-Student (paired samples t-test when appropriate) and Chi-squared $P< 0.05$ were considered as significant (MedCalc Version 12.7.1.0). Differential expression analysis and pathway analysis on RNA-sequencing data were performed as previously described (11). Genes were considered as differentially expressed at family-wise error rate (FWER) < 0.01 (Bonferroni correction) and with absolute fold change higher than 2.

RESULTS

Specific isolation of PHHs and impact of lentiviral transduction on their proliferative capabilities

As previously described (12), PHHs are non-dividing cells resting in G_0-phase of the cell cycle. Morphological analysis using light microscopy 7 days after isolation showed cubic binucleated cells that formed a confluent monolayer. They maintained this morphology throughout the three weeks culture period. By immunofluorescence (IF), PHHs exhibited expression of hepatocyte markers [CK18$^{(+)}$, albumin$^{(+)}$], and absence of cholangiocyte [CK7$^{(-)}$, CK19$^{(-)}$], liver progenitor [EpCAM$^{(-)}$, CD133$^{(-)}$] and mesenchymal cell [vimentin$^{(-)}$] markers (Supplementary Fig. S1).

After lentiviral transduction of PHHs, the ectopic expression of transgenes was verified by western-blotting (Supplementary Fig. S2) and the morphology of cells assessed by phase contrast microscopy. PHH-EV cells resembled the parental hepatocytes, while the PHH-HRAS^{V12} cells displayed an oncogene-induced senescence phenotype (Fig. 1A). The PHH- SV40^{LT+ST} and PHH-SV40^{LT+ST}/HRAS^{V12} transduced cells dramatically changed morphology (Fig.1A) and re-entered the cell cycle as confirmed by FACS analysis (Fig. 1B). The growth rate was similar in PHH-SV40^{LT+ST} and PHH-SV40^{LT+ST}/HRAS^{V12} cells when cultured in 10% FCS (Fig. 1C). Under conditions of serum starvation (1% FCS), PHH-SV40^{LT+ST} transduced cells reduced their growth rate while the PHH-SV40^{LT+ST}/HRAS^{V12} cells continued to grow rapidly, indicating a markedly reduced dependence on external mitogen stimuli, one of the hallmarks of *in vitro* transformation (Fig. 1D).

Transformation of PHH and tumorigenicity

The assessment of anchorage-independent growth, another hallmark of *in vitro* transformation, showed that only the combination of SV40^{LT+ST}/HRAS^{V12} or SV40^{LT+ST}/HRAS^{V12}/hTERT expressed in the PHHs was associated with the ability to form colonies > 0.15 mm diameter in soft agar (Fig. 2). Six colonies from the PHH-SV40^{LT+ST}/HRAS^{V12} and PHH-SV40^{LT+ST}/HRAS^{V12}/hTERT cells were picked and subsequently expanded *in vitro* in 2D-cell subcultures: 6/6 PHH-SV40^{LT+ST}/HRAS^{V12}/hTERT agar colonies grew, while only 2/6 for PHH-SV40^{LT+ST}/HRAS^{V12}. Indeed, the majority (4/6) PHH-SV40^{LT+ST}/HRAS^{V12} subcultures underwent senescence (data not shown). All sub-clones that continued to grow were

characterized by the same morphology, the same growth rate and formed similar number of anchorage-independent colonies as their parental cells after a second soft agar sub-cloning assay (data not shown). In the two PHH-SV40^{LT+ST}/HRAS^{V12} clones that survived without replicative senescence, endogenous hTERT mRNA was detected (Supplementary Fig. S3). Interestingly hTERT mRNA showed a gradual increase in levels as the cells progressed towards a more transformed phenotype suggesting that the acquisition of hTERT expression is critical in this process (Table 1 and Supplementary Fig. S3).

To test the *in vivo* tumorigenic potential of the different cells, 10^6 PHH-SV40^{LT+ST}/HRAS^{V12}, or PHH-SV40^{LT+ST}/HRAS^{V12}/hTERT cells isolated after two rounds of soft agar growth and sub-culturing, were subcutaneously injected into immuno-deficient nude mice (two independent experiments with two animals per cell line). After three months of follow-up, tumors were detected in animals injected with both sub-clones (Fig. 3A). In contrast, injection of either 10^6 PHH-EV or PHH-SV40^{LT+ST} cells failed to give rise to tumors in nude mice within 6 months of follow-up, an observation consistent with previous data obtained from two human immortalized hepatocyte cell lines (9). Pathological analysis of the tumors arising in nude mice showed a poorly differentiated pattern of HCC infiltrating adjacent tissues (Fig. 3B, C). A second tumorigenic assay was performed by using an independent batch of transduced-cell lines, giving the same results.

Transcriptomic analysis

A transcriptomic analysis was carried out to identify the genes that showed altered expression profiles during the immortalization and transformation processes. A comparison of the immortalized PHHs (PHH-SV40^{LT+ST}) with the PHH-EV showed that this process was associated with a dramatic change in gene expression with 4,003 differentially expressed genes (DEGs) (FWER<0.01, FC>2): 2,139 down-regulated genes in PHH-SV40^{LT+ST} (among which was 186 lncRNAs) and 1,864 up-regulated (135 lncRNAs) compared to PHH-EV (Fig. 4A). 1,428 genes were differentially expressed (FWER<0.01, FC>2) in the next transformation stage: 692 genes were down-regulated (40 lncRNAs) and 736 up-regulated (83 lncRNAs) when the profiles of PHH SV40^{LT+ST}/HRAS^{V12} cells were compared to PHH-SV40^{LT+ST} (Fig. 4B). Most up-regulated genes showed an increased expression only in the later stages of this

immortalization/transformation process with changes being noted only in the PHH-SV40^{LT+ST}/HRAS^{V12} cells and with no differential expression between the PHH-EV and PHH-SV40^{LT+ST} cells (Fig. 4B). The DEGs clustered clearly in three sub-groups: i) one showing high expression in PHH-EV that was reduced in the PHH-SV40^{LT+ST} cells and remained low in the PHH-SV40^{LT+ST}/HRAS^{V12} cells; ii) a second showing an up-regulation only in the PHH-SV40^{LT+ST} cells; and iii) a third showing a gradual increase in expression as the cells move from the "normal" phenotype seen in the PHH-EV cells to intermediate levels in PHH-SV40^{LT+ST} cells and the highest levels in the fully transformed PHH-SV40^{LT+ST}/HRAS^{V12} cells.

Pathway analysis showed that genes up-regulated in PHH-SV40^{LT+ST} *vs.* PHH-EV cells are involved in cell cycle and cell proliferation pathways (including histone coding genes) (Fig. 4C). Interestingly, down-regulated genes in PHH-SV40^{LT+ST} were mostly associated with hepatic metabolism. Loss of HNF4A expression and its target genes (ALB, CYP450 and coagulation factor genes) indicated that immortalization was associated with a loss of liver cell differentiation (Fig. 4D). A comparison of PHH-SV40^{LT+ST}/HRAS^{V12} *vs.* PHH-SV40^{LT+ST} transcriptome showed that the up-regulated genes were mostly involved in the PI3k-Akt pathway (Fig. 4E) while down-regulated genes were enriched in cell-cell interaction pathways, although this trend was not very consistent across the different interrogated databases (Fig. 4F). Taken together, these results suggest that these two pathways are critical to induce the transformation of immortalized cells.

Most of the altered lncRNAs were upregulated during the transition from immortalized PHH-SV40^{LT+ST} towards the transformed PHH-SV40^{LT+ST}/HRAS^{V12} cells (Supplementary Fig. S4). The majority of them have not been previously identified associated with HCC, although a number of them have been described to be cancer-related (for example CCAT, CRNDE, LUCAT1, CASC8, CASC19). In contrast, HOTAIR, a well-known cancer promoting lncRNA, was found up-regulated already in the immortalized PHH-SV40^{LT+ST} cells, suggesting that its up-regulation is an early event in HCC development. These data showed that the PHH-EV cells clustered and were distinct from the immortalized (PHH-SV40^{LT+ST}) and transformed cells (PHH-SV40^{LT+ST}/HRAS^{V12}) (Supplementary Fig. S5).

Immortalization and transformation of PHH is associated with a dedifferentiation process

As suggested by the large-scale transcriptome analysis, hepatocyte dedifferentiation occurred during the immortalization/transformation process as confirmed by the assessment of the expression of a panel of gene transcripts by RT-qPCR (Table 1). In comparison to the PHH-EV cells, the PHH-SV40^{LT+ST} and PHH-SV40^{LT+ST}/HRAS^{V12} cells harbored a striking decrease of hepatocyte-specific markers: *ALBUMIN*, *AAT*, *CYP3A4*, *CYP2B6*, *HNF4*, *TAT*, *TDO*. The levels of *KRT18* epithelial marker were already lowered in the PHH-SV40^{LT+ST} cells and showed no further decrease in the PHH-SV40^{LT+ST}/HRAS^{V12} cells, while the *KRT19* progenitor marker showed high levels in the immortalized PHH-SV40^{LT+ST} cells and lower levels in the poorly differentiated transformed PHH-SV40^{LT+ST}/HRAS^{V12} cells. Those data were confirmed at the protein level by IF in the PHH-SV40^{LT+ST} and PHH-SV40^{LT+ST}/HRAS^{V12} cells (Fig. 5) by comparison to PHH (Supplementary Fig. S1): a sequential decrease of hepatocyte and epithelial markers (Albumin, CK18) and appearance of mesenchymal markers (vimentin, N-cadherin) were noted. Also, CK19, a progenitor cell marker was up-regulated in PHH-SV40^{LT+ST} and its expression lost in PHH-SV40^{LT+ST}/HRAS^{V12} cells. Similar data were observed in HCC growing after heterotopic injection in nude mice (Table 1). In order to confirm that the transduced cells had changed differentiation status, we used HCV infection as an end point, as this can only occur in mature hepatocytes. Indeed, both the PHH-SV40^{LT+ST} and PHH-SV40^{LT+ST}/HRAS^{V12} cells had lost their functional capability to support HCV infection (Supplementary Fig. S6).

Transformation of PHHs is associated with acquisition of stemness markers and cancer stem cell (CSC) properties

As assessed by RT-qPCR, stemness markers such as DLK1, EpCAM, BMI, NANOG, OCT4, and SOX2 were mainly up-regulated in transformed PHH-SV40^{LT+ST}/HRas^{V12} compared to PHH-EV cells and were absent or modestly over-expressed in immortalized PHH-SV40^{LT+ST} cells. However, FZD7 and ΔNp73, associated to immaturity in several tissues, were strikingly up-regulated in the early steps of transformation, as suggested by an up-regulation in PHH-SV40^{LT+ST} cells and remained at higher levels in our model of fully transformed cells (PHH-SV40^{LT+ST}/HRAS^{V12} cells) (Table 1). FACS analysis showed that PHH-SV40^{LT+ST} and PHH-

SV40^{LT+ST}/HRAS^{V12} cells carried CD90 surface stemness marker as well as ALDH labeling, whereas they both were negative for others stemness markers, such as CD44v6 and CD133 (Supplementary Fig. S7). Confirming the increased stem-like phenotype of PHH-SV40^{LT+ST}/HRAS^{V12}, only these cells could give rise to hepatospheres in low attachment conditions, a classical assay for stem cells (Fig. 6). Taken together, these *in vitro* molecular and cellular characterizations indicate that dedifferentiation accompanied the immortalization step and was reinforced during full-transformation.

DISCUSSION

This study reports the use of normal differentiated adult hepatocytes of human origin (PHHs) to establish a model of *in vitro* hepatocarcinogenesis in which HCC cells with features of immaturity and CSC-like properties are generated. The *in vitro* transformation of hepatocytes of human origin has been previously reported although the cells used were not fully normal hepatocytes but the pre-immortalized HL-7702 and HL-7703 cell lines, transformed either by the SV40^{LT+ST}/RAS/hTERT combination (9) or RhoC (13). The transformed cells that we obtained showed a dedifferentiation program although keeping some features of their hepatocyte origin (expression of hepatocyte-specific markers), a phenomenon also described in rodent models (8). It is recognized that both the cell of origin and the type of cancer-predisposing genomic/epigenomic alterations will contribute to the phenotypic and molecular diversity of HCC. Both hepatic stem/progenitor cells and differentiated hepatocytes have been implicated as the potential cells of origin of HCCs. The expansion of progenitor cells in rodent hepatocarcinogenesis models and the frequent expression of stem/progenitor cell markers in experimental and human HCCs favor the hypothesis of progenitor cell origin at least for some HCCs (14-17). However in rodent, Holczbauer and collaborators provided conclusive evidence that the acquisition of stemness properties in HCCs is independent of the cell of origin (8). In their model, the expression of both SV40^{LT} and oncogenic HRAS^{V12} forced diverse hepatic cell lineages (primary hepatic progenitor cells, lineage-committed hepatoblasts and differentiated mature adult hepatocytes) to reprogram into HCC cells with some stemness and EMT traits, as also found in human tumors (18, 19). However, this present study is the first demonstration of *in vitro* transformation of human hepatocytes with these same traits involved.

While it is clear that cancers arise from the accumulation of genetic and/or epigenetic abnormalities that endow the malignant cell with the properties of uncontrolled growth and proliferation, the precise sequence of these events that program human hepatocarcinogenesis remains heterogeneous and unclear. The study of the transforming proteins derived from DNA tumor viruses in experimental models of transformation has provided fundamental insights into the process of cell transformation. Weinberg and collaborators reported for the first time that the co-expression of $SV40^{LT}$ and $SV40^{ST}$, *hTERT*, and $HRAS^{V12}$into normal human cells such as fibroblasts, kidney and mammary epithelia, converted these cells into a tumorigenic state (3, 20). However, this has never been investigated in hepatocytes. In the present study, we showed for the first time that the $SV40^{LT+ST}$ co-expression could immortalize PHHs and that the addition of $HRAS^{V12}$ could transform these cells. This process required the reactivation of telomerase either by spontaneous upregulation of the endogenous *hTERT* or directly by lentiviral transduction of *hTERT*. Transcriptome analysis showed that immortalization induced the greatest change in the gene expression profiles with a partial loss of cell identity, including a decrease of hepatocyte markers, such as albumin, CYP genes, coagulation factors, lineage-specific transcription factors, e.g. HNF4A being found. These results suggest that the loss of cell identity/dedifferentiation may be an early event in HCC development. Similar loss was also detected in the transcriptomic analysis from cirrhotic livers (P. Gifu, personal communication), which is recognized to be pre-cancerous tissue.

Although being a key driver for cancer development (21), the Ras oncoprotein provokes oncogene-induced senescence by activation of the p53/pRb gatekeepers, which serves as a major barrier to Ras-driven transformation in different kind of cells including hepatocytes (22). Indeed, in our model system the ectopic expression of $HRAS^{V12}$ alone, without previous immortalization by $SV40^{LT+ST}$, led to oncogene-induced senescence of PHH, strengthening the need of immortalization prior to transformation as has been reported in many models (23). In our experiments, $SV40^{LT+ST}$ expression allowed the G_0 phase-resting PHH cells to re-enter the cell cycle and reach immortalization as has been described with other proteins such as HCV core or HPV E6-E7 (24, 25). It is well established that expression of $SV40^{LT}$ in combination with an oncogenic allele of HRAS suffices to transform normal rodent cells (26) including hepatocytes (8). One of the mechanisms is the inactivation of the p53 and

retinoblastoma (pRb) tumor suppressor proteins through their interaction with $SV40^{LT}$. However, similar attempts to transform normal cells of human origin through immortalization with $SV40^{LT}$ alone, have mostly failed due to the cells entering into an irreversible growth arrest or undergoing apoptosis (27). Interestingly, $SV40^{ST}$ is able to boost $SV40^{LT}$ expression (28). This will, for instance, perturb the expression of the phosphatase 2A protein (4), and allow the $SV40^{LT}$-mediated inhibition of p53 that has been shown to contribute to the acquisition and maintenance of CSC properties (29) in addition to cell transformation.

We found that, among the lentivirus transduced PHHs giving rise to colonies in soft agar, all the PHH-$SV40^{LT+ST}$/$HRAS^{V12}$/hTERT-derived colonies were able to grow after subsequent subculture, whereas only one third of the PHH-$SV40^{LT+ST}$/$HRAS^{V12}$-derived colonies displayed the same capabilities. These latter colonies showed reactivation of the endogenous *hTERT*, thus preventing replicative senescence and enhancing cancerous transformation. The role of telomerase expression as an essential requirement for the neoplastic conversion of human cells has been controversial. In models in which normal human cells were converted to cancer cells by the combination of SV40 and oncogenic RAS, hTERT was originally described as essential (3). In other approaches using primary cultures of colon smooth muscle cells isolated from surgical specimens, ectopic SV40 and oncogenic HRAS rapidly transformed the cells growing *in vitro*, and they were tumorigenic in immunodeficient mice without a previous selection in culture (30). However, the cells in the resulting cancers showed morphological evidence of crisis, consistent with their lack of telomerase, thus supporting the concept that $HRAS^{V12}$ and SV40 form a minimal set of genes that can convert normal human cells to cancer cells without a requirement for hTERT (30). Another hypothesis would be that the $SV40^{LT+ST}$ and $HRAS^{V12}$ combination is able to reactivate the endogenous telomerase, either by direct impact or by a stepwise manner as described in mammary models of transformation driven by Wnt signaling (31).

In conclusion, the *in vitro* and *in vivo* characterization of the immortalized and transformed human, adult, mature hepatocytes has generated for the first time a paradigm for the study of the molecular and cellular events involved in hepatocarcinogenesis. This study highlights that hepatocytes are the cells targeted in this process as they are able to reacquire stemness and CSC properties, and the transcriptomic changes that are involved in this process.

This proof of concept model with the well-established SV40 and RAS combination could provide the experimental basis for the assessment of the contribution of other genetic and epigenetic changes implicated in human hepatocarcinogenesis and provides an assay system for the development of more effective therapeutic strategies.

ACKNOWLEDGEMENTS: RNA-sequencing was performed at the platform "Biopuce et sequençage" of the Institut de Biologie Moléculaire and Cellulaire, Strasbourg. The authors thank Sabrina Chesnais for her support in mice injections and Janet Hall for helpful discussions and English proofreading.

AUTHORSHIP CONTRIBUTIONS: F. P., P.G., D.D-E., N.F., A.L., L.L., M.M. performed experiments and data analysis. M.R. provided patients' samples. B.B. performed the histological analysis of mice tumors. B.S. and Z.H. were involved in the design of the study and revised the manuscript. F.P., C.C.F. and P.M. designed the study, analyzed data and wrote the paper.

REFERENCES

1. Ferlay J, Shin HR, Bray F, Forman D, Mathers C, Parkin DM. Estimates of worldwide burden of cancer in 2008: GLOBOCAN 2008. *Int J Cancer* 2010; 127: 2893-917.

2. Farazi PA, DePinho RA. Hepatocellular carcinoma pathogenesis: from genes to environment. *Nat Rev Cancer* 2006; 6: 674-87.

3. Hahn WC, Counter CM, Lundberg AS, Beijersbergen RL, Brooks MW, Weinberg RA. Creation of human tumour cells with defined genetic elements. *Nature* 1999; 400: 464-8.

4. Hahn WC, Dessain SK, Brooks MW, King JE, Elenbaas B, Sabatini DM, et al. Enumeration of the simian virus 40 early region elements necessary for human cell transformation. *Mol Cell Biol* 2002; 22: 2111-23.

5. Hahn WC. Experimental models of human cancer. *Cell Cycle* 2004; 3: 604-5.

6. Isom HC, Woodworth CD, Meng Y, Kreider J, Miller T, Mengel L. Introduction of the Ras oncogene transforms a simian virus 40-immortalized hepatocyte cell line without loss of expression of albumin and other liver-specific genes. *Cancer Res* 1992; 52: 940-8.

7. Jacob JR, Tennant BC. Transformation of immortalized woodchuck hepatic cell lines with the c-Ha-ras proto-oncogene. *Carcinogenesis* 1996; 17: 631-6.

8. Holczbauer A, Factor VM, Andersen JB, Marquardt JU, Kleiner DE, Raggi C, et al. Modeling pathogenesis of primary liver cancer in lineage-specific mouse cell types. *Gastroenterology* 2013; 145: 221-31.

9. Sun B, Chen M, Hawks C, Hornsby PJ, Wang X. Tumorigenic study on hepatocytes coexpressing SV40 with Ras. *Mol Carcinog* 2006; 45: 213-9.

10. Gripon P, Diot C, Guguen-Guillouzo C. Reproducible high level infection of cultured adult human hepatocytes by hepatitis B virus: effect of polyethylene glycol on adsorption and penetration. *Virology* 1993; 192: 534-40.

11. Degli Esposti D, Hernadenz-Vargas H, Voegele C, Fernandez-Jimenez N, Forey N, Bancel B, et al. Identification of novel long non coding RNAs deregulated in hepatocellular carcinoma using RNA-sequencing. *Oncotarget* 2016; 7: 31862-77.

12. Bhogal RH, Hodson J, Bartlett DC, Weston CJ, Curbishley SM, Haughton E, et al. Isolation of primary human hepatocytes from normal and diseased liver tissue: a one hundred liver experience. *PLoS One* 2011;6:e18222.

13. Xie S, Zhu M, Lv G, Geng Y, Chen G, Ma J, et al. Overexpression of Ras homologous C (RhoC) induces malignant transformation of hepatocytes in vitro and in nude mouse xenografts. *PLoS One* 2013;8:e54493.

14. Hytiroglou P. Morphological changes of early human hepatocarcinogenesis. *Semin Liver Dis* 2004;24:65-75.

15. Roskams T. Liver stem cells and their implication in hepatocellular and cholangiocarcinoma. *Oncogene* 2006; 25: 3818-22.

16. Woo HG, Lee JH, Yoon JH, Kim CY, Lee HS, Jang JJ, et al. Identification of a cholangiocarcinoma-like gene expression trait in hepatocellular carcinoma. *Cancer Res* 2010; 70: 3034-41.

17. Yeh MM. Pathology of combined hepatocellular-cholangiocarcinoma. *J Gastroenterol Hepatol* 2010; 25: 1485-92.

18. Polyak K, Weinberg RA. Transitions between epithelial and mesenchymal states: acquisition of malignant and stem cell traits. *Nat Rev Cancer* 2009; 9: 265-73.

19. Seok JY, Na DC, Woo HG, Roncalli M, Kwon SM, Yoo JE, et al. A fibrous stromal component in hepatocellular carcinoma reveals a cholangiocarcinoma-like gene expression trait and epithelial-mesenchymal transition. *Hepatology* 2012; 55: 1776-86.

20. Elenbaas B, Spirio L, Koerner F, Fleming MD, Zimonjic DB, Donaher JL, et al. Human breast cancer cells generated by oncogenic transformation of primary mammary epithelial cells. *Genes Dev* 2001; 15: 50-65.

21. De Vita G, Bauer L, da Costa VM, De Felice M, Baratta MG, De Menna M, et al. Dose-dependent inhibition of thyroid differentiation by RAS oncogenes. *Mol Endocrinol* 2005; 19: 76–89.

22. Donninger H, Calvisi DF, Barnoud T, Clark J, Schmidt ML, Vos MD, et al. NORE1A is a Ras senescence effector that controls the apoptotic/senescent balance of p53 via HIPK2. *J Cell Biol* 2015; 208: 777-89.

23. Newbold RF, Overell RW, Connell JR. Induction of immortality is an early event in malignant transformation of mammalian cells by carcinogens. *Nature* 1982; 299: 633-5.

24. Ray RB, Meyer K, Ray R. Hepatitis C virus core protein promotes immortalization of primary human hepatocytes. Virology 2000; 271: 197-204.

25. Tsuruga Y, Kiyono T, Matsushita M, Takahashi T, Kasai H, Matsumoto S, et al. Establishment of immortalized human hepatocytes by introduction of HPV16 E6/E7 and hTERT as cell sources for liver cell-based therapy. *Cell Transplant* 2008; 17: 1083-94.

26. Michalovitz D, Fischer-Fantuzzi L, Vesco C, Pipas JM, Oren M. Activated Ha-ras can cooperate with defective simian virus 40 in the transformation of non-established rat embryo fibroblasts. *J Virol* 1987; 61: 2648-54.

27. Sager R, Tanaka K, Cau CC, Ebina Y, Anisowicz A. Resistance of human cells to tumorigenesis induced by cloned transforming genes. *Proc Natl Acad Sci USA* 1983; 80: 7601-5.

28. Kolzau T, Hansen RS, Zahra D, Reddel RR, Braithwaite AW. Inhibition of SV40 large T antigen induced apoptosis by small T antigen. *Oncogene* 1999; 18: 5598-603.

29. Yi L, Lu C, Hu W, Sun Y, Levine AJ. Multiple roles of p53 related pathways in somatic cell reprogramming and stem cell differentiation. *Cancer Res* 2012; 72: 5635–45.

30. Liang S, Kahlenberg MS, Rousseau DL, Hornsby PJ. Neoplastic conversion of human colon smooth muscle cells: No requirement for telomerase. *Mol Carcinog* 2008; 47: 478-84.

31. Ayyanan A, Civenni G, Ciarloni L, Morel C, Mueller N, Lefort K, et al. Increased Wnt signaling triggers oncogenic conversion of human breast epithelial cells by a Notch-dependent mechanism. *Proc Natl Acad Sci USA* 2006; 103: 3799-804.

FIGURES AND TABLES

Table 1. Gene expression assessed by RT-qPCR in PHH-EV, PHH-SV40^{LT+ST} and PHH-SV40^{LT+ST}/HRAS^{V12} and in in PHH-SV40 $^{LT+ST}$ /HRAS^{V12} tumors developing subcutaneously in nude mice. Data were generated from 3 independent experiments, and normalized to PHH-EV. ND, not determined.

Gene expression Arbitrary value ± SD	PHH-EV	PHH-SV40	PHH-SV40/HRAS^{V12}	Subcutaneous tumors arising in nude mice
ALBUMIN	1 ± 0.1	$3.7\ 10^{-6} \pm 0.9\ 10^{-6}$	$3.9\ 10^{-5} \pm 0.6\ 10^{-5}$	$7\ 10^{-4} \pm 1\ 10^{-4}$
AAT	1 ± 0.21	$2\ 10^{-3} \pm 5\ 10^{-5}$	8.5 10-3 ± $3\ 10^{-4}$	4 10-3 ± $4\ 10^{-4}$
CYP3A4	1 ± 0.20	1.3 10-2 ± $3\ 10^{-3}$	$8\ 10^{-3} \pm 3\ 10^{-3}$	$5\ 10^{-4} \pm 5\ 10^{-5}$
CYP2B6	1 ± 0.26	0.002 ± 0.0005	0.013 ± 0.001	1.31 ± 0.55
HNF4	1 ± 0.16	$3\ 10^{-4} \pm 1\ 10^{-4}$	$4\ 10^{-4} \pm 2\ 10^{-4}$	$6\ 10^{-4} \pm 1\ 10^{-5}$
TAT	1 ± 0.31	$2\ 10^{-4} \pm 8\ 10^{-5}$	$4\ 10^{-4} \pm 1\ 10^{-6}$	$4\ 10^{-5} \pm 2\ 10^{-5}$
TDO	1 ± 0.14	0.01 ± 0.0002	0.01 ± 0.0002	0.001 ± 0.00001
KRT18 (CK18)	1 ± 0.31	0.24 ± 0.09	0.25 ± 0.02	0.57 ± 0.006
KRT19 (CK19)	1 ± 0.17	6.63 ± 1.18	0.33 ± 0.09	0.01 ± 0.005
hTERT	1 ± 0.29	1.93 ± 0.32	4.06 ± 0.15	3.72 ± 0.38
AFP	1 ± 0.26	0.01 ± 0.003	0.009 ± 0.003	ND
DLK1	1 ± 0.34	1.88 ± 0.89	7.32 ± 0.35	ND
EpCAM	1 ± 0.36	0.11 ± 0.02	1.76 ± 0.44	ND
BMI	1 ± 0.29	1.69 ± 0.29	2.15 ± 0.17	ND
NANOG	1 ± 0.31	0.78 ± 0.15	1.98 ± 0.40	ND
OCT4	1 ± 0.60	1.54 ± 0.59	2.21 ± 0.27	ND
SOX2	1 ± 0.22	1.30 ± 1.02	2.53 ± 0.05	ND
FZD7	1 ± 0.60	3.90 ± 0.30	5.40 ± 0.05	ND
ΔNp73	1 ± 0.01	24.0 ± 10.0	18.0 ± 0.05	ND

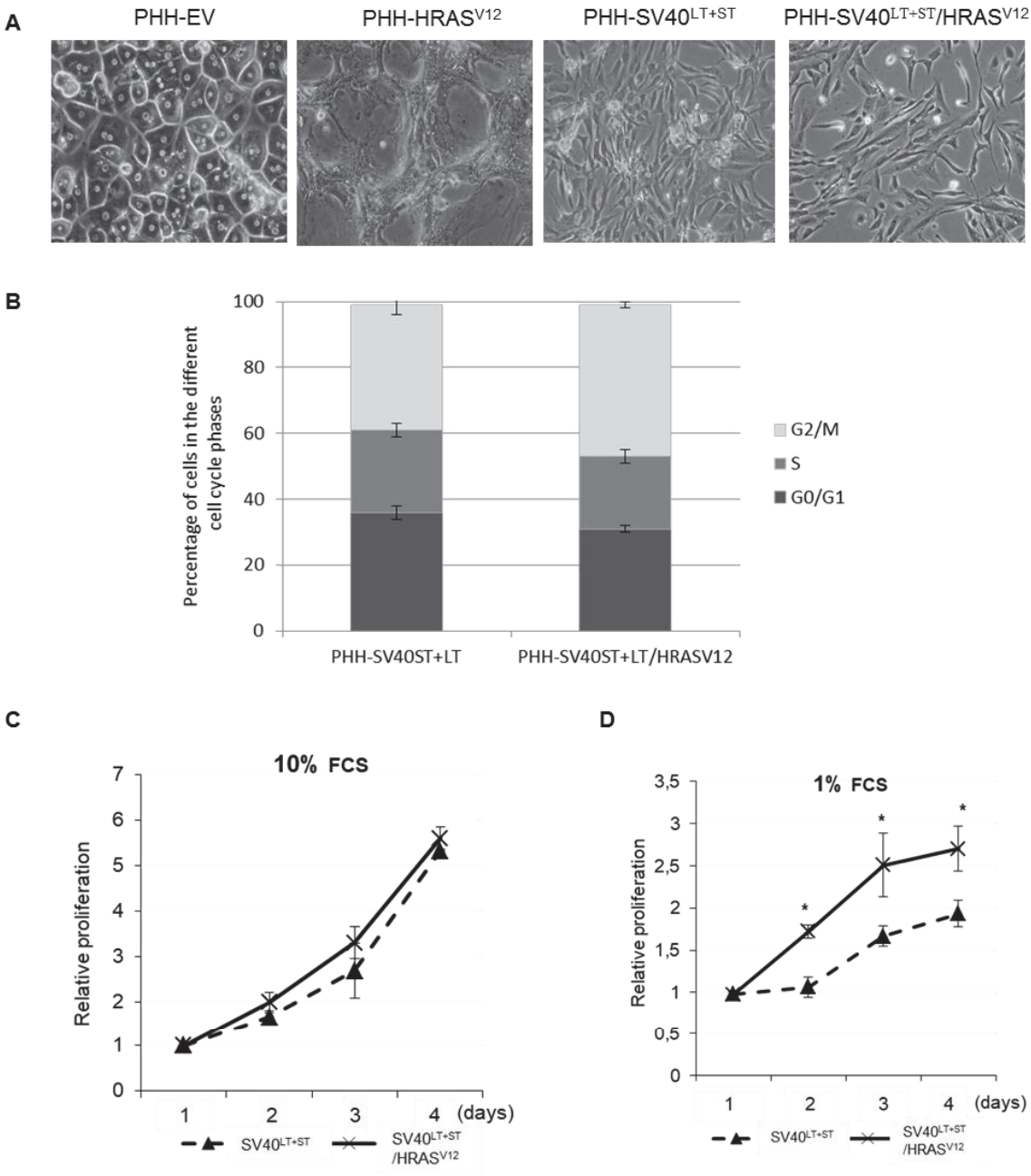

Figure 1. Morphology, cell cycle and proliferation of lentiviral-transduced cells. PHH-SV40^{LT+ST} and PHH-SV40 $^{LT+ST}$/HRAS^{V12}. Phase-contrast microscopy reveals a hepatocyte morphology for the PHH-EV cells, whereas PHH-HRAS^{V12} display a senescent phenotype and PHH-SV40^{LT+ST} and PHH-SV40^{LT+ST}/HRAS^{V12} resemble an epithelial non-hepatocyte morphology. Pictures are representative of those obtained in three independent experiments (magnification, 200x) (A). Propidium Iodide staining and FACS analysis shows that PHH-SV40^{LT+ST} and PHH-SV40^{LT+ST}/HRAS^{V12} cells are actively cycling; n=3 (B). Cell growth, as evaluated by MTS, of PHH-SV40^{LT+ST}/HRAS^{V12} and PHH-SV40^{LT+ST} is similar in the presence of 10% FCS (C), but only PHH-SV40^{LT+ST}/HRAS^{V12} showed a significant growth in serum-deprived medium (D). Non-parametric Mann-Whitney test between PHH-SV40^{LT+ST}/HRAS^{V12} *vs.* PHH-SV40^{LT+ST} was used for each time-point, from three independent experiments; (*) $P < 0.05$.

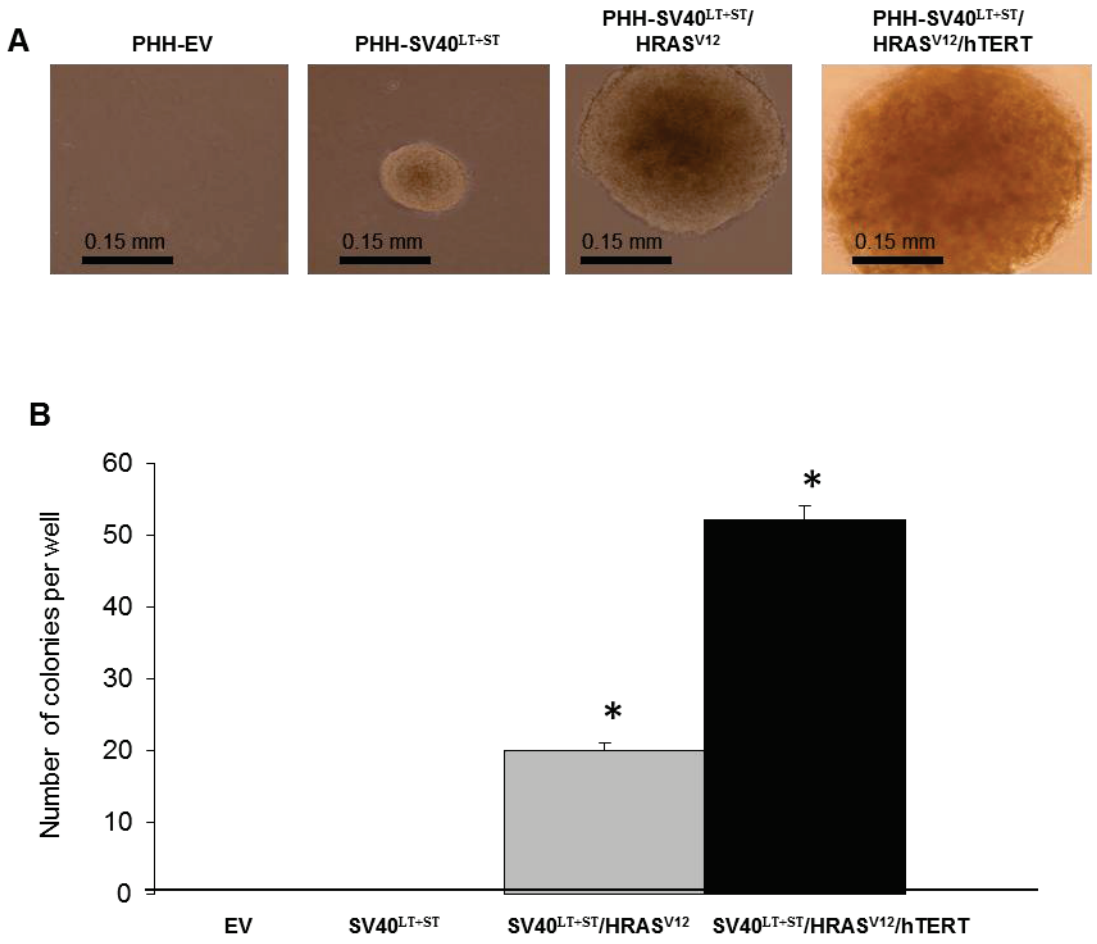

Figure 2. PHH-EV, PHH-SV40^{LT+ST}, PHH-SV40^{LT+ST}/HRAS^{V12} and PHH-SV40^{LT+ST}/HRAS^{V12}/hTERT growth in anchorage-independent conditions. (A) Microscopic view of colonies from soft agar assays in 6-well plates (magnification, 100x). (B) Colonies > 0.15 mm diameter were counted. Data is the mean of three independent experiments in duplicate. Non-parametric Mann-Whitney test between PHH-SV40/HRAS^{V12} and PHH-SV40 *versus* PHH-EV; * $P < 0.05$.

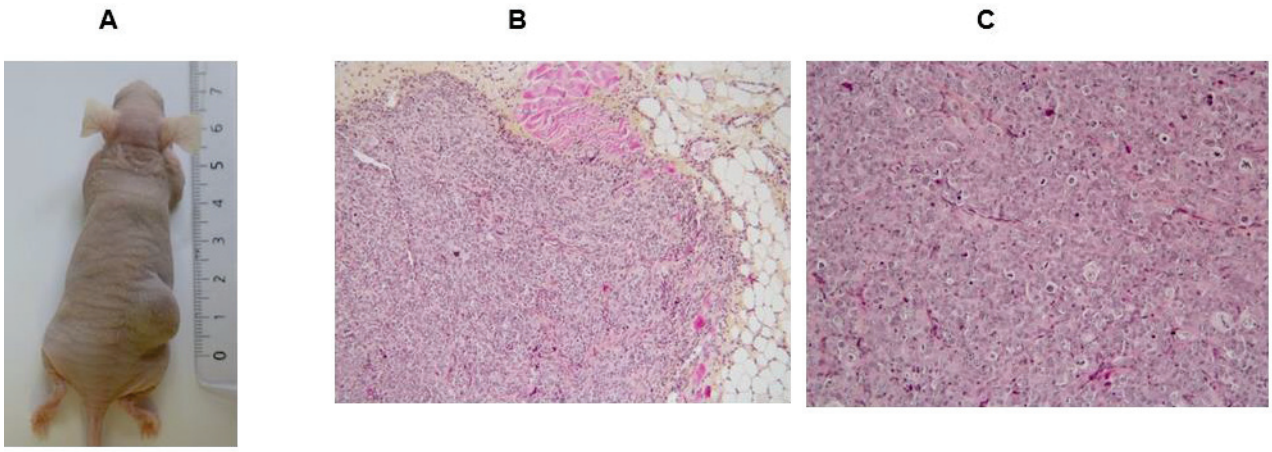

Figure 3. PHH-SV40^{LT+ST}/HRAS^{V12} are tumorigenic in nude mice. (A) Development of tumors in a nude mouse 3 months after subcutaneous injection of 10^6 PHH-SV40^{LT+ST}/HRAS^{V12} cells. (B) Poorly differentiated HCC with a solid trabecular pattern infiltrates hypoderm and muscle tissues (Hematoxylin and Eosin staining (H&E), 100x). (C) Higher magnification details morphology showing abundant eosinophilic cytoplasm and irregular pleomorphic nuclei with distinct nucleoli, numerous mitosis (some of them being atypical), absence of glycogen, bile pigment, or steatosis (H&E, 400x).

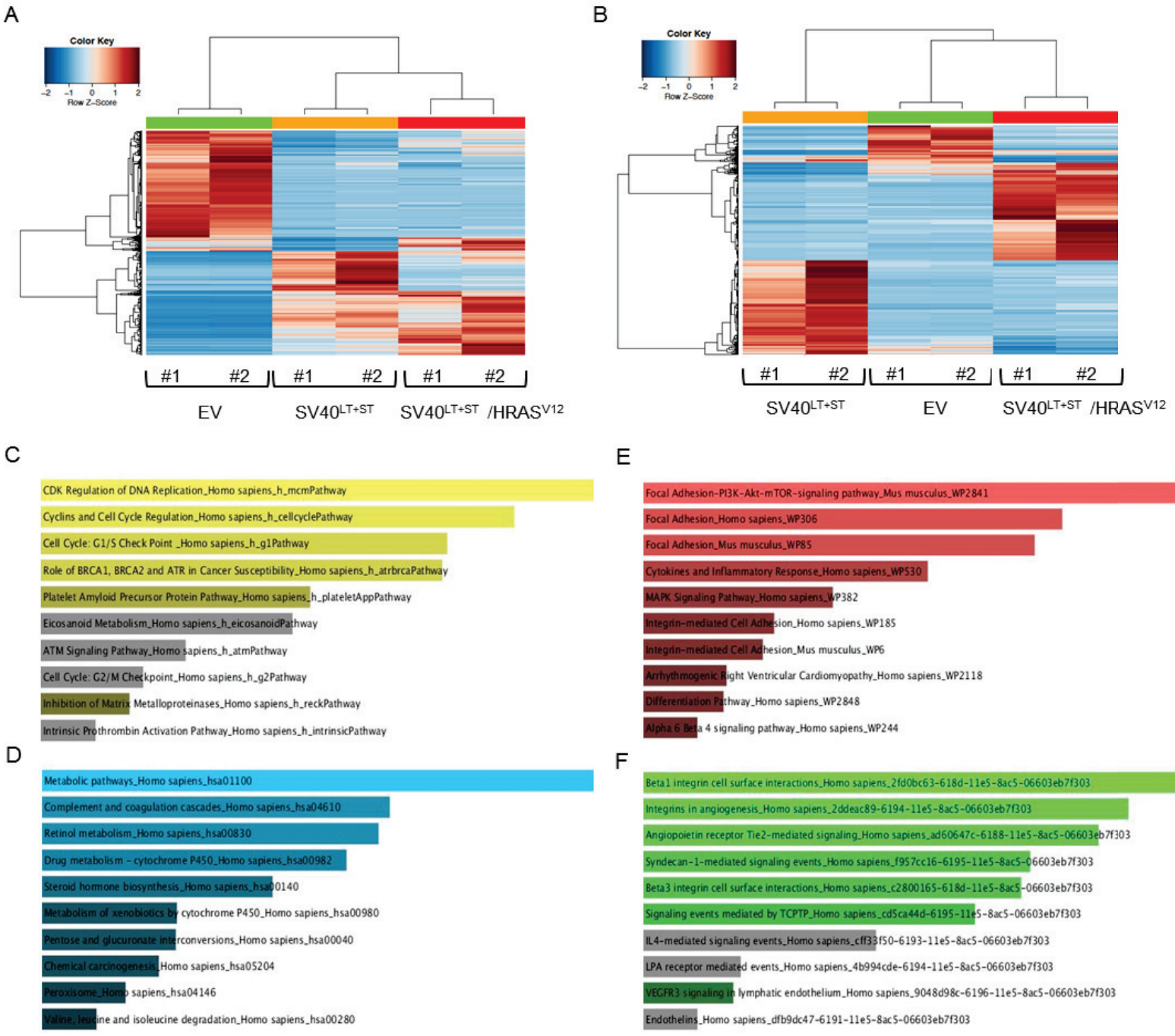

Figure 4. PHH-EV, PHH-SV40^{LT+ST} and PHH-SV40 $^{LT+ST}$/HRAS^{V12} were assessed and compared by transcriptome analysis. (A) Comparison between two batches of PHH-EV and PHH-SV40^{LT+ST}; 2,139 genes being down-regulated and 1,864 up-regulated in PHH-SV40^{LT+ST}, Fold change > 2, Bonferroni adjusted p-value FWER < 0.01. (B) Comparison between two batches of PHH-SV40^{LT+ST} and PHH-SV40^{LT+ST}/HRAS^{V12}; 692 genes being down-regulated and 736 up-regulated in PHH-SV40^{LT+ST}/HRAS^{V12}, Fold change > 2, Bonferroni adjusted p-value FWER < 0.01. (C) Up-regulated genes and (D) Down-regulated genes in PHH-SV40^{LT+ST} *vs.* PHH-EV. (E) Up-regulated genes and (F) Down-regulated genes in PHH-SV40^{LT+ST}/HRAS^{V12} *vs.* PHH-SV40^{LT+ST}.

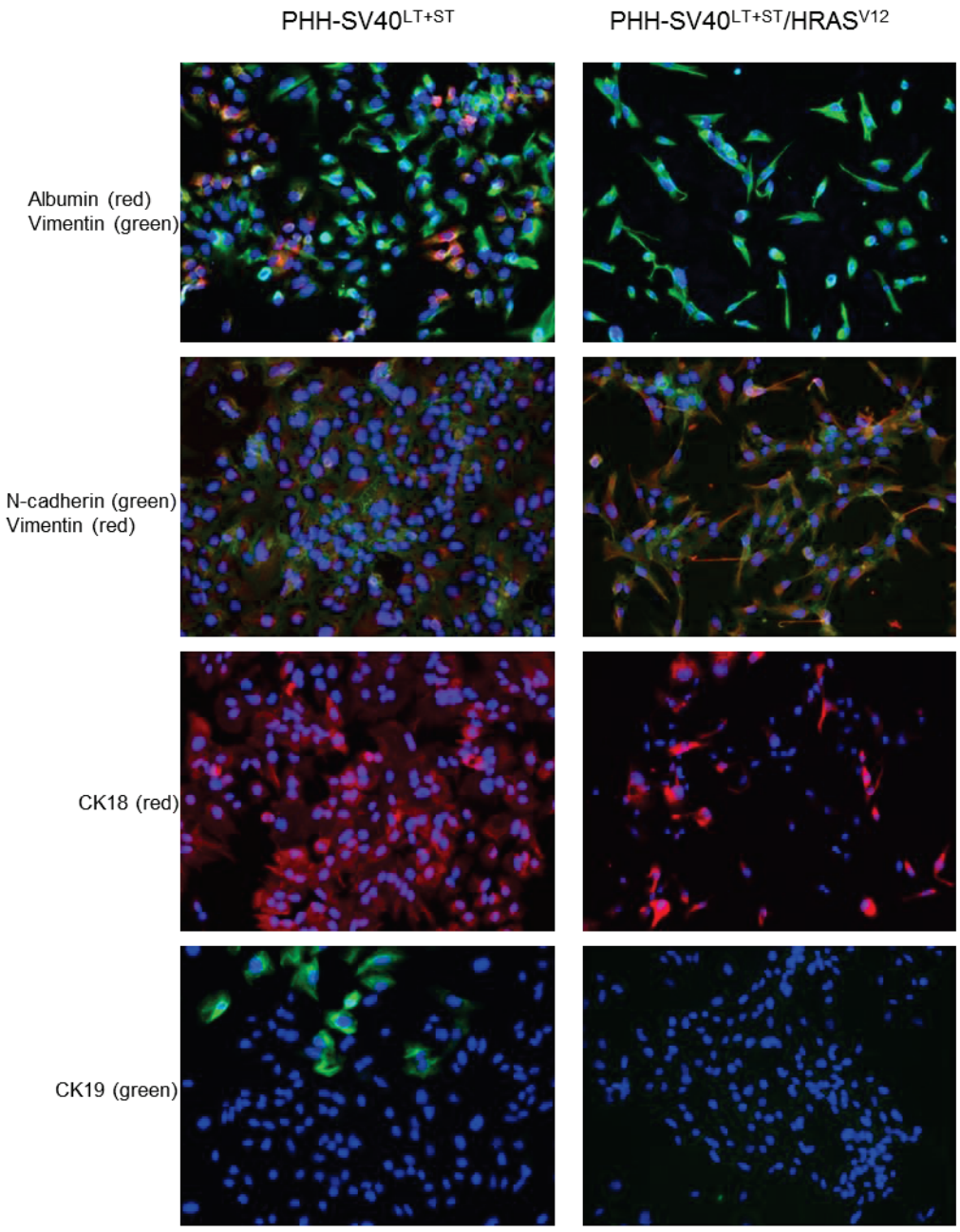

Figure 5. Expression of some phenotypic markers in PHH-SV40^{LT+ST} and PHH-SV40 $^{LT+ST}$/HRAS^{V12}. Cells were assessed for different markers by indirect immunofluorescence: Albumin and CK18 for hepatocyte lineage, CK19 for cholangiocyte or hepatic progenitor lineage. N-Cadherin and Vimentin are mesenchymal markers. Double staining of Albumin and vimentin was performed to evaluate the proportion of cell harboring an epithelial or mesenchymal phenotype. Double staining of N-Cadherin and vimentin confirmed that almost all cells have a mesenchymal phenotype. Nuclei were stained by DAPI (blue). Pictures are representative of those obtained in three independent experiments (magnification, 200x).

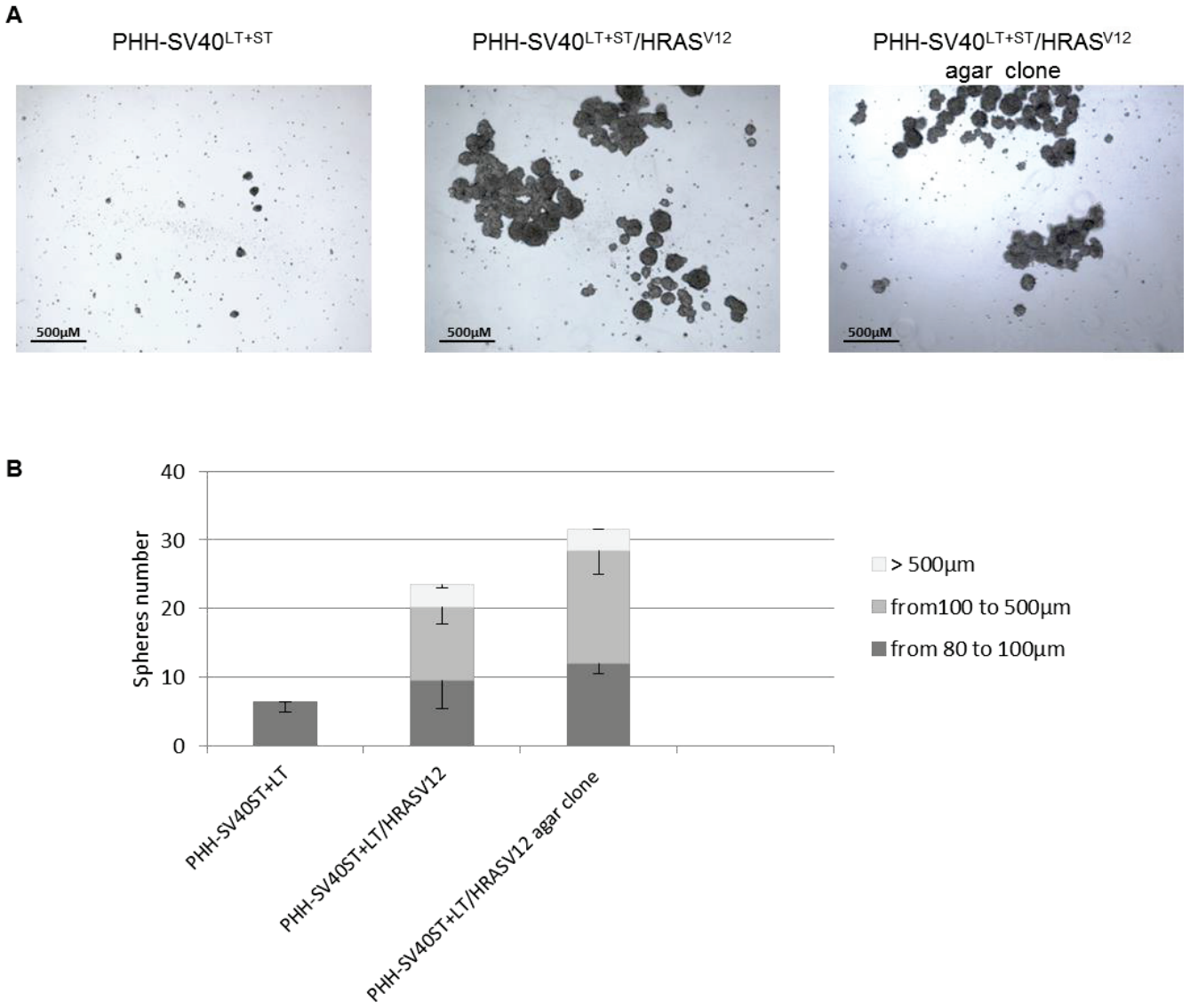

Figure 6. Total population or agar clones from PHH-SV40LT+ST/HRASV12 cells, but not PHH-SV40LT+ST cells were able to form large hepatospheres. Cells were cultured in low attachment conditions. (A) Pictures were taken after 4 days culture (x40). (B) Hepatospheres > 80 µm diameter were counted in each well (2 independent experiments in duplicate) and the mean +/- SEM was calculated.

SUPPLEMENTARY

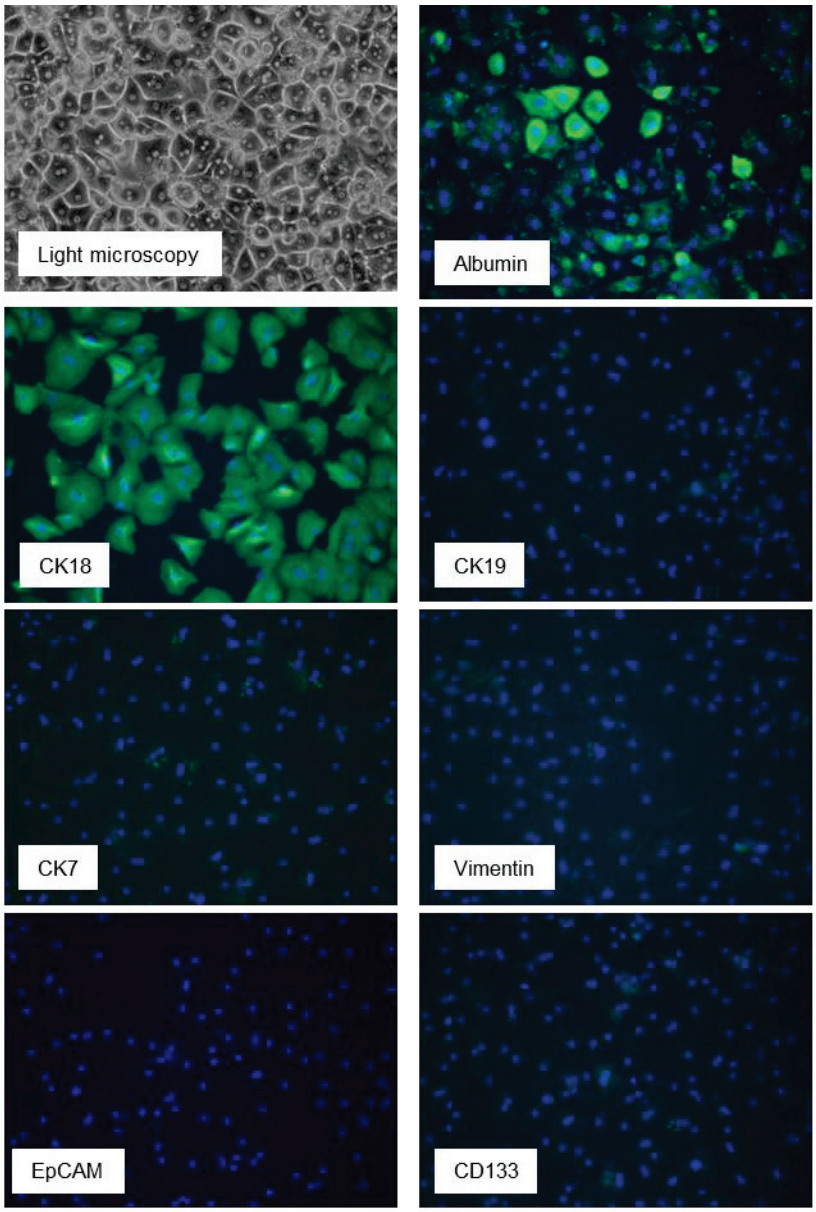

Supplementary Figure S1. *In vitro* cultured PHHs express differentiated hepatocyte-specific markers. PHHs were plated at high density. Phase-contrast microscopy examination of cells and the expression of different markers by indirect immunofluorescence are shown: Albumin and CK18 are indicative of hepatocyte lineage, CK19 for cholangiocyte or hepatic progenitor lineage and CK7 for hepatic progenitor lineage; Vimentin is a mesenchymal marker; EpCAM and CD133 are progenitor-associated markers. Nuclei were stained by DAPI (blue). Pictures are representative of those obtained in three independent experiments (magnification, 200x).

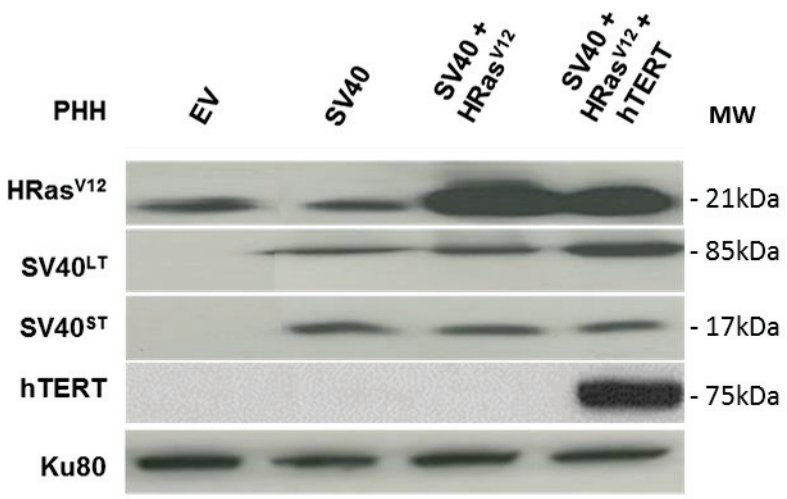

Supplementary Figure S2. Lentiviral transgene expression in PHH-EV, PHH-SV40^{LT+ST}, PHH-SV40^{LT+ST}/HRAS^{V12} and PHH-SV40^{LT+ST}/HRAS^{V12}/hTERT. The transgene intracellular levels were evaluated by Western blotting analysis on the total protein lysate. The anti-HRas antibody binds both the ectopic mutated HRas^{V12} and the endogenous wild-type HRas proteins. Ku80 was used as loading control. MW, molecular weight.

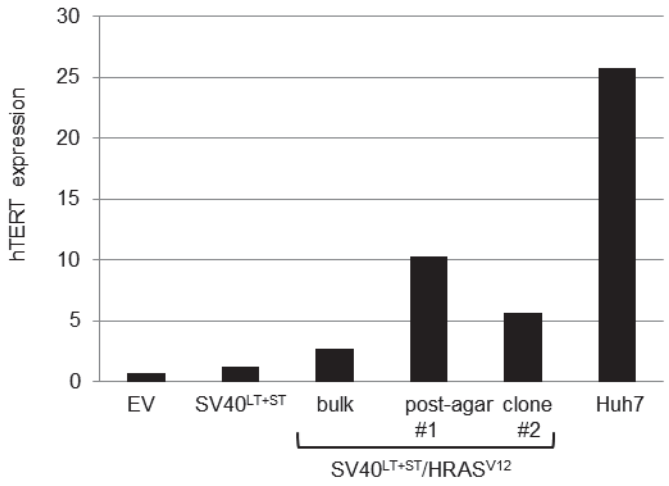

Supplementary Figure S3. Endogenous hTERT expression is increased in PHH-SV40^{LT+ST}/HRAS^{V12} cells from soft agar colonies. Expression of endogenous hTERT was assessed by RT-qPCR in PHH-EV and PHH-SV40^{LT+ST}. For PHH-SV40^{LT+ST}/HRAS^{V12}, hTERT expression was evaluated in the total population (bulk), and in two clones isolated from soft agar (post-agar clone #1, #2). PHH-EV hTERT mRNA served as the reference and the Huh7 HCC cell line as the positive control. hTERT levels are reported relative to the 18S ribosomal gene.

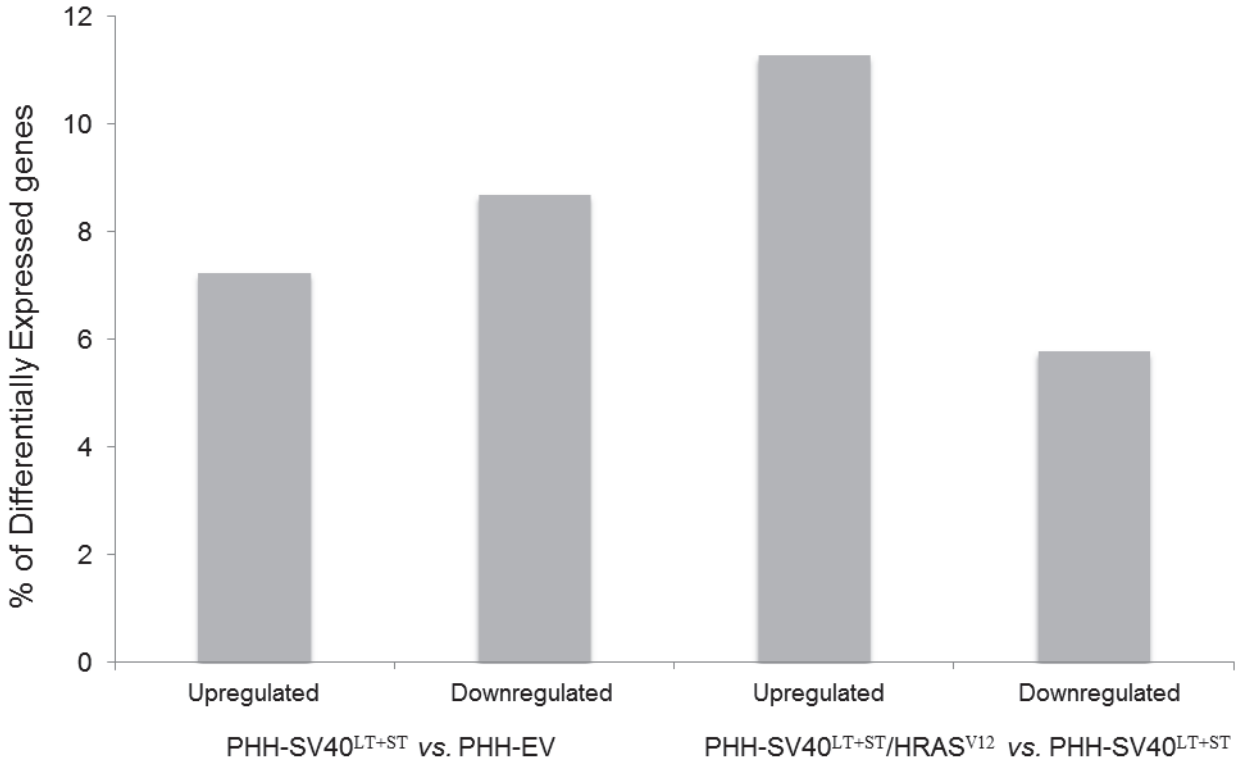

Supplementary Figure S4. Differential expression analysis of lncRNAs between PHH-EV, PHH-SV40^{LT+ST} and PHH-SV40 $^{LT+ST}$/HRAS^{V12}. The y axis show the percentage of deregulated lncRNAs based on the totality of differentially expressed genes.

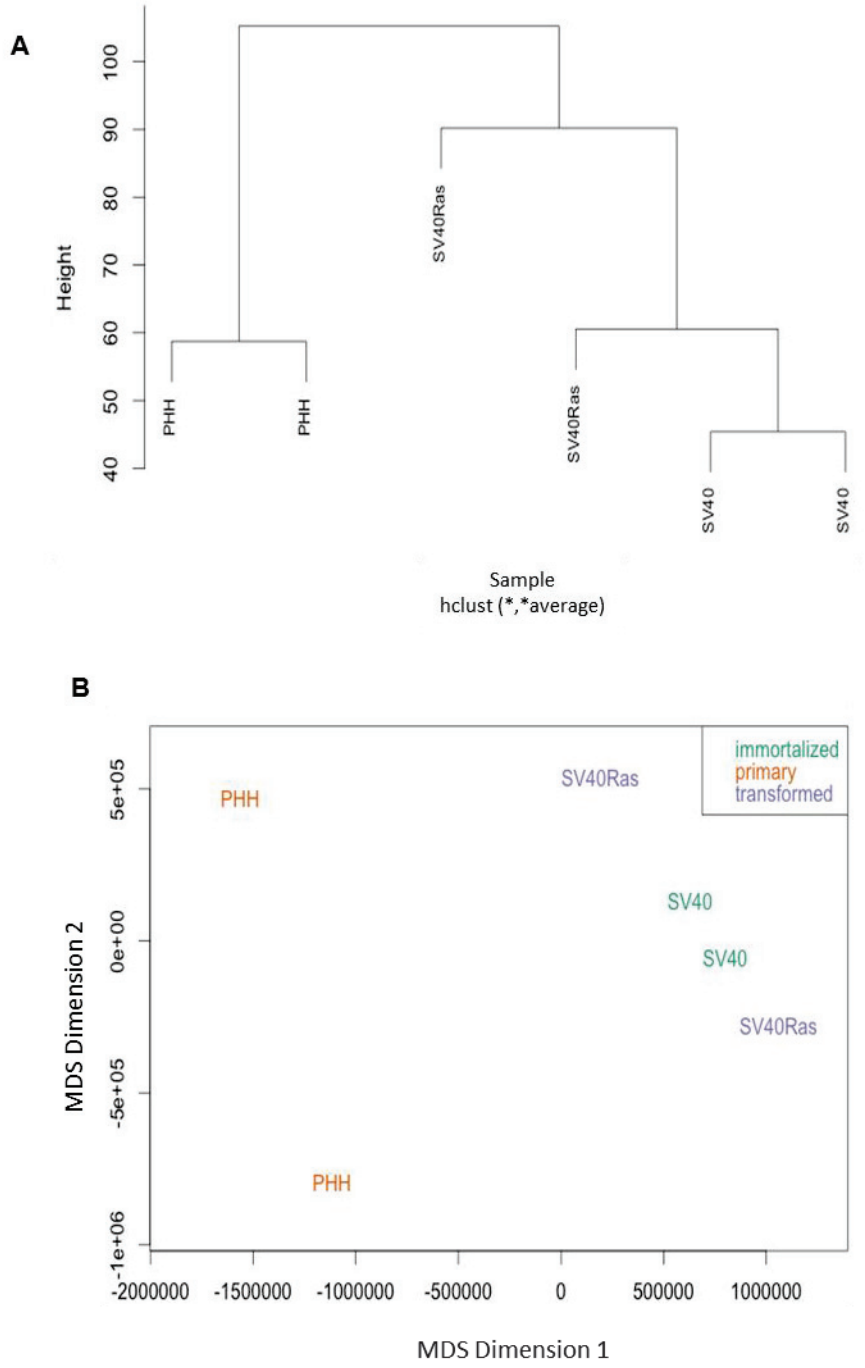

Supplementary Figure S5. PHH-EV clearly clustered separately to immortalized PHH-SV40^{LT+ST} or transformed PHH-SV40 $^{LT+ST}$/HRAS^{V12}. (A) Clustering based on whole transcriptome with sample relations based on 17,727 genes. (B) MDS plot based on 10% most variable genes (MDS 1,773 most variable positions).

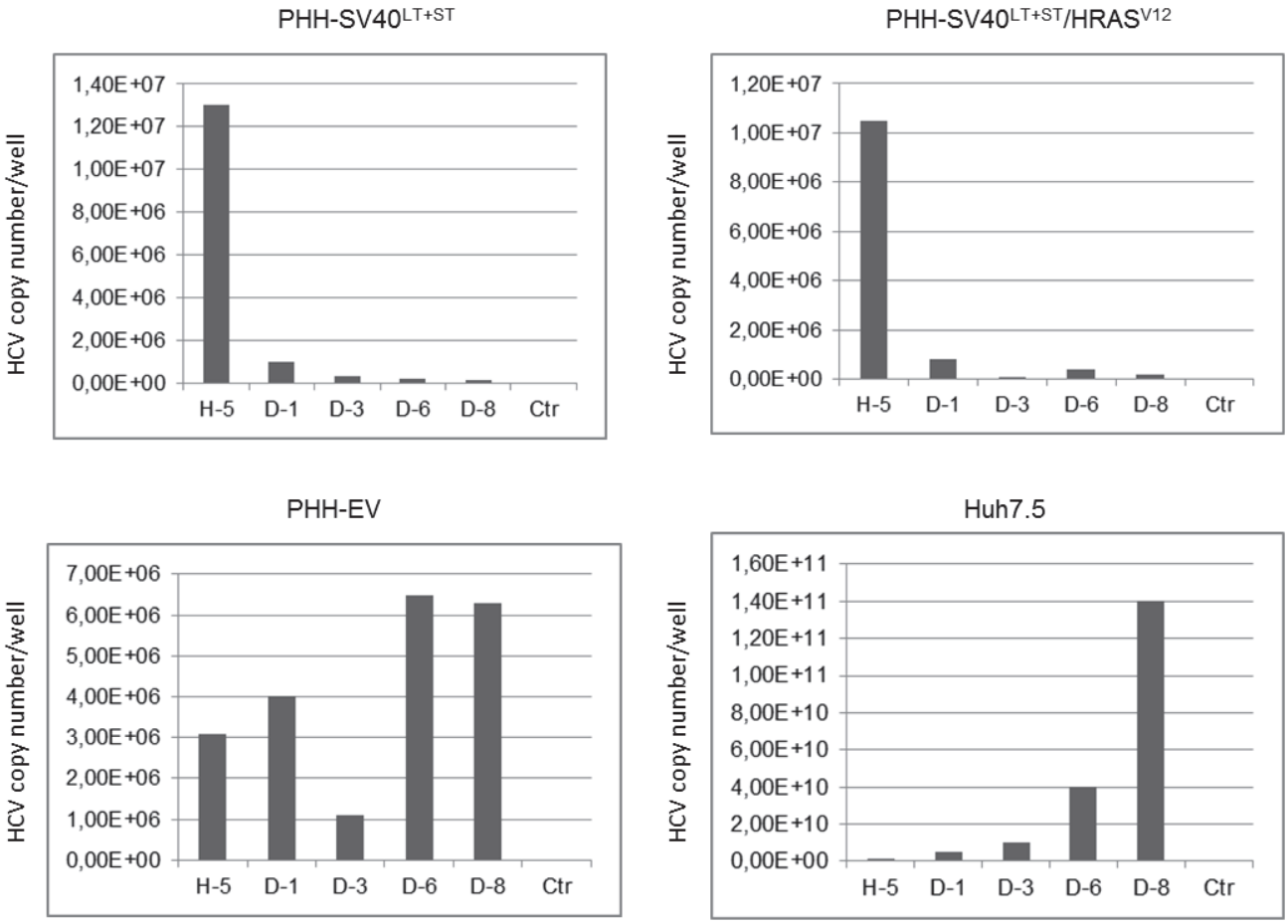

Supplementary Figure S6. Loss of HCV infection capability in PHH-SV40^{LT+ST} and PHH-SV40 $^{LT+ST}$/HRAS^{V12}. Transduced-PHHs were infected with HCV (HCV strain JFH1). Detection of intracellular HCV RNA was performed by RT-qPCR at different time points after HCV inoculation: 5 hours (H-5), day-1 (D-1), 3 (D-3), 6 (D-6) and 8 (D-8). HCV infection capability is maintained in the PHH-EV cells, but lost in the PHH-SV40^{LT+ST} and PHH-SV40 $^{LT+ST}$/HRAS^{V12} cells. Data were generated from 3 independent experiments. Huh7.5 cell line was used as positive control of HCV infection. Ctr, non-infected cells.

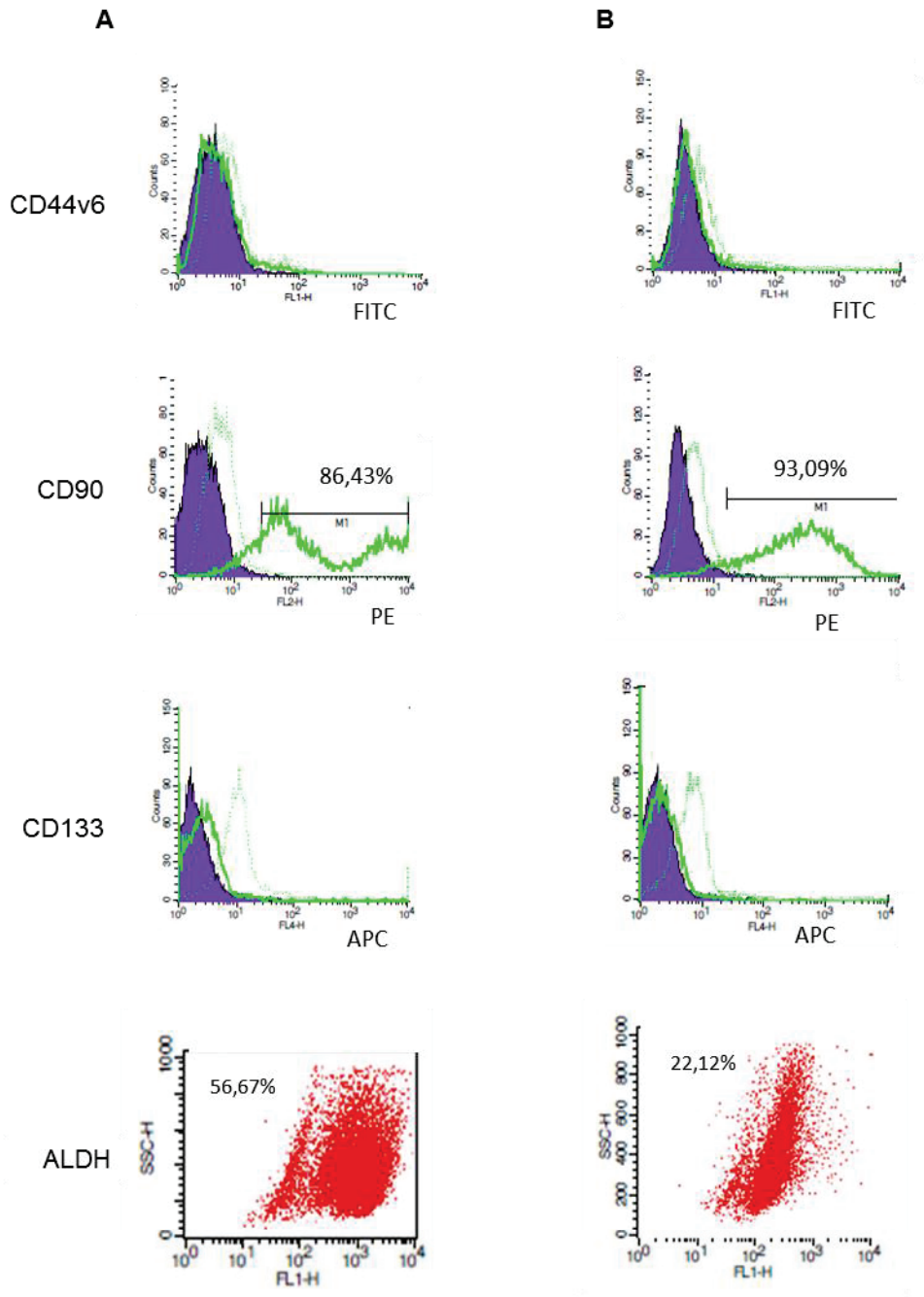

Supplementary Figure S7. PHH-SV40^{LT+ST} and PHH-SV40^{LT+ST}/HRAS^{V12} express some stem cells-associated markers. FACS analysis was performed to evaluate the expression of CD44v6, CD90, CD133 and ALDH in (A) PHH-SV40^{LT+ST} and (B) PHH-SV40^{LT+ST}/HRAS^{V12}. Both cells were positive for CD90 and ALDH and negative for CD44v6 and CD133. Full purple curve = non-labeled cells; hatched green lines = control isotype; bold green line = labeled cells.

Supplementary Materials and Methods

RNA extraction, RNA sequencing and real-time quantitative PCR (RT-qPCR)

About 1µg of total RNA was DNAse I-digested (Roche) and then reverse transcribed (RT) with random primers and MMLV-RT (Life technologies). Quantitative real-time PCR (qPCR) was performed with a LightCycler 480 (Roche) using QuantiFast SYBR Green PCR Kit (Qiagen). Levels of gene expression were determined using the Ct method with 18S gene as housekeeping gene. Each experiment was conducted three times in triplicate. Oligonucleotide sequences are available on request.

Immunofluorescence

Cells were plated on collagen-coated glass coverslips in a 12-well plate. Twenty four hours later, cells were fixed in 4% paraformaldehyde and then permeabilized in PBS-0.1% saponin (30min/ room temperature (RT)). After saturation in PBS-3% BSA-0.1% saponin, cells were incubated (1hour/ RT) with a primary antibody against either vimentin (EP21), CK19 (EP72), CK18 (EP30) (Epitomics), CK7 (OV-TL 12/30, Dako), albumin (15C7; AbCam), EpCAM (ab32392, Epitomics), or CD133 (ab19898, AbCam). After washing with PBS-0.1% saponin an alexaFluor488-conjugated secondary antibody against mouse or rabbit IgG (Dako) was added (30min/ RT). Finally, coverslips were washed with PBS-0.1% saponin, incubated (5min/ RT) with 0.25µg/mL DAPI prior to mounting in Vectashield medium (Vector Laboratories) and analyzed using a Nikon fluorescence microscope.

Protein extraction and Western blotting

Proteins were extracted with RIPA (50 mM Tris-HCl, pH 8.0, 150 mM NaCl, 1% Nonidet P-40, 0.5% sodium deoxycholate, 0.1% SDS, 1mM Na3VO4, protease cocktail inhibitor (Roche)) and protein concentrations were determined using the BCA assay (Pierce). Whole-cell extracts were resolved by SDS-PAGE, transferred onto a PVDF membrane and probed with a specific primary antibody against $SV40^{ST+LT}$ (PAb419, Harlow E et al., J Virol. 1981); HRas (SC520, Santa Cruz Biotechnology); Ku80 (AHP317, Serotec); hTERT (H-231, Santa Cruz Biotechnology) and then with a HRP-conjugated secondary goat anti-rabbit or goat anti-mouse antibody (Sigma). Protein revelation was performed by using enhanced chemiluminescence kit (Amersham). All blots were standardized for equal protein loading with Ku80 staining.

HCV infection

PHH were infected with HCV (HCVcc: JFH1) and harvested 5 hours (H-5), 1 day (D-1), 3 days (D-3), 6 days (D-6) or 8 days after HCV inoculation (D-8). Detection of intracellular HCV RNA was performed by RT-qPCR. Primers sequences are available on request.

Flow cytometry

Cells were harvested by trypsinization in 15mL tubes containing 8mL of complete media and centrifuged for 5min at 200g. The supernatant was discarded and the pellets were resuspended in PBS buffer at 106cells/mL. For each staining condition, 0.5mL of the cell suspension was dispensed in 1.5mL Eppendorf tubes and centrifuged for 5min at 400g. The supernatants were discarded, the pellet were resuspended in 100µL of staining buffer (1X PBS, 2% BSA) and incubated on ice for 10min for non-specific antigen saturation. For CD44v6, CD90 and CD133 detection, the following antibodies were used for staining at dilution factors and incubation times indicated by the manufacturer, in the dark and on ice: CD44v6-FITC (eBiosciences ref:BMS 125FI), CD90-PE (BD Biosciences, ref: 555596), CD133-APC (Miltenyi ref: 130-090-826). At the end of the incubation period, cells were washed with 1mL of staining buffer and centrifuged for 5min at 400g. Supernatants were discarded and pellets were suspended in 0.5mL of staining buffer. Cells were incubated with isotype controls according to the same protocol. Staining analysis was performed with the same cytometer and for each condition at least ten thousand events were recorded.

Study 2

p73 and cancer stem cells

Several lines of evidence prove the existence of cancer stem cells in solid tumours, including hepatocellular carcinoma. In contrast there is only emerging data showing the importance of truncated isoforms of the p73 in the maintenance of the stem cells pool and in particular of the cancer stem cells.

During my PhD thesis, I initiated a study dedicated to investigating the link between p73 expression profile in HCC and cancer stem cells features. This study was performed on HCC biopsies by gene transcription analysis as well as by studying HCC cell lines *in vitro*.

ΔNp73 favors the developpement of CSCs

Introduction

It has been proposed that resistance to treatment and relapse could be mainly due to a small population of highly aggressive cancer cells, which are the cancer stem cells (CSCs). These cells represent a small population of tumour cells with stemness features. They have infinite proliferation potential and are highly resistant to drugs. Therefore, targeting liver cancer stem cells could represent an excellent strategy for preventing cancer resistance and tumour relapse. However, the mechanisms and factors that are unique for CSCs are still poorly understood.

Several studies have shown that in HCC the p73 truncated isoforms are over-expressed and are of poor prognosis. Mechanistic studies suggested that during carcinogenesis, there is a switch in the expression of p73 isoforms. In non-neoplastic cells the balance is in favour of the anti-oncogenic TAp73, while in transformed cells the transcription of the truncated isoforms ΔTAp73 increases.

The aim of this study was to investigate the pattern of expression of p73 in liver biopsies from healthy and HCC patients undergoing tumour resection and correlate their expression with clinical data, patients' outcome and expression of stemness markers.

Results

p73 expression in human primary HCC

RNA extraction was performed on an HCC cohort comprising 138 tumour and adjacent non-tumour samples and gene expression was performed by RT-qPCR. In parallel, a second cohort was studied comprising 11 healthy liver tissues without any clinical history of acute or chronic liver disease. The expression of four p73 isoforms ΔNp73, TAp73, ΔEx2p73, and ΔEx2/3p73 was analysed at the mRNA level in the two cohorts. In parallel the expression of *NANOG*, *OCT4*, *SOX2*, *CD133*, *CK19* and *EPCAM* genes was quantified in the same manner.

ΔNp73 is generated from the internal promoter P2 of *TP73* while TAp73, ΔEx2p73 and ΔEx2/3p73 isoforms are transcribed from the conventional P1 promoter. ΔEx2p73 and ΔEx2/3p73 are obtained by alternative splicing of the pre-mRNA that also serves for TAp73 translation. The expression profile of ΔEx2p73 and ΔEx2/3p73 isoforms reflects both the activity of the P1 promoter and the intensity of alternative splicing events.

The expression data of the four isoforms across the cohorts of HCC samples and healthy livers is presented on the dot plots in **Figure 1**. The first column is dedicated to the expression in the healthy livers (HL), the second one to the HCC non-tumour tissues (NT) and the third one represents the HCC samples (T).

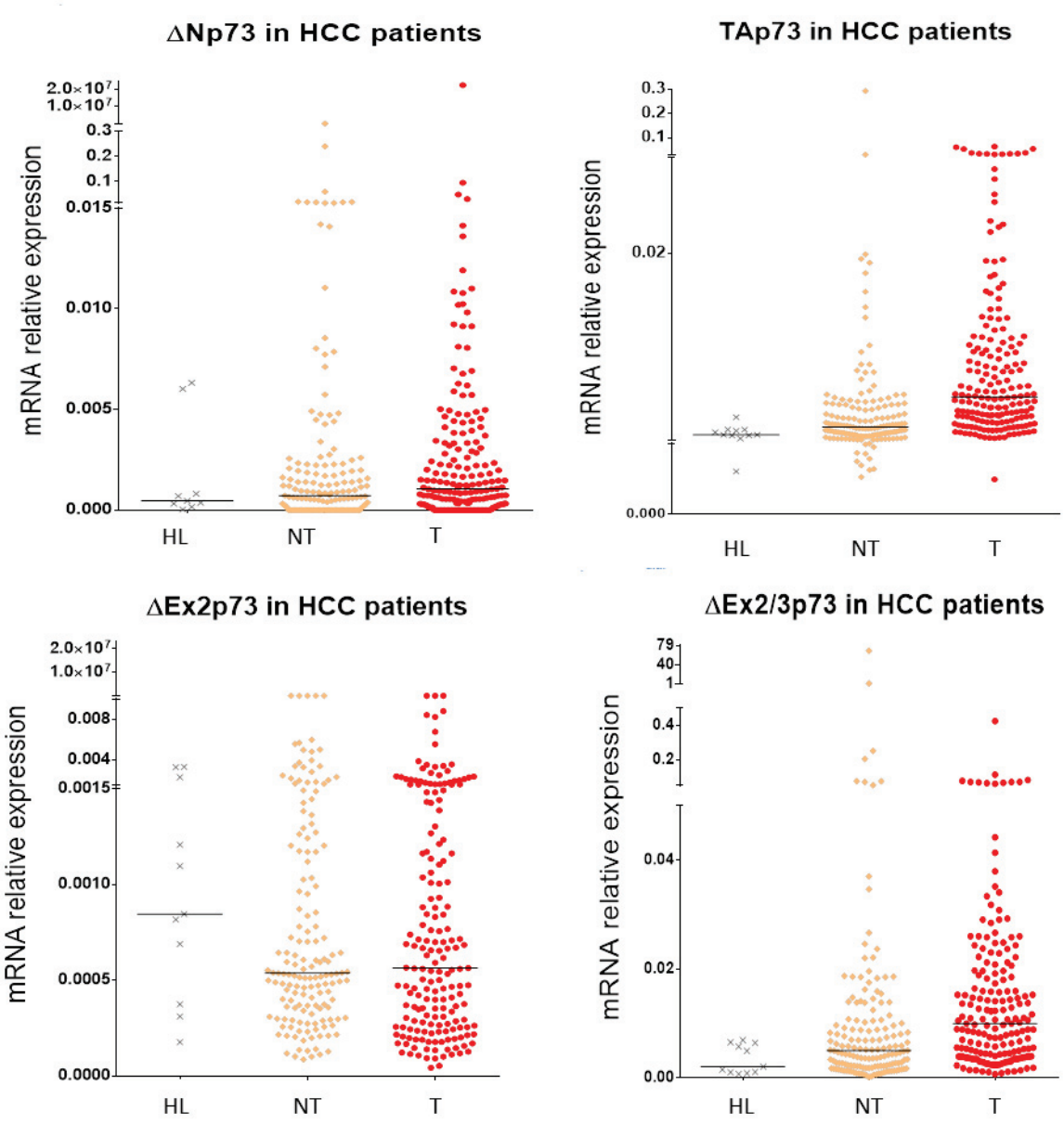

Figure 1. Expression of p73 in healthy and tumoural human liver tissues. The expression of the p73 isoforms ΔNp73, ΔEx2p73, ΔEx2/3p73 and TAp73 was quantified by RT-qPCR from frozen liver biopsies of healthy liver (HL) (no known chronic liver disease), tumour (T) and surrounding non-tumour (NT) tissue originating from patients with HCC. Expression data are presented as the result of the relative quantification after normalization to the housekeeping gene on a logarithmic scale. Horizontal black bars represent the median of expression.

For each of the four p73 isoforms, the wide expression range reflects the high variability in the transcriptional activity among the population of HCC patients. For three of the four isoforms, ΔNp73, TAp73 and ΔEx2/3p73, the median of expression is lower in the healthy liver tissue compared to the HCC non-tumoural and tumoural tissue. However, this tendency could be biased by the small size of the healthy liver cohort (11 samples versus more than 150 samples for the HCC cohort). Increased level of these three transcripts in the liver tissue adjacent to the HCC nodule suggests that chronic liver stress (in our cohort due to HCV and HBV chronic infection, alcohol abuse and NASH) could favour their production. Further, the median of expression of ΔNp73, TAp73 and ΔEx2/3p73 is higher in HCC than in adjacent liver non-tumoural tissue. These observations suggest that the expression of the three isoforms is progressively increased in human liver during the transition healthy liver → chronic liver disease → hepatocellular carcinoma.

Regarding the isoform ΔEx2p73, the range of expression in the healthy liver is wider in comparison to the three isoforms mentioned above. The median of expression in the non-tumour liver surrounding the HCC nodule does not seem to be higher than in the healthy livers. However, the same tendency was found in the HCC cohort where the median of expression is higher in the tumour than in the non-tumoural tissue, even though the difference is less striking than for the isoforms TAp73, ΔNp73 and ΔEx2/3p73.

In conclusion, for the four p73 isoforms the median of expression is higher in the tumour samples compared to the matching non-tumour and could be due to an individual increase in the level of each of these isoforms. To have an overview of this aspect, the expression in each tumour sample was graphically represented as linked to the matching non-tumoural samples (**Figure 2**). The arrows between the non-tumour and tumour samples are not all directed upwards, which would have indicated a systematic increased expression in tumours compared to the matching non-tumour. Patients with high levels in the tumour presented lower levels in the non-tumour and *vice versa*, while for other patients the levels were roughly the same in the tumoural and matching non-tumoural tissue. However, for TAp73 and ΔEx2/3p73 a higher proportion of arrows are directed upwards, suggesting a more systematic increase in the tumour. This question was more profondly explored statistically here below.

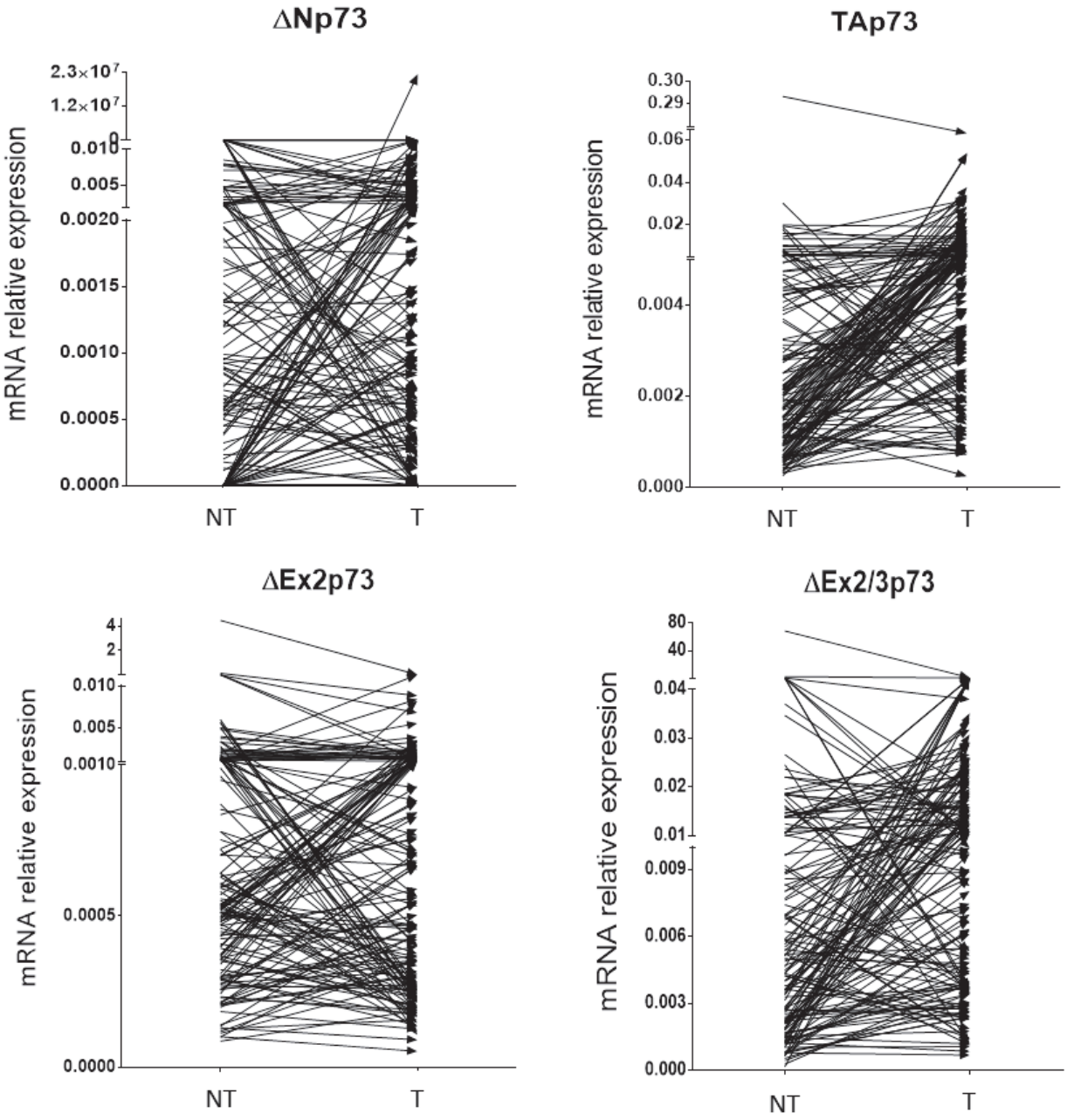

Figure 2. Correlation between the over-expression in the tumoural HCC (T) and matching non-tumoural (NT) tissue for each of the investigated p73 isoforms (ΔNp73, ΔEx2p73, ΔEx2/3p73 and TAp73). Each arrow represents a pair tumour (T) / surrounding non-tumour (NT). The overall higher median of expression of each p73 isoform in the tumour observed in **Figure 1** does not seem to result from a systematic increase of the expression between the non-tumoural and tumoural tissue pairs of the same patient.

Differential regulation of *TP73* in tumour and adjacent non-tumoural tissue

The overall increase of p73 transcripts in the HCC cohort compared to the healthy livers led to the identification of patients in whom the two transcripts were over-expressed.

The expression of the four p73 isoforms in the HCC nodules and matching non-tumoural tissues was compared to the healthy liver samples in order to identify the groups of patients over-expressing each of these isoforms. Over-expression was established when the expression level was higher than the mean plus two standard deviations of that of healthy livers.

We found that each of the four isoforms was over-expressed from 15% to 60% of HCC samples and from 15% to 25% of the non-tumoural tissues.

The full length isoform TAp73 was found to be over-expressed in 58.6% of HCC and 25.8% of the surrounding non-tumour tissues and overexpression between the two regions was found to be associated (p=0.023, r=0.183.). In the non-tumour tissues, the overexpression of TAp73 was associated with those of ΔNp73 (p<0.001, r=0.318), ΔEx2p73 (p=0.003, r=0.237) and ΔEx2/3p73 (p<0.001, r=0.342) as presented in **Table 1**. In HCC samples, overexpression of TAp73 only correlated with overexpression of the P1 promoter-related isoforms ΔEx2p73 (p=0.004, r=0.213) and ΔEx2/3p73 (p<0.001, r=0.522) but not with ΔNp73 (p=0.722), transcribed from the P2 internal promoter. This suggests that in tumour cells, the P1 and P2 promoters are differentially activated whereas in the adjacent tissue they could be activated simultaneously.

	TAp73 NT_up_HL		TAp73 T_up_HL	
Total prevalence	25.8% up		58.6% up	
	Pearson's Chi-Square 2-Sided			
	p	χ^2	p	χ^2
ΔNp73 NT_up_HL	<0.001	15.691		
ΔNp73 T_up_HL			0.722	0.127
ΔEx2p73 NT_up_HL	0.003	8.681		
ΔEx2p73 T_up_HL			0.004	8.286
ΔEx2/3p73 NT_up_HL	<0.001	18.202		
ΔEx2/3p73 T_up_HL			<0.001	49.8
TAp73 NT_up_HL	-		0.023	5.204
TAp73 T_up_HL	0.023	5.204	-	

Table 1. Correlation between the over-expression of TAp73 and ΔNp73, ΔEx2p73 and ΔEx2/3p73 in tumoural (T_up_HL) and adjacent non-tumoural (NT_up_HL) tissue. Overexpression was determined with respect to the threshold in the healthy liver (HL) tissue. In non-tumour samples, TAp73 overexpression is correlated with that of all the other isoforms

(middle column), whereas in tumour samples it is correlated with all, except ΔNp73 (right column). For statistical analysis the Chi-2 Squared 2-sided test was employed, and significance was established for $p<0.05$.

To have a more quantitative visual idea, we represented the expression of TAp73 in function of that of ΔNp73, ΔEx2p73 and ΔEx2/3p73 (**Figure 3**). Graphs clearly show that when TAp73 expression increases in tumours, the expression of ΔEx2p73 and ΔEx2/3 increases but this is not the case for ΔNp73. However, in the non-tumour tissue, the expression of all three isoforms ΔNp73, ΔEx2p73 and ΔEx2/3p73 seems to increase at the same time as TAp73. Secondly, the expression of ΔEx2p73 and ΔEx2/3p73 seems to be more correlated to TAp73 in the tumoural compared to the non-tumour tissue. This is perhaps due to alterations of the alternative-splicing machinery in HCC cancer cells which would favour the production of truncated isoforms.

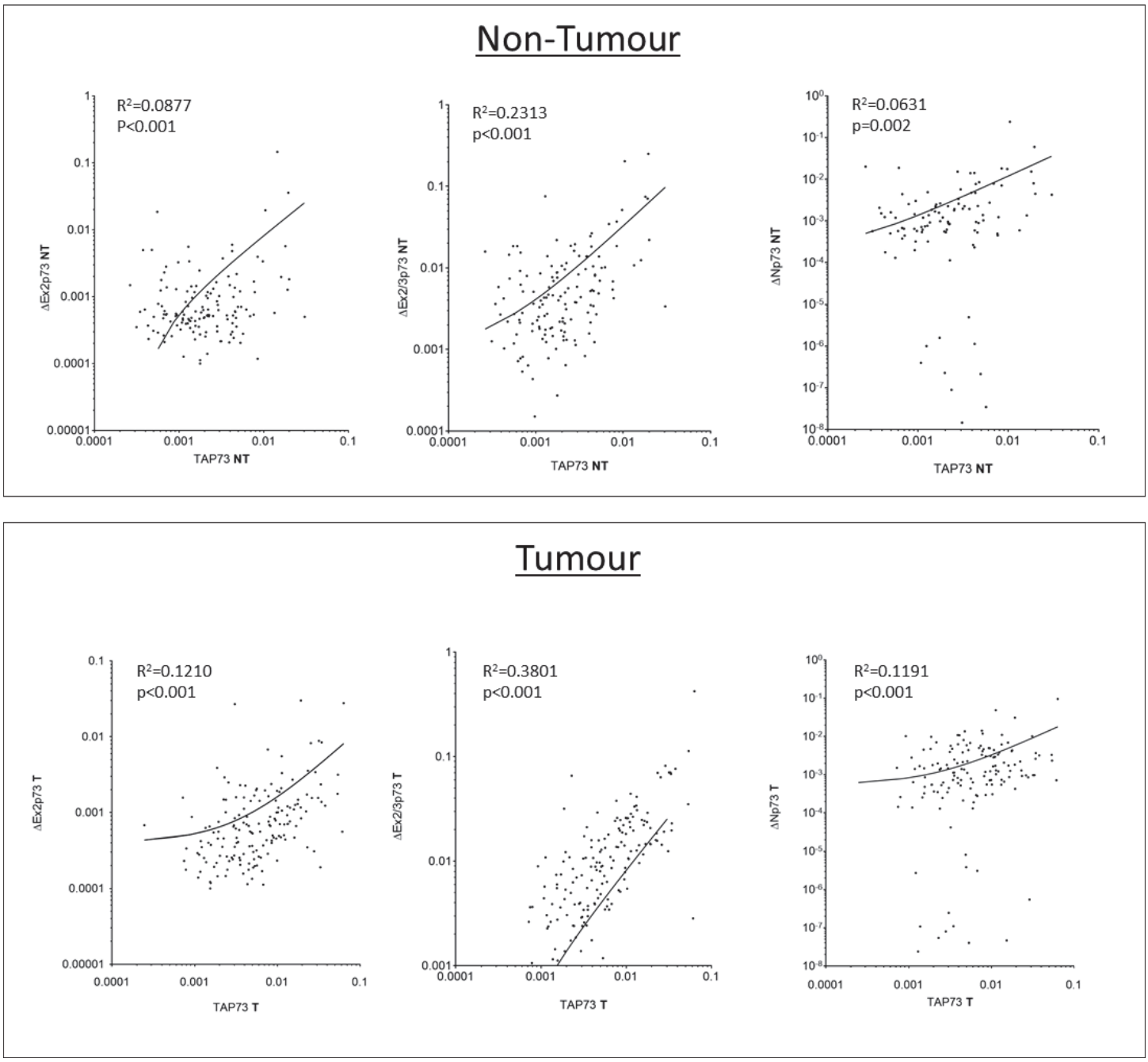

Figure 3. Correlation between TAp73 and ΔNp73, ΔEx2p73 and ΔEx2/3p73 mRNA expression (log scale). Increase of TAp73 seemed to correlate with ΔEx2p73, ΔEx2/3p73 and ΔNp73 in non-tumoural (NT) tissue and with ΔEx2p73, ΔEx2/3p73 but NOT with ΔNp73 in the tumoural (T) tissue. Data were modelised using the linear regression approach. Fisher F-test was employed to tesh whether the slope is significantly non-zero.

The transcripts ΔEx2p73 and ΔEx2/3p73 were found to be overexpressed in 16.7% and 37.0% of tumours, respectively, and in 15.5% and 16.1% of non-tumours compared to healthy livers, respectively (**Table 2** and **Table 3**). Moreover, the two transcripts were overexpressed in approximately the same proportion in non-tumoural liver samples and their overexpression was statistically correlated ($p<0.05$). In HCC samples, ΔEx2/3p73 was more frequently overexpressed than ΔEx2p73. Both transcripts are obtained by alternative splicing from the P1 promoter. Until now, no specific alternative splicing mechanism has been described that would preferentially lead to the ΔEx2/3p73 transcript. Castillo and collaborators showed that the EGFR ligand amphiregulin favours the alternative splicing leading to the formation of the ΔEx2p73 (Castillo et al., 2009).

	ΔEx2p73 NT_up_HL		**ΔEx2p73 T_up_HL**	
Total prevalence	15.5% up		16.7% up	
	Pearson's Chi-Square 2-Sided			
	P	χ^2	p	χ^2
ΔNp73 NT_up_HL ΔNp73 T_up_HL	<0.001	39.842	<0.001	15.540
ΔEx2p73 NT_up_HL	-		0.248	1.335
ΔEx2p73 T_up_HL	0.248	1.335	-	
ΔEx2/3p73 NT_up_HL ΔEx2/3p73 T_up_HL	<0.001	18.522	0.003	8.649
TAp73 NT_up_HL TAp73 T_up_HL	0.003	8.681	0.004	8.286

Table 2. Correlation between the over-expression of ΔEx2p73 and ΔNp73, ΔEx2/3p73 and TAp73 in tumoural (T_up_HL) and adjacent non-tumoural (NT_up_HL) tissue. Overexpression was determined with respect to the threshold in the healthy liver (HL) tissue. In both cases, ΔEx2p73 overexpression correlated with that of all the other isoforms (numbers in red). For statistical analysis the Chi-2 Squared 2-sided test was employed, and significance was established for $p<0.05$.

	ΔEx2/3p73 NT_up_HL		ΔEx2/3p73 T_up_HL	
Total prevalence	16.1% up		37.0% up	
	Pearson's Chi-Square 2-Sided			
	p	χ^2	p	χ^2
ΔNp73 NT_up_HL	<0.001	13.690		
ΔNp73 T_up_HL			0.077	3.137
ΔEx2p73 NT_up_HL	<0.001	18.522		
ΔEx2p73 T_up_HL			0.003	8.6493
ΔEx2/3p73 NT_up_HL	-		<0.001	14.332
ΔEx2/3p73 T_up_HL	<0.001	14.332	-	
TAp73 NT_up_HL	<0.001	18.202		
TAp73 T_up_HL			<0.001	49.8

Table 3. Correlation between the over-expression of ΔEx2/3p73 and ΔNp73, ΔEx2p73 and TAp73 in tumoural (T_up_HL) and adjacent non-tumoural (NT_up_HL) tissue. Overexpression was determined with respect to the threshold in the healthy liver (HL) tissue. In both cases, ΔEx2/3p73 overexpression correlated with that of ΔNp73, ΔEx2p73, and TAp73 (numbers in red) (at the borderline of significance for the couple ΔEx2/3p73 – ΔNp73 in tumours - numbers in black). For statistical analysis the Chi-2 Squared 2-sided test was employed, and significance was established for $p<0.05$.

ΔEx2/3p73 overexpression observed in tumours was also found in the matching non-tumoural tissues ($p<0.001$, $r=0.305$) but this was not the case for ΔEx2p73 ($p=0.248$). This suggests that ΔEx2p73 overexpression is proper to HCC cells. High ΔEx2/3p73 and ΔEx2p73 expression in tumours and non-tumours correlated with high ΔNp73 expression, with the correlation ΔEx2/3p73 and ΔNp73 overexpression in tumours at the borderline of significance ($p=0.077$).

Finally, ΔNp73, the only isoform originating from the activation of the internal promoter P2 of *TP73*, was found overexpressed in 15.5% of tumours and 16.1% of non-tumour tissues compared to healthy liver tissue (**Table 4**).

	ΔNp73 NT_up_HL		ΔNp73 T_up_HL	
Total prevalence	15.5% up		16.1% up	
	Pearson's Chi-Square 2-Sided			
	p	χ^2	p	χ^2
ΔNp73 NT_up_HL	-		0.019	5.483
ΔNp73 T_up_HL	0.019	5.483	-	
ΔEx2p73 NT_up_HL	<0.001	39.842		
ΔEx2p73 T_up_HL			<0.001	15.540
ΔEx2/3p73 NT_up_HL	<0.001	13.690		
ΔEx2/3p73 T_up_HL			0.077	3.137
TAp73 NT_up_HL	<0.001	15.691		
TAp73 T_up_HL			0.722	0.127

Table 4. Correlation between the over-expression of ΔNp73 and ΔEx2p73, ΔEx2/3p73 and TAp73 in tumoural (T_up_HL) and adjacent non-tumoural (NT_up_HL) tissue. Overexpression was determined with respect to the threshold in the healthy liver (HL) tissue. In both cases, ΔNp73 overexpression correlated with that of ΔEx2p73 and ΔEx2/3p73 (numbers in red) (at the borderline of significance for the couple ΔEx2/3p73 – ΔEx2/3p73 in tumours - numbers in black). TAp73 and ΔNp73 overexpression correlated in non-tumoural tissues but not in the tumoural ones. For statistical analysis the Chi-2 Squared 2-sided test was employed, and significance was established for $p<0.05$.

As for ΔEx2/3p73, overexpression of ΔNp73 in tumours and non-tumours were found correlated ($p=0.019$, $r=0.188$). As described here above, both in tumours and non-tumours, ΔNp73 overexpression was associated with the overexpression of the other isoforms, except for TAp73 in the tumours ($p=0.722$). These observations were graphically represented in **Figure 4**.

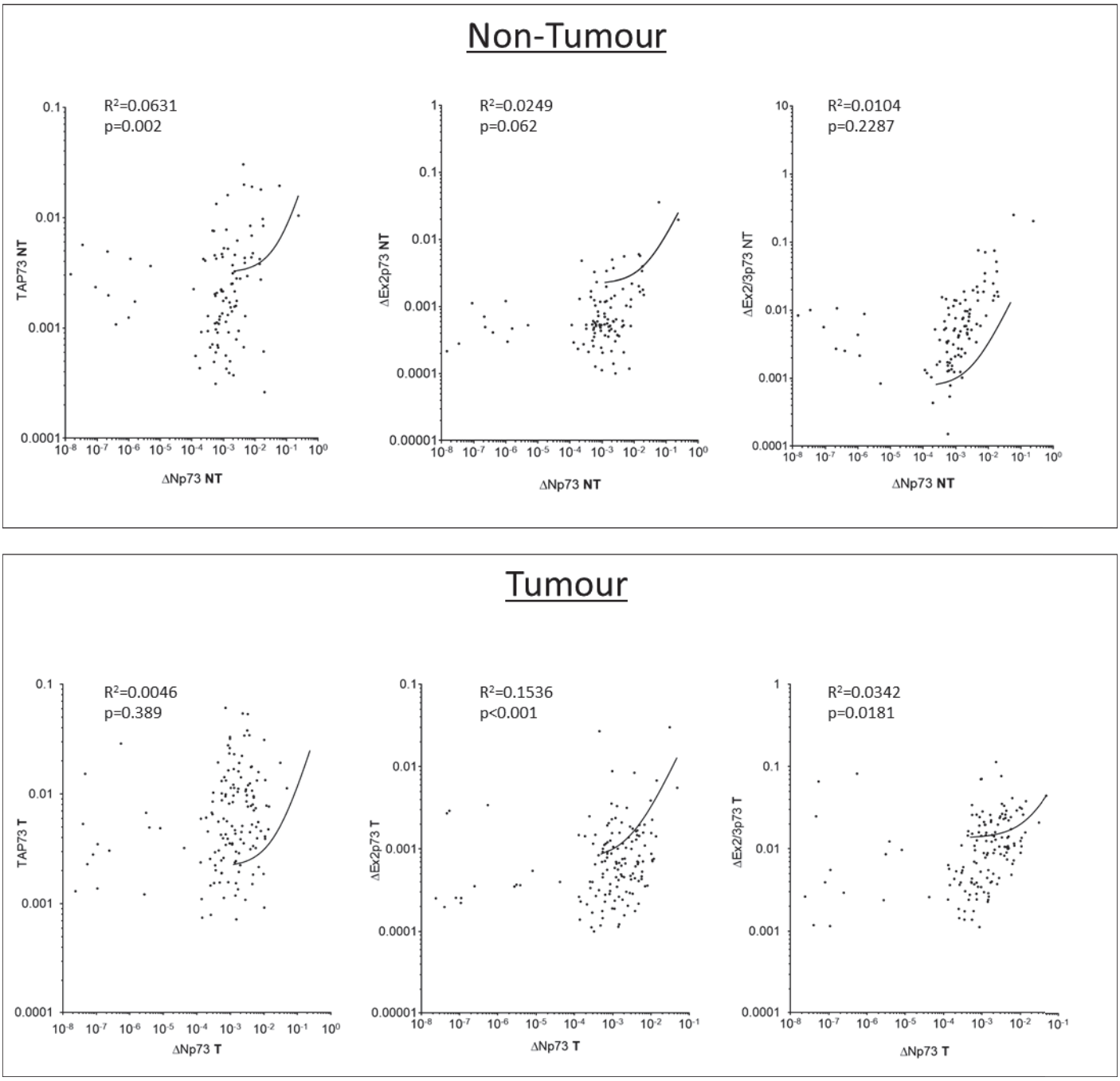

Figure 4. Correlation between ΔNp73 vs. TAp73 and ΔEx2p73 vs ΔEx2/3p73 regarding mRNA expression (log scale). Increase of ΔNp73 seemed to correlate with TAp73 in non-tumoural tissue but not in tumours. Data were modelised using the linear regression approach. Fisher F-test was employed to tesh whether the slope is significantly non-zero.

***TP73* over-expression correlates with stemness markers and clinicopathologic features**

We investigated whether *TP73* over-expression correlated with the clinicopathologic data of patients, such as the presence or absence of cirrhosis, microvascular invasion, or tumour differentiation, as well as the overexpression of the stemness factors Sox2, Nanog and Oct4 or the stem-like markers CD133, CK19 and EpCAM.

Over-expression of ΔNp73 in tumours and surrounding non-tumoural tissue correlated with stemness factors Nanog, Oct4 and Sox2 ($p<0.05$) (**Table 5**). From a clinicopathological point of view, over-expression of ΔNp73 in non-tumoural tissues negatively correlated with HCC multinodularity ($p=0.030$, $r=-0.179$) and high AFP levels (>200ng/mL) ($p=0.030$, $r=-0.186$) while over-expression in the tumours correlated with the absence of NASH ($p=0.020$, $r=-0.2$).

Clinico-biology, pathology	**ΔNp73 NT_up_HL**		**ΔNp73 T_up_HL**	
	Pearson's Chi-Square 2-Sided			
	p	χ^2	p	χ^2
Etiology: HBV *vs.* HCV *vs.* alcohol *vs.* NASH vs. others	0.668	2.370	0.020	11.640
Presence *vs.* absence of cirrhosis	0.830	0.040	0.360	0.820
Tumour size > 50 mm *vs.* ≤ 50 mm	0.580	0.300	0.730	0.110
Presence *vs.* absence of HCC multinodularity	0.030	4.320	0.180	1.740
Poor *vs.* moderate *vs.* good differentiation	0.450	1.580	0.850	0.310
AFP > 200 *vs.* ≤ 200 ng/mL	0.030	4.370	0.440	0.590
Microscopic portal invasion	0.710	0.130	0.740	0.100
Presence *vs.* absence of satellite nodules	0.550	0.340	0.350	0.860
Recurrence: extra-hepatic *vs.* hepatic multifocal *vs.* hepatic uninodular	0.730	0.620	0.960	0.060
Vascular emboli	0.930	0.006	0.320	0.980
CD133 T_up_HL			0.770	0.080
CK19 T_up_HL			0.520	0.400
EpCAM T_up_HL			0.740	0.100
Nanog NT_up_HL	<0.001	23.510		
Nanog T_up_HL			<0.001	16.051
Oct4 NT_up_HL	<0.001	13.240		
Oct4 T__up_HL			0.007	7.050
Sox2 NT_up_HL	<0.001	30.470		
Sox2 T_up_HL			0.040	3.910

Table 5. Correlation between the over-expression of ΔNp73 in HCC (T) and the surounding non-tumoural (NT) tissues and clinicopathological data, over-expression of stemness factors (Nanog, Oct4, Sox2) and of stem markers (CD133, CK19, EpCAM). For statistical analysis the Chi-2 Squared 2-sided test was employed, and significance was established for $p<0.05$.

Over-expression of TAp73 in non-tumours positively correlated with cirrhosis (p=0.011, r=0.078) and over-expression of the stemness factors Nanog (p=0.027, r=0.195), Oct4 (p=0.001, r=0.299) and Sox2 (p=0.001, r=0.283) (**Table 6**). In tumours, it positively correlated with the stem-like marker EpCAM (p=0.021, r=0.196) and the stemness factors Nanog (p=0.012, r=0.221) and Oct4 (p=0.012, r=0.221). No correlation was found in tumoural or non-tumoural tissue with HCC aetiology (HBV, HCV, alcohol and NASH).

Clinico-biology, pathology	TAp73 NT_up_HL		TAp73 T_up_HL	
Total prevalence	Pearson's Chi-Square 2-Sided			
	p-value	χ^2	p	χ^2
Etiology: HBV *vs.* HCV *vs.* alcohol *vs.* NASH vs. others	0.035	10.312	0.012	12.825
Presence *vs.* absence of cirrhosis	0.011	6.497	0.775	0.082
Tumour size > 50 mm *vs.* ≤ 50 mm	0.430	0.622	0.305	1.051
Presence *vs.* absence of HCC multinodularity	0.267	1.232	0.298	1.081
Poor *vs.* moderate *vs.* good differentiation	0.210	3.126	0.146	3.842
AFP > 200 *vs.* ≤ 200 ng/mL	0.554	0.349	0.947	0.005
Microscopic portal invasion	0.081	3.044	0.238	1.390
Presence *vs.* absence of satellite nodules	0.077	3.126	0.377	0.780
Recurrence: extra-hepatic *vs.* hepatic multifocal *vs.* hepatic uninodular	0.470	1.510	0.053	5.870
Vascular emboli	0.768	0.087	0.836	0.043
CD133 T_up_HL			0.978	0.001
CK19 T_up_HL			0.128	2.313
EpCAM T_up_HL			0.021	5.303
Nanog NT_up_HL	0.027	4.878		
Nanog T_up_HL			0.012	6.308
Oct4 NT_up_HL	0.001	11.467		
Oct4 T_up_HL			0.012	6.308
Sox2 NT_up_HL	0.001	10.264		
Sox2 T_up_HL			0.566	0.330

Table 6. Correlation between the over-expression of TAp73 in tumoural (T) and the surounding non-tumoural (NT) tissue and clinicopathological data, over-expression of stemness factors (Nanog, Oct4, Sox2) and of stem markers (CD133, CK19, EpCAM). For statistical analysis the Chi-2 Squared 2-sided test was employed, and significance was established for p<0.05.

Both in tumours and in the non-tumours, over-expression of ΔEx2p73 and ΔEx2/3p73 isoforms correlated with high expression of the stemness factors Nanog, Sox2 and Oct4 ($p<0.05$) except for ΔEx2p73 and Nanog that were not found to be significantly correlated in HCC samples ($p=0.437$) (**Table 7** and **Table 8**).

Regarding the association with the clinicopathological data, ΔEx2p73 over-expression in the tumoural tissue correlated with microscopic portal invasion ($p=0.037$, $r=0.182$). Over-expression of ΔEx2/3p73 in tumours was associated to poor differentiation ($p=0.041$), microscopic portal invasion ($p=0.008$, $r=0.230$), and recurrence ($p=0.039$) but no association was found with the HCC aetiology (HBV, HCV, alcohol abuse or NASH).

Clinico-biology, pathology	**ΔEx2p73 NT_up_HL**		**ΔEx2p73 T_up_ HL**	
Total prevalence	**Pearson's Chi-Square 2-Sided**			
	P	χ^2	p	χ^2
Etiology: HBV *vs.* HCV *vs.* alcohol *vs.* NASH vs. others	0.508	3.300	0.420	3.840
Presence *vs.* absence of cirrhosis	0.230	1.410	0.644	0.213
Tumour size > 50 mm *vs.* ≤ 50 mm	0.150	2.030	0.301	1.060
Presence *vs.* absence of HCC multinodularity	0.340	0.880	0.650	0.200
Poor *vs.* moderate *vs.* good differentiation	0.939	0.127	0.707	0.693
AFP > 200 *vs.* ≤ 200 ng/mL	0.843	0.039	0.686	0.164
Microscopic portal invasion	1.000	0.000	0.037	4.360
Presence *vs.* absence of satellite nodules	0.380	0.760	0.938	0.006
Recurrence: extra-hepatic *vs.* hepatic multifocal *vs.* hepatic uninodular	0.340	2.120	0.320	2.224
Vascular emboli	0.400	0.690	0.343	0.896
CD133 T_up_HL			0.770	0.082
CK19 T_up_HL			0.315	1.007
EpCAM T_up_HL			0.872	0.026
Nanog NT_up_HL	<0.001	24.589		
Nanog T_up_HL			0.437	0.603
Oct4 NT_up_HL	<0.001	32.809		
Oct4 T__up_HL			<0.001	15.123
Sox2 NT_up_HL	<0.001	38.081		
Sox2 T_up_HL			0.001	10.670

Table 7. Correlation between the over-expression of ΔEx2p73 in tumours (T) and the surounding non-tumoural (NT) tissue and clinicopathological data, over-expression of stemness factors (Nanog, Oct4, Sox2) and of stemness markers (CD133, CK19, EpCAM). For statistical analysis the Chi-2 Squared 2-sided test was employed, and significance was established for $p<0.05$.

Clinico-biology, pathology	ΔEx2/3p73 NT_up_HL		ΔEx2/3p73 T_up_HL	
	Pearson's Chi-Square 2-Sided			
	p	χ^2	p	χ^2
Etiology: HBV *vs.* HCV *vs.* alcohol *vs.* NASH vs. others	0.020	11.667	0.045	9.724
Presence *vs.* absence of cirrhosis	0.127	2.324	0.165	1.926
Tumour size > 50 mm *vs.* ≤ 50 mm	0.353	0.864	0.648	0.208
Presence *vs.* absence of HCC multinodularity	0.400	0.708	0.074	3.195
Poor *vs.* moderate *vs.* good differentiation	0.829	0.375	0.041	6.388
AFP > 200 *vs.* ≤ 200 ng/mL	0.665	0.187	0.251	1.318
Microscopic portal invasion	0.579	0.307	0.008	6.960
Presence *vs.* absence of satellite nodules	0.626	0.237	0.144	2.132
Recurrence: extra-hepatic *vs.* hepatic multifocal *vs.* hepatic uninodular	0.531	1.268	0.039	6.474
Vascular emboli	0.317	1.003	0.385	0.754
CD133 T_up_HL			0.603	0.270
CK19 T_up_HL			0.025	5.012
EpCAM T_up_HL			0.320	0.988
Nanog NT_up_HL	<0.001	20.160		
Nanog T_up_HL			0.001	10.971
Oct4 NT_up_HL	<0.001	28.233		
Oct4 T__up_HL			<0.001	22.465
Sox2 NT_up_HL	<0.001	33.438		
Sox2 T_up_HL			0.018	5.573

Table 8. Correlation between the over-expression of ΔEx2/3p73 in tumoural (T) and the surounding non-tumoural (NT) tissue and clinicopathological data, over-expression of stemness factors (Nanog, Oct4, Sox2) and of stemness markers (CD133, CK19, EpCAM). For statistical analysis the Chi-2 Squared 2-sided test was employed, and significance was established for $p<0.05$.

The expression of each of the p73 isoforms was graphically represented in function of the expression of the stemness factors Nanog, Sox2 and Oct4 both in tumours and in the adjacent liver tissue (**Figure 5** and **Figure 6**). In both cases, the correlation between the expression of the p73 isoforms and the stemness factors found by statistical tests was also observed on the graphical representation. Additionally, the graphical representation clearly suggested that in HCC nodules, the level of p73 isoforms is closely correlated to the expression level of the three stemness factors Sox2, Nanog and Oct4.

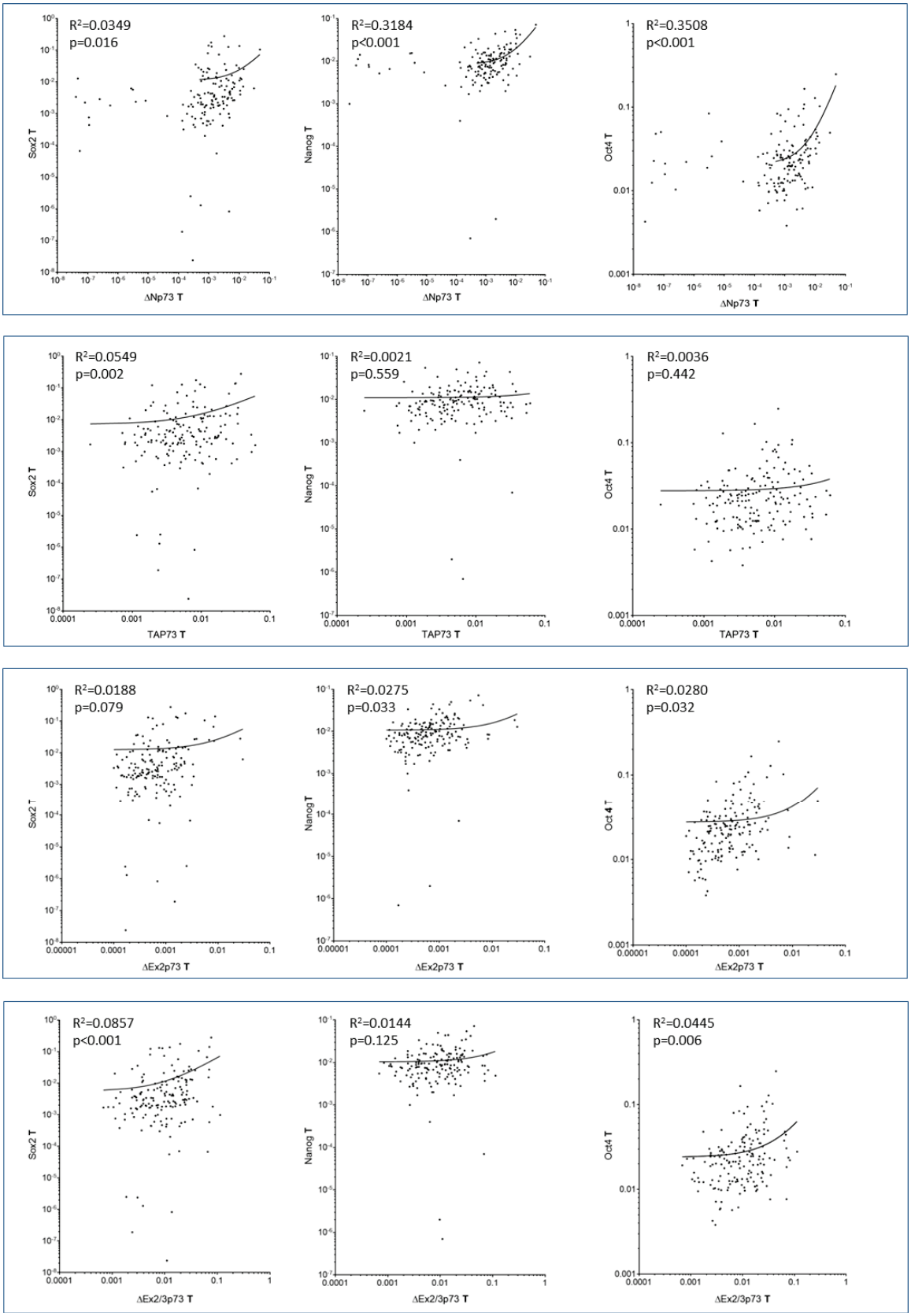

Figure 5. Correlation between the mRNA expression of each p73 isoform and the stemness factors Sox2, Nanog and Oct4 in the TUMOURAL tissue (log scale). Data were modelised using the linear regression approach. Fisher F-test was employed to tesh whether the slope is significantly non-zero.

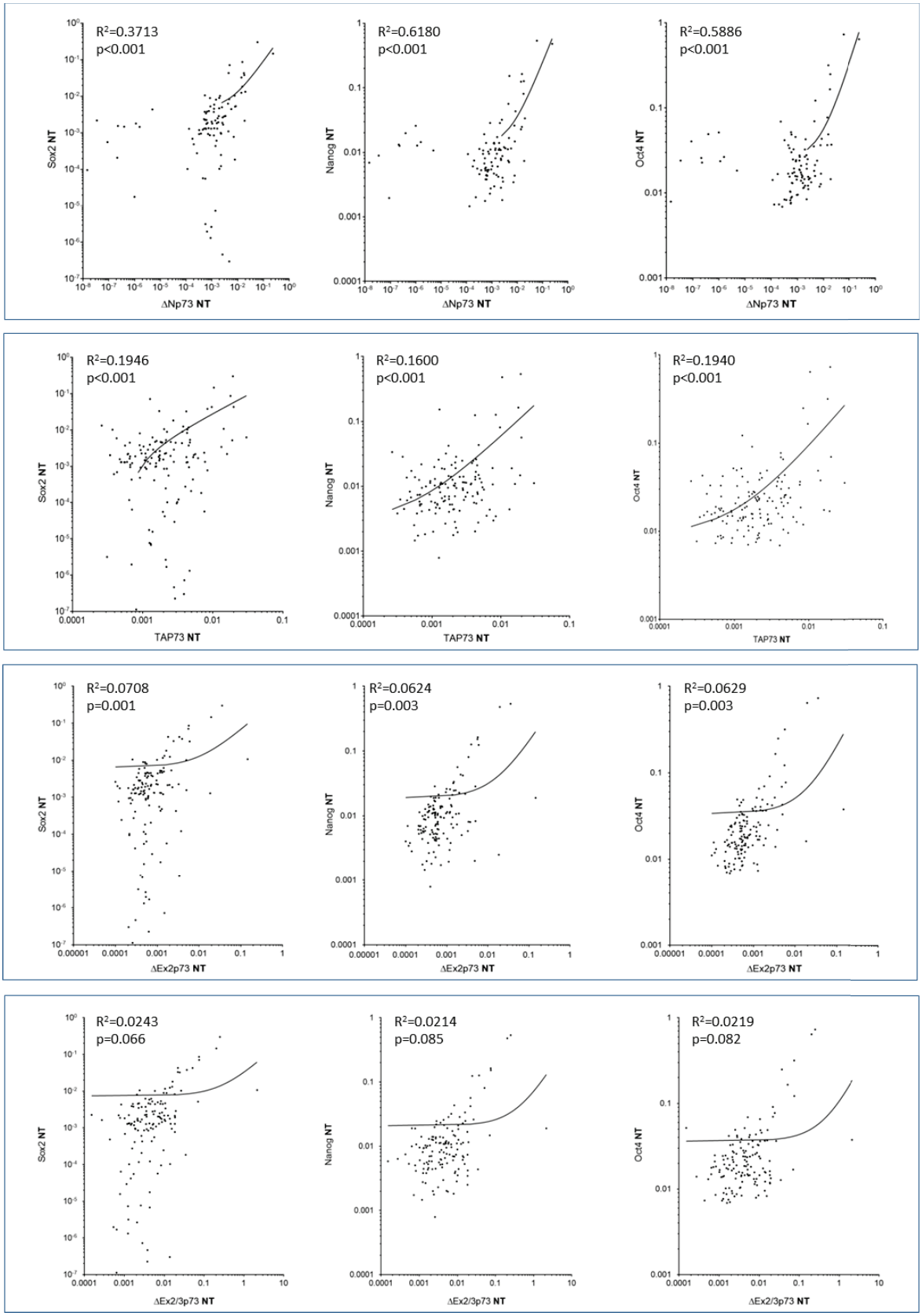

Figure 6. Correlation between the mRNA expression of each p73 isoform and the stemness factors Sox2, Nanog and Oct4 in the NON-TUMOURAL tissue (log scale). Data were modelised using the linear regression approach. Fisher F-test was employed to tesh whether the slope is significantly non-zero.

ΔNp73 over-expression is a factor of poor overall survival

We investigated the association between p73 isoforms over-expression and patients overall survival (OS), progression free survival (PFS), early recurrence-free survival and late recurrence-free survival. Patients were divided in two separate groups with respect to the over-expression of each p73 isoform. Overexpression was defined by three methods: tumours versus matching non-tumoural tissue, tumours versus healthy liver or non-tumoural tissue versus healthy liver. We performed univariate analysis separately for each of these groups of patients with respect to each of the end-points mentioned here above. Results are presented in **Table 9**.

Univariate analysis of survivals regarding variables *vs.* rest	Overall survival		Early recurrence-free survival (< 24 months)		Progression free survival (PFS)		Late recurrence-free survival (>24 months)	
	HR (95% CI)	*P*	HR (95% CI)	*P*	HR (95% CI)	*P*	HR (95% CI)	*P*
ΔNp73 NT_up_HL	0.88 (0.34-2.23)	0.780	1.21 (0.64-2.312)	0.56	1.34 (0.75-2.38)	0.321	2.06 (0.59-7.19)	0.258
ΔNp73 T_up_HL	0.89 (0.40-1.99)	0.776	1.11 (0.59-2.07)	0.748	1.08 (0.63-1.86)	0.771	1.09 (0.37-3.22)	0.874
ΔNp73 T_up_NT	1.56 (0.86-2.82)	0.140	1.55 (0.96-2.51)	0.074	1.28 (0.84-1.92)	0.247	0.74 (0.31-1.74)	0.485
ΔEx2p73 NT_up_HL	0.81 (0.34-1.92)	0.632	1.20 (0.65-2.25)	0.559	1.03 (0.58-1.82)	0.92	0.55 (0.13-2.34)	0.414
ΔEx2p73 T_up_HL	1.51 (0.78-2.93)	0.222	1.16 (0.63-2.13)	0.628	1.22 (0.73-2.02)	0.446	1.35 (0.53-3.42)	0.526
ΔEx2p73 T_up_NT	1.60 (0.88-2.89)	0.121	1.24 (0.77-1.99)	0.378	1.208 (0.80-1.82)	0.366	1.16 (0.52-2.59)	0.719
ΔEx2/3p73 NT_up_HL	0.69 (0.27-1.74)	0.429	1.06 (0.56-2.03)	0.852	1.23 (0.72-2.11)	0.454	1.83 (0.68-4.92)	0.234
ΔEx2/3p73 T_up_HL	0.79 (0.42-1.49)	0.464	1.41 (0.87-2.28)	0.162	1.19 (0.78-1.81)	0.417	0.70 (0.29-1.70)	0.433
ΔEx2/3p73 T_up_NT	0.98 (0.52-1.88)	0.960	1.15 (0.68-1.95)	0.605	1.11 (0.71-1.75)	0.653	1.04 (0.43-2.50)	0.938
TAp73 NT_up_HL	1.46 (0.73-2.91)	0.284	1.17 (0.68-2.04)	0.567	1.24 (0.77-2.01)	0.376	1.51 (0.56-4.06)	0.42
TAp73 T_up_HL	0.72 (0.40-1.30)	0.279	0.94 (0.580-1.51)	0.784	0.99 (0.66-1.50)	0.979	1.17 (0.52-2.70)	0.703
TAp73 T_up_NT	1.07 (0.50-2.30)	0.864	1.09 (0.60-2.01)	0.768	1.08 (0.64-1.84)	0.77	1.08 (0.36-3.21)	0.89
Tumour size > 50 mm	1.65 (0.92-2.96)	0.095	2.59 (1.58-4.24)	<0.001	2.17 (1.43-3.29)	<0.001	1.25 (0.52-2.97)	0.619
HCC multinodularity	0.98 (0.46-2.12)	0.967	1.26 (0.71-2.24)	0.437	1.23 (0.74-2.05)	0.418	1.15 (0.39-3.40)	0.801
AFP > 200 ng/mL	1.17 (0.55- 2.46)	0.685	1.98 (1.14-3.46)	0.016	1.47 (0.88-2.45)	0.139	0.45 (0.11-1.92)	0.28
Satellite nodules	2.23 (1.20-4.15)	0.011	2.05 (1.25-3.37)	0.004	2.07 (1.32-3.23)	0.001	2.34 (0.84-6.52)	0.104
Recurrence: extra-hepatic *vs.* hepatic multifocal *vs.* hepatic uninodular	1.56 (1.02-2.38)	0.038	1.48 (1.06-2.06)	0.023	1.33 (0.99-1.78)	0.059	0.89 (0.47-1.69)	0.719
Cirrhosis	2.39 (1.27-4.53)	0.007	1.23 (0.75-2.00)	0.416	1.53 (0.99-2.35)	0.053	2.97 (1.25-7.07)	0.014
vascular emboli	2.72 (1.50-4.94)	0.001	3.66 (2.23-6.00)	<0.001	2.60 (1.70-3.97)	<0.001	0.75 (0.25-2.22)	0.597
Microscopic portal invasion	0.68 (0.29-1.62)	0.387	1.30 (0.71-2.39)	0.397	1.20 (0.70-2.07)	0.507	0.90 (0.26-3.08)	0.862
CD133 T_up_HL	1.26 (0.62-2.55)	0.519	0.90(0.49-1.69)	0.752	1.13 (0.68-1.88)	0.634	1.95 (0.80-4.76)	0.142
CK19 T_up_HL	1.29 (0.64-2.60)	0.484	1.35 (0.78-2.36)	0.299	1.31 (0.80-2.16)	0.287	1.19 (0.40-3.53)	0.75
EpCAM T_up_HL	1.05 (0.56-1.95)	0.889	1.01 (0.60-1.69)	0.978	1.01 (0.65-1.56)	0.983	0.99 (0.42-2.33)	0.991
FZD7 T_up_HL	0.67 (0.36-1.27)	0.219	1.14 (0.70-1.85)	0.599	1.19 (0.78-1.80)	0.417	1.33 (0.59-2.97)	0.494
Oct4 T _up_ HL	0.50 (0.18-1.42)	0.193	1.31 (0.69-2.46)	0.409	1.25 (0.71-2.18)	0.444	1.04 (0.31-3.54)	0.946
Oct4 NT _up_ HL	1.31 (0.51-3.36)	0.572	1.21 (0.55-2.67)	0.633	1.19 (0.59-2.38)	0.625	1.10 (0.26-4.73)	0.897
Oct4 T _up_ NT	0.96 (0.51-1.80)	0.894	1.57 (0.93-2.67)	0.092	1.41 (0.91-2.20)	0.123	1.12 (0.49-2.53)	0.793
Nanog T _up_ HL	0.81 (0.32-2.07)	0.661	1.28 (0.65-2.53)	0.481	1.38 (0.76-2.50)	0.296	1.77 (0.52-6.00)	0.360
Nanog NT _up_ HL	0.95 (0.45-2.01)	0.894	0.96 (0.52-1.77)	0.884	0.93 (0.55-1.56)	0.773	0.84 (0.31-2.28)	0.738
Nanog T _up_ NT	1.34 (0.71-2.52)	0.361	1.32 (0.79-2.20)	0.289	1.42 (0.92-2.21)	0.115	1.80 (0.78-4.11)	0.166
Sox2 T _up_ HL	1.59 (0.78-3.26)	0.203	1.32 (0.71-2.43)	0.383	1.05 (0.60-1.85)	0.86	0.49 (0.11-2.09)	0.333
Sox2 NT _up_ HL	1.20 (0.37-3.91)	0.758	1.19 (0.43-3.29)	0.738	1.57 (0.68-3.62)	0.29	4.03 (0.90-18.08)	0.069
Sox2 T _up_ NT	1.38 (0.69-2.77)	0.366	0.88 (0.52-1.50)	0.645	0.78 (0.50-1.22)	0.27	0.55 (0.23-1.31)	0.177

Table 9. Univariate survival analysis performed with the Cox-2 hazard ratio method. In red are represented the statistically significant results.

The over-expression of ΔNp73 in tumours compared to the matching non-tumoural tissue was found as a prognosis factor in favour of early recurrence, at the borderline of significance (HR=1.551, 95%CI[0.958-2.510], p=0.074). The results were also represented with the Kaplan-Meier method and confirmed by the log rank test (**Figure 7A**). The other transcripts were not found to have a significant impact on patient outcome. In multivariate analysis, ΔNp73 was found to be a prognostic factor for early recurrence versus the other factors. This result could be attributed to specific gain of function properties of ΔNp73, since this observation was not true for the two other truncated isoforms ΔEx2p73 and ΔEx2/3p73.

Strikingly, no association was found between the expression level of TAp73 and patients outcome. TAp73 is considered as a tumour suppressor and it was shown that during an oncogenic stimulus, in absence of functional p53, TAp73 expression increases in order to replace part of the cellular functions of p53. In this case, cells were shown to be more sensitive to apoptosis. In our cohort of HCC patients, the Kaplan-Meyer diagram representing the overall survival of patients overexpressing TAp73 versus the rest, showed a tendency towards a better outcome for the first group, but not statistically significant (HR=0.723, 95%CI[0.401-1.301,], p=0.279) (**Figure 7B**).

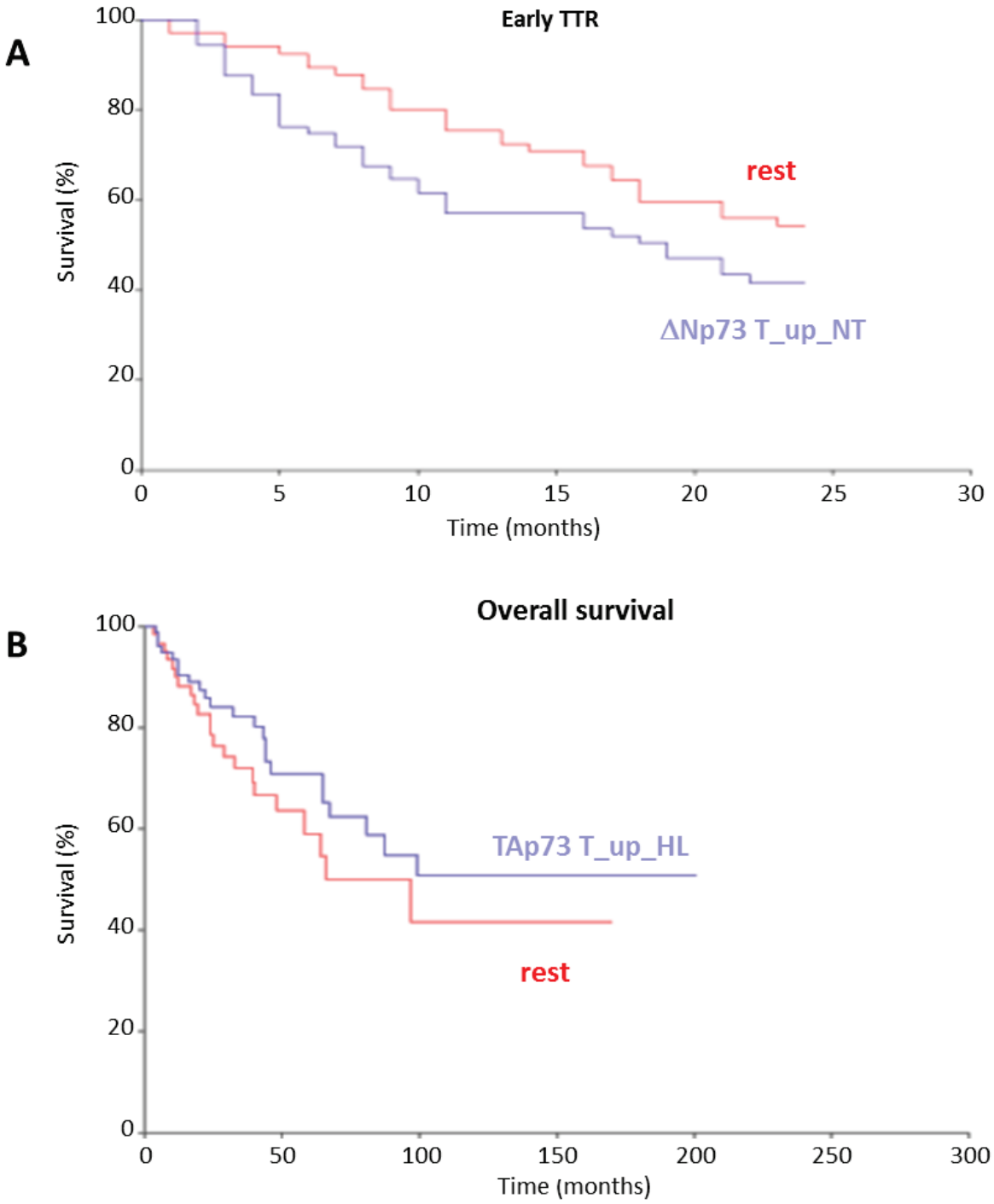

Figure 7. Kaplan Meier curves regarding **A.** Early recurrence probability when ΔNp73 is over-expressed in tumours compared to the matching non-tumoural (T_up_NT) tissue; and **B.** Overall survival probability when TAp73 is over-expressed in tumours compared to healthy liver (HL).

The balance between the truncated isoforms and TAp73 impacts the patients' late recurrence and presence of stemness factors.

It has been previously reported that in leukemia, rather then the over-expression of one single truncated isoforms, it is the balance between the relative cellular amounts of ΔNp73 and TAp73 that has the strongest impact on patient outcome (Chapter 3.3.5 of the Introduction). A high ratio ΔNp73/TAp73 is a prognosis factor for recurrence and poor overall survival in patients treated with chemotherapy. The value of this balance has two consequences. First, it is linked to the dominant negative effect of ΔNp73 on TAp73. If the balance is in favour of ΔNp73 (high ΔNp73/TAp73), TAp73 is outweighted by ΔNp73 and will not be capable of transactivating target genes involved in cell cycle arrest or apoptosis. Second, this impacts on the gain of function properties of ΔNp73, because TAp73 can act in its turn as a dominant negative of this truncated isoform. In this case, even if ΔNp73 is highly expressed, simultaneous high levels of TAp73 will inhibit the specific activity of ΔNp73. In both cases, switching the balance in favour of ΔNp73 has a rather pro-oncogenic than anti-oncogenic effect. For each patient included in our HCC cohort, the value of the expression ratio ΔNp73/TAp73 was calculated in both tumours and surrounding non-tumour tissue. The result is represented in **Figure 8A** for each patient, with the horizontal lines representing the median of expression. We found that the median of ΔNp73/TAp73 ratio is lower in tumoural than in the non-tumoural samples. This result was unexpected since we hypothesized that the balance in favour of ΔNp73 would benefit tumoural cells and thus would increase during tumourigenesis.

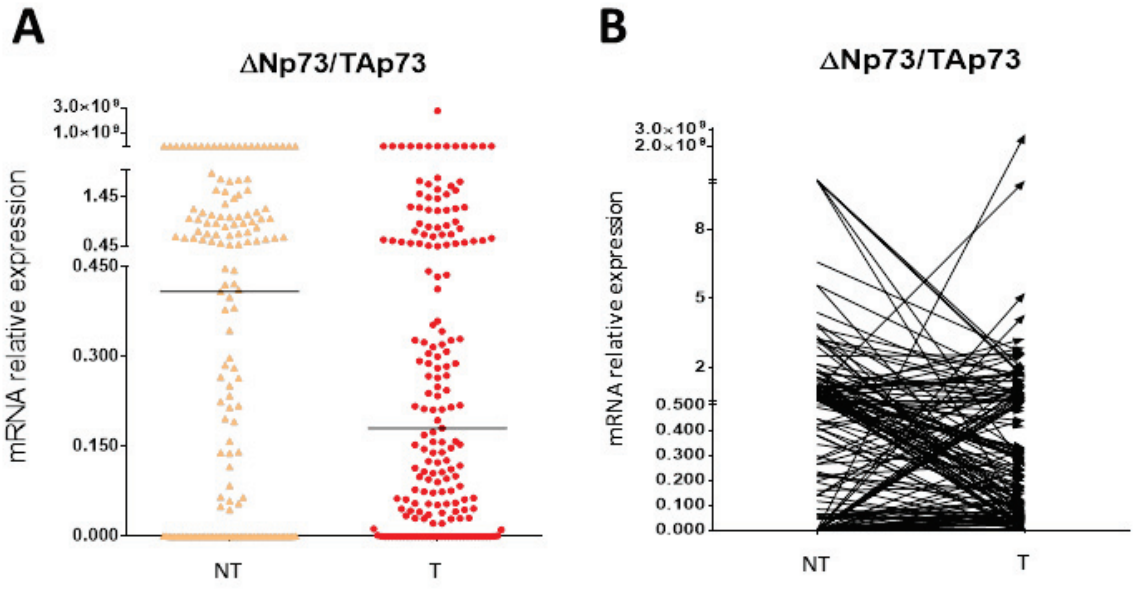

Figure 8. Ratio ΔNp73/TAp73 in liver tissue. A. Relative expression in HCC tumoural (T) and surrounding non-tumoural (NT) tissue. Horizontal black lines represent the median of expression. **B** Comparison of the ratio ΔNp73/TAp73 between each tumour (T) and the corresponding non-tumoural (NT) tissue. Each arrow represents a pair tumour/surrounding tissue.

The value of the ration ΔNp73/TAp73 is determined both by the variation of ΔNp73 and TAp73. Therefore, an increase in the ratio can be due either to a ΔNp73 increase or to a TAp73 decrease and *vice versa* for low values of the ratio. To better understand how this ratio varies in non-tumoural and tumoural tissue, we graphically represented the value of the ratio ΔNp73/TAp73 both in tumours and non-tumours in function of ΔNp73 or TAp73 (**Figure 9**). We found that the value of this ratio was much more impacted by the variations in the expression of ΔNp73 than that of TAp73. When TAp73 expression increased, small variations of this ratio were observed.

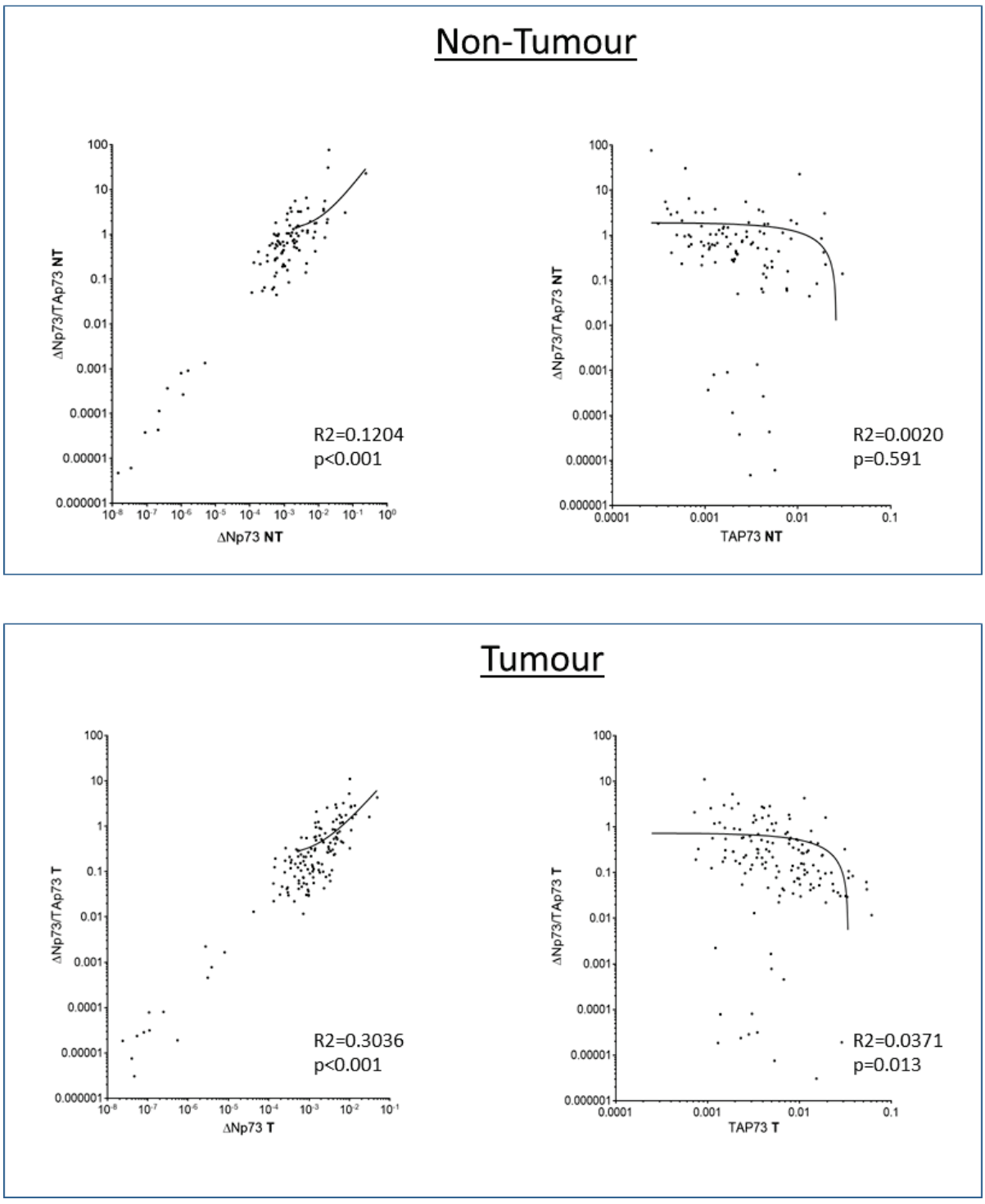

Figure 9. Correlation between the value of ΔNp73/TAp73 ratio and the mRNA expression of ΔNp73 or TAp73. Data were modelised using the linear regression approach. Fisher F-test was employed to tesh whether the slope is significantly non-zero.

We divided patients in two groups based on the value of the ratio ΔNp73/TAp73: the first group was formed of patients with a higher ratio ΔNp73/TAp73 in the tumour than in the matching non-tumour (n=91) and the second group with a lower ratio (n=63). The impact of a low or a high ratio was then evaluated on patients overall survival, progression free survivial and early and late recurrence (**Table 10**). Univariate survival analysis indicated that a higher ratio ΔNp73/TAp73 in tumours than in corresponding non-tumours could be a prognostic factor for late recurrence (HR=2.71, 95%CI [0.92-7.94], p=0.07) (**Table 10**). Late recurrence is recognised when a tumour is detected more than 2 years after tumour resection and is associated to the intrinsic capacity of the surrounding tissue to develop *de novo* hepatocellular tumours. This suggests that an increase in the ΔNp73/TAp73 ratio in cells from the surrounding tissue could be involved in the emergence of *de novo* tumour. To confirm this observation, we represented the results with the Kaplan-Meier method and confirmed them by the log rank test (**Figure 10**).

Univariate analysis of survivals regarding variables *vs.* rest	Overall survival		Early recurrence-free survival (< 24 months)		Progression free survival (PFS)		Late recurrence-free survival (>24 months)	
	HR (95% CI)	*P*	HR (95% CI)	*P*	HR (95% CI)	*P*	HR (95% CI)	*P*
ΔNp73/TAp73 T_up_NT	0.96 (0.53-1.77)	0.907	0.87 (0.54-1.41)	0.566	1.11 (0.73-1.71)	0.623	2.71 (0.92-7.94)	0.07

Table 10. Univariate analysis between increased ratio ΔNp73/TAp73 in tumours compared to the corresponding non-tumours (T_up_NT).

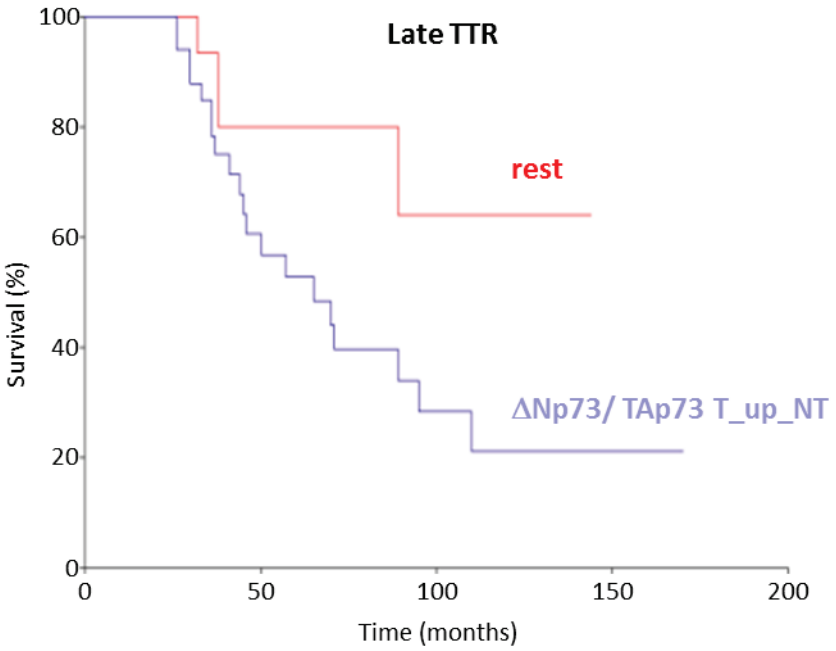

Figure 10. Kaplan- Meier curve representing the influence of the increased ΔNp73/TAp73 ratio in tumours (T) compared to the corresponding non-tumour (NT) on late recurrence free survival.

ΔNp73 is downregulated during the differentiation of HepaRG

Of the four p73 isoforms studied in the HCC cohort, ΔNp73 was the only one that we found to be a prognosis factor for early recurrence. Early recurrence is related to the tumour initiating capacity of cancer cells remaining in the liver after tumour resection. Studies showed that these cells are considered as cancer stem cells. For these reasons we investigated the role of ΔNp73 in the progenitor phenotype of liver cells and the emergence of the CSCs.

We studied *in-vitro* the expression status of ΔNp73 during the differentiation process of liver progenitor cells. For this, we used HepaRG cells which are a liver bipotent progenitor cell line. When cultured in sub-confluent conditions, HepaRG cells proliferate and have the morphology intermediate between epithelial cells and mesenchymal cells and express progenitor markers (Parent et al., 2004). In confluent conditions, cells stop proliferating and engage into a differentiation program towards hepatic cells. After maintaining cells for 2 weeks in confluent conditions followed by two other weeks of culture in presence of DMSO, cells will organize into a monolayer formed of the two epithelial liver cell types: hepatocytes and cholangiocytes. As shown in **Figure 11A**, hepatocytes appear as small cells, organized in longitudinal cords, with inter-cellular bile canaliculi and surrounded by cholangiocytes while are larger cells. At this time point and during the proliferative stage, cells were collected and the expression of the p73 isoform ΔNp73, albumin and EpCAM were measured by RT-qPCR. We found a decreased expression of ΔNp73 isoform in differentiated cells compared to proliferative cells. The expression of EpCAM, associated to liver progenitor phenotype and albumin, associated to hepatocyte phenotype were assessed in order to confirm cell phenotype. As expected, proliferating HepaRG cells express a higher level of EpCAM and lower level of albumin compared to differentiated HepaRG cells (**Figure 11B**).

We confirmed the results at the protein level by Western Blot analysis on total cell extracts with a specific antibody against ΔNp73. In differentiated HepaRG cells ΔNp73 was undetectable while a band corresponding to this isoform (at 72kDa) appeared in the sample lane corresponding to non-differentiated HepaRG cells.

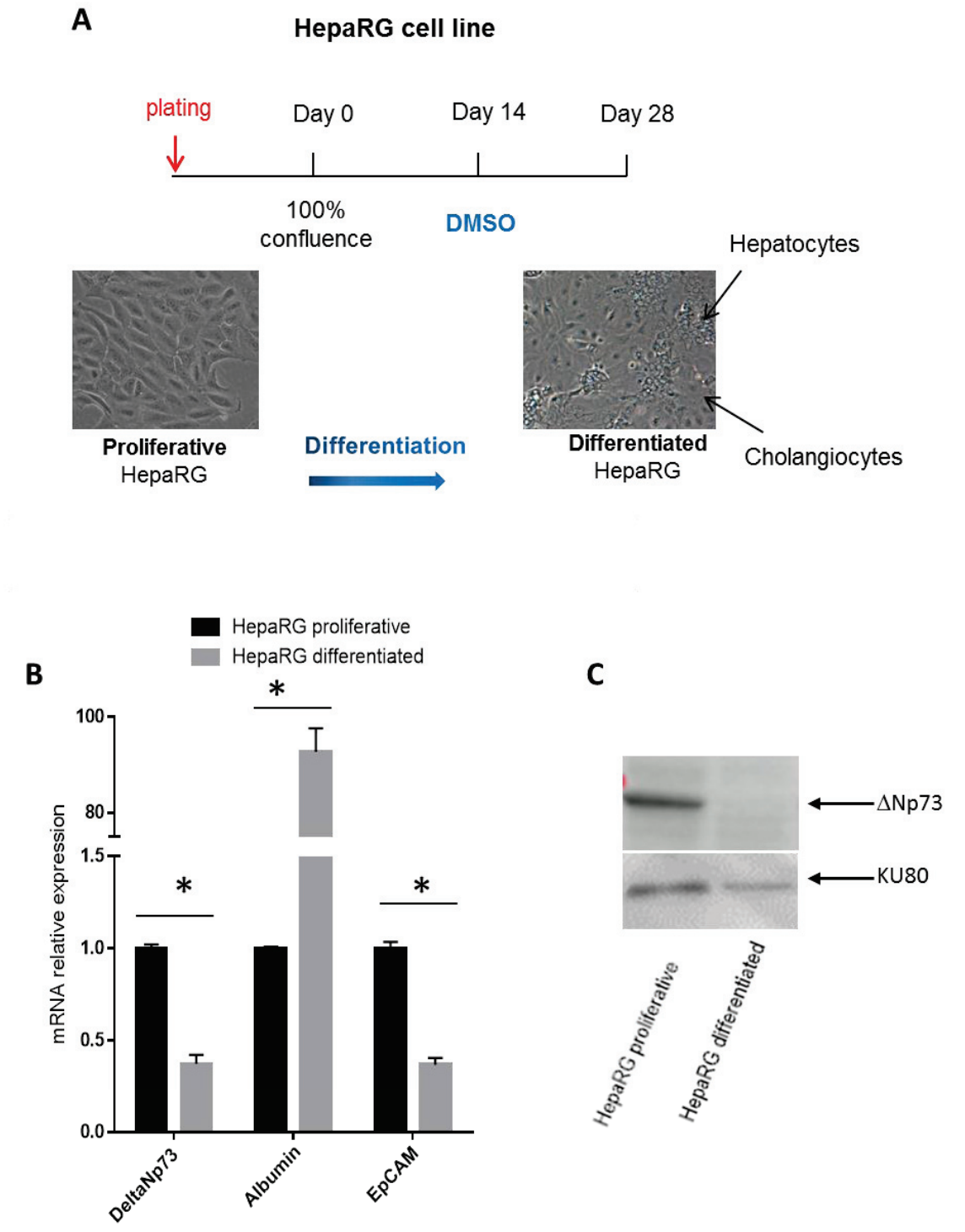

Figure 11. Expression of ΔNp73 in proliferating and differentiated HepaRG cells. **A.** Differentiation protocol of the liver progenitor cell line HepaRG. **B.** RT-qPCR analysis of the expression of ΔNp73, the hepatic marker albumin and the progenitor marker EpCAM in proliferating and differentiated HepaRG. **C.** Western Blot result confirming the absence of ΔNp73 at the protein level in differentiated HepaRG cells and its presence in progenitor proliferating HepaRG cells. The Ku80 protein was used as a loading control.

ΔNp73 expression increases during the early stages of hepatocarcinogenesis

Since we and others found that ΔNp73 is overexpressed in HCC, we investigated the level of expression of this isoform in an *in vitro* model of cell transformation established in the lab. PHHs were immortalized *in vitro* by ectopic expression of the SV40 oncoviral proteins small T (ST) and large T (LT) and further transformed with the mutant active form of H-Ras^{V12} (**Figure 12A**).

The expression of ΔNp73 was investigated in parental primary human hepatocytes, transformed hepatocytes and a sub-population of these transformed hepatocytes isolated by agar colony formation. We found that ΔNp73 expression increased during transformation and was enhanced in transformed hepatocytes sub-clones from agar assay, thought to possess aggressive features. In this model of hepatic immortalization and transformation, cells acquire EMT (such as vimentin) and progenitor markers (such as CK19) (*Pez, Gifu et al, in prep*).

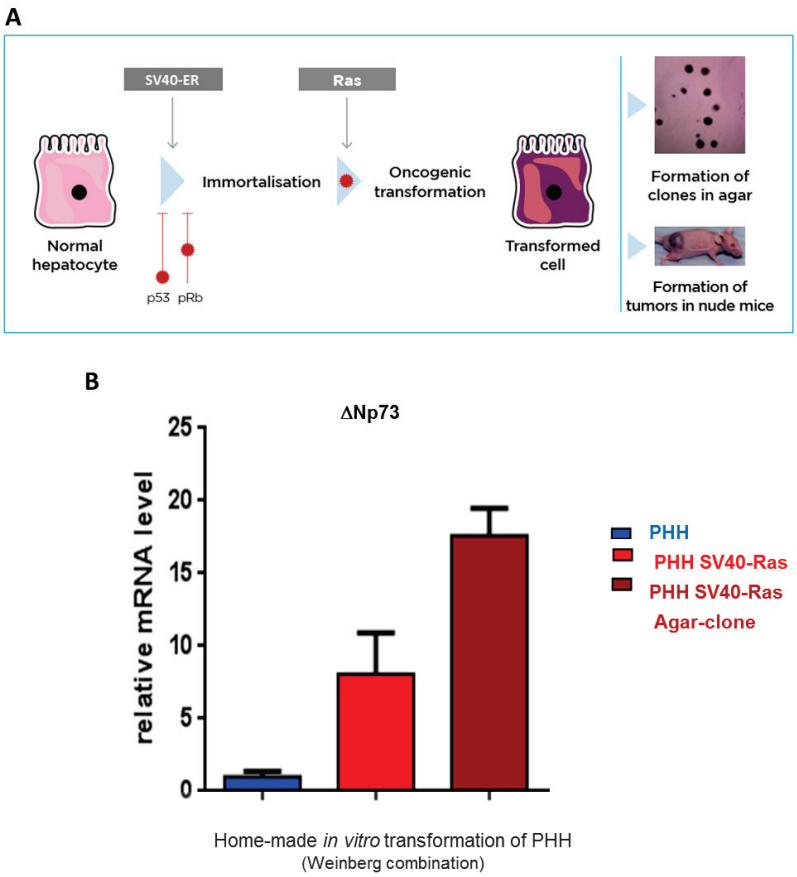

Figure 12. Expression of ΔNp73 during the *in vitro* transformation of primary human hepatocytes. **A.** Model of *in vitro* transformation by expression of the SV40 oncoviral proteins and a constitutively active mutant form of RAS. **B.** Expression of ΔNp73 in PHHs, transformed hepatocytes and in an agar clone-derived population of these transformed hepatocytes.

ΔNp73 is overexpressed in cancer stem cells

We than investigated whether ΔNp73 was specifically overexpressed in liver cancer progenitor cells, as this isoform is thought to promote cell stemness. We isolated the most immature cells from three HCC cell lines: HuH7, Hep3B and Focus by culturing the entire cell population in non-adherent conditions and in absence of serum. In these *in-vitro* conditions, only immature/cancer stem cells can develop and form hepatospheres, mainly composed of cancer progenitor cells. We performed gene expression analysis by RT-qPCR in the parental heterogeneous population and derived 4-days old hepatospheres. We confirmed that hepatospheres are formed of a subpopulation with progenitor traits since they overexpressed stemness factors such as Sox2, Oct4, Klf4 and Nanog. We found that ΔNp73 was overexpressed in the isolated cancer progenitor cell population (**Figure 13**). The presence of ΔNp73 in HCC progenitor cells could be either a driver to the emergence of this subpopulation or the consequence of the progenitor phenotype.

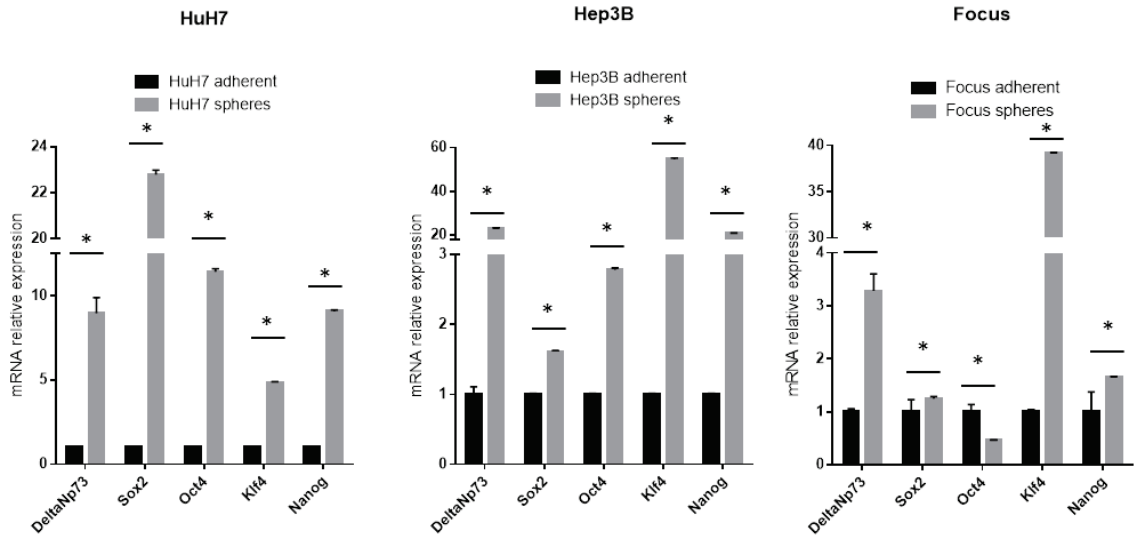

Figure 13. Expression of ΔNp73 and the stemness factors Sox2, Oct4, Klf4 and Nanog in three HCC cell lines (HuH7, Hep3B and Focus) in adherent conditions (black) or in spheres obtained after culture in low-adherent conditions (grey).

ΔNp73 ectopic expression increases the expression of stemness markers

In order to determine if ΔNp73 could drive the expression of immaturity markers, we ectopically expressed this isoform in the p53-null HCC cell line Hep3B and in the p53 wild-type (WT) progenitor cell line HepaRG. The stable cell lines overexpressed the exogenous protein ΔNp73 as shown by Western-Blot in **Figure 14A**. The expression of stemness factors in the ΔNp73 stable cell lines was analyzed at the mRNA level and compared to the parental cell lines. We observed that independently of the status of p53, ΔNp73 expression increased the transcription of stemness factors Oct4, Klf4 and Nanog as well as IGF1R and TAp73 (**Figure 14B**). The morphology of cells did not change after transduction suggesting than ΔNp73 would not contribute to the epithelial-to-mesenchymal transition (data not shown). Furthermore, it has been shown that in melanoma and lung cancer cells, ΔNp73 induces the expression of IGF1R, which has been shown to maintain pluripotency by blocking differentiation of embryonic stem cells into somatic cells. We found that in hepatocellular carcinoma ΔNp73 also regulates IGF1R.

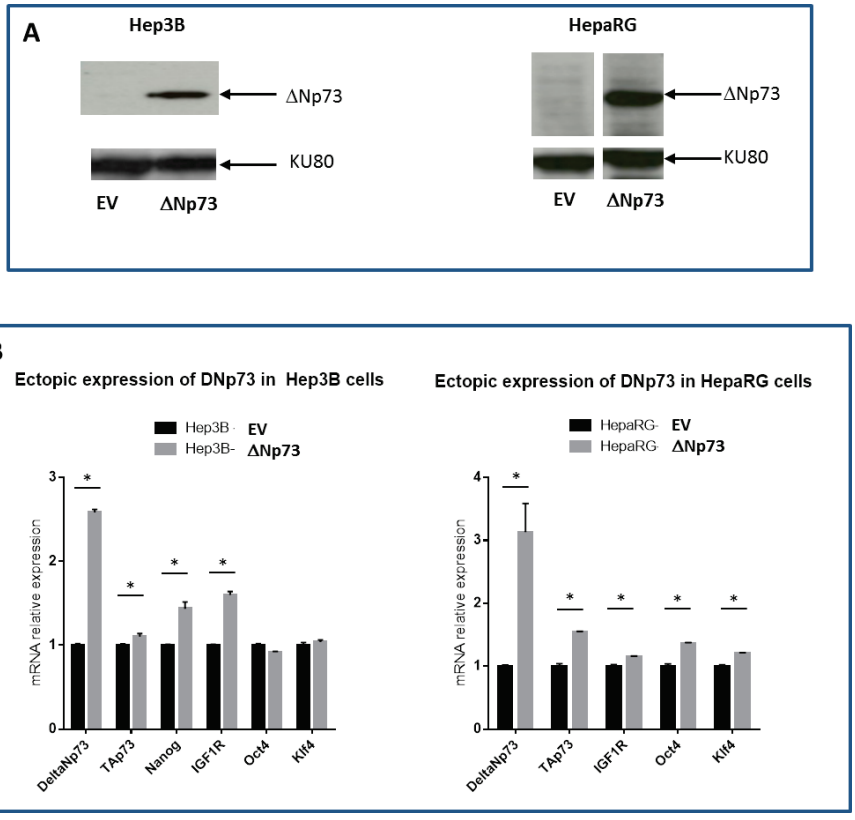

Figure 14. Expression of ΔNp73 and stemness factors in ΔNp73 stably transduced Hep3B and HepaRG cell lines. A. Western Blot results confirming the expression of ΔNp73 protein in stably transduced Hep3B and HepaRG cell lines; EV, cells transduced with an empty lentivirus. Ku80 was used a load control. **B.** Expression of ΔNp73, TAp73, Nanog, IGF1F, Oct4 and Klf4 in ΔNp73-overexpressing cells and the control empty vector (black).

ΔNp73 expression increases the efficacy of holoclones formation

It has been described that epithelial stem cells and progenitor cells can be distinguished thanks to their capacity to generate colonies starting from single cells. More cells of origin are de-differentiated, more the resulting colony is bigger, with sizes described as small, medium and large and formation of paraclones, meroclones and holoclones, respectively.

We examined the colony formation potential of ΔNp73-transduced cell lines in comparison to the EV control cell lines. Paraclones were counted separately and called here 'small colonies' while medium and large colonies were counted together and called 'large colonies'. We observed that ΔNp73 expression modifies the size, but not the number of colonies. When ΔNp73 was present, cells formed larger colonies, which means that the ΔNp73 stable cell line contains a similar number of immature cancer cells compared to control cells, but these immature cells are composed of more early progenitors and cancer stem cells (**Figure 15**).

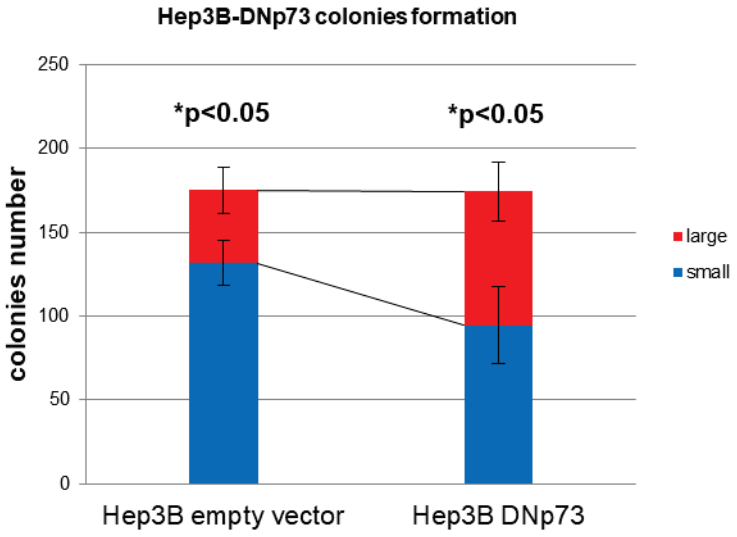

Figure 15. Quantification of small and large colonied formed by ΔNp73-expressing and empty vector Hep3B cells.

ΔNp73 does not enhance the proliferative capacity of HCC or liver progenitor cells

It has been shown that TAp73 inhibits cell proliferation but it is not known whether ΔNp73 could favor cell proliferation, in particular by blocking TAp73 and p53 through its dominant negative properties (Jost et al., 1997; Kaghad et al., 1997; Zhu et al., 1998). To answer this question, the growth rate of Hep3B (p53 null) and HepaRG (p53 WT) cells stably transduced with ΔNp73 was compared to cells transduced with empty vector. No difference was observed between the control and the ΔNp73-expressing cells the two first days. However, ΔNp73-expressing cells showed a higher proliferation rate at day 3 and 4, suggesting that they are less sensitive to cell contact inhibition or to growth factors deprivation than control cells (**Figure 16).** Additional experiments should be performed to further investigate into this hypothesis.

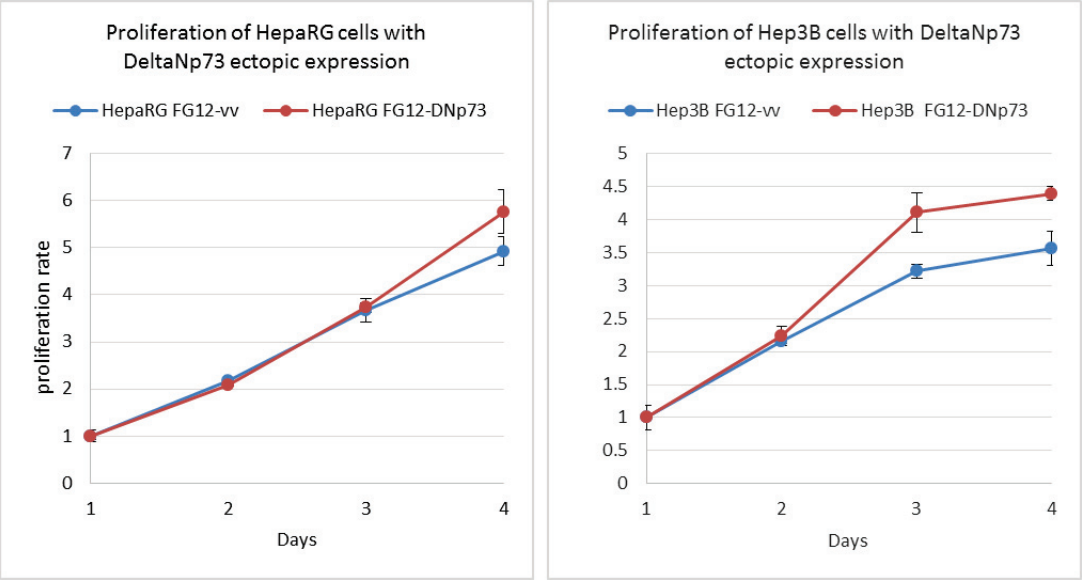

Figure 16. Proliferation assay of HepaRG and Hep3B cells ectopically expressing ΔNp73 versus control cells (empty vector). Cells were cultured for 4 days in 96 well plates. Proliferation was measured by MTS assay.

Discusion

Hepatocellular carcinoma patients have a very poor outcome. This cancer type is highly refractory to conventional chemotherapeutic agents and patients undergoing tumour removal show a high incidence of cancer relapse. Moreover, patients treated by Sorafenib rapidly develop secondary resistance. It is thought that drug resistance and relapse post-surgery are due to the existence of cancer stem cells inside hepatocellular tumours.

Little is known about the factors contributing to the emergence and maintenance of the CSCs pool. Increasing number of studies show that the of the p53 family members p63 and p73 are not only important in regulating apoptosis and cell cycle arrest but also play a role in the maintenance of the CSCs pool.

Our results show that in the non-tumoural liver tissue surrounding the HCC nodules, the four N-terminal truncated p73 isoforms are overexpressed in about the same proportion of cases (with TAp73 having a slightly superior incidence). In the tumours, we found that the transcripts ΔEx2/3p73 and TAp73 corresponding to the P1 promoter are much more frequent. This suggests that the P1 promoter is activated more frequently in tumours than in non-tumour tissues. Secondly, this result also suggests that in HCC cells, alterations of the transcription-splicing coupling regulation or of the elongation rate could appear, thus explaining why we observed more often ΔEx2/3p73 overexpression than ΔEx2p73. Such alterations have already been reported in which activation of the EGFR pathway triggers aberrant IR-A/IR-B ratio (IR:insulin receptor) in HCC cells through the upregulation of several splicing factors (Chettouh et al., 2013).

Although ΔNp73 is a target-gene of the transcriptionally competent p53 family members, in particular TAp73, we did not observe correlation between TAp73 and ΔNp73 overexpression in the tumoural tissue, contrary to the non-tumour. This is probably due to the involvement of other transcription factors in the regulation of the P1 and P2 promoters, for example the oncogenic factor c-myc for P2 and the transcription factor E2F1 for P1, both of them previously described to be overexpressed in HCC.

In the liver non-tumour tissue, activation of the P1 and P2 promoters correlate but in HCC, P2 activation does not seem to occur at the same time as P1 in terms of frequency. It has been shown that the P2 promoter contains responsive elements to the oncogene c-Myc and E2F1, both described to be overexpressed in cancer and proliferating cells.

We hypothesised that ΔNp73 overexpression triggers the expression of stemness features in HCC. We and others showed that ΔNp73 counteracts the p53-dependent inhibition of Sox2,

Oct4 and Nanog expression and that Nanog is a true ΔNp73-target gene, probably by synergizing the transactivation activity of a non-identified transcription factor (Lin et al., 2012, Voeltzel et al., submitted). Here, we found that besides the ΔNp73 isoform, TAp73, ΔEx2/p73 and ΔEx2/3p73 also correlate with stemness factors Sox2, Oct4 and Nanog in HCC. However, this result should be carefully interpreted as it does not necessarily mean that these isoforms trigger the transcription of these stemness factors. First, this could be an artefact due to the simultaneous overexpression of TAp73, ΔEx2p73 and ΔEx2/3p73 and of ΔNp73 in the same tumour. Events that lead to ΔNp73 overexpression also lead to overexpression of TAp73, ΔEx2p73 and ΔEx2/3p73. Since ΔNp73 triggers the transcription of Oct4, Sox2 and Nanog, this could explain the significance of the correlation tests between the isoforms ΔEx2/p73 and ΔEx2/3p73 and the three stemness factors. Secondly, since ΔNp73 and ΔEx2p73 and ΔEx2/3p73 share the same DNA binding domain, these two last truncated isoforms can also block the p53-dependent inhibition of Oct4, Sox2 and Nanog expression.

TP73 expression is tissue specific. For example, several studies found a link between *TP73* hypermethylation and overexpression in haematological diseases, but similar reports in the liver reported absence of aberrant methylation of the gene while the protein was still found to be overexpressed. In the same manner, two studies showed the link between deregulation of the balance ΔNp73/TAp73 and patient outcome (discussed in the Introduction, Chapter 3). However, in our study we did not found a significant impact on patient overall survival or recurrence. This suggests once again that p73 overexpression is regulated differently depending on the type of tissue that is being studied.

It is possible that by stratifying patients based on the p53 status (wild type or mutated) we could observe even to a higher extent the importance of TAp73 overexpression on patients overall survival when p53 is mutated. In these patients, activation of the P1 promoter is needed to activate the transcription of TAp73. But, the combination between P1 activation and the deregulation of splicing could favour the formation of splicing products rather than the full-length isoform.

The result that ΔNp73 overexpression in HCC correlates with that of stemness factors is a strong argument for implicating this isoform in the emergence of CSCs. Correlation data between overexpression of each p73 isoform and stemness factors showed significant associations in all cases, both in the tumours and the non-tumours. However, at this level it is very difficult to assess whether there is a relation between ΔNp73 expression and CSCs population, since the latter represent a very small population inside the tissue sample investigated.

It is of importance to note that our approach does not take into account the mRNA level of ΔN'p73. This transcript is obtained from the activation of the P1 promoter but integrates the sequence of the 3' exon exon (located in the intron 3 and coding for the N-terminal specific part of ΔNp73). The inclusion of the 3' exon generates a stop codon upstream from the AUG contained in this exon and therefore the protein obtained is exactly the same as the one obtained from the ΔNp73 transcript. The primers that we used in the cohort study allowed us specifically to amplify ΔNp73, not ΔN'p73. By not taking into consideration the amount of the ΔN'p73 transript, we underestimate the protein amount of the ΔNp73 isoforms and therefore i) we have false-negative cases for the overexpression of ΔNp73 protein and ii) the balance between the cellular amount of full length and truncated isoforms cannot be well estimated. This is extremely important since we consider that the cell outcome dependends on the total amount of ΔTAp73 protein. Our survival analysis shows that ΔNp73 overexpression is not predictive of patients overall survival, contrary to other studies clearly showing that patients having positive immunostaining inside the tumour have a shorter overall survival than the rest. However, these studies did take into consideration the total amount of the ΔNp73 protein inside the cell. It could be very interesting to perform immunohistochemistry analysis of ΔNp73 expression at least on some samples from our cohort and to compare with the transcript level.

The initial aim of this work was to prove that ΔNp73 would promote by itself the expression of stemness factors that would favour the appearace of an HCC cancer stem cells population. However, as we showed here, the overexpression of the ΔNp73 is accompagnied by the overexpression of TAp73 (both in HCC samples and *in vitro*). It would be important to verify the functionality of the TAp73 protein present in these tumours. Indeed, like for p53, some proteins have been shown to decrease or abolish TAp73 activity. For example, by binding on its N-terminus, MDM2 induces TAp73 neddylation and its subsequent cytoplasmic localization, thus decreasing TAp73 transactivation function (Watson et al., 2006). Also, ΔNp63 isoform promotes survival of breast cancer cells by interacting with TAp73 and thereby inhibiting its proapoptotic activity (Leong et al., 2007).

The moderate effect that we observe on stemness factors expression after overexpressing ΔNp73 can be explained by the inhibition TAp73-mediated. Indeed, if we admit that ΔNp73 posses gain of function properties, for example by binding and cooperating with transcription factors, then TAp73 behaves as a dominant negative of ΔNp73, quite in the same manner as this last acts on the former one.

We observed that ΔNp73 expression is progressively increased during hepatocarcinonegesis. If considering that ΔNp73 acts as a stemnes factor during this process, this result is in accordance to other data in the literrature reporting the progressive enrichment in stemness features during multistep hepatocarcinogenesis in HCC patients and murine HCC models (Kowalik et al., 2015; Yoo et al., 2017). Preneoplastic cells retained a certain plasticity potential and can acquire additional markers during complete transformation.

Materials and Methods

Human Tissue Samples

138 HCC and matched non-tumour surrounding liver samples were obtained from patients with resectable HCC. Patients with all HCC aetiologies were included (HBV, HVB, alcohol abuse, NASH) and clinicopathological data was collected together with patients follow-up. The distributon of aetiology in the cohort was HCV 28.3% (n=39), HBV 21.0% (n=29), alcohol abuse 35.5% (n=49), NASH 16.7% (n=23) and for 10.1% (n=14) of patients the aetiological factors were unknown. 52.2% of patients developed the HCC on a cirrhotic background. The grade of HCC differentiation was estimated according to the Edmonson-Steiner criteria that take into consideration the size, morphology and mitotic figures and grouped in the present study as well-differentiated. Healthy liver tissues were collected from patients with liver metastasis from colon cancers undergoing surgery for tumour resection at Centre Léon Berard in Lyon, France. Total RNA was extracted from liver biopsies with Extract-All as described here bellow.

RNA extraction

Nucleic acids were extracted with Extract-All (Eurobio) following manufacturer's instructions and precipitated with isopropanol. The RNA pellet was washed two times with ethanol 95% and 70% and then dissolved in distilled water.

Lentivirus transduction

Hep3B and HepaRG cells were transduced with FG12-empty vector (EV) of FG12-ΔNp73 lentiviruses in presence of polybrene 8 µg/mL at a multiplicity of infection (MOI) of 1. The FG12 empty vector and the FG12 containing the coding sequence of ΔNp73a were provided by the lab. The selection for the integration of the FG12 vector in eukaryote cells is done based on the resistance to puromycin. Lentiviruses were produced in the 293T cells. Brieffly, cells were transfected with FG12 EV or ΔNp73 together with the packaging and the envelope vectors (VSVG and 8.9.1) in relative amounts 5:1:5 by using the CalPhos kit (Clontech) and following the manufacter's instructions. The lentivirus production was harvested after 24 and 48h, mixed and concentrated by centrifugation. The lentiviral production was titrated in order to determine the number of virions per volume unit.

Real time quantitative PCR (RT-qPCR)

RNA was isolated from liver biopsies as described here above and for the cell lines, cells were first washed with PBS, harvested by scrapping and the RNA was isolated in the same manner. One µg of total RNA was submitted to retrotranscription (RT) for the synthesis of complementary DNA (cDNA) with the SuperScript III kit following provider's instructions (ThermoFisher). The RT was performed with a Biorad Thermocycler. The qPCR was performed

on the synthesized cDNA corresponding to 10ng, mixed with 1X quantifast Qiagen SYBR Green, and 500nM of each primer in 10µL total volume. Reactions were performed using LightCycler 480 (Roche). The thermal cycling conditions comprised an initial step at 95°C for 5 minutes, followed by 40 cycles at 95°C for 10 seconds, and 60°C for 30 seconds. Experiments were performed in duplicate. All primers were designed with Primer3 plus software : TAp73 forward 5'- GCACCACGTTTGAGCACCTCT -3' and reverse: 5'- GCAGATTGAACTGGGCCATGA -3'; ΔNp73 forward 5'- AAGCGAAAATGCCAACAAAC -3' and reverse: 5'- CACCGACGTACAGCATGGTA -3'; ΔEx2p73 forward 5'- GACGGCTGCAGGGAACCAGA -3' and reverse: 5'- TGCCCTCCAGGTGGAAGACG -3'; ΔEx2/3p73 forward 5'- TGCAGGCCCAGTTCAATCTGC -3' and reverse: 5'- TCGGTGTTGGAGGGGATGACA -3'. GUS and TBP were used as internat control in parallel for each run and for the quantification. The -ΔΔCt or Pfaffl method was used to analyse the ratio of the target gene in the test sample to the calibrator sample, normalized to the expression of the reference gene. Normalizing the expression of the target gene to that of the reference gene compensates for any difference in the amount of sample tissue.

Cell line culture

Hep3B cells were maintained in EMEM medium (ATCC) supplemented with 10% heat-decomplemented fetal calf serum (FCS, Invitrogen), 100U/mL penicillin, 100µg/mL streptomycin. HepaRG cells were maintained in William's medium supplemented with 10% FCS, 100U/mL penicillin, 100µg/mL streptomycin, 2mM GlutaMAX (Invitrogen), 5µg/mL bovine insulin and $5*10^{-5}$ M hydrocortisone hemisuccinate (Roche Diagnostics). Cells were kept in 5% CO_2, at 37°C in an atmosphere saturated in H_2O. Hep3B stable cell lines transduced with the FG12 vector were selected with 2 mg/mL puromycin while HepaRG cell lines transduced with the FG12 vector were selected with 2.3 mg/mL puromycin.

Cell proliferation

Cell proliferation was determined by using the MTS kit by following the indications of the commercial assay manufacturer's instructions (Promega).

Western blot analysis

The expression of ΔNp73 and the load control Ku80 were assessed in cell lines by Western-blot on total cell lysates. Cell were washed with PBS and harvested by scrapping. Total cellular protein extraction was done with the (RIPA) lysis buffer (50 mM Tris-Cl (pH 8.0), 1 mM EDTA, 0.5 mM EGTA, 1% Triton X-100, 0.1% sodium deoxycholate, 0.1% SDS, 140 mM NaCl) supplemented with Protease Inhibitor Cocktail (Roche). Protein quantification was performed with the Pierce protein kit according to the manufacturer's instructions (ThermoFicher) and using the bovine serum albumin (BSA) as standard. Proteins (40µg) were heat-denaturated,

fractionated on sodium dodecyl sulphate (SDS) polyacrylamide 8% W/v gel and transferred to PVDF membranes. Membranes were blocked with 5% non-fatty milk in PBS. Membranes were incubated overnight at 4°C with commercial primary antibodies against ΔNp73 (Imgenex 313A 1/200) and KU80 (Serotec 1/40000). Excess of antibody was removed by washing the membranes three times with PBS-NP40 0.05% followed by incubation for 1 hour at room temperature with a horseradish peroxidase-conjugated secondary antibody (Dako 1/1000). Excess of antibody was removed by washing the membranes several times with PBS-NP40 0.05%. Detection of the proteins was carried out by using an enhanced chemiluminescence Western blotting system (GE Healthcare).

Colony assay

Cells were plated in 6 well plates at a cell density of 2000 cells/well. Coloy growth was followed under the microscope and the experiment was stopped 3 weeks latter. Cells were fixed with methanol and stained with crystal violet by incubating cells with a fixation and staining solution containing acetic acid/methanol 1/7 (v/v) and 0.5% crystal violet for 10 min. The excess of crystal violet was washed with H2O and dishes were let to air dry. Plates were scanned and the area of colonies was measured with the ImageJ software.

Sphere assay

Total cell population was seeded in sphere media (complete cell media without FCS and supplemented with B27 (Life Technologies), 20ng/mL EGF (R&D Systems), 20ng/mL bFGF (StemCell Technologies) and 4µg/mL heparin) and distributed in ultra low adherence 24-well cell culture plates (Corning). Spheres were harvested 96h later. Spheres either used for RNA extraction or were dissociated by trypsination and seeded for cell viability assays.

Statistical analysis

Pearson's chi-squared test was employed to define significance of the correlation between expression of p73 isoforms and clinicopathological features as well as expression of stemness markers. Univariate and multivariate survival analysis were performed by the Cox proportional hazard ratio (HR) method in order to asses the impact of p73 overexpression in patient overall survival, progression-free survival as well as early and late recurence. Results of the univariate analysis were confirmed by the Kaplan-Meier method and the log rank test. The Mann-Whitney test was employed to test the hypothesis whether two populations are identical. The software Medcal, NCSS and Prism GraphPad were used.

Study 3

Preclinical development of the SLC Inhibitor GNS561 against Hepatocellular Carcinoma

In the aim of discovering novel small molecules against cancer, the company Genoscience Pharma screened a library of quinoline derivatives on a panel on cancer cell lines. It was found that the compound GNS561 has a high efficacy against hepatocellular carcinoma cell lines and showed no particular toxicity for normal hepatocytes *in vitro*. *In vivo* pharmacological studies showed that GNS561 has a strong hepatotropism, justifying the interest of its use in the treatment of liver tumours. *In vivo*, the anti-tumourigenic activity of GNS561 was assessed on two models of murine HCC (orthotopic xenograft and chemically-induced) and it was found that GNS561 has a strong anti-tumourigenic capacity, at least comparable to Sorafenib. *In vitro*, GNS561 was shown to induce lysosome membrane permeabilisation, as well as activation of caspase 3/7. Biochemical analysis of molecular interactions allowed the identification of the molecular target of GNS561, for the moment under confidence.

In the laboratory we investigated the anti-tumour capacity of GNS561 and studied the profile of expression of its molecular target in HCC cells and tumours.

Introduction

In spite of successful approval and wide application of Sorafenib for advanced hepatocellular carcinoma (HCC) treatment, the prognostic remains poor.

A highly tumourigenic subpopulation of cancer cells named Cancer Stem Cells (CSCs) have been claimed as participating to tumour recurrence. Indeed, CSCs are resistant to chemotherapy, and they have the ability to regenerate the tumour bulk with its heterogeneous cell populations. For this reason, innovative drugs with original mechanism of action which target CSC properties would likely improve cancer treatment of patients.

We investigated the *in vitro* antitumour activity of GNS561 in view of its potential use in targeted therapy against HCC. The antitumour activity was explored *in vitro* both on the bulk of cells and on a sub-population of HCC cells enriched in CSCs. We also studied the expression of the molecular target of GNS561 in HCC patient tumours and its association with CSCs markers.

Results

EC50 GNS561 and Sorafenib

The cytotoxic effect of GNS561 was assessed on three HCC cell lines Hep3B, HuH7 and Focus at 48 hours and 72 hours post treatment. Experiments were performed in parallel with Sorafenib, the gold standard targeted therapy for HCC. Results were compared between the two drugs. After treatment with GNS561 or Sorafenib, cells responded in a dose dependent manner. After 48 hours or 72 hours post-treatment and at equimolar concentrations, GNS561 exhibited a higher cytotoxicity than Sorafenib. We found that for the two time points, 48 hours and 72 hours, the dose of drug needed to kill half of cells (defined here as EC50) was lower for GNS561 than for Sorafenib (**Figure 1**). The cytotoxicity of GNS561 did not change significantly between 48 hours and 72 hours since the EC50 for the two time points were not significantly different (**Table 1**). The EC50 of GNS561 for the three cell lines, Hep3B, Focus and HuH7 remained in the same range, between 2.4µM and 1.8 µM. The EC50 of Sorafenib showed a higher variability due to an unexpectedly high EC50 for the HuH7 cell line.

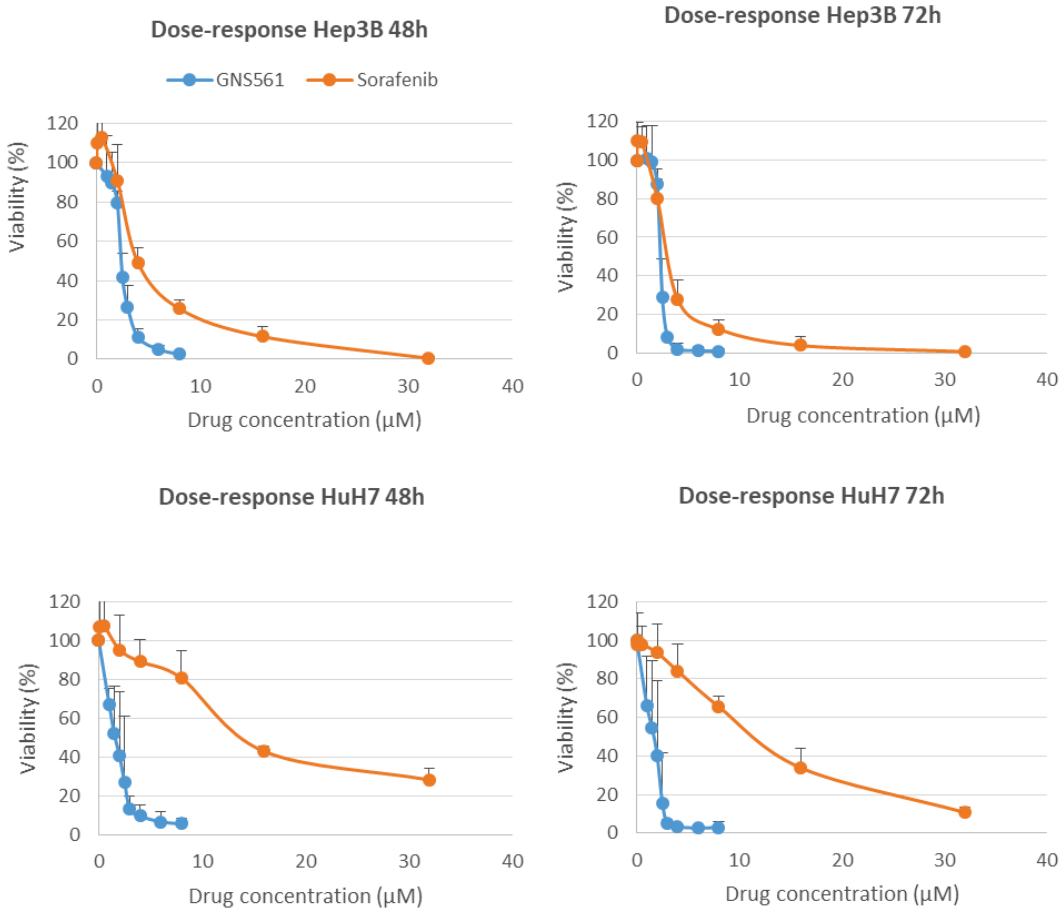

Figure 1. *In vitro* anti-tumourigenic activity of Sorafenib and GNS561 on the Hep3B and HuH7 cells lines.

	Hep3B		HuH7		Focus	
	GNS561	Sorafenib	GNS561	Sorafenib	GNS561	Sorafenib
48h	2,40 ± 0,10 µM	4,03 ± 0,45 µM	1,70 ± 0,69 µM	14,48 ± 0,22 µM	1.8 µM	4 µM
72h	2,35 ± 0,21 µM	3,10 ± 0,10 µM	1,73 ± 0,64 µM	12,03 ± 1,12 µM	1.8 µM	4 µM

Table 1. EC50 of Sorafenib and GNS561 on the HCC cell lines Hep3B, HuH7 and Focus after treatment for 48 or 72 hours.

Sphere-derived cells are not resistant to GNS561 or Sorafenib

Since cancer cell lines are heterogeneous, we explored the sensitivity of a cell sub-population enriched in cancer progenitor cells to both Sorafenib and GNS561. We confirmed by RT-qPCR analysis that the CSCs enriched population overexpressed liver progenitor factors such as Sox2, Oct4, Klf4 or Nanog (**Figure 2**). The enriched population was obtained by culturing the entire cell population of two HCC cell lines, Focus and Hep3B, in sphere conditions during 96 hours. Then, spheres were dissociated and plated in cell culture dishes in adherent conditions and at the same cellular density as the parental total population for the cytotoxic assays.

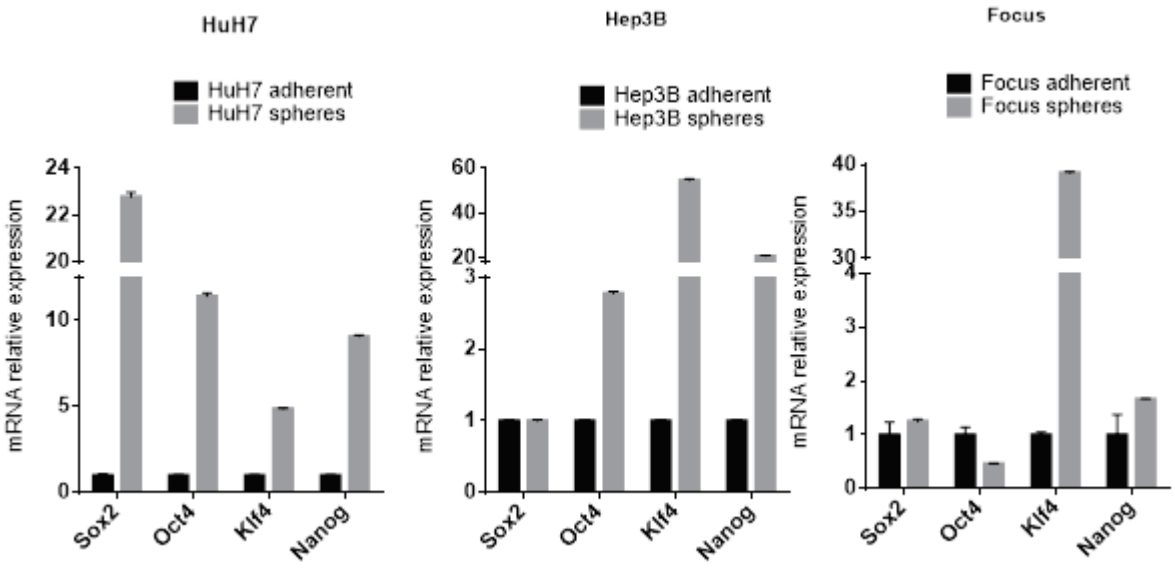

Figure 2. Expression of the stemness factors Sox2, Oct4, Klf4 and Nanog in adherent cell conditions and in spheres.

Compared to the total cell population, CSCs enriched population did not show resistance to Sorafenib or GNS561 when treated in monolayer for 24h, 48h or 72h (**Figure 3**). The EC50 obtained were within the same range as what has been determined previously. Since cells with

progenitor phenotype have a higher plasticity when cultured *in vitro*, we hypothesise that they could have derived after 24 hours of monolayer culture and restored the initial heterogeneous population. We repeated the experiment and assessed cytotoxicity at shorter time lapses (6h, 8h and 24h) and with higher doses. Similarly, no resistance has been observed between the cancer bulk cells and the CSCs enriched population to Sorafenib or GNS561 (**Figure 4**).

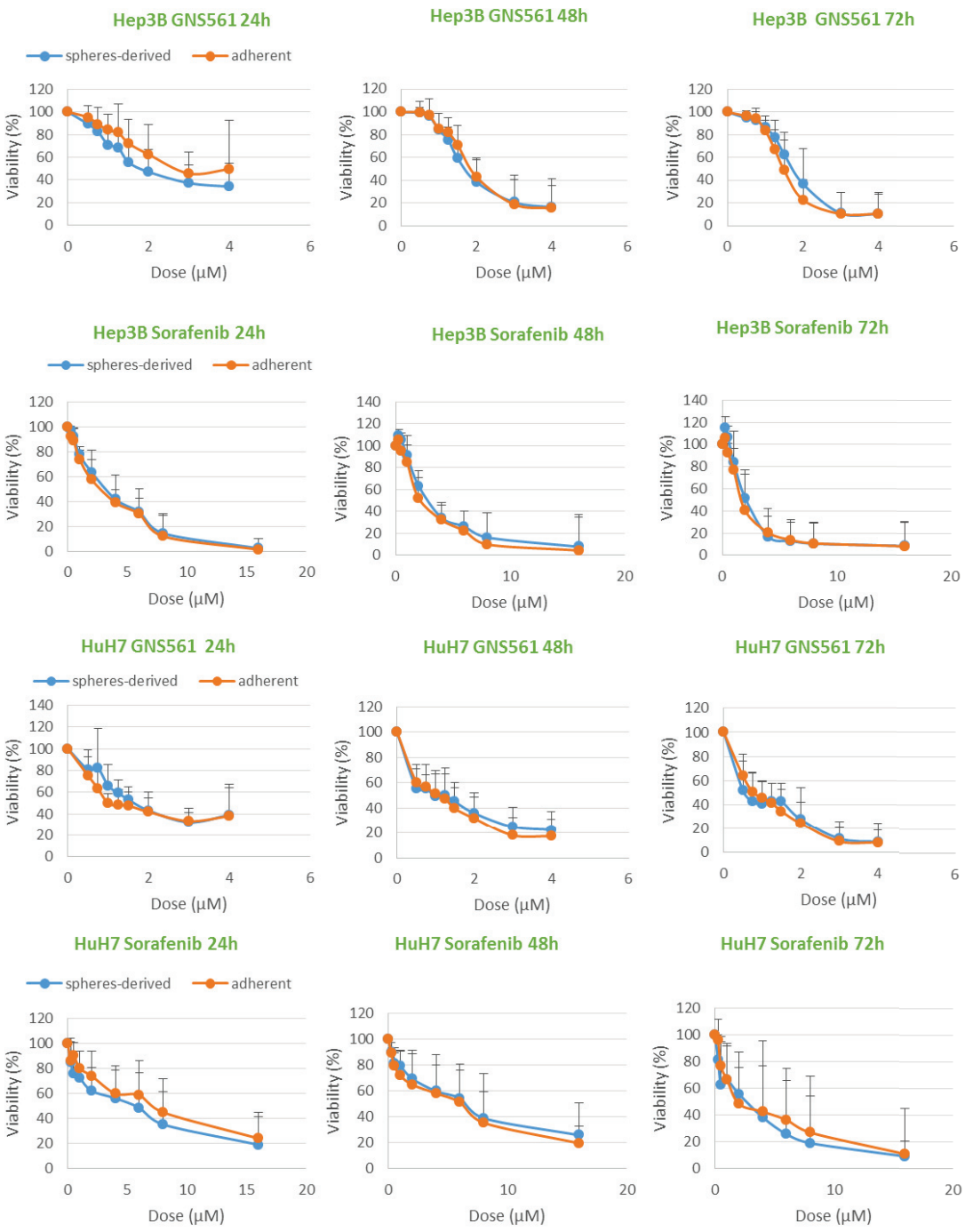

Figure 3. Anti-tumourigenic activity of Sorafenib and GNS561 on total populations (adherent) (orange) or CSCs enriched populations (spheres derived) (blue) of HCC cell lines Hep3B and HuH7 after 24, 48 or 72 hours of treatment.

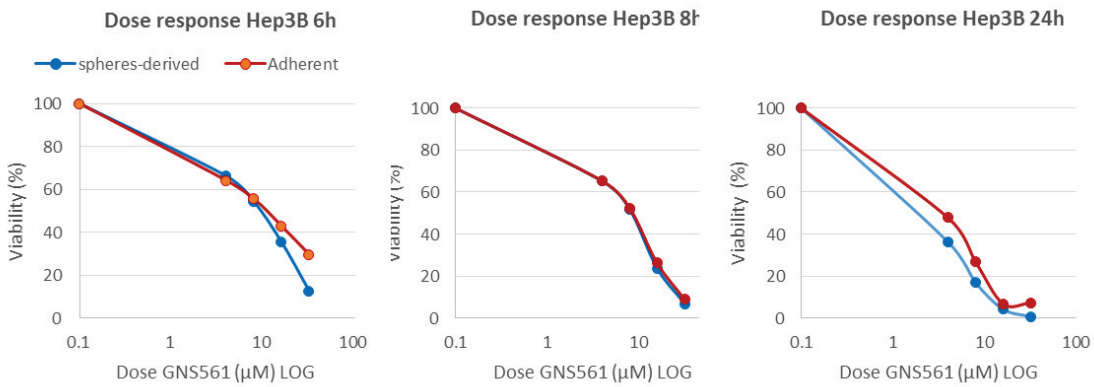

Figure 4. Anti-tumourigenic activity of Sorafenib and GNS561 on total populations (adherent) (orange) or CSCs enriched populations (spheres derived) (blue) of HCC cell lines Hep3B and HuH7 after SHORT treatment periods of 6, 8 or 24 hours and with high drug concentrations (up to 64µM).

GNS561 inhibits formation of hepatospheres

The possibility that among the CSC-enriched population only a very small amount would be resistant to GNS561 was explored. We cultured two HCC cell lines, Hep3B and Focus, in non-adherent conditions and in absence of serum in order to specifically favour the proliferation of CSCs.

At the time of platting, cells were treated with Sorafenib or GNS561 at several concentrations. Contrary to Sorafenib which allowed the formation of spheres, GNS561 completely inhibited these, even at low concentrations (0.33*EC50) (**Figure 5**). At 1*EC50, Sorafenib treatment significantly decreased the average sphere size, showing therefore a partial inhibitory effect on the capacity of cancer progenitor cells to develop into spheres (unpaired Mann-Whitney test, $p<0.001$) (sphere size refers to area). It should be noted that the EC50 in this case was calculated for the adherent total population. Similar results have been obtained after treatment with Sorafenib of the Focus cell line, for which GNS561 also completely inhibits the capacity of cells to form spheres. These results demonstrate the high efficacy of GNS561 to counteract the proliferation and survival of isolated immature cell sub-populations from HCC cell lines.

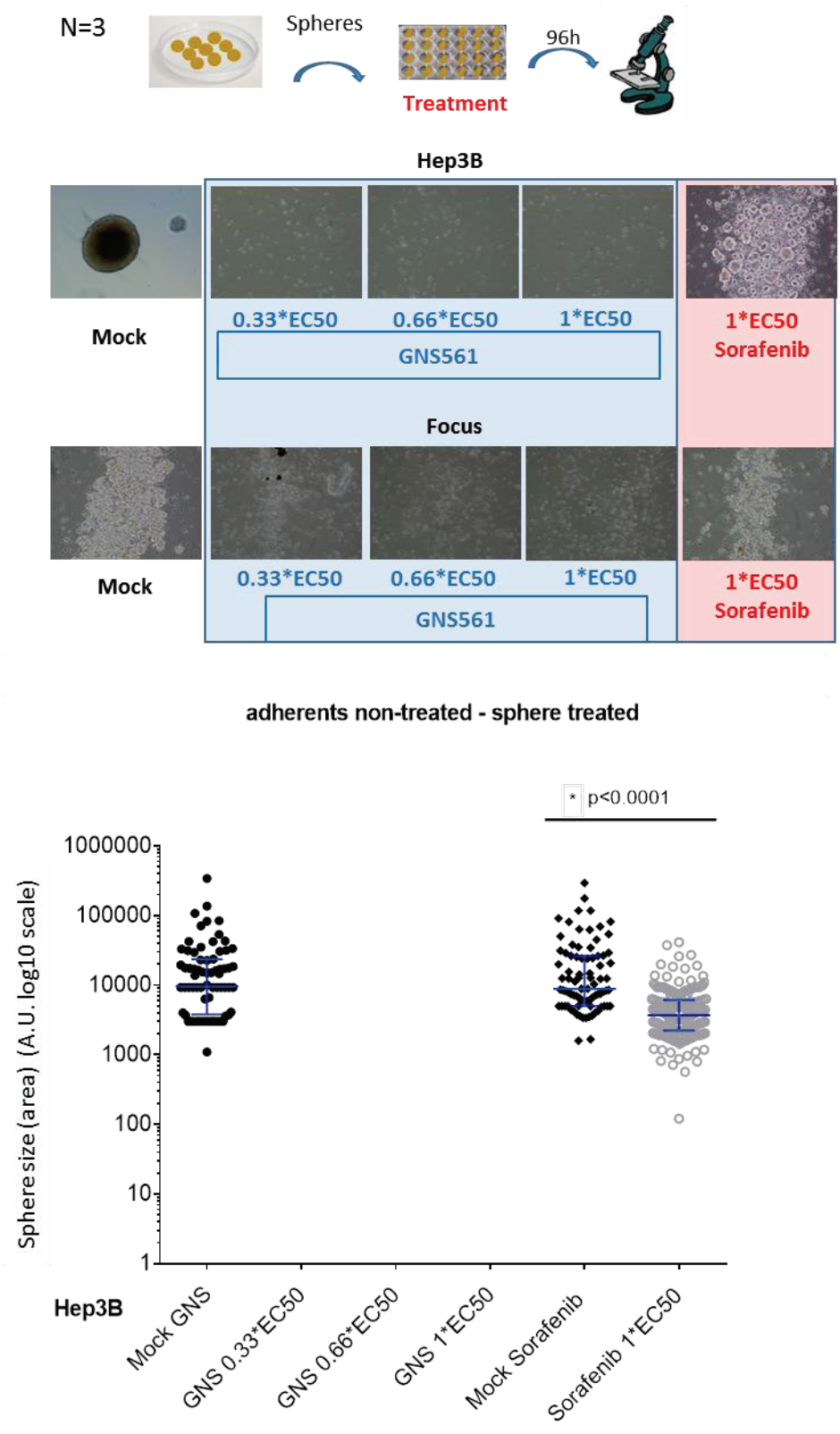

Figure 5. Anti-tumour effect of GNS561 and Sorafenib on HCC cell lines Hep3B and Focus cultured in sphere conditions. On the quantification panel, each dot represents an individual sphere and its position is related to its size. Statistical analysis was performed with unpaired Mann-Whitney test.

Cancer stem cells are less sensitive to GNS561 when pre-treated in adherent conditions

In order to confirm that low concentrations of GNS561 completely eliminates CSCs, we pre-treated the total cell population in adherent conditions with GNS561 at 0.33*EC50, 0.66*EC50 and 1*EC50 or Sorafenib 1*EC50 for 72h. Cells were further cultured in hepatospheres conditions and for each condition the same number of cells was seeded without continuing drug treatment (GNS561 or Sorafenib). Prior treatment with GNS561 or Sorafenib did not affect the capacity of cells to develop hepatospheres after 96h of culture (**Figure 6**). For each of GNS561 concentrations tested, we did not observe significant decrease in the size or number of spheres formed by treated cells. However, for Sorafenib we obtained the same tendency regarding a decreased size of spheres that were formed. If we consider that GNS561 eliminated the entire CSCs population during adherent treatment but the remaining bulk cells are still able to form hepatospheres, it means that these cells are able to regenerate the cancer stem cells population in the *in vitro* conditions tested here.

This observation has already been reported in the case of breast cancer (Gupta et al., 2011). When researchers sorted by FACS luminal, basal and stem-like from a heterogeneous cell population and cultured them separately, the three sub-populations initially homogenous reconstituted the heterogeneous population. This highlights that there is an equilibrium in a cancer cell population due to cancer cell plasticity.

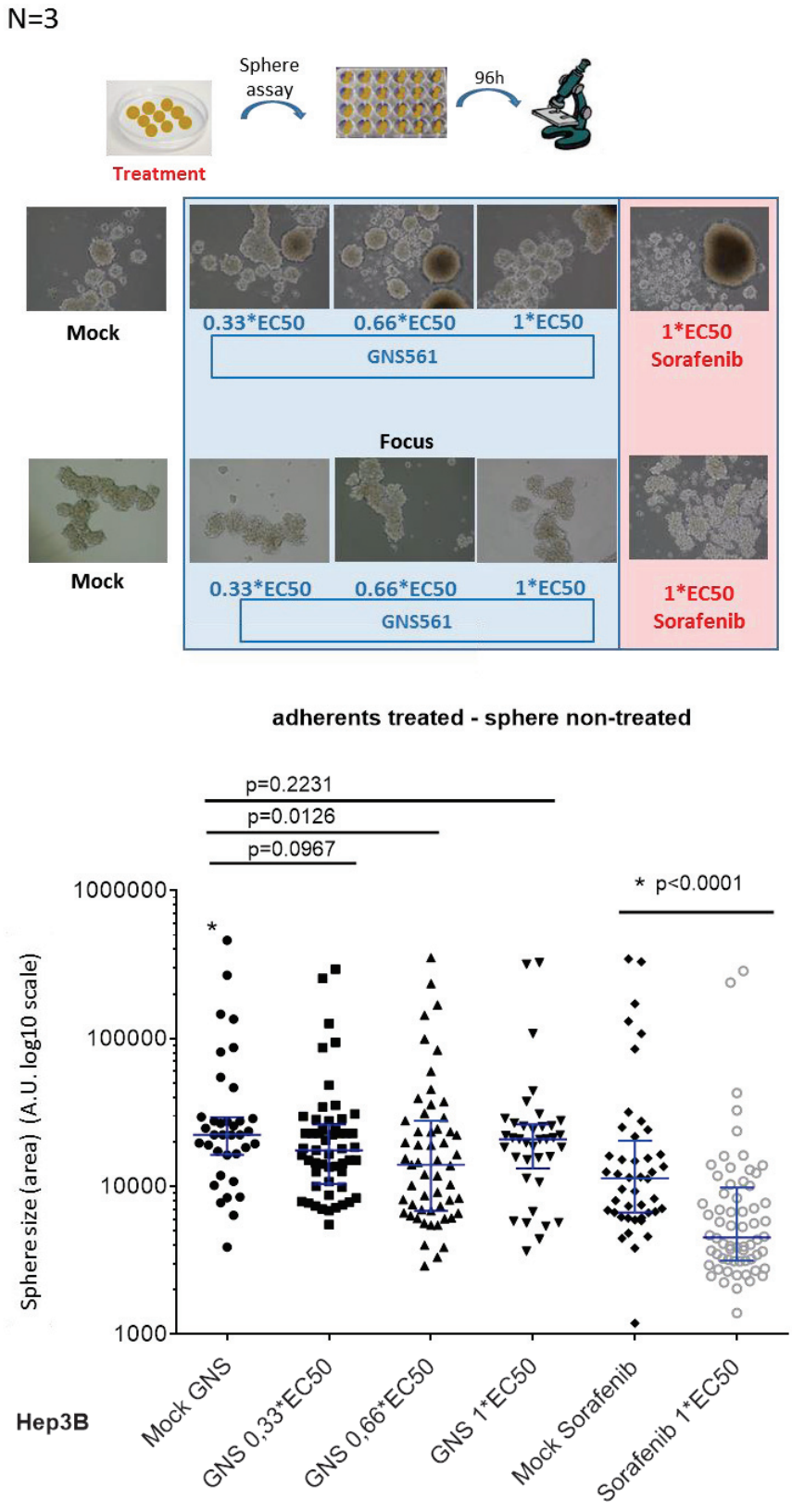

Figure 6. Anti-tumour effect of GNS561 and Sorafenib on HCC cell lines Hep3B and Focus pretreated and then cultured in sphere conditions. On the quantification panel, each dot represents an individual sphere and its position is related to its size. Statistical analysis was performed with unpaired Mann-Whitney test.

GNS561 molecular target is downregulated in sphere-derived CSCs

The molecular target of GNS561 was previously identified and corresponds to a specific SLC transporter (here called SLCt). Since we showed that GNS561 has a cytotoxic activity on liver cancer stem cells, we investigated the level of expression of the SLC transporter in cancer stem cells isolated from Hep3B, Focus and Huh7 HCC cell lines, by spheres formation. The level of expression of the SLC transporter was measured in 4-days old hepatospheres as well as the initial total cell population. We found that for the 3 cell lines, the mRNA of the SLC transporter was lower in hepatospheres compared to the initial parental cell population (**Figure 7**). This result was unexpected as it is considered that a given drug is more efficient on cells with high levels of the molecular target. One explanation could be that in bulk cells, partial inhibition of the transporter will probably not trigger sufficient low concentration of the solute incompatible with cell growth and viability. On the contrary, in the case of cancer stem cells the inhibition of the transporter will lead to drastic decrease in the cellular level of the solute, probably below the threshold concentration, thus leading to impaired stem-specific cell functions.

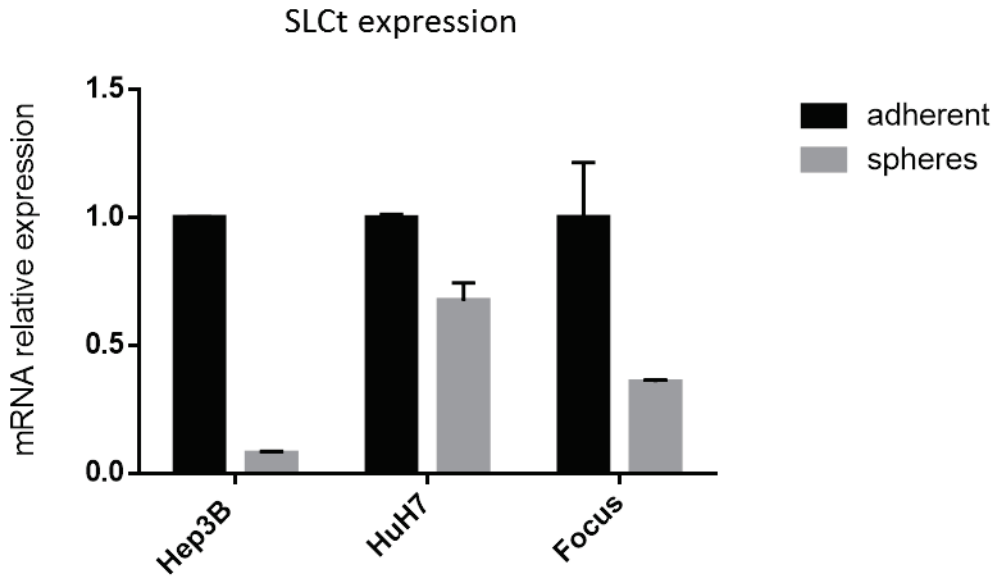

Figure 7. Expression of the molecular target of GNS561, SLCt in bulk and spheres forming cancer cells of three HCC cell lines Hep3B, HuH7 and Focus. SLCt mRNA levels is reduced in the spheres forming cells. Unpaired Mann-Whitney test ($p<0.05$).

GNS561 treatment rapidly diminishes the mRNA level its target

We explored the hypothesis whether GNS561 also has an effect on the expression of SLCt, besides acting as a structural inhibitor of this transporter. We treated the HCC cell line Hep3B in adherent conditions with GNS561 at three concentrations for 4, 8 and 24 hours. At the end of each time point cells were collected and the expression of the SLCt target was assessed at the mRNA level. We observed that GNS561 decreases the level of the SLCt mRNA in a time dependent manner (**Figure 8**). We observed that after 4 hours treatment, the mRNA level of SLCt already decreased by 30%. The fast inhibitor activity of GNS561 suggests that the drug might rather affect the stability of the SLCt mRNA rather than its transcription rate. The inhibition was found to be rather time dependent than concentration dependent. Indeed, for each time point we did not observe a significant difference when treating with 1*EC50, 2*EC50 or 4*EC50.

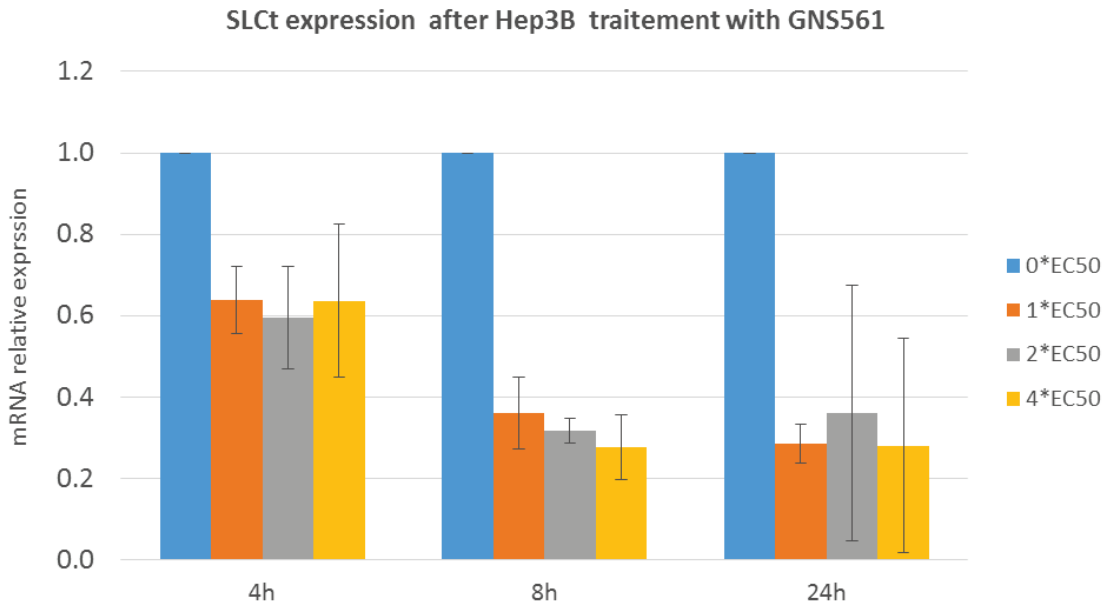

Figure 8. Expression of SLCt in Hep3B cells after treatment with increasing doses of GNS561 for 4, 8 or 24 hours.

GNS561 target expression in HCC patients

One of the requirements justifying GNS561 as a targeted therapy in HCC patients is the expression of the GNS561 target SLC transporter in tumours. The expression of SLCt was investigated by RT-qPCR in surgically resected hepatocellular tumours (T) and the matched non-tumour (NT) liver tissues (n=180) as well as in healthy livers (HL) devoid of chronic or

acute disease (n=10). Healthy liver tissues were collected from liver resection coming from patients undergoing surgery for colorectal liver metastases.

We found that the SLC transporter was overexpressed in 40.5% of tumours and 33.3 % of the non-tumour tissue compared to the healthy liver samples. As shown in the **Figure 9,** there is not a systematic increase of SLCt transcription in hepatocellular tumours compared to the matching non-tumour liver. While some patients have a lower level of SLCt in tumours than in non-tumours, others show increased levels in tumours compared to matching non-tumoural

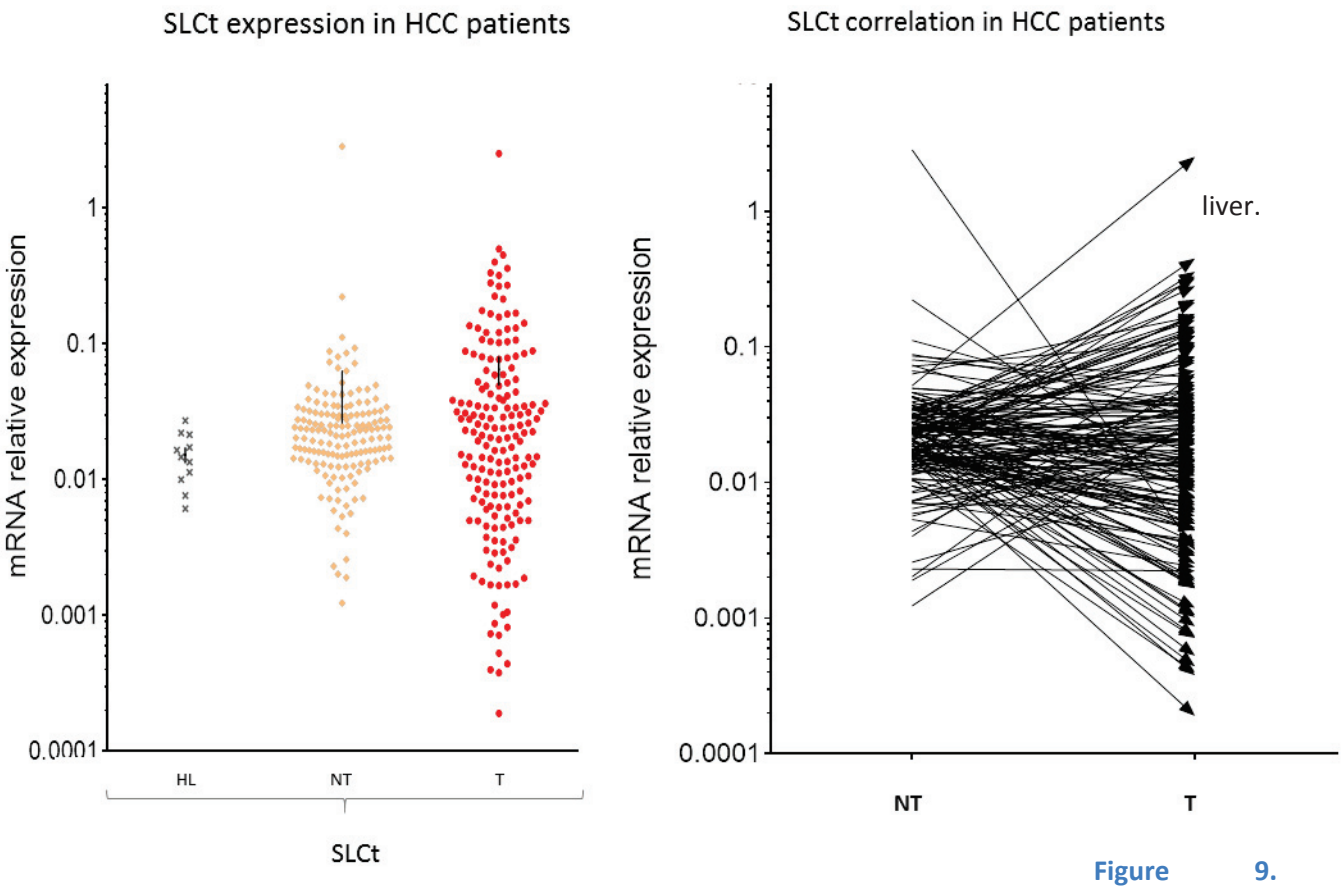

Figure 9. Expression of SLCt in human HCC biopsies and healthy liver parenchyma. Left panel. The expression of the SLCt was quantified by RT-qPCR from frozen biopsies of healthy livers (HL) (no known chronic liver disease), tumours (T) and surrounding non-tumour (NT) tissue originating from patients with HCC. Expression data are presented as the result of the relative quantification after normalization to the housekeeping gene. Horizontal black bars represent the median of expression. **Right panel.** Correlation between the overexpression of SLCt in the tumoural HCC (T) and the matching non-tumoural (NT) tissue. Each arrow represents a pair tumour (T) / surrounding non-tumour (NT).

We then investigated whether SLCt overexpression correlated with the clinicopathologic data of patients and expression of immaturity markers. High SLCt in HCC samples was associated with microvascular emboli (p=0.034) and with the expression of the stem cell factor Sox2 (p=0.025) and the stem marker CD133 (p=0.034) (**Table 2**). High SLCt in non-tumoural liver correlated with cirrhosis (p=0.009) and presence of satellite nodules (p<0.001). Univariate analysis showed an association between overexpression of SLCt in tumours and shortened overall survival (OS) (HR=1.08, p=0.020), lower progression-free survival (PFS) (HR=1.76, p=0.006) as well as early recurrence-free survival (ERFS) (within 2 years post-surgery) (HR=1.88, p=0.008) (**Table 3**). In multivariate analysis, high SLCt tended to be an independent factor for OS, and this was strongly significant for PFS and ERFS (**Table 4**). High SLCt in non-tumoural liver, is quite a poor outcome factor on late recurrence-free survival (LRFS) (HR=2.33, p=0.056) together with cirrhosis in univariate analysis, but remained dependent of cirrhosis in multivariate analysis. Late recurrence is linked to the intrinsic tumourigenic status of the liver and associated with development of *de-novo* HCC nodules. Results were confirmed by Kaplan Meier method and the log rank test (**Figure 10**).

Total prevalence	SLCt **T_up_HL** **40,5% up**		SLCt **NT_up_HL** **30,3% up**	
Clinico-biology, pathology	Chi-Square 2-Sided			
	p	χ^2	p	χ^2
Etiology: HBV *vs.* HCV *vs.* alcohol *vs.* NASH vs. others	0,96	0,64	0,45	3,69
Presence *vs.* absence of cirrhosis	0,29	1,13	0,009	6,77
Tumour size > 50 mm *vs.* ≤ 50 mm	0,98	<0.001	0,98	<0.001
Presence *vs.* absence of HCC multinodularity	0,24	1,37	0,75	0,10
Poor *vs.* moderate *vs.* good differentiation	0,33	2,20	0,82	0,39
AFP > 200 *vs.* ≤ 200 ng/mL	0,41	0,68	0,77	0,08
Microscopic portal invasion	0,478	0,50	0,45	0,56
Presence *vs.* absence of satellite nodules	0,32	0,99	<0.001	0,98
Recurrence: extra-hepatic *vs.* hepatic multifocal *vs.* hepatic uninodular	0,17	3,55	2,58	0,28
Vascular emboli	0,03	4,49	0,35	0,87
CD133 T_up_HL	0,03	4,49	0,11	2,54
CK19 T_up_HL	0,35	0,89	0,60	0,28
EpCAM T_up_HL	0,96	0,003	0,47	0,52
Nanog T_up_HL	0,25	1,34		
Oct4 T_up_HL	0,08	3,16		
Sox2 T_up_HL	0,03	4,99		
SLCt T_up_HL	-	-	0,002	9,94
new Nanog NT_up_HL			0,20	1,63
Oct4 NT_up_HL			0,41	0,69
Sox2 NT_up_HL			0,37	0,79
SLCt NT_up_HL	0,002	9,9369	-	-

Table 2. Correlation between the overexpression of SLCt and clinicopathological data as well as stem-cells molecular features.

Univariate analysis of survivals regarding variables *vs.* rest	Overall survival		Early recurrence-free survival (TTR) (< 24 mo)		Progression free survival (PFS)		Late recurrence-free survival (TTR) (> 24 mo)	
	HR (95% CI)	*P*	HR (95% CI)	*P*	HR (95% CI)	*P*	HR (95% CI)	*P*
SLCt T_up_HL	**1.08 (1.88-3.28)**	**0,020**	**1.88 (1.18-3.01)**	**0,008**	**1.76 (1.17-2.64)**	**0,006**	1.4 (0.60-3.24)	0,420
SLCt NT_up_HL	1.27 (0.65-2.48)	0,460	1.22 (0.72-2.07)	0,450	1.44 (0.91-2.27)	0,110	**2.33 (0.97-5.58)**	**0,050**
SLCt T_up_NT	0.94 (0.50-1.78)	0,860	1.27 (0.76-2.11)	0,340	1.28 (0.83-1.99)	0,250	0.78 (0.33-1.87)	0,590
Tumour size > 50 mm		0,190	**2.16 (1.35-3.44)**	**0,001**	**2.03 (1.35-3.03)**	**<0.001**	1.66 (0.74-3.72)	0,210
HCC multinodularity	1.43 (0.82-2.48)	0,470	1.34 (0.79-2.27)	0,270	1.38 (0.87-2.18)	0,160	1.5 (0.59-3.76)	0,380
AFP > 200 ng/mL	1.39 (0.72-2.69)	0,320	**1.89 (1.10-3.24)**	**0,020**	1.43 (0.88-2.34)	0,140	0.56 (0.16-1.89)	0,350
Satellite nodules	**2.20 (1.23-3.92)**	**0,007**	**2.3 (1.42-3.71)**	**<0.001**	**2.2 (1.43-3.38)**	**<0.001**	1.98 (0.72-5.38)	0,180
Recurrence: extra-hepatic vs. hepatic multifocal vs. hepatic uninodular	**1.49 (1.01-2.20)**	**0,040**	**1.38 (1.00-1.91)**	**0,040**	1.27 (0.95-1.68)	0,090	0.93 (0.50-1.71)	0,816
Cirrhosis	**3.29 (1.64-6.63)**	**<0.001**	1.34 (0.81-2.24)	0,250	**1.72 (1.10-2.68)**	**0,010**	**3.33 (1.37-8.08)**	**0,007**
Vascular emboli	**1.94 (1.11-3.39)**	**0,010**	**2.7 (1.68-4.33)**	**<0.001**	**1.95 (1.29-2.94)**	**0,001**	0.59 (0.20-1.73)	0,330
Microscopic portal invasion	0.68 (0.30-1.53)	0,360	1.19 (0.65-2.18)	0,560	1.16 (0.68-1.97)	0,570	1.05 (0.35-3.10)	0,920
CD133 T_up_HL	1.52 (0.82-2.81)	0,180	1.14 (0.65-2.00)	0,620	1.35 (0.84-2.14)	0,200	2.02 (0.87-4.71)	0,10
CK19 T_up_HL	1.32 (0.69-2.53)	0,390	1.42 (0.83-2.43)	0,190	1.4 (0.87-2.25)	0,150	1.33 (0.49-3.56)	0,570
EpCAM T_up_HL	1.21 (0.68-2.14)	0,500	1.16 (0.71-1.90)	0,540	1.13 (0.74-1.72)	0,550	1.03 (0.45-2.32)	0,934
Oct4 T_up_HL	0.4 (0.14-1.12)	0,080	1.17 (0.62-2.18)	0,610	1.2 (0.70-2.07)	0,490	1.3 (0.44-3.83)	0,620
Oct4 NT_up_HL	1.2 (0.49-3.23)	0,620	1.15 (0.52-2.53)	0,720	1.13 (0.56-2.26)	0,720	1.06 (0.24-4.55)	0,930
Oct4 T_up_NT	0.88 (0.47-1.64)	0,690	1.41 (0.83-2.37)	0,190	1.28 (0.83-1.99)	0,250	1.05 (0.46-2.39)	0,890
Nanog T_up_HL	0.84 (0.37-1.87)	0,670	1.04 (0.54-1.99)	0,880	1.31 (0.76-2.26)	0,310	**2.68 (1.00-7.19)**	**0,050**
Nanog NT_up_HL	1.06 (0.51-2.17)	0,860	1.05 (0.57-1.90)	0,870	0.99 (0.59-1.66)	0,996	0.86 (0.31-2.32)	0,760
Nanog T_up_NT	1.22 (0.65-2.27)	0,520	1.18 (0.71-1.97)	0,500	1.29 (0.83-2.00)	0,240	1.67 (0.72-3.83)	0,220
Sox2 T_up_HL	1.66 (0.89-3.07)	0,100	1.24 (0.70-2.16)	0,450	1.12 (0.68-1.84)	0,640	0.86 (0.29-2.52)	0,790
Sox2 NT_up_HL	1.15 (0.35-3.75)	0,810	1.13 (0.41-3.14)	0,801	1.5 (0.65-3.46)	0,340	3.84 (0.85-17.23)	0,070
Sox2 T_up_NT	1.2 (0.61-2.37)	0,590	0.77 (0.46-1.30)	0,340	0.68 (0.43-1.06)	0,090	0.48 (0.20-1.13)	0,090

Table 3. Univariate analysis regarding the prognosis of each molecular and clinicopathological parameter on patient outcome.

Multivariate analysis of survivals regarding variables vs. rest	HR (95% CI)	p
Overall survival		
	GNS561 target receptor T_up_HL	
Satellite nodules	1.87 (0.89-3.92)	0,090
Recurrence: extra-hepatic *vs.* hepatic multifocal *vs.* hepatic uninodular	1.95 (0.61-6.19)	0,250
Cirrhosis	2.98 (0.86-10.33)	0,080
Vascular emboli	1.87 (0.89-3.92)	0,090
TTR		
	GNS561 target receptor T_up_HL	
Tumour size > 50 mm	1.94 (1.28-2.943)	0,001
Satellite nodules	1.55 (1.02-2.35)	0,030
Cirrhosis	1.74 (1.15-2.65)	0,008
Vascular emboli	1.49 (0.98-2.27)	0,060
Early recurrence-free survival (< 24 mo)		
	GNS561 target receptor T_up_HL	
Tumour size > 50 mm	2.01 (1.25-3.23)	0,003
AFP > 200 ng/mL	1.74 (1.08-2.82)	0,020
Satellite nodules	1.67 (1.04-2.71)	0,030
Recurrence: extra-hepatic vs. hepatic multifocal vs. hepatic uninodular	1.30 (0.78-2.17)	0,290
Vascular emboli	1.56 (0.96-2.53)	0,060
PFS		
	GNS561 target receptor T_up_HL	
Tumour size > 50 mm	1.94 (1.28-2.94)	0,002
Satellite nodules	1.55 (1.02-2.35)	0,030
Cirrhosis	1.74 (1.15-2.65)	0,008
Vascular emboli	1.49 (0.98-2.27)	0,060
late TTR		
	GNS561 target receptor NT_up_HL	
Cirrhosis	1.55 (0.61-3.94)	0,350
Nanog T_up_HL	2.55 (1.04-6.20)	0,030

Table 4. Multivariate analysis regarding the combined prognosis of SLCt overexpression with each clinicopathological factor on patient outcome.

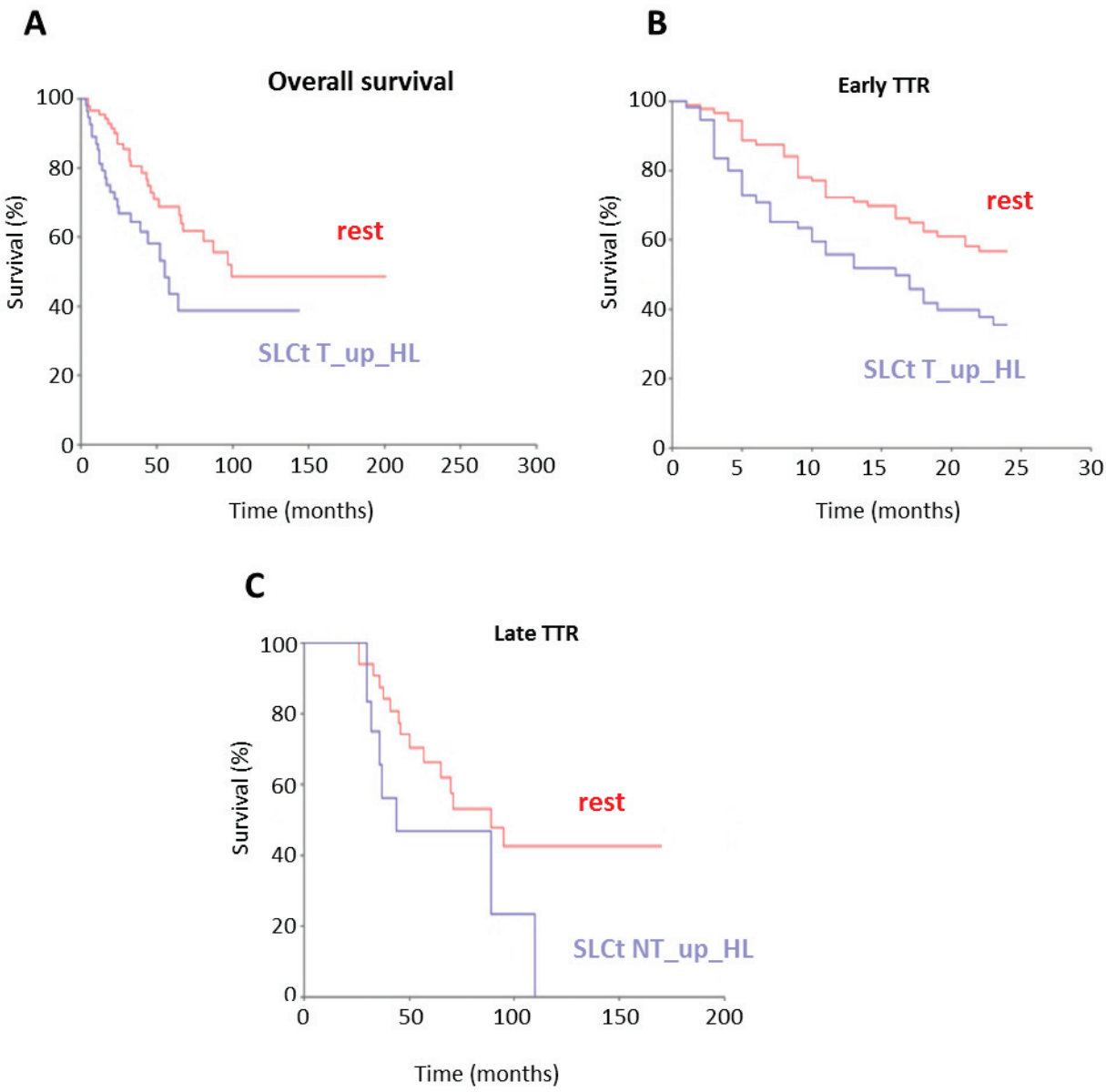

Figure 10. Kaplan Meier curves regarding **A.** Impact of SLCt overexpression in tumours (T) compared to healthy liver (HL) tissue on patients overall survival. Log rank test Chi2=5.192 p=0.023. **B.** Impact of SLCt overexpression in tumours (T) compared to healthy liver (HL) tissue on early recurrence. Log rank test Chi2=7.288; p=0.007. C. Prognosis of SLCt overexpression in non-tumour (NT) liver tissue compared to healthy liver (HL) tissue on late recurrence. Log rank test Chi2=3.787; p=0.0517.

Discusion

HCC is refractory to most conventional chemotherapies and only the tyrosine kinase inhibitor (TKI) Sorafenib has shown a significant benefit in the treatment of HCC patients with non-resectable HCC. One of the reasons for the high mortality rate is the existence of a small population of cancer stem cells with high tumourigenic features. CSCs are resistant to therapies because, like normal stem cells, they have put in place defence mechanisms endowing them with genomic stability and detoxification mechanisms in order to resist stressful conditions.

GNS561 is small molecule belonging to the family of quinoline derivatives. Another member of this family is the well known chloroquine, used in clinic for the treatment of malaria and in research thanks to its capacity to inhibit autophagy.

The antitumoural effect of GNS561 on HCC bulk cells and on cancer stem cells can be both explained by its capacity to inhibit autophagy as well as its action on the membrane transporter SLCt.

Autophagy is a very important mechanism with a dual role in cancer. In the precancerous stage, autophagy is thought to inhibit tumour initiation. In the advanced stages, autophagy has a pro-tumour activity by favouring the survival of cancer cells in stressful conditions such as hypoxia and low-nutriment. In the cancer stem cell population, autophagy is particularly important since these cells are those that have the highest genetic stability and are supposed to resist in the toughest conditions. Studies showed that inhibition of autophagy depletes the cancer stem cell pool. It is possible that in our case, inhibition of autophagy by GNS561 render cancer stem cells more vulnerable to the cytotoxic effect of the molecule. Moreover, inhibition of autophagy impacts also on the plasticity of these cells and impairs the biological features related to cell stemness. Therefore it is possible that GNS561 blocks cancer stem cells to act as stem cells by favouring their behaviour rather as cancer bulk cells.

Secondly, the solute transported by the SLC was shown to be involved in cellular stemness features. Inhibition of the SLCt leads to low levels of the solute and specific cellular stemness mechanisms will be impaired. However, once the molecule GNS561 is withdrawn, the intracellular concentration of the solute is restored and thus conditions become favourable for the development of the cancer stem cells population that has been shown in the case of breast cancer to derive from the bulk cell population thanks to their remarkable plasticity.

Besides the direct molecular interaction between the small molecule GNS561 and the SLCt transporter, we showed that after treatment, GNS561 diminisHes the SLCt mRNA level in a

time dependent manner. It should be noted that the decrease is remarkably rapid, as after 4 hours of treatment the pool of SLCt mRNA decreased by 40%. This rapid decrease suggests that it is rather the consequence of SLCt mRNA instability than the transcription rate of the SLCt coding gene.

Furthermore, the cohort study results clearly showed that the mRNA overexpression of this transporter correlates with overexpression of stemness factors Oct4 and Sox2. Several studies demonstrated that cancer stem cells have tumour initiating properties and can be responsible both for initiation of the primary tumour and tumour relapse. In our case, we found indeed that overexpression of SLCt in the tumours was correlated with relapse post-surgery while overexpression in the adjacent liver parenchyma correlates with late recurrence, linked to the capacity of the liver to reform tumours. Therefore, this study also identifies SLCt as a putative prognostic factor for early recurrence and potentially a predictive factor for primary HCC initiation. Validation cohorts and prospective assessments are needed to define high SLCt as a potential biomarker.

In conclusion, our results show that in comparison to Sorafenib, the gold standard treatment for advanced HCC, GNS561 has a lower EC50 and a higher antitumour activity *in vitro* and it is more efficient to kill the immature sub-population of HCC cancer cell lines, considered as tumour initiating cells. Together with its high hepatotropism and the frequent overexpression of its target, GNS561 represents a promising new therapeutic agent for HCC therapy.

Materials and Methods

Cell culture

Hep3B and Focus cells were maintained in EMEM medium (ATCC) supplemented with 10% heat-decomplemented fetal calf serum (FCS), 100U/mL penicillin, 100µg/mL streptomycin. HuH7 cells were maintained in DMEM medium supplemented with 10% FCS, 100U/mL penicillin, 100µg/mL streptomycin, 2mM GlutaMAX (Invitrogen), and 1mM Sodium Pyruvate. Cells were kept in 5% CO2, at 37°C in an atmosphere saturated in H2O.

Cell viability assay

Hep3B and Huh7. Cells were seeded in 96 well plated at 12 000 cells/well. GNS561, Sorafenib or vehicle (H_2O for GNS561 and DMSO for Sorafenib) were added at appropriate concentrations 24 hours later. At the indicated time points cell viability was assayed using a standard MTS assay (Promega). EC50 was calculated as the dose needed to eliminate half of the cell population.

Sphere assay

Total cell population was seeded in sphere medium (complete cell culture medium without FCS and supplemented with B27 (Life Technologies), 20ng/mL EGF (R&D Systems), 20ng/mL bFGF (StemCell Technologies) and 4µg/mL heparin) and distributed in ultra low adherence cell culture plates (Corning). Spheres were harvested 96h later. Spheres were dissociated by trypsination and seeded for cell viability assays.

Cytotoxic activity on cancer cells cultured in sphere conditions

Hep3B cells (pre-treated or not) were seeded in sphere conditions as described above. At the time of seeding, GNS561, Sorafenib or vehicle (H_2O for GNS561 and DMSO for Sorafenib) were added to the media. Spheres were observed 96h later to assess the effect of the treatment.

Expression of GNS561 target gene in HCC liver biopsies

The effect of GNS561 treatment was also studied by evaluating the mRNA expression of a specific SLC transporter, previously identified as the molecular target of GNS561. The expression of this SLC transporter was measured by RT-qPCR at several time points post-treatment and for three different GNS561 concentrations. The expression of the target SCLt was investigated by RT-qPCR in liver biopsies coming from patients with (n=180) and without HCC (n=10). In the population of HCC patients, 21% were HBV positive, 28% were HCV, 36% were reported as abusive alcohol consumers, 17% were diagnosed with NASH while for 10% of patients the aetiology of the disease remained unknown. Correlation studies were performed

regarding associations between the overexpression of the target SLC transporter, clinicopathological features and expression of stemness markers.

RNA extraction

Nucleic acids were extracted with Extract-All (Eurobio) following manufacturer's instructions and precipitated with isopropanol. The RNA pellet was washed two times with ethanol 95% and 70% and then dissolved in demineralised water.

Real time semi-quantitative PCR (RT-qPCR)

RNA was isolated from liver biopsies as described here above and for the cell lines, cells were first washed with PBS, harvested by scrapping or centrifugation (for spheres) and the RNA was isolated in the same manner. One µg of total RNA was submitted to retrotranscription (RT) for the synthesis of complementary DNA (cDNA) with the SuperScript III kit following providers' instructions (ThermoFisher). The RT was performed with a Biorad Thermocycler. The RT-qPCR was performed on the synthesized cDNA corresponding to 10ng RNA equivalent, mixed with 1X quantifast Qiagen SYBR Green, and 500nM of each primer in 10µL total volume. Reactions were performed using LightCycler 480 (Roche). The thermal cycling conditions comprised an initial step at 95°C for 5 minutes, followed by 40 cycles at 95°C for 10 seconds, and 60°C for 30 seconds. Experiments were performed in duplicate. All primers were designed with Primer3 plus software. GUS and TBP were used as internal control in parallel for each run and for the quantification. The -ΔΔCt or Pfaffl method was used to analyse the ratio of the target gene in the test sample to the calibrator sample, normalized to the expression of the reference gene. Normalizing the expression of the target gene to that of the reference gene compensates for any difference in the amount in sample tissue.

Statistical analysis

Pearson's chi-squared test was employed to define significance of the correlation between expression of the target SLC transporter and clinicopathological features as well as expression of stemness markers. Univariate and multivariate survival analysis were performed by the Cox proportional hazard ratio (HR) method in order to assess the impact of the SLC transporter expression in patient overall survival, progression-free survival as well as early and late recurrence. Results of the univariate analysis were confirmed by the Kaplan-Meier method and the log rank test. The Mann-Whitney test was employed to test the hypothesis whether two populations are identical. The software Medcal, NCSS and Prism GraphPad were used.

General Conclusions and Perspectives

The studies presented in this manuscript are focused around cancer stem cells in HCC and the development of *in vivo* and *in vitro* models of HCC. One of the aims is to contribute to the development of more efficient therapies against HCC as well as a more optimal administration.

***

One of the studies showed that truncated p73 isoforms expression in HCC correlates with stemness features, previously found to be associated with poor prognosis. *In vitro* data showed that the truncated isoform ΔNp73 itseld drives the expression of transcription factors regulating cell stemness (Oct4, Sox2, Nanog). This suggests that specific inhibition of p73 truncated isoforms could downregulate the expression of these stemness features, and possibly render HCC more sensitive to therapy. This hypothesis could be tested in the near feature as specific inhibitory strategies against these isoforms have already been developed (described in the introduction, Chapter 3.5 ”Drugable actions of the p73 axis”). Since cohort studies showed that not only ΔNp73 isoform, but also ΔEx2p73 and ΔEx2/3p73 correlate with stemness factors, wide spectrum inhibitors against all ΔTAp73 isoforms should be tested in parallel to ΔNp73-specific inhibitors. *In vitro* testing the effect of these inhibitors on the stemness characteristics of HCC could also clarify whether ΔNp73 alone drives stemness by gain of function properties or whether all ΔTAp73 isoforms have this property.

Indeed, in the perspective of this work, it should be tested if inhibition of ΔTAp7A could represent a therapy *per se* or rather be considered as a cotherapy that would synergise with classical therapeutic interventions (both chemo and radiotherapy).

Sorafenib has proven to be efficient in HCC treatment but data showed that the main drawback of this molecule is that it engenders resistance. It is possible that coupling ΔTAp73 inhibitors to Sorafenib could reveal to have a better effect than Sorafenib alone. Secondly, HCC has proven to be extremely resistant to chemotherapeutic drugs and radiotherapy but administration of ΔTAp73 inhibitors coupled to chemotherapeutic drugs or radiotherapy could render these tumours more sensititve to these therapies. However, it remains to be discussed if the best responders to the therapies are those that overexpress these isoforms, in which case, a stratification of patients should be done based on the level of expression of p73 isoforms in HCC biopsies.

***

The third study regarding the pre-clinical development of GNS561 against HCC and targeting cancer stem cells is a step closer to clinical development than ΔTAp73 inhibitors for which the pre-clinical proof of concept still remains to be performed. We showed here the pre-clinical development of GNS561 *in vitro* as well as the pertinence of its molecular target through cohort sudies. The *in vitro* part clearly shows the important anti-tumourigenic effect of GNS561 againts cancer stem cells as well as the wide expression of the GNS561 target in human HCC and its correlation with the stemness marker CD133 and stemness factors Oct4 and Sox2, justifying its potential efficacy in at least one third of cases. Several complementary *in vivo* experiments were performed by our collaborators that demonstrate the efficacy of GNS561 in pre-clinical rodent models of HCC. They also showed the weak *in vitro* toxicity of the molecule on normal hepatocytes. If Phase 1 clinical trial succeeds, it will remain to be determined whether GNS561 could be employed as a monotherapy or in combination with Sorafenib or other therapeutic agents.

***

Our participation to IMODI consortium concluded to the development of one HCC PDX model IM-LIV-516, derived from a patient HBV spontaneously cured and infected by HCV. The histological characterization confirmed that the model retained the characteristics of the initial tumour. Pharmacological characterisation of the model remains to be performed, principally by studying the anti-tumoural effect after treatment with Sorafenib. This part of the project is managed by the bio-pharmaceutical companies of the consortium.

However, the efficiency of xenografting of HCC fragments subcutaneously in immunodeficient mice was very low, as estimated on the thirty tumours that were engrafted. For reasons that are not clear to date, while some types of tumours can easily be engrafted in mice such as breast or ovary, HCC models have rarely been described in the literature. In order to try to enhance the efficiency of engraftment, it could be interested to try to orthotopically implant human HCC fragments in immunodeficient mice with humanised livers. This approach would provide the implanted tumour a tissue microenviroment closely to what is found in humans livers. It is possible that in the case of hepatocellular carcinoma, the tumours microenvironment plays a much stronger role in terms of angiogenesis as well as release of hepato-specific growing factors. In the case of HCC, the nodules generally develop on the background of a chronic liver disease environment which means that the surrounding tissue releases specific soluble factors which are not normally found in healthy organs.

The two studies that described the successful development of HCC PDX models employed human samples coming from patients with southeastern asian origins. In this part of the world, the molecular epidemiology of the HCC is different from Europe, and from France in particular. While the main risk factor in China is HBV chronic infection, in Europe HBV-associated HCC is less frequent due to vaccination campaigns. In our study, HBV chronic infection represented 10% of cases. However, it should be noted that the only PDX model that was established originated from a patients previously infected by HBV.

Bibliography

Abe, H., Hayashi, A., Kunita, A., Sakamoto, Y., Hasegawa, K., Shibahara, J., Kokudo, N., and Fukayama, M. (2015). Altered expression of AT-rich interactive domain 1A in hepatocellular carcinoma. Int. J. Clin. Exp. Pathol. *8*, 2763–2770.

Afreen, S., and Dermime, S. (2014). The immunoinhibitory B7-H1 molecule as a potential target in cancer: killing many birds with one stone. Hematol. Oncol. Stem Cell Ther. *7*, 1–17.

Agami, R., Blandino, G., Oren, M., and Shaul, Y. (1999). Interaction of c-Abl and p73alpha and their collaboration to induce apoptosis. Nature *399*, 809–813.

Albano, E., French, S.W., and Ingelman-Sundberg, M. (1999). Hydroxyethyl radicals in ethanol hepatotoxicity. Front. Biosci. J. Virtual Libr. *4*, D533-540.

Albini, A., and Sporn, M.B. (2007). The tumour microenvironment as a target for chemoprevention. Nat. Rev. Cancer *7*, 139–147.

Alexandrov, L.B., Nik-Zainal, S., Wedge, D.C., Aparicio, S.A.J.R., Behjati, S., Biankin, A.V., Bignell, G.R., Bolli, N., Borg, A., Børresen-Dale, A.-L., et al. (2013). Signatures of mutational processes in human cancer. Nature *500*, 415–421.

Ali, N., Allam, H., May, R., Sureban, S.M., Bronze, M.S., Bader, T., Umar, S., Anant, S., and Houchen, C.W. (2011). Hepatitis C virus-induced cancer stem cell-like signatures in cell culture and murine tumor xenografts. J. Virol. *85*, 12292–12303.

Alla, V., Kowtharapu, B.S., Engelmann, D., Emmrich, S., Schmitz, U., Steder, M., and Pützer, B.M. (2012). E2F1 confers anticancer drug resistance by targeting ABC transporter family members and Bcl-2 via the p73/DNp73-miR-205 circuitry. Cell Cycle Georget. Tex *11*, 3067–3078.

Allen, C., Opyrchal, M., Aderca, I., Schroeder, M.A., Sarkaria, J.N., Domingo, E., Federspiel, M.J., and Galanis, E. (2013). Oncolytic measles virus strains have significant antitumor activity against glioma stem cells. Gene Ther. *20*, 444–449.

Altman, B.J., Jacobs, S.R., Mason, E.F., Michalek, R.D., MacIntyre, A.N., Coloff, J.L., Ilkayeva, O., Jia, W., He, Y.-W., and Rathmell, J.C. (2011). Autophagy is essential to suppress cell stress and to allow BCR-Abl-mediated leukemogenesis. Oncogene *30*, 1855–1867.

Amaddeo, G., Guichard, C., Imbeaud, S., and Zucman-Rossi, J. (2012). Next-generation sequencing identified new oncogenes and tumor suppressor genes in human hepatic tumors. Oncoimmunology *1*, 1612–1613.

Amaravadi, R., Kimmelman, A.C., and White, E. (2016). Recent insights into the function of autophagy in cancer. Genes Dev. *30*, 1913–1930.

Amelio, I., Markert, E.K., Rufini, A., Antonov, A.V., Sayan, B.S., Tucci, P., Agostini, M., Mineo, T.C., Levine, A.J., and Melino, G. (2014). p73 regulates serine biosynthesis in cancer. Oncogene *33*, 5039–5046.

An, F.Q., Matsuda, M., Fujii, H., Tang, R.F., Amemiya, H., Dai, Y.M., and Matsumoto, Y. (2001). Tumor heterogeneity in small hepatocellular carcinoma: analysis of tumor cell proliferation, expression and mutation of p53 AND beta-catenin. Int. J. Cancer *93*, 468–474.

Anfuso, B., El-Khobar, K.E., Sukowati, C.H.C., and Tiribelli, C. (2015). The multiple origin of cancer stem cells in hepatocellular carcinoma. Clin. Res. Hepatol. Gastroenterol. *39 Suppl 1*, S92-97.

Anilkumar, T.V., Golding, M., Edwards, R.J., Lalani, E.N., Sarraf, C.E., and Alison, M.R. (1995). The resistant hepatocyte model of carcinogenesis in the rat: the apparent independent development of oval cell proliferation and early nodules. Carcinogenesis *16*, 845–853.

Arzumanyan, A., Friedman, T., Ng, I.O.L., Clayton, M.M., Lian, Z., and Feitelson, M.A. (2011). Does the hepatitis B antigen HBx promote the appearance of liver cancer stem cells? Cancer Res. *71*, 3701–3708.

Arzumanyan, A., Reis, H.M.G.P.V., and Feitelson, M.A. (2013). Pathogenic mechanisms in HBV- and HCV-associated hepatocellular carcinoma. Nat. Rev. Cancer *13*, 123–135.

Asher, G., Tsvetkov, P., Kahana, C., and Shaul, Y. (2005). A mechanism of ubiquitin-independent proteasomal degradation of the tumor suppressors p53 and p73. Genes Dev. *19*, 316–321.

Avasarala, S., Yang, L., Sun, Y., Leung, A.W.C., Chan, W.Y., Cheung, W.T., and Lee, S.S.T. (2006). A temporal study on the histopathological, biochemical and molecular responses of CCl4-induced hepatotoxicity in Cyp2e1-null mice. Toxicology *228*, 310–322.

Avivar-Valderas, A., Bobrovnikova-Marjon, E., Alan Diehl, J., Bardeesy, N., Debnath, J., and Aguirre-Ghiso, J.A. (2013). Regulation of autophagy during ECM detachment is linked to a selective inhibition of mTORC1 by PERK. Oncogene *32*, 4932–4940.

Aydinlik, H., Nguyen, T.D., Moennikes, O., Buchmann, A., and Schwarz, M. (2001). Selective pressure during tumor promotion by phenobarbital leads to clonal outgrowth of beta-catenin-mutated mouse liver tumors. Oncogene *20*, 7812–7816.

Azuma, H., Paulk, N., Ranade, A., Dorrell, C., Al-Dhalimy, M., Ellis, E., Strom, S., Kay, M.A., Finegold, M., and Grompe, M. (2007). Robust expansion of human hepatocytes in Fah−/−/Rag2−/−/Il2rg −/− mice. Nat. Biotechnol. *25*, 903–910.

Babinet, C., Farza, H., Morello, D., Hadchouel, M., and Pourcel, C. (1985). Specific expression of hepatitis B surface antigen (HBsAg) in transgenic mice. Science *230*, 1160–1163.

Bailey, S.G., Cragg, M.S., and Townsend, P.A. (2011). Family friction as ΔNp73 antagonises p73 and p53. Int. J. Biochem. Cell Biol. *43*, 482–486.

Baskaran, R., Wood, L.D., Whitaker, L.L., Canman, C.E., Morgan, S.E., Xu, Y., Barlow, C., Baltimore, D., Wynshaw-Boris, A., Kastan, M.B., et al. (1997). Ataxia telangiectasia mutant protein activates c-Abl tyrosine kinase in response to ionizing radiation. Nature *387*, 516–519.

Bastians, H. (2015). Causes of Chromosomal Instability. Recent Results Cancer Res. Fortschritte Krebsforsch. Progres Dans Rech. Sur Cancer *200*, 95–113.

Basu, S., and Murphy, M.E. (2016). p53 family members regulate cancer stem cells. Cell Cycle Georget. Tex *15*, 1403–1404.

Baxter, R.C. (2014). IGF binding proteins in cancer: mechanistic and clinical insights. Nat. Rev. Cancer *14*, 329–341.

Becker, R., Lüthgens, B., Oesch, F., Dienes, H.P., and Steinberg, P. (1996). Ha-rasVal12 but not p53Ser247 leads to a significant neoplastic transformation rate of the putative rat liver stem cells (oval cell). Carcinogenesis *17*, 2635–2640.

Beitzinger, M., Oswald, C., Beinoraviciute-Kellner, R., and Stiewe, T. (2006). Regulation of telomerase activity by the p53 family member p73. Oncogene *25*, 813–826.

Beitzinger, M., Hofmann, L., Oswald, C., Beinoraviciute-Kellner, R., Sauer, M., Griesmann, H., Bretz, A.C., Burek, C., Rosenwald, A., and Stiewe, T. (2008). p73 poses a barrier to malignant transformation by limiting anchorage-independent growth. EMBO J. *27*, 792–803.

Bell, R.J.A., Rube, H.T., Kreig, A., Mancini, A., Fouse, S.D., Nagarajan, R.P., Choi, S., Hong, C., He, D., Pekmezci, M., et al. (2015). Cancer. The transcription factor GABP selectively binds and activates the mutant TERT promoter in cancer. Science *348*, 1036–1039.

Belyi, V.A., Ak, P., Markert, E., Wang, H., Hu, W., Puzio-Kuter, A., and Levine, A.J. (2010). The Origins and Evolution of the p53 Family of Genes. Cold Spring Harb. Perspect. Biol. *2*.

Ben-Yehoyada, M., Ben-Dor, I., and Shaul, Y. (2003). c-Abl tyrosine kinase selectively regulates p73 nuclear matrix association. J. Biol. Chem. *278*, 34475–34482.

Berghauser Pont, L.M.E., Kleijn, A., Kloezeman, J.J., van den Bossche, W., Kaufmann, J.K., de Vrij, J., Leenstra, S., Dirven, C.M.F., and Lamfers, M.L.M. (2015). The HDAC Inhibitors Scriptaid and LBH589 Combined with the Oncolytic Virus Delta24-RGD Exert Enhanced Anti-Tumor Efficacy in Patient-Derived Glioblastoma Cells. PloS One *10*, e0127058.

Bertino, G., Demma, S., Ardiri, A., Proiti, M., Gruttadauria, S., Toro, A., Malaguarnera, G., Bertino, N., Malaguarnera, M., Malaguarnera, M., et al. (2014). Hepatocellular carcinoma: novel molecular targets in carcinogenesis for future therapies. BioMed Res. Int. *2014*, 203693.

Bertotti, A., Migliardi, G., Galimi, F., Sassi, F., Torti, D., Isella, C., Corà, D., Di Nicolantonio, F., Buscarino, M., Petti, C., et al. (2011). A molecularly annotated platform of patient-derived xenografts ("xenopatients") identifies HER2 as an effective therapeutic target in cetuximab-resistant colorectal cancer. Cancer Discov. *1*, 508–523.

Billon, N., Terrinoni, A., Jolicoeur, C., McCarthy, A., Richardson, W.D., Melino, G., and Raff, M. (2004). Roles for p53 and p73 during oligodendrocyte development. Dev. Camb. Engl. *131*, 1211–1220.

Bissell, M.J., and Radisky, D. (2001). Putting tumours in context. Nat. Rev. Cancer *1*, 46–54.

Bisso, A., Collavin, L., and Del Sal, G. (2011). p73 as a pharmaceutical target for cancer therapy. Curr. Pharm. Des. *17*, 578–590.

Biswas, S.K., and Mantovani, A. (2010). Macrophage plasticity and interaction with lymphocyte subsets: cancer as a paradigm. Nat. Immunol. *11*, 889–896.

Blum, R., and Kloog, Y. (2014). Metabolism addiction in pancreatic cancer. Cell Death Dis. *5*, e1065.

Bonnet, D., and Dick, J.E. (1997). Human acute myeloid leukemia is organized as a hierarchy that originates from a primitive hematopoietic cell. Nat. Med. *3*, 730–737.

Bosetti, C., Levi, F., Boffetta, P., Lucchini, F., Negri, E., and La Vecchia, C. (2008). Trends in mortality from hepatocellular carcinoma in Europe, 1980-2004. Hepatol. Baltim. Md *48*, 137–145.

Bouchard, M.J., and Schneider, R.J. (2004). The enigmatic X gene of hepatitis B virus. J. Virol. *78*, 12725–12734.

Boya, P., Reggiori, F., and Codogno, P. (2013). Emerging regulation and functions of autophagy. Nat. Cell Biol. *15*, 713–720.

Boyault, S., Rickman, D.S., de Reyniès, A., Balabaud, C., Rebouissou, S., Jeannot, E., Hérault, A., Saric, J., Belghiti, J., Franco, D., et al. (2007). Transcriptome classification of HCC is related to gene alterations and to new therapeutic targets. Hepatol. Baltim. Md *45*, 42–52.

Bréchot, C., Gozuacik, D., Murakami, Y., and Paterlini-Bréchot, P. (2000). Molecular bases for the development of hepatitis B virus (HBV)-related hepatocellular carcinoma (HCC). Semin. Cancer Biol. *10*, 211–231.

Breuhahn, K., Vreden, S., Haddad, R., Beckebaum, S., Stippel, D., Flemming, P., Nussbaum, T., Caselmann, W.H., Haab, B.B., and Schirmacher, P. (2004). Molecular profiling of human hepatocellular carcinoma defines mutually exclusive interferon regulation and insulin-like growth factor II overexpression. Cancer Res. *64*, 6058–6064.

Broadhead, M.L., Dass, C.R., and Choong, P.F.M. (2009). Cancer cell apoptotic pathways mediated by PEDF: prospects for therapy. Trends Mol. Med. *15*, 461–467.

Bruix, J., Gores, G.J., and Mazzaferro, V. (2014). Hepatocellular carcinoma: clinical frontiers and perspectives. Gut *63*, 844–855.

Bruix, J., Qin, S., Merle, P., Granito, A., Huang, Y.-H., Bodoky, G., Pracht, M., Yokosuka, O., Rosmorduc, O., Breder, V., et al. (2017). Regorafenib for patients with hepatocellular carcinoma who progressed on sorafenib treatment (RESORCE): a randomised, double-blind, placebo-controlled, phase 3 trial. Lancet Lond. Engl. *389*, 56–66.

Bruno, S., Crosignani, A., Maisonneuve, P., Rossi, S., Silini, E., and Mondelli, M.U. (2007). Hepatitis C virus genotype 1b as a major risk factor associated with hepatocellular carcinoma in patients with cirrhosis: a seventeen-year prospective cohort study. Hepatol. Baltim. Md *46*, 1350–1356.

Buhlmann, S., and Pützer, B.M. (2008). DNp73 a matter of cancer: mechanisms and clinical implications. Biochim. Biophys. Acta *1785*, 207–216.

Bunjobpol, W., Dulloo, I., Igarashi, K., Concin, N., Matsuo, K., and Sabapathy, K. (2014). Suppression of acetylpolyamine oxidase by selected AP-1 members regulates DNp73 abundance: mechanistic insights for overcoming DNp73-mediated resistance to chemotherapeutic drugs. Cell Death Differ. *21*, 1240–1249.

Cai, Q., Yan, L., and Xu, Y. (2015). Anoikis resistance is a critical feature of highly aggressive ovarian cancer cells. Oncogene *34*, 3315–3324.

Calderaro, J., Couchy, G., Imbeaud, S., Amaddeo, G., Letouzé, E., Blanc, J.-F., Laurent, C., Hajji, Y., Azoulay, D., Bioulac-Sage, P., et al. (2017). Histological subtypes of hepatocellular carcinoma are related to gene mutations and molecular tumour classification. J. Hepatol. *67*, 727–738.

Cam, H., Griesmann, H., Beitzinger, M., Hofmann, L., Beinoraviciute-Kellner, R., Sauer, M., Hüttinger-Kirchhof, N., Oswald, C., Friedl, P., Gattenlöhner, S., et al. (2006). p53 family members in myogenic differentiation and rhabdomyosarcoma development. Cancer Cell *10*, 281–293.

Campbell, L.L., and Polyak, K. (2007). Breast tumor heterogeneity: cancer stem cells or clonal evolution? Cell Cycle Georget. Tex *6*, 2332–2338.

Capurro, M., Wanless, I.R., Sherman, M., Deboer, G., Shi, W., Miyoshi, E., and Filmus, J. (2003). Glypican-3: a novel serum and histochemical marker for hepatocellular carcinoma. Gastroenterology *125*, 89–97.

Carastro, L.M., Lin, H.-Y., Park, H.Y., Kim, D., Radlein, S., Hampton, K.K., Hakam, A., Zachariah, B., Pow-Sang, J., and Park, J.Y. (2014). Role of p73 Dinucleotide Polymorphism in Prostate Cancer and p73 Protein Isoform Balance. Prostate Cancer *2014*.

Casciano, I., Mazzocco, K., Boni, L., Pagnan, G., Banelli, B., Allemanni, G., Ponzoni, M., Tonini, G.P., and Romani, M. (2002a). Expression of DeltaNp73 is a molecular marker for adverse outcome in neuroblastoma patients. Cell Death Differ. *9*, 246–251.

Casciano, I., Banelli, B., Croce, M., Allemanni, G., Ferrini, S., Tonini, G.P., Ponzoni, M., and Romani, M. (2002b). Role of methylation in the control of DeltaNp73 expression in neuroblastoma. Cell Death Differ. *9*, 343–345.

Cascio, S.M. (2001). Novel strategies for immortalization of human hepatocytes. Artif. Organs *25*, 529–538.

Castillo, J., Goñi, S., Latasa, M.U., Perugorría, M.J., Calvo, A., Muntané, J., Bioulac-Sage, P., Balabaud, C., Prieto, J., Avila, M.A., et al. (2009). Amphiregulin induces the alternative splicing of p73 into its oncogenic isoform DeltaEx2p73 in human hepatocellular tumors. Gastroenterology *137*, 1805-1815.e1-4.

Cervello, M., McCubrey, J.A., Cusimano, A., Lampiasi, N., Azzolina, A., and Montalto, G. (2012). Targeted therapy for hepatocellular carcinoma: novel agents on the horizon. Oncotarget *3*, 236–260.

Cevik, D., Yildiz, G., and Ozturk, M. (2015). Common telomerase reverse transcriptase promoter mutations in hepatocellular carcinomas from different geographical locations. World J. Gastroenterol. *21*, 311–317.

Chamuleau, R.A.F.M., Deurholt, T., and Hoekstra, R. (2005). Which are the right cells to be used in a bioartificial liver? Metab. Brain Dis. *20*, 327–335.

Chan, J.Y. (2011). A clinical overview of centrosome amplification in human cancers. Int. J. Biol. Sci. *7*, 1122–1144.

Chan, H.L.-Y., Wong, M.L., Hui, A.Y., Hung, L.C.-T., Chan, F.K.-L., and Sung, J.J.-Y. (2003). Hepatitis B virus genotype C takes a more aggressive disease course than hepatitis B virus genotype B in hepatitis B e antigen-positive patients. J. Clin. Microbiol. *41*, 1277–1279.

Chang, Y., Lin, J., and Tsung, A. (2012a). Manipulation of autophagy by MIR375 generates antitumor effects in liver cancer. Autophagy *8*, 1833–1834.

Chang, Y., Yan, W., He, X., Zhang, L., Li, C., Huang, H., Nace, G., Geller, D.A., Lin, J., and Tsung, A. (2012b). miR-375 inhibits autophagy and reduces viability of hepatocellular carcinoma cells under hypoxic conditions. Gastroenterology *143*, 177–187.e8.

Chao, M.P., Alizadeh, A.A., Tang, C., Myklebust, J.H., Varghese, B., Gill, S., Jan, M., Cha, A.C., Chan, C.K., Tan, B.T., et al. (2010). Anti-CD47 antibody synergizes with rituximab to promote phagocytosis and eradicate non-Hodgkin lymphoma. Cell *142*, 699–713.

Chaudhary, N., and Maddika, S. (2014). WWP2-WWP1 Ubiquitin Ligase Complex Coordinated by PPM1G Maintains the Balance between Cellular p73 and ΔNp73 Levels. Mol. Cell. Biol. *34*, 3754–3764.

Chen, C.-J., Yang, H.-I., Su, J., Jen, C.-L., You, S.-L., Lu, S.-N., Huang, G.-T., Iloeje, U.H., and REVEAL-HBV Study Group (2006). Risk of hepatocellular carcinoma across a biological gradient of serum hepatitis B virus DNA level. JAMA *295*, 65–73.

Chen, H., Luo, Z., Dong, L., Tan, Y., Yang, J., Feng, G., Wu, M., Li, Z., and Wang, H. (2013a). CD133/prominin-1-mediated autophagy and glucose uptake beneficial for hepatoma cell survival. PloS One *8*, e56878.

Chen, H., Luo, Z., Sun, W., Zhang, C., Sun, H., Zhao, N., Ding, J., Wu, M., Li, Z., and Wang, H. (2013b). Low glucose promotes CD133mAb-elicited cell death via inhibition of autophagy in hepatocarcinoma cells. Cancer Lett. *336*, 204–212.

Chen, W.-J., Ho, C.-C., Chang, Y.-L., Chen, H.-Y., Lin, C.-A., Ling, T.-Y., Yu, S.-L., Yuan, S.-S., Chen, Y.-J.L., Lin, C.-Y., et al. (2014a). Cancer-associated fibroblasts regulate the plasticity of lung cancer stemness via paracrine signalling. Nat. Commun. *5*, 3472.

Chen, X., Cheung, S.T., So, S., Fan, S.T., Barry, C., Higgins, J., Lai, K.-M., Ji, J., Dudoit, S., Ng, I.O.L., et al. (2002). Gene expression patterns in human liver cancers. Mol. Biol. Cell *13*, 1929–1939.

Chen, Y.-L., Jeng, Y.-M., Chang, C.-N., Lee, H.-J., Hsu, H.-C., Lai, P.-L., and Yuan, R.-H. (2014b). TERT promoter mutation in resectable hepatocellular carcinomas: a strong association with hepatitis C infection and absence of hepatitis B infection. Int. J. Surg. Lond. Engl. *12*, 659–665.

Cheng, Z., Li, X., and Ding, J. (2016). Characteristics of liver cancer stem cells and clinical correlations. Cancer Lett. *379*, 230–238.

Chettouh, H., Fartoux, L., Aoudjehane, L., Wendum, D., Clapéron, A., Chrétien, Y., Rey, C., Scatton, O., Soubrane, O., Conti, F., et al. (2013). Mitogenic insulin receptor-A is overexpressed in human hepatocellular carcinoma due to EGFR-mediated dysregulation of RNA splicing factors. Cancer Res. *73*, 3974–3986.

Cheung, P.F.Y., Yip, C.W., Ng, L.W.C., Lo, K.W., Chow, C., Chan, K.F., Cheung, T.T., and Cheung, S.T. (2016). Comprehensive characterization of the patient-derived xenograft and the paralleled primary hepatocellular carcinoma cell line. Cancer Cell Int. *16*, 41.

Chiang, D.Y., Villanueva, A., Hoshida, Y., Peix, J., Newell, P., Minguez, B., LeBlanc, A.C., Donovan, D.J., Thung, S.N., Solé, M., et al. (2008). Focal gains of VEGFA and molecular classification of hepatocellular carcinoma. Cancer Res. *68*, 6779–6788.

Chiba, T., Zheng, Y.-W., Kita, K., Yokosuka, O., Saisho, H., Onodera, M., Miyoshi, H., Nakano, M., Zen, Y., Nakanuma, Y., et al. (2007). Enhanced self-renewal capability in hepatic stem/progenitor cells drives cancer initiation. Gastroenterology *133*, 937–950.

Chilakapati, J., Shankar, K., Korrapati, M.C., Hill, R.A., and Mehendale, H.M. (2005). Saturation toxicokinetics of thioacetamide: role in initiation of liver injury. Drug Metab. Dispos. Biol. Fate Chem. *33*, 1877–1885.

Chisari, F.V., Pinkert, C.A., Milich, D.R., Filippi, P., McLachlan, A., Palmiter, R.D., and Brinster, R.L. (1985). A transgenic mouse model of the chronic hepatitis B surface antigen carrier state. Science *230*, 1157–1160.

Chisari, F.V., Klopchin, K., Moriyama, T., Pasquinelli, C., Dunsford, H.A., Sell, S., Pinkert, C.A., Brinster, R.L., and Palmiter, R.D. (1989). Molecular pathogenesis of hepatocellular carcinoma in hepatitis B virus transgenic mice. Cell *59*, 1145–1156.

Choi, D.S., Blanco, E., Kim, Y.-S., Rodriguez, A.A., Zhao, H., Huang, T.H.-M., Chen, C.-L., Jin, G., Landis, M.D., Burey, L.A., et al. (2014). Chloroquine eliminates cancer stem cells through deregulation of Jak2 and DNMT1. Stem Cells Dayt. Ohio *32*, 2309–2323.

Choudhury, S., Kolukula, V.K., Preet, A., Albanese, C., and Avantaggiati, M.L. (2013). Dissecting the pathways that destabilize mutant p53. Cell Cycle *12*, 1022–1029.

Clarke, M.F., Dick, J.E., Dirks, P.B., Eaves, C.J., Jamieson, C.H.M., Jones, D.L., Visvader, J., Weissman, I.L., and Wahl, G.M. (2006). Cancer stem cells--perspectives on current status and future directions: AACR Workshop on cancer stem cells. Cancer Res. *66*, 9339–9344.

Clement, V., Sanchez, P., de Tribolet, N., Radovanovic, I., and Ruiz i Altaba, A. (2007). HEDGEHOG-GLI1 signaling regulates human glioma growth, cancer stem cell self-renewal, and tumorigenicity. Curr. Biol. CB *17*, 165–172.

Concin, N., Hofstetter, G., Berger, A., Gehmacher, A., Reimer, D., Watrowski, R., Tong, D., Schuster, E., Hefler, L., Heim, K., et al. (2005). Clinical relevance of dominant-negative p73 isoforms for responsiveness to chemotherapy and survival in ovarian cancer: evidence for a crucial p53-p73 cross-talk in vivo. Clin. Cancer Res. Off. J. Am. Assoc. Cancer Res. *11*, 8372–8383.

Conforti, F., Sayan, A.E., Sreekumar, R., and Sayan, B.S. (2012). Regulation of p73 activity by post-translational modifications. Cell Death Dis. *3*, e285.

Cufí, S., Vazquez-Martin, A., Oliveras-Ferraros, C., Martin-Castillo, B., Vellon, L., and Menendez, J.A. (2011). Autophagy positively regulates the CD44(+) CD24(-/low) breast cancer stem-like phenotype. Cell Cycle Georget. Tex *10*, 3871–3885.

Cui, R., Nguyen, T.T., Taube, J.H., Stratton, S.A., Feuerman, M.H., and Barton, M.C. (2005). Family members p53 and p73 act together in chromatin modification and direct repression of alpha-fetoprotein transcription. J. Biol. Chem. *280*, 39152–39160.

Damhofer, H., Ebbing, E.A., Steins, A., Welling, L., Tol, J.A., Krishnadath, K.K., van Leusden, T., van de Vijver, M.J., Besselink, M.G., Busch, O.R., et al. (2015). Establishment of patient-derived xenograft models and cell lines for malignancies of the upper gastrointestinal tract. J. Transl. Med. *13*, 115.

Dandri, M., Burda, M.R., Török, E., Pollok, J.M., Iwanska, A., Sommer, G., Rogiers, X., Rogler, C.E., Gupta, S., Will, H., et al. (2001). Repopulation of mouse liver with human hepatocytes and in vivo infection with hepatitis B virus. Hepatol. Baltim. Md *33*, 981–988.

Dash, S., Saxena, R., Myung, J., Rege, T., Tsuji, H., Gaglio, P., Garry, R.F., Thung, S.N., and Gerber, M.A. (2000). HCV RNA levels in hepatocellular carcinomas and adjacent non-tumorous livers. J. Virol. Methods *90*, 15–23.

Daskalos, A., Logotheti, S., Markopoulou, S., Xinarianos, G., Gosney, J.R., Kastania, A.N., Zoumpourlis, V., Field, J.K., and Liloglou, T. (2011). Global DNA hypomethylation-induced ΔNp73 transcriptional activation in non-small cell lung cancer. Cancer Lett. *300*, 79–86.

De Laurenzi, V.D., Catani, M.V., Terrinoni, A., Corazzari, M., Melino, G., Costanzo, A., Levrero, M., and Knight, R.A. (1999). Additional complexity in p73: induction by mitogens in lymphoid cells and identification of two new splicing variants epsilon and zeta. Cell Death Differ. *6*, 389–390.

Degenhardt, K., Mathew, R., Beaudoin, B., Bray, K., Anderson, D., Chen, G., Mukherjee, C., Shi, Y., Gélinas, C., Fan, Y., et al. (2006). Autophagy promotes tumor cell survival and restricts necrosis, inflammation, and tumorigenesis. Cancer Cell *10*, 51–64.

Degos, F., Christidis, C., Ganne-Carrie, N., Farmachidi, J., Degott, C., Guettier, C., Trinchet, J., Beaugrand, M., and Chevret, S. (2000). Hepatitis C virus related cirrhosis: time to occurrence of hepatocellular carcinoma and death. Gut *47*, 131–136.

Deng, M., Jiang, Z., Li, Y., Zhou, Y., Li, J., Wang, X., Yao, Y., Wang, W., Li, P., and Xu, B. (2016). Effective elimination of adult B-lineage acute lymphoblastic leukemia by disulfiram/copper complex in vitro and in vivo in patient-derived xenograft models. Oncotarget *7*, 82200–82212.

Deretic, V., Saitoh, T., and Akira, S. (2013). Autophagy in infection, inflammation and immunity. Nat. Rev. Immunol. *13*, 722–737.

Désert, R., Rohart, F., Canal, F., Sicard, M., Desille, M., Renaud, S., Turlin, B., Bellaud, P., Perret, C., Clément, B., et al. (2017). Human hepatocellular carcinomas with a periportal phenotype have the lowest potential for early recurrence after curative resection. Hepatol. Baltim. Md.

Díaz, R., Peña, C., Silva, J., Lorenzo, Y., García, V., García, J.M., Sánchez, A., Espinosa, P., Yuste, R., Bonilla, F., et al. (2008). p73 Isoforms affect VEGF, VEGF165b and PEDF expression in human colorectal tumors: VEGF165b downregulation as a marker of poor prognosis. Int. J. Cancer *123*, 1060–1067.

Dierks, C., Grbic, J., Zirlik, K., Beigi, R., Englund, N.P., Guo, G.-R., Veelken, H., Engelhardt, M., Mertelsmann, R., Kelleher, J.F., et al. (2007). Essential role of stromally induced hedgehog signaling in B-cell malignancies. Nat. Med. *13*, 944–951.

Dimri, G.P., Lee, X., Basile, G., Acosta, M., Scott, G., Roskelley, C., Medrano, E.E., Linskens, M., Rubelj, I., and Pereira-Smith, O. (1995). A biomarker that identifies senescent human cells in culture and in aging skin in vivo. Proc. Natl. Acad. Sci. U. S. A. *92*, 9363–9367.

Ding, J., and Wu, J. (2015). Epigenetic regulation of hepatic tumor-initiating cells. Front. Biosci. Landmark Ed. *20*, 946–963.

Ding, L., Ellis, M.J., Li, S., Larson, D.E., Chen, K., Wallis, J.W., Harris, C.C., McLellan, M.D., Fulton, R.S., Fulton, L.L., et al. (2010). Genome remodelling in a basal-like breast cancer metastasis and xenograft. Nature *464*, 999–1005.

Dixit, D., Ghildiyal, R., Anto, N.P., and Sen, E. (2014). Chaetocin-induced ROS-mediated apoptosis involves ATM-YAP1 axis and JNK-dependent inhibition of glucose metabolism. Cell Death Dis. *5*, e1212.

Domínguez, G., García, J.M., Peña, C., Silva, J., García, V., Martínez, L., Maximiano, C., Gómez, M.E., Rivera, J.A., García-Andrade, C., et al. (2006). DeltaTAp73 upregulation correlates with poor prognosis in human tumors: putative in vivo network involving p73 isoforms, p53, and E2F-1. J. Clin. Oncol. Off. J. Am. Soc. Clin. Oncol. *24*, 805–815.

Dontu, G., Abdallah, W.M., Foley, J.M., Jackson, K.W., Clarke, M.F., Kawamura, M.J., and Wicha, M.S. (2003). In vitro propagation and transcriptional profiling of human mammary stem/progenitor cells. Genes Dev. *17*, 1253–1270.

Dore, M.P., Realdi, G., Mura, D., Onida, A., Massarelli, G., Dettori, G., Graham, D.Y., and Sepulveda, A.R. (2001). Genomic instability in chronic viral hepatitis and hepatocellular carcinoma. Hum. Pathol. *32*, 698–703.

Dumble, M.L., Croager, E.J., Yeoh, G.C.T., and Quail, E.A. (2002). Generation and characterization of p53 null transformed hepatic progenitor cells: oval cells give rise to hepatocellular carcinoma. Carcinogenesis *23*, 435–445.

Durnez, A., Verslype, C., Nevens, F., Fevery, J., Aerts, R., Pirenne, J., Lesaffre, E., Libbrecht, L., Desmet, V., and Roskams, T. (2006). The clinicopathological and prognostic relevance of cytokeratin 7 and 19 expression in hepatocellular carcinoma. A possible progenitor cell origin. Histopathology *49*, 138–151.

Egan, D.F., Shackelford, D.B., Mihaylova, M.M., Gelino, S., Kohnz, R.A., Mair, W., Vasquez, D.S., Joshi, A., Gwinn, D.M., Taylor, R., et al. (2011). Phosphorylation of ULK1 (hATG1) by AMP-activated protein kinase connects energy sensing to mitophagy. Science *331*, 456–461.

El-Din, H.G., Ghafar, N.A., Saad, N.E., Aziz, M., Rasheed, D., and Hassan, E.M. (2010). Relationship between codon 249 mutation in exon 7 of p53 gene and diagnosis of hepatocellular carcinoma. Arch. Med. Sci. AMS *6*, 348–355.

Elgendy, M., Sheridan, C., Brumatti, G., and Martin, S.J. (2011). Oncogenic Ras-induced expression of Noxa and Beclin-1 promotes autophagic cell death and limits clonogenic survival. Mol. Cell *42*, 23–35.

Ellinger-Ziegelbauer, H., Aubrecht, J., Kleinjans, J.C., and Ahr, H.-J. (2009). Application of toxicogenomics to study mechanisms of genotoxicity and carcinogenicity. Toxicol. Lett. *186*, 36–44.

El-Serag, H.B. (2011). Hepatocellular carcinoma. N. Engl. J. Med. *365*, 1118–1127.

El-Shamy, A., Pendleton, M., Eng, F.J., Doyle, E.H., Bashir, A., and Branch, A.D. (2016). Impact of HCV core gene quasispecies on hepatocellular carcinoma risk among HALT-C trial patients. Sci. Rep. *6*.

Emmrich, S., Wang, W., John, K., Li, W., and Pützer, B.M. (2009). Antisense gapmers selectively suppress individual oncogenic p73 splice isoforms and inhibit tumor growth in vivo. Mol. Cancer *8*, 61.

Engelmann, D., Meier, C., Alla, V., and Pützer, B.M. (2015). A balancing act: orchestrating amino-truncated and full-length p73 variants as decisive factors in cancer progression. Oncogene *34*, 4287–4299.

Espina, V., Mariani, B.D., Gallagher, R.I., Tran, K., Banks, S., Wiedemann, J., Huryk, H., Mueller, C., Adamo, L., Deng, J., et al. (2010). Malignant precursor cells pre-exist in human breast DCIS and require autophagy for survival. PloS One *5*, e10240.

Facciorusso, A., Villani, R., Bellanti, F., Mitarotonda, D., Vendemiale, G., and Serviddio, G. (2016). Mitochondrial Signaling and Hepatocellular Carcinoma: Molecular Mechanisms and Therapeutic Implications. Curr. Pharm. Des. *22*, 2689–2696.

Fan, H., Zhang, H., Pascuzzi, P.E., and Andrisani, O. (2016). Hepatitis B virus X protein induces EpCAM expression via active DNA demethylation directed by RelA in complex with EZH2 and TET2. Oncogene *35*, 715–726.

Fan, X., Khaki, L., Zhu, T.S., Soules, M.E., Talsma, C.E., Gul, N., Koh, C., Zhang, J., Li, Y.-M., Maciaczyk, J., et al. (2010). NOTCH pathway blockade depletes CD133-positive glioblastoma cells and inhibits growth of tumor neurospheres and xenografts. Stem Cells Dayt. Ohio *28*, 5–16.

Fang, C.-H., Gong, J.-Q., and Zhang, W. (2004). Function of oval cells in hepatocellular carcinoma in rats. World J. Gastroenterol. *10*, 2482–2487.

Fantini, M., Benvenuto, M., Masuelli, L., Frajese, G.V., Tresoldi, I., Modesti, A., and Bei, R. (2015). In vitro and in vivo antitumoral effects of combinations of polyphenols, or polyphenols and anticancer drugs: perspectives on cancer treatment. Int. J. Mol. Sci. *16*, 9236–9282.

Faouzi, S., Le Bail, B., Neaud, V., Boussarie, L., Saric, J., Bioulac-Sage, P., Balabaud, C., and Rosenbaum, J. (1999). Myofibroblasts are responsible for collagen synthesis in the stroma of human hepatocellular carcinoma: an in vivo and in vitro study. J. Hepatol. *30*, 275–284.

Farazi, P.A., and DePinho, R.A. (2006). Hepatocellular carcinoma pathogenesis: from genes to environment. Nat. Rev. Cancer *6*, 674–687.

Farinati, F., Cardin, R., Degan, P., De Maria, N., Floyd, R.A., Van Thiel, D.H., and Naccarato, R. (1999). Oxidative DNA damage in circulating leukocytes occurs as an early event in chronic HCV infection. Free Radic. Biol. Med. *27*, 1284–1291.

Ferlay, J., Shin, H.-R., Bray, F., Forman, D., Mathers, C., and Parkin, D.M. (2010). Estimates of worldwide burden of cancer in 2008: GLOBOCAN 2008. Int. J. Cancer *127*, 2893–2917.

Fernandez-Banet, J., Lee, N.P., Chan, K.T., Gao, H., Liu, X., Sung, W.-K., Tan, W., Fan, S.T., Poon, R.T., Li, S., et al. (2014). Decoding complex patterns of genomic rearrangement in hepatocellular carcinoma. Genomics *103*, 189–203.

Fernández-Checa, J.C., Kaplowitz, N., García-Ruiz, C., and Colell, A. (1998). Mitochondrial glutathione: importance and transport. Semin. Liver Dis. *18*, 389–401.

Fichtner, I., Rolff, J., Soong, R., Hoffmann, J., Hammer, S., Sommer, A., Becker, M., and Merk, J. (2008). Establishment of patient-derived non-small cell lung cancer xenografts as models for the identification of predictive biomarkers. Clin. Cancer Res. Off. J. Am. Assoc. Cancer Res. *14*, 6456–6468.

Fiebig, H.H., Neumann, H.A., Henss, H., Koch, H., Kaiser, D., and Arnold, H. (1985). Development of three human small cell lung cancer models in nude mice. Recent Results Cancer Res. Fortschritte Krebsforsch. Progres Dans Rech. Sur Cancer *97*, 77–86.

Forner, A., Llovet, J.M., and Bruix, J. (2012). Hepatocellular carcinoma. Lancet Lond. Engl. *379*, 1245–1255.

Frese, K.K., and Tuveson, D.A. (2007). Maximizing mouse cancer models. Nat. Rev. Cancer *7*, 645–658.

Friedman, S.L. (2008). Mechanisms of hepatic fibrogenesis. Gastroenterology *134*, 1655–1669.

Friedman, S.L., Roll, F.J., Boyles, J., and Bissell, D.M. (1985). Hepatic lipocytes: the principal collagen-producing cells of normal rat liver. Proc. Natl. Acad. Sci. U. S. A. *82*, 8681–8685.

Fruman, D.A., and Rommel, C. (2014). PI3K and cancer: lessons, challenges and opportunities. Nat. Rev. Drug Discov. *13*, 140–156.

Fu, X., Guadagni, F., and Hoffman, R.M. (1992). A metastatic nude-mouse model of human pancreatic cancer constructed orthotopically with histologically intact patient specimens. Proc. Natl. Acad. Sci. U. S. A. *89*, 5645–5649.

Fujimoto, A., Totoki, Y., Abe, T., Boroevich, K.A., Hosoda, F., Nguyen, H.H., Aoki, M., Hosono, N., Kubo, M., Miya, F., et al. (2012). Whole-genome sequencing of liver cancers identifies etiological influences on mutation patterns and recurrent mutations in chromatin regulators. Nat. Genet. *44*, 760–764.

Gaiddon, C., Lokshin, M., Gross, I., Levasseur, D., Taya, Y., Loeffler, J.-P., and Prives, C. (2003). Cyclin-dependent kinases phosphorylate p73 at threonine 86 in a cell cycle-dependent manner and negatively regulate p73. J. Biol. Chem. *278*, 27421–27431.

Galavotti, S., Bartesaghi, S., Faccenda, D., Shaked-Rabi, M., Sanzone, S., McEvoy, A., Dinsdale, D., Condorelli, F., Brandner, S., Campanella, M., et al. (2013). The autophagy-associated factors DRAM1 and p62 regulate cell migration and invasion in glioblastoma stem cells. Oncogene *32*, 699–712.

Galle, P.R., Hagelstein, J., Kommerell, B., Volkmann, M., Schranz, P., and Zentgraf, H. (1994). In vitro experimental infection of primary human hepatocytes with hepatitis B virus. Gastroenterology *106*, 664–673.

Galluzzi, L., Pietrocola, F., Levine, B., and Kroemer, G. (2014). Metabolic control of autophagy. Cell *159*, 1263–1276.

Galluzzi, L., Pietrocola, F., Bravo-San Pedro, J.M., Amaravadi, R.K., Baehrecke, E.H., Cecconi, F., Codogno, P., Debnath, J., Gewirtz, D.A., Karantza, V., et al. (2015). Autophagy in malignant transformation and cancer progression. EMBO J. *34*, 856–880.

Gao, H., Korn, J.M., Ferretti, S., Monahan, J.E., Wang, Y., Singh, M., Zhang, C., Schnell, C., Yang, G., Zhang, Y., et al. (2015). High-throughput screening using patient-derived tumor xenografts to predict clinical trial drug response. Nat. Med. *21*, 1318–1325.

Gao, J.-Z., Li, J., Du, J.-L., and Li, X.-L. (2016). Long non-coding RNA HOTAIR is a marker for hepatocellular carcinoma progression and tumor recurrence. Oncol. Lett. *11*, 1791–1798.

Garin-Chesa, P., Old, L.J., and Rettig, W.J. (1990). Cell surface glycoprotein of reactive stromal fibroblasts as a potential antibody target in human epithelial cancers. Proc. Natl. Acad. Sci. U. S. A. *87*, 7235–7239.

Garrido-Laguna, I., Uson, M., Rajeshkumar, N.V., Tan, A.C., de Oliveira, E., Karikari, C., Villaroel, M.C., Salomon, A., Taylor, G., Sharma, R., et al. (2011). Tumor engraftment in nude mice and enrichment in stroma- related gene pathways predict poor survival and resistance to gemcitabine in patients with pancreatic cancer. Clin. Cancer Res. Off. J. Am. Assoc. Cancer Res. *17*, 5793–5800.

Garufi, A., Pucci, D., D'Orazi, V., Cirone, M., Bossi, G., Avantaggiati, M.L., and D'Orazi, G. (2014). Degradation of mutant p53H175 protein by Zn(II) through autophagy. Cell Death Dis. *5*, e1271.

Geismann, C., Arlt, A., Sebens, S., and Schäfer, H. (2014). Cytoprotection "gone astray": Nrf2 and its role in cancer. OncoTargets Ther. *7*, 1497–1518.

Geller, S.A., Nichols, W.S., Kim, S., Tolmachoff, T., Lee, S., Dycaico, M.J., Felts, K., and Sorge, J.A. (1994). Hepatocarcinogenesis is the sequel to hepatitis in Z#2 alpha 1-antitrypsin transgenic mice: histopathological and DNA ploidy studies. Hepatol. Baltim. Md *19*, 389–397.

Gerber, M.A., Shieh, Y.S., Shim, K.S., Thung, S.N., Demetris, A.J., Schwartz, M., Akyol, G., and Dash, S. (1992). Detection of replicative hepatitis C virus sequences in hepatocellular carcinoma. Am. J. Pathol. *141*, 1271–1277.

Giuliano, M., Herrera, S., Christiny, P., Shaw, C., Creighton, C.J., Mitchell, T., Bhat, R., Zhang, X., Mao, S., Dobrolecki, L.E., et al. (2015). Circulating and disseminated tumor cells from breast cancer patient-derived xenograft-bearing mice as a novel model to study metastasis. Breast Cancer Res. BCR *17*, 3.

Glebe, D., Berting, A., Broehl, S., Naumann, H., Schuster, R., Fiedler, N., Tolle, T.K., Nitsche, S., Seifer, M., Gerlich, W.H., et al. (2001). Optimised conditions for the production of hepatitis B virus from cell culture. Intervirology *44*, 370–378.

Goel, S., Wang, Q., Watt, A.C., Tolaney, S.M., Dillon, D.A., Li, W., Ramm, S., Palmer, A.C., Yuzugullu, H., Varadan, V., et al. (2016). Overcoming Therapeutic Resistance in HER2-Positive Breast Cancers with CDK4/6 Inhibitors. Cancer Cell *29*, 255–269.

Gong, C., Bauvy, C., Tonelli, G., Yue, W., Deloménie, C., Nicolas, V., Zhu, Y., Domergue, V., Marin-Esteban, V., Tharinger, H., et al. (2013). Beclin 1 and autophagy are required for the tumorigenicity of breast cancer stem-like/progenitor cells. Oncogene *32*, 2261–2272, 2272e.1-11.

Gong, G., Waris, G., Tanveer, R., and Siddiqui, A. (2001). Human hepatitis C virus NS5A protein alters intracellular calcium levels, induces oxidative stress, and activates STAT-3 and NF-kappa B. Proc. Natl. Acad. Sci. U. S. A. *98*, 9599–9604.

Gong, S.-J., Feng, X.-J., Song, W.-H., Chen, J.-M., Wang, S.-M., Xing, D.-J., Zhu, M.-H., Zhang, S.-H., and Xu, A.-M. (2015). Upregulation of PP2Ac predicts poor prognosis and contributes to aggressiveness in hepatocellular carcinoma. Cancer Biol. Ther. *17*, 151–162.

González, R., De la Rosa, Á.J., Rufini, A., Rodríguez-Hernández, M.A., Navarro-Villarán, E., Marchal, T., Pereira, S., De la Mata, M., Müller-Schilling, M., Pascasio-Acevedo, J.M., et al. (2017). Role of p63 and p73 isoforms on the cell death in patients with hepatocellular carcinoma submitted to orthotopic liver transplantation. PloS One *12*, e0174326.

Gordon, G.J., Coleman, W.B., Hixson, D.C., and Grisham, J.W. (2000). Liver regeneration in rats with retrorsine-induced hepatocellular injury proceeds through a novel cellular response. Am. J. Pathol. *156*, 607–619.

Gordon, S.C., Bayati, N., and Silverman, A.L. (1998). Clinical outcome of hepatitis C as a function of mode of transmission. Hepatol. Baltim. Md *28*, 562–567.

GOUMARD, C., DESBOIS-MOUTHON, C., WENDUM, D., CALMEL, C., MERABTENE, F., SCATTON, O., and PRAZ, F. (2017). Low Levels of Microsatellite Instability at Simple Repeated Sequences Commonly Occur in Human Hepatocellular Carcinoma. Cancer Genomics Proteomics *14*, 329–339.

Gozuacik, D., and Kimchi, A. (2004). Autophagy as a cell death and tumor suppressor mechanism. Oncogene *23*, 2891–2906.

Green, D.R., Galluzzi, L., and Kroemer, G. (2011). Mitochondria and the autophagy-inflammation-cell death axis in organismal aging. Science *333*, 1109–1112.

Gregorieff, A., and Clevers, H. (2005). Wnt signaling in the intestinal epithelium: from endoderm to cancer. Genes Dev. *19*, 877–890.

Gripon, P., Diot, C., Thézé, N., Fourel, I., Loreal, O., Brechot, C., and Guguen-Guillouzo, C. (1988). Hepatitis B virus infection of adult human hepatocytes cultured in the presence of dimethyl sulfoxide. J. Virol. *62*, 4136–4143.

Gripon, P., Diot, C., and Guguen-Guillouzo, C. (1993). Reproducible high level infection of cultured adult human hepatocytes by hepatitis B virus: effect of polyethylene glycol on adsorption and penetration. Virology *192*, 534–540.

Gripon, P., Rumin, S., Urban, S., Seyec, J.L., Glaise, D., Cannie, I., Guyomard, C., Lucas, J., Trepo, C., and Guguen-Guillouzo, C. (2002). Infection of a human hepatoma cell line by hepatitis B virus. Proc. Natl. Acad. Sci. *99*, 15655–15660.

Gu, Q., Zhang, B., Sun, H., Xu, Q., Tan, Y., Wang, G., Luo, Q., Xu, W., Yang, S., Li, J., et al. (2015). Genomic characterization of a large panel of patient-derived hepatocellular carcinoma xenograft tumor models for preclinical development. Oncotarget *6*, 20160–20176.

Guan, J.-L., Simon, A.K., Prescott, M., Menendez, J.A., Liu, F., Wang, F., Wang, C., Wolvetang, E., Vazquez-Martin, A., and Zhang, J. (2013). Autophagy in stem cells. Autophagy *9*, 830–849.

Guerrieri, F., Piconese, S., Lacoste, C., Schinzari, V., Testoni, B., Valogne, Y., Gerbal-Chaloin, S., Samuel, D., Bréchot, C., Faivre, J., et al. (2013). The sodium/iodide symporter NIS is a transcriptional target of the p53-family members in liver cancer cells. Cell Death Dis. *4*, e807.

Guichard, C., Amaddeo, G., Imbeaud, S., Ladeiro, Y., Pelletier, L., Maad, I.B., Calderaro, J., Bioulac-Sage, P., Letexier, M., Degos, F., et al. (2012). Integrated analysis of somatic mutations and focal copy-number changes identifies key genes and pathways in hepatocellular carcinoma. Nat. Genet. *44*, 694–698.

Guo, J.Y., Chen, H.-Y., Mathew, R., Fan, J., Strohecker, A.M., Karsli-Uzunbas, G., Kamphorst, J.J., Chen, G., Lemons, J.M.S., Karantza, V., et al. (2011). Activated Ras requires autophagy to maintain oxidative metabolism and tumorigenesis. Genes Dev. *25*, 460–470.

Guo, J.Y., Xia, B., and White, E. (2013). Autophagy-mediated tumor promotion. Cell *155*, 1216–1219.

Gupta, P.B., Fillmore, C.M., Jiang, G., Shapira, S.D., Tao, K., Kuperwasser, C., and Lander, E.S. (2011). Stochastic state transitions give rise to phenotypic equilibrium in populations of cancer cells. Cell *146*, 633–644.

Hai, H., Tamori, A., and Kawada, N. (2014). Role of hepatitis B virus DNA integration in human hepatocarcinogenesis. World J. Gastroenterol. *20*, 6236–6243.

Ham, J., Costa, C., Sano, R., Lochmann, T.L., Sennott, E.M., Patel, N.U., Dastur, A., Gomez-Caraballo, M., Krytska, K., Hata, A.N., et al. (2016). Exploitation of the Apoptosis-Primed State of MYCN-Amplified Neuroblastoma to Develop a Potent and Specific Targeted Therapy Combination. Cancer Cell *29*, 159–172.

Hamdy, M.S.A.-D., El-Saadany, Z.A., Makhlouf, M.M., Salama, A.I., Ibrahim, N.S., and Gad, A.A. (2016). TAp73 and ΔNp73 relative expression in Egyptian patients with lymphoid neoplasms. Tumori 0.

Han, S., Han, L., Yao, Y., Sun, H., Zan, X., and Liu, Q. (2014). Activated hepatic stellate cells promote hepatocellular carcinoma cell migration and invasion via the activation of FAK-MMP9 signaling. Oncol. Rep. *31*, 641–648.

Hanahan, D., and Weinberg, R.A. (2000). The hallmarks of cancer. Cell *100*, 57–70.

Hanahan, D., and Weinberg, R.A. (2011). Hallmarks of Cancer: The Next Generation. Cell *144*, 646–674.

Hanif, R., and Mansoor, S. (2014). Hep par-1: a novel immunohistochemical marker for differentiating hepatocellular carcinoma from metastatic carcinoma. J. Coll. Physicians Surg.--Pak. JCPSP *24*, 186–189.

Hara, E. (2015). Relationship between Obesity, Gut Microbiome and Hepatocellular Carcinoma Development. Dig. Dis. Basel Switz. *33*, 346–350.

Hara, T., Nakamura, K., Matsui, M., Yamamoto, A., Nakahara, Y., Suzuki-Migishima, R., Yokoyama, M., Mishima, K., Saito, I., Okano, H., et al. (2006). Suppression of basal autophagy in neural cells causes neurodegenerative disease in mice. Nature *441*, 885–889.

Harms, K.L., and Chen, X. (2005). The C terminus of p53 family proteins is a cell fate determinant. Mol. Cell. Biol. *25*, 2014–2030.

Harouaka, D., Engle, R.E., Wollenberg, K., Diaz, G., Tice, A.B., Zamboni, F., Govindarajan, S., Alter, H., Kleiner, D.E., and Farci, P. (2016). Diminished viral replication and

compartmentalization of hepatitis C virus in hepatocellular carcinoma tissue. Proc. Natl. Acad. Sci. U. S. A. *113*, 1375–1380.

Haruna, Y., Hayashi, N., Kamada, T., Hytiroglou, P., Thung, S.N., and Gerber, M.A. (1994). Expression of hepatitis C virus in hepatocellular carcinoma. Cancer *73*, 2253–2258.

Hassan, M., Ghozlan, H., and Abdel-Kader, O. (2004). Activation of RB/E2F signaling pathway is required for the modulation of hepatitis C virus core protein-induced cell growth in liver and non-liver cells. Cell. Signal. *16*, 1375–1385.

He, C., Xu, J., Zhang, J., Xie, D., Ye, H., Xiao, Z., Cai, M., Xu, K., Zeng, Y., Li, H., et al. (2012a). High expression of trimethylated histone H3 lysine 4 is associated with poor prognosis in hepatocellular carcinoma. Hum. Pathol. *43*, 1425–1435.

He, X.-X., Chang, Y., Meng, F.-Y., Wang, M.-Y., Xie, Q.-H., Tang, F., Li, P.-Y., Song, Y.-H., and Lin, J.-S. (2012b). MicroRNA-375 targets AEG-1 in hepatocellular carcinoma and suppresses liver cancer cell growth in vitro and in vivo. Oncogene *31*, 3357–3369.

He, Z., Liu, H., Agostini, M., Yousefi, S., Perren, A., Tschan, M.P., Mak, T.W., Melino, G., and Simon, H.U. (2013). p73 regulates autophagy and hepatocellular lipid metabolism through a transcriptional activation of the ATG5 gene. Cell Death Differ. *20*, 1415–1424.

Heddleston, J.M., Li, Z., McLendon, R.E., Hjelmeland, A.B., and Rich, J.N. (2009). The hypoxic microenvironment maintains glioblastoma stem cells and promotes reprogramming towards a cancer stem cell phenotype. Cell Cycle Georget. Tex *8*, 3274–3284.

Heindryckx, F., Colle, I., and Van Vlierberghe, H. (2009). Experimental mouse models for hepatocellular carcinoma research. Int. J. Exp. Pathol. *90*, 367–386.

Herencia, C., Martínez-Moreno, J.M., Herrera, C., Corrales, F., Santiago-Mora, R., Espejo, I., Barco, M., Almadén, Y., de la Mata, M., Rodríguez-Ariza, A., et al. (2012). Nuclear translocation of β-catenin during mesenchymal stem cells differentiation into hepatocytes is associated with a tumoral phenotype. PloS One *7*, e34656.

Hermann, P.C., Huber, S.L., Herrler, T., Aicher, A., Ellwart, J.W., Guba, M., Bruns, C.J., and Heeschen, C. (2007). Distinct populations of cancer stem cells determine tumor growth and metastatic activity in human pancreatic cancer. Cell Stem Cell *1*, 313–323.

Hernando, E., Nahlé, Z., Juan, G., Diaz-Rodriguez, E., Alaminos, M., Hemann, M., Michel, L., Mittal, V., Gerald, W., Benezra, R., et al. (2004). Rb inactivation promotes genomic instability by uncoupling cell cycle progression from mitotic control. Nature *430*, 797–802.

Higgs, M.R., Lerat, H., and Pawlotsky, J.-M. (2013). Hepatitis C virus-induced activation of β-catenin promotes c-Myc expression and a cascade of pro-carcinogenetic events. Oncogene *32*, 4683–4693.

Higgs, M.R., Chouteau, P., and Lerat, H. (2014). "Liver let die": oxidative DNA damage and hepatotropic viruses. J. Gen. Virol. *95*, 991–1004.

Ho, T.-C., Chen, S.-L., Yang, Y.-C., Liao, C.-L., Cheng, H.-C., and Tsao, Y.-P. (2007). PEDF induces p53-mediated apoptosis through PPAR gamma signaling in human umbilical vein endothelial cells. Cardiovasc. Res. *76*, 213–223.

Homayounfar, K., Schwarz, A., Enders, C., Cameron, S., Baumhoer, D., Ramadori, G., Lorf, T., Gunawan, B., and Sander, B. (2013). Etiologic influence on chromosomal aberrations in European hepatocellular carcinoma identified by CGH. Pathol. Res. Pract. *209*, 380–387.

Hooper, C., Tavassoli, M., Chapple, J.P., Uwanogho, D., Goodyear, R., Melino, G., Lovestone, S., and Killick, R. (2006). TAp73 isoforms antagonize Notch signalling in SH-SY5Y neuroblastomas and in primary neurones. J. Neurochem. *99*, 989–999.

Horiike, N., Nonaka, T., Kumamoto, I., Kajino, K., Onji, M., and Ohta, Y. (1993). Hepatitis C virus plus- and minus- strand RNA in hepatocellular carcinoma and adjoining nontumorous liver. J. Med. Virol. *41*, 312–315.

Hoshida, Y., Villanueva, A., Kobayashi, M., Peix, J., Chiang, D.Y., Camargo, A., Gupta, S., Moore, J., Wrobel, M.J., Lerner, J., et al. (2008). Gene expression in fixed tissues and outcome in hepatocellular carcinoma. N. Engl. J. Med. *359*, 1995–2004.

Hoshida, Y., Nijman, S.M.B., Kobayashi, M., Chan, J.A., Brunet, J.-P., Chiang, D.Y., Villanueva, A., Newell, P., Ikeda, K., Hashimoto, M., et al. (2009). Integrative transcriptome analysis reveals common molecular subclasses of human hepatocellular carcinoma. Cancer Res. *69*, 7385–7392.

Hoshida, Y., Toffanin, S., Lachenmayer, A., Villanueva, A., Minguez, B., and Llovet, J.M. (2010). Molecular classification and novel targets in hepatocellular carcinoma: recent advancements. Semin. Liver Dis. *30*, 35–51.

Houghton, J.A., Houghton, P.J., and Green, A.A. (1982). Chemotherapy of childhood rhabdomyosarcomas growing as xenografts in immune-deprived mice. Cancer Res. *42*, 535–539.

Hsia, C.C., Evarts, R.P., Nakatsukasa, H., Marsden, E.R., and Thorgeirsson, S.S. (1992). Occurrence of oval-type cells in hepatitis B virus-associated human hepatocarcinogenesis. Hepatol. Baltim. Md *16*, 1327–1333.

Hsia, C.C., Thorgeirsson, S.S., and Tabor, E. (1994). Expression of hepatitis B surface and core antigens and transforming growth factor-alpha in “oval cells” of the liver in patients with hepatocellular carcinoma. J. Med. Virol. *43*, 216–221.

Hsu, H.C., Wu, T.T., Sheu, J.C., Wu, C.Y., Chiou, T.J., Lee, C.S., and Chen, D.S. (1989). Biologic significance of the detection of HBsAg and HBcAg in liver and tumor from 204 HBsAg-positive patients with primary hepatocellular carcinoma. Hepatol. Baltim. Md *9*, 747–750.

Hsu, H.C., Cheng, W., and Lai, P.L. (1997). Cloning and expression of a developmentally regulated transcript MXR7 in hepatocellular carcinoma: biological significance and temporospatial distribution. Cancer Res. *57*, 5179–5184.

Hsu, H.C., Jeng, Y.M., Mao, T.L., Chu, J.S., Lai, P.L., and Peng, S.Y. (2000). Beta-catenin mutations are associated with a subset of low-stage hepatocellular carcinoma negative for hepatitis B virus and with favorable prognosis. Am. J. Pathol. *157*, 763–770.

Hsu, I.C., Metcalf, R.A., Sun, T., Welsh, J.A., Wang, N.J., and Harris, C.C. (1991). Mutational hotspot in the p53 gene in human hepatocellular carcinomas. Nature *350*, 427–428.

Huang, D.-S., Wang, Z., He, X.-J., Diplas, B.H., Yang, R., Killela, P.J., Meng, Q., Ye, Z.-Y., Wang, W., Jiang, X.-T., et al. (2015). Recurrent TERT promoter mutations identified in a large-scale study of multiple tumour types are associated with increased TERT expression and telomerase activation. Eur. J. Cancer Oxf. Engl. 1990 *51*, 969–976.

Huang, H., Fujii, H., Sankila, A., Mahler-Araujo, B.M., Matsuda, M., Cathomas, G., and Ohgaki, H. (1999). Beta-catenin mutations are frequent in human hepatocellular carcinomas associated with hepatitis C virus infection. Am. J. Pathol. *155*, 1795–1801.

Huang, J., Deng, Q., Wang, Q., Li, K.-Y., Dai, J.-H., Li, N., Zhu, Z.-D., Zhou, B., Liu, X.-Y., Liu, R.-F., et al. (2012). Exome sequencing of hepatitis B virus-associated hepatocellular carcinoma. Nat. Genet. *44*, 1117–1121.

Hussain, S.P., Schwank, J., Staib, F., Wang, X.W., and Harris, C.C. (2007). TP53 mutations and hepatocellular carcinoma: insights into the etiology and pathogenesis of liver cancer. Oncogene *26*, 2166–2176.

Hüttinger-Kirchhof, N., Cam, H., Griesmann, H., Hofmann, L., Beitzinger, M., and Stiewe, T. (2006). The p53 family inhibitor DeltaNp73 interferes with multiple developmental programs. Cell Death Differ. *13*, 174–177.

Iizuka, N., Oka, M., Yamada-Okabe, H., Nishida, M., Maeda, Y., Mori, N., Takao, T., Tamesa, T., Tangoku, A., Tabuchi, H., et al. (2003). Oligonucleotide microarray for prediction of early intrahepatic recurrence of hepatocellular carcinoma after curative resection. Lancet Lond. Engl. *361*, 923–929.

Imamura, H., Matsuyama, Y., Tanaka, E., Ohkubo, T., Hasegawa, K., Miyagawa, S., Sugawara, Y., Minagawa, M., Takayama, T., Kawasaki, S., et al. (2003). Risk factors contributing to early and late phase intrahepatic recurrence of hepatocellular carcinoma after hepatectomy. J. Hepatol. *38*, 200–207.

Irwin, M., Marin, M.C., Phillips, A.C., Seelan, R.S., Smith, D.I., Liu, W., Flores, E.R., Tsai, K.Y., Jacks, T., Vousden, K.H., et al. (2000). Role for the p53 homologue p73 in E2F-1-induced apoptosis. Nature *407*, 645–648.

Ishimoto, O., Kawahara, C., Enjo, K., Obinata, M., Nukiwa, T., and Ikawa, S. (2002). Possible oncogenic potential of DeltaNp73: a newly identified isoform of human p73. Cancer Res. *62*, 636–641.

Ito, M., Hiramatsu, H., Kobayashi, K., Suzue, K., Kawahata, M., Hioki, K., Ueyama, Y., Koyanagi, Y., Sugamura, K., Tsuji, K., et al. (2002). NOD/SCID/gamma(c)(null) mouse: an excellent recipient mouse model for engraftment of human cells. Blood *100*, 3175–3182.

Iwama, A., Oguro, H., Negishi, M., Kato, Y., Morita, Y., Tsukui, H., Ema, H., Kamijo, T., Katoh-Fukui, Y., Koseki, H., et al. (2004). Enhanced self-renewal of hematopoietic stem cells mediated by the polycomb gene product Bmi-1. Immunity *21*, 843–851.

Jang, J.-W., Song, Y., Kim, S.-H., Kim, J., and Seo, H.R. (2017). Potential mechanisms of CD133 in cancer stem cells. Life Sci. *184*, 25–29.

Jemal, A., Bray, F., Center, M.M., Ferlay, J., Ward, E., and Forman, D. (2011). Global cancer statistics. CA. Cancer J. Clin. *61*, 69–90.

Jiang, Z., Jhunjhunwala, S., Liu, J., Haverty, P.M., Kennemer, M.I., Guan, Y., Lee, W., Carnevali, P., Stinson, J., Johnson, S., et al. (2012). The effects of hepatitis B virus integration into the genomes of hepatocellular carcinoma patients. Genome Res. *22*, 593–601.

Joerger, A.C., Rajagopalan, S., Natan, E., Veprintsev, D.B., Robinson, C.V., and Fersht, A.R. (2009). Structural evolution of p53, p63, and p73: implication for heterotetramer formation. Proc. Natl. Acad. Sci. U. S. A. *106*, 17705–17710.

John, K., Alla, V., Meier, C., and Pützer, B.M. (2011). GRAMD4 mimics p53 and mediates the apoptotic function of p73 at mitochondria. Cell Death Differ. *18*, 874–886.

Jost, C.A., Marin, M.C., and Kaelin, W.G. (1997). p73 is a simian [correction of human] p53-related protein that can induce apoptosis. Nature *389*, 191–194.

Julien, S., Merino-Trigo, A., Lacroix, L., Pocard, M., Goéré, D., Mariani, P., Landron, S., Bigot, L., Nemati, F., Dartigues, P., et al. (2012). Characterization of a large panel of patient-derived tumor xenografts representing the clinical heterogeneity of human colorectal cancer. Clin. Cancer Res. Off. J. Am. Assoc. Cancer Res. *18*, 5314–5328.

Junttila, M.R., and de Sauvage, F.J. (2013). Influence of tumour micro-environment heterogeneity on therapeutic response. Nature *501*, 346–354.

Kabbach, G., Assi, H.A., Bolotin, G., Schuster, M., Lee, H.J., and Tadros, M. (2015). Hepatobiliary Tumors: Update on Diagnosis and Management. J. Clin. Transl. Hepatol. *3*, 169–181.

Kaghad, M., Bonnet, H., Yang, A., Creancier, L., Biscan, J.C., Valent, A., Minty, A., Chalon, P., Lelias, J.M., Dumont, X., et al. (1997). Monoallelically expressed gene related to p53 at 1p36, a region frequently deleted in neuroblastoma and other human cancers. Cell *90*, 809–819.

Kalluri, R., and Zeisberg, M. (2006). Fibroblasts in cancer. Nat. Rev. Cancer *6*, 392–401.

Kan, Z., Zheng, H., Liu, X., Li, S., Barber, T.D., Gong, Z., Gao, H., Hao, K., Willard, M.D., Xu, J., et al. (2013). Whole-genome sequencing identifies recurrent mutations in hepatocellular carcinoma. Genome Res. *23*, 1422–1433.

Kang, J.S., Wanibuchi, H., Morimura, K., Wongpoomchai, R., Chusiri, Y., Gonzalez, F.J., and Fukushima, S. (2008). Role of CYP2E1 in thioacetamide-induced mouse hepatotoxicity. Toxicol. Appl. Pharmacol. *228*, 295–300.

Kang, S.-M., Kim, S.-J., Kim, J.-H., Lee, W., Kim, G.-W., Lee, K.-H., Choi, K.-Y., and Oh, J.-W. (2009). Interaction of hepatitis C virus core protein with Hsp60 triggers the production of reactive oxygen species and enhances TNF-alpha-mediated apoptosis. Cancer Lett. *279*, 230–237.

Karin, M., and Dhar, D. (2016). Liver carcinogenesis: from naughty chemicals to soothing fat and the surprising role of NRF2. Carcinogenesis *37*, 541–546.

Karsli-Uzunbas, G., Guo, J.Y., Price, S., Teng, X., Laddha, S.V., Khor, S., Kalaany, N.Y., Jacks, T., Chan, C.S., Rabinowitz, J.D., et al. (2014). Autophagy is required for glucose homeostasis and lung tumor maintenance. Cancer Discov. *4*, 914–927.

Kasim, V., Huang, C., Zhang, J., Jia, H., Wang, Y., Yang, L., Miyagishi, M., and Wu, S. (2014). Synergistic cooperation of MDM2 and E2F1 contributes to TAp73 transcriptional activity. Biochem. Biophys. Res. Commun. *449*, 319–326.

Kasper, M., Regl, G., Frischauf, A.-M., and Aberger, F. (2006). GLI transcription factors: mediators of oncogenic Hedgehog signalling. Eur. J. Cancer Oxf. Engl. 1990 *42*, 437–445.

Kawai, H., Suda, T., Aoyagi, Y., Isokawa, O., Mita, Y., Waguri, N., Kuroiwa, T., Igarashi, M., Tsukada, K., Mori, S., et al. (2000). Quantitative evaluation of genomic instability as a possible predictor for development of hepatocellular carcinoma: comparison of loss of heterozygosity and replication error. Hepatol. Baltim. Md *31*, 1246–1250.

Kawai-Kitahata, F., Asahina, Y., Tanaka, S., Kakinuma, S., Murakawa, M., Nitta, S., Watanabe, T., Otani, S., Taniguchi, M., Goto, F., et al. (2016). Comprehensive analyses of mutations and hepatitis B virus integration in hepatocellular carcinoma with clinicopathological features. J. Gastroenterol. *51*, 473–486.

Kenific, C.M., and Debnath, J. (2015). Cellular and metabolic functions for autophagy in cancer cells. Trends Cell Biol. *25*, 37–45.

Kessler, S.M., Laggai, S., Barghash, A., Schultheiss, C.S., Lederer, E., Artl, M., Helms, V., Haybaeck, J., and Kiemer, A.K. (2015). IMP2/p62 induces genomic instability and an aggressive hepatocellular carcinoma phenotype. Cell Death Dis. *6*, e1894.

Keysar, S.B., Astling, D.P., Anderson, R.T., Vogler, B.W., Bowles, D.W., Morton, J.J., Paylor, J.J., Glogowska, M.J., Le, P.N., Eagles-Soukup, J.R., et al. (2013). A patient tumor transplant model of squamous cell cancer identifies PI3K inhibitors as candidate therapeutics in defined molecular bins. Mol. Oncol. *7*, 776–790.

Killela, P.J., Reitman, Z.J., Jiao, Y., Bettegowda, C., Agrawal, N., Diaz, L.A., Friedman, A.H., Friedman, H., Gallia, G.L., Giovanella, B.C., et al. (2013). TERT promoter mutations occur frequently in gliomas and a subset of tumors derived from cells with low rates of self-renewal. Proc. Natl. Acad. Sci. U. S. A. *110*, 6021–6026.

Killick, R., Niklison-Chirou, M., Tomasini, R., Bano, D., Rufini, A., Grespi, F., Velletri, T., Tucci, P., Sayan, B.S., Conforti, F., et al. (2011). p73: A Multifunctional Protein in Neurobiology. Mol. Neurobiol. *43*, 139–146.

Kim, T.-M., and Park, P.J. (2014). A genome-wide view of microsatellite instability: old stories of cancer mutations revisited with new sequencing technologies. Cancer Res. *74*, 6377–6382.

Kim, B.H., Sung, S.R., Choi, E.H., Kim, Y.I., Kim, K.J., Dong, S.H., Kim, H.J., Chang, Y.W., Lee, J.I., and Chang, R. (2000). Dedifferentiation of conditionally immortalized hepatocytes with long-term in vitro passage. Exp. Mol. Med. *32*, 29–37.

Kim, C.M., Koike, K., Saito, I., Miyamura, T., and Jay, G. (1991). HBx gene of hepatitis B virus induces liver cancer in transgenic mice. Nature *351*, 317–320.

Kim, H., Choi, G.H., Na, D.C., Ahn, E.Y., Kim, G.I., Lee, J.E., Cho, J.Y., Yoo, J.E., Choi, J.S., and Park, Y.N. (2011). Human hepatocellular carcinomas with “Stemness”-related marker expression: keratin 19 expression and a poor prognosis. Hepatol. Baltim. Md *54*, 1707–1717.

Kim, J., Kim, Y.C., Fang, C., Russell, R.C., Kim, J.H., Fan, W., Liu, R., Zhong, Q., and Guan, K.-L. (2013). Differential regulation of distinct Vps34 complexes by AMPK in nutrient stress and autophagy. Cell *152*, 290–303.

Kim, M., Lee, H.C., Tsedensodnom, O., Hartley, R., Lim, Y.-S., Yu, E., Merle, P., and Wands, J.R. (2008). Functional interaction between Wnt3 and Frizzled-7 leads to activation of the Wnt/beta-catenin signaling pathway in hepatocellular carcinoma cells. J. Hepatol. *48*, 780–791.

Kisseleva, T., and Brenner, D.A. (2008). Mechanisms of fibrogenesis. Exp. Biol. Med. Maywood NJ *233*, 109–122.

Knight, B., Yeoh, G.C., Husk, K.L., Ly, T., Abraham, L.J., Yu, C., Rhim, J.A., and Fausto, N. (2000). Impaired preneoplastic changes and liver tumor formation in tumor necrosis factor receptor type 1 knockout mice. J. Exp. Med. *192*, 1809–1818.

Knight, B., Tirnitz-Parker, J.E.E., and Olynyk, J.K. (2008). C-kit inhibition by imatinib mesylate attenuates progenitor cell expansion and inhibits liver tumor formation in mice. Gastroenterology *135*, 969–979, 979.e1.

Knoll, S., Fürst, K., Thomas, S., Villanueva Baselga, S., Stoll, A., Schaefer, S., and Pützer, B.M. (2011). Dissection of cell context-dependent interactions between HBx and p53 family members in regulation of apoptosis: a role for HBV-induced HCC. Cell Cycle Georget. Tex *10*, 3554–3565.

Kobayashi, S., Hayashi, H., Itoh, Y., Asano, T., and Isono, K. (1994). Detection of minus-strand hepatitis C virus RNA in tumor tissues of hepatocellular carcinoma. Cancer *73*, 48–52.

Koike, K., and Miyoshi, H. (2006). Oxidative stress and hepatitis C viral infection. Hepatol. Res. Off. J. Jpn. Soc. Hepatol. *34*, 65–73.

Koike, K., Moriya, K., Iino, S., Yotsuyanagi, H., Endo, Y., Miyamura, T., and Kurokawa, K. (1994). High-level expression of hepatitis B virus HBx gene and hepatocarcinogenesis in transgenic mice. Hepatol. Baltim. Md *19*, 810–819.

Koike, K., Moriya, K., Yotsuyanagi, H., Shintani, Y., Fujie, H., Tsutsumi, T., and Kimura, S. (1998). Compensatory apoptosis in preneoplastic liver of a transgenic mouse model for viral hepatocarcinogenesis. Cancer Lett. *134*, 181–186.

Komatsu, M., Waguri, S., Ueno, T., Iwata, J., Murata, S., Tanida, I., Ezaki, J., Mizushima, N., Ohsumi, Y., Uchiyama, Y., et al. (2005). Impairment of starvation-induced and constitutive autophagy in Atg7-deficient mice. J. Cell Biol. *169*, 425–434.

Komatsu, M., Waguri, S., Koike, M., Sou, Y.-S., Ueno, T., Hara, T., Mizushima, N., Iwata, J.-I., Ezaki, J., Murata, S., et al. (2007). Homeostatic levels of p62 control cytoplasmic inclusion body formation in autophagy-deficient mice. Cell *131*, 1149–1163.

Kondo, Y., Kanai, Y., Sakamoto, M., Mizokami, M., Ueda, R., and Hirohashi, S. (2000). Genetic instability and aberrant DNA methylation in chronic hepatitis and cirrhosis--A comprehensive study of loss of heterozygosity and microsatellite instability at 39 loci and DNA hypermethylation on 8 CpG islands in microdissected specimens from patients with hepatocellular carcinoma. Hepatol. Baltim. Md *32*, 970–979.

Korenaga, M., Wang, T., Li, Y., Showalter, L.A., Chan, T., Sun, J., and Weinman, S.A. (2005). Hepatitis C Virus Core Protein Inhibits Mitochondrial Electron Transport and Increases Reactive Oxygen Species (ROS) Production. J. Biol. Chem. *280*, 37481–37488.

Kowalik, M.A., Sulas, P., Ledda-Columbano, G.M., Giordano, S., Columbano, A., and Perra, A. (2015). Cytokeratin-19 positivity is acquired along cancer progression and does not predict cell origin in rat hepatocarcinogenesis. Oncotarget *6*, 38749–38763.

Kreso, A., O'Brien, C.A., van Galen, P., Gan, O.I., Notta, F., Brown, A.M.K., Ng, K., Ma, J., Wienholds, E., Dunant, C., et al. (2013). Variable clonal repopulation dynamics influence chemotherapy response in colorectal cancer. Science *339*, 543–548.

Kresse, S.H., Meza-Zepeda, L.A., Machado, I., Llombart-Bosch, A., and Myklebost, O. (2012). Preclinical xenograft models of human sarcoma show nonrandom loss of aberrations. Cancer *118*, 558–570.

Krivtsov, A.V., Twomey, D., Feng, Z., Stubbs, M.C., Wang, Y., Faber, J., Levine, J.E., Wang, J., Hahn, W.C., Gilliland, D.G., et al. (2006). Transformation from committed progenitor to leukaemia stem cell initiated by MLL-AF9. Nature *442*, 818–822.

Kroemer, G., Mariño, G., and Levine, B. (2010). Autophagy and the integrated stress response. Mol. Cell *40*, 280–293.

Kulik, L.M., and Chokechanachaisakul, A. (2015). Evaluation and management of hepatocellular carcinoma. Clin. Liver Dis. *19*, 23–43.

Kurinna, S., Stratton, S.A., Tsai, W.-W., Akdemir, K.C., Gu, W., Singh, P., Goode, T., Darlington, G.J., and Barton, M.C. (2010). Direct activation of forkhead box O3 by tumor suppressors p53 and p73 is disrupted during liver regeneration in mice. Hepatol. Baltim. Md *52*, 1023–1032.

Kurtova, A.V., Xiao, J., Mo, Q., Pazhanisamy, S., Krasnow, R., Lerner, S.P., Chen, F., Roh, T.T., Lay, E., Ho, P.L., et al. (2015). Blocking PGE2-induced tumour repopulation abrogates bladder cancer chemoresistance. Nature *517*, 209–213.

Lachenmayer, A., Alsinet, C., Savic, R., Cabellos, L., Toffanin, S., Hoshida, Y., Villanueva, A., Minguez, B., Newell, P., Tsai, H.-W., et al. (2012). Wnt-pathway activation in two molecular classes of hepatocellular carcinoma and experimental modulation by sorafenib. Clin. Cancer Res. Off. J. Am. Assoc. Cancer Res. *18*, 4997–5007.

Lade, A., Noon, L.A., and Friedman, S.L. (2014). Contributions of metabolic dysregulation and inflammation to nonalcoholic steatohepatitis, hepatic fibrosis, and cancer. Curr. Opin. Oncol. *26*, 100–107.

Lai, J., Nie, W., Zhang, W., Wang, Y., Xie, R., Wang, Y., Gu, J., Xu, J., Song, W., Yang, F., et al. (2014). Transcriptional regulation of the p73 gene by Nrf-2 and promoter CpG methylation in human breast cancer. Oncotarget *5*, 6909–6922.

Lai, Y., Wei, X., Lin, S., Qin, L., Cheng, L., and Li, P. (2017). Current status and perspectives of patient-derived xenograft models in cancer research. J. Hematol. Oncol.J Hematol Oncol *10*, 106.

Lambert, M.-P., Ancey, P.-B., Esposti, D.D., Cros, M.-P., Sklias, A., Scoazec, J.-Y., Durantel, D., Hernandez-Vargas, H., and Herceg, Z. (2015). Aberrant DNA methylation of imprinted loci in

hepatocellular carcinoma and after in vitro exposure to common risk factors. Clin. Epigenetics *7*, 15.

Lapidot, T., Sirard, C., Vormoor, J., Murdoch, B., Hoang, T., Caceres-Cortes, J., Minden, M., Paterson, B., Caligiuri, M.A., and Dick, J.E. (1994). A cell initiating human acute myeloid leukaemia after transplantation into SCID mice. Nature *367*, 645–648.

Laplante, M., and Sabatini, D.M. (2012). mTOR signaling in growth control and disease. Cell *149*, 274–293.

Lau, L.M.S., Wolter, J.K., Lau, J.T.M.L., Cheng, L.S., Smith, K.M., Hansford, L.M., Zhang, L., Baruchel, S., Robinson, F., and Irwin, M.S. (2009). Cyclooxygenase inhibitors differentially modulate p73 isoforms in neuroblastoma. Oncogene *28*, 2024–2033.

Laurent-Puig, P., Legoix, P., Bluteau, O., Belghiti, J., Franco, D., Binot, F., Monges, G., Thomas, G., Bioulac-Sage, P., and Zucman-Rossi, J. (2001). Genetic alterations associated with hepatocellular carcinomas define distinct pathways of hepatocarcinogenesis. Gastroenterology *120*, 1763–1773.

Laurenzi, M.A., Beccari, T., Stenke, L., Sjölinder, M., Stinchi, S., and Lindgren, J.A. (1998). Expression of mRNA encoding neurotrophins and neurotrophin receptors in human granulocytes and bone marrow cells--enhanced neurotrophin-4 expression induced by LTB4. J. Leukoc. Biol. *64*, 228–234.

Laurenzi, V.D., Raschellá, G., Barcaroli, D., Annicchiarico-Petruzzelli, M., Ranalli, M., Catani, M.V., Tanno, B., Costanzo, A., Levrero, M., and Melino, G. (2000). Induction of Neuronal Differentiation by p73 in a Neuroblastoma Cell Line. J. Biol. Chem. *275*, 15226–15231.

Lavoie, H., and Therrien, M. (2015). Regulation of RAF protein kinases in ERK signalling. Nat. Rev. Mol. Cell Biol. *16*, 281–298.

Lawson, D.A., Bhakta, N.R., Kessenbrock, K., Prummel, K.D., Yu, Y., Takai, K., Zhou, A., Eyob, H., Balakrishnan, S., Wang, C.-Y., et al. (2015). Single-cell analysis reveals a stem-cell program in human metastatic breast cancer cells. Nature *526*, 131–135.

Lazova, R., Camp, R.L., Klump, V., Siddiqui, S.F., Amaravadi, R.K., and Pawelek, J.M. (2012). Punctate LC3B expression is a common feature of solid tumors and associated with proliferation, metastasis, and poor outcome. Clin. Cancer Res. Off. J. Am. Assoc. Cancer Res. *18*, 370–379.

LeCluyse, E.L., Alexandre, E., Hamilton, G.A., Viollon-Abadie, C., Coon, D.J., Jolley, S., and Richert, L. (2005). Isolation and culture of primary human hepatocytes. Methods Mol. Biol. Clifton NJ *290*, 207–229.

Lee, C.W., and La Thangue, N.B. (1999). Promoter specificity and stability control of the p53-related protein p73. Oncogene *18*, 4171–4181.

Lee, A.F., Ho, D.K., Zanassi, P., Walsh, G.S., Kaplan, D.R., and Miller, F.D. (2004a). Evidence that DeltaNp73 promotes neuronal survival by p53-dependent and p53-independent mechanisms. J. Neurosci. Off. J. Soc. Neurosci. *24*, 9174–9184.

Lee, J.-S., Chu, I.-S., Heo, J., Calvisi, D.F., Sun, Z., Roskams, T., Durnez, A., Demetris, A.J., and Thorgeirsson, S.S. (2004b). Classification and prediction of survival in hepatocellular carcinoma by gene expression profiling. Hepatol. Baltim. Md *40*, 667–676.

Leenders, M.W.H., Nijkamp, M.W., and Borel Rinkes, I.H.M. (2008). Mouse models in liver cancer research: a review of current literature. World J. Gastroenterol. *14*, 6915–6923.

Lemon, S.M., and McGivern, D.R. (2012). Is hepatitis C virus carcinogenic? Gastroenterology *142*, 1274–1278.

Leonardi, G.C., Candido, S., Cervello, M., Nicolosi, D., Raiti, F., Travali, S., Spandidos, D.A., and Libra, M. (2012). The tumor microenvironment in hepatocellular carcinoma (review). Int. J. Oncol. *40*, 1733–1747.

Leong, C.-O., Vidnovic, N., DeYoung, M.P., Sgroi, D., and Ellisen, L.W. (2007). The p63/p73 network mediates chemosensitivity to cisplatin in a biologically defined subset of primary breast cancers. J. Clin. Invest. *117*, 1370–1380.

Lerat, H., Honda, M., Beard, M.R., Loesch, K., Sun, J., Yang, Y., Okuda, M., Gosert, R., Xiao, S.-Y., Weinman, S.A., et al. (2002). Steatosis and liver cancer in transgenic mice expressing the structural and nonstructural proteins of hepatitis C virus. Gastroenterology *122*, 352–365.

Leung, T.H.-Y., Wong, S.C.-S., Chan, K.K.-L., Chan, D.W., Cheung, A.N.-Y., and Ngan, H.Y.-S. (2013). The interaction between C35 and ΔNp73 promotes chemo-resistance in ovarian cancer cells. Br. J. Cancer *109*, 965–975.

Levrero, M., and Zucman-Rossi, J. (2016). Mechanisms of HBV-induced hepatocellular carcinoma. J. Hepatol. *64*, S84–S101.

Levy, J.M.M., and Thorburn, A. (2011). Targeting Autophagy During Cancer Therapy to Improve Clinical Outcomes. Pharmacol. Ther. *131*, 130–141.

Levy, D., Adamovich, Y., Reuven, N., and Shaul, Y. (2007). The Yes-associated protein 1 stabilizes p73 by preventing Itch-mediated ubiquitination of p73. Cell Death Differ. *14*, 743–751.

Levy, D., Adamovich, Y., Reuven, N., and Shaul, Y. (2008). Yap1 phosphorylation by c-Abl is a critical step in selective activation of proapoptotic genes in response to DNA damage. Mol. Cell *29*, 350–361.

Li, J., Davies, B.R., Han, S., Zhou, M., Bai, Y., Zhang, J., Xu, Y., Tang, L., Wang, H., Liu, Y.J., et al. (2013). The AKT inhibitor AZD5363 is selectively active in PI3KCA mutant gastric cancer, and sensitizes a patient-derived gastric cancer xenograft model with PTEN loss to Taxotere. J. Transl. Med. *11*, 241.

Li, M., Zhao, H., Zhang, X., Wood, L.D., Anders, R.A., Choti, M.A., Pawlik, T.M., Daniel, H.D., Kannangai, R., Offerhaus, G.J.A., et al. (2011). Inactivating mutations of the chromatin remodeling gene ARID2 in hepatocellular carcinoma. Nat. Genet. *43*, 828–829.

Lin, Q., and Yun, Z. (2010). Impact of the hypoxic tumor microenvironment on the regulation of cancer stem cell characteristics. Cancer Biol. Ther. *9*, 949–956.

Lin, W., Tsai, W.-L., Shao, R.-X., Wu, G., Peng, L.F., Barlow, L.L., Chung, W.J., Zhang, L., Zhao, H., Jang, J.-Y., et al. (2010). Hepatitis C virus regulates transforming growth factor beta1 production through the generation of reactive oxygen species in a nuclear factor kappaB-dependent manner. Gastroenterology *138*, 2509–2518, 2518.e1.

Lin, Y., Cheng, Z., Yang, Z., Zheng, J., and Lin, T. (2012). DNp73 improves generation efficiency of human induced pluripotent stem cells. BMC Cell Biol. *13*, 9.

Lin, Y.-H., Huang, Y.-C., Chen, L.-H., and Chu, P.-M. (2015). Autophagy in cancer stem/progenitor cells. Cancer Chemother. Pharmacol. *75*, 879–886.

Lin, Y.-L., Sengupta, S., Gurdziel, K., Bell, G.W., Jacks, T., and Flores, E.R. (2009). p63 and p73 transcriptionally regulate genes involved in DNA repair. PLoS Genet. *5*, e1000680.

Lissy, N.A., Davis, P.K., Irwin, M., Kaelin, W.G., and Dowdy, S.F. (2000). A common E2F-1 and p73 pathway mediates cell death induced by TCR activation. Nature *407*, 642–645.

Liu, F., Liu, L., Li, B., Wei, Y.-G., Yan, L.-N., Wen, T.-F., Xu, M.-Q., Wang, W.-T., and Yang, J.-Y. (2011a). p73 G4C14-A4T14 polymorphism and cancer risk: a meta-analysis based on 27 case-control studies. Mutagenesis *26*, 573–581.

Liu, J., Wang, Z., Tang, J., Tang, R., Shan, X., Zhang, W., Chen, Q., Zhou, F., Chen, K., Huang, A., et al. (2011b). Hepatitis C virus core protein activates Wnt/β-catenin signaling through multiple regulation of upstream molecules in the SMMC-7721 cell line. Arch. Virol. *156*, 1013–1023.

Liu, J., Fan, L., Wang, H., and Sun, G. (2016a). Autophagy, a double-edged sword in anti-angiogenesis therapy. Med. Oncol. Northwood Lond. Engl. *33*, 10.

Liu, L., Liao, J.-Z., He, X.-X., and Li, P.-Y. (2017). The role of autophagy in hepatocellular carcinoma: friend or foe. Oncotarget *8*, 57707–57722.

Liu, S., Dontu, G., Mantle, I.D., Patel, S., Ahn, N., Jackson, K.W., Suri, P., and Wicha, M.S. (2006a). Hedgehog signaling and Bmi-1 regulate self-renewal of normal and malignant human mammary stem cells. Cancer Res. *66*, 6063–6071.

Liu, S.S., Leung, R.C.-Y., Chan, K.Y.-K., Chiu, P.-M., Cheung, A.N.-Y., Tam, K.-F., Ng, T.-Y., Wong, L.-C., and Ngan, H.Y.-S. (2004). p73 expression is associated with the cellular radiosensitivity in cervical cancer after radiotherapy. Clin. Cancer Res. Off. J. Am. Assoc. Cancer Res. *10*, 3309–3316.

Liu, S.S., Chan, K.Y.-K., Cheung, A.N.-Y., Liao, X.-Y., Leung, T.-W., and Ngan, H.Y.-S. (2006b). Expression of deltaNp73 and TAp73alpha independently associated with radiosensitivities and prognoses in cervical squamous cell carcinoma. Clin. Cancer Res. Off. J. Am. Assoc. Cancer Res. *12*, 3922–3927.

Liu, W.-R., Shi, Y.-H., Peng, Y.-F., and Fan, J. (2012a). Epigenetics of hepatocellular carcinoma: a new horizon. Chin. Med. J. (Engl.) *125*, 2349–2360.

Liu, Y., Chang, C.-C.H., Marsh, G.M., and Wu, F. (2012b). Population attributable risk of aflatoxin-related liver cancer: systematic review and meta-analysis. Eur. J. Cancer Oxf. Engl. 1990 *48*, 2125–2136.

Liu, Y.-L., Patman, G.L., Leathart, J.B.S., Piguet, A.-C., Burt, A.D., Dufour, J.-F., Day, C.P., Daly, A.K., Reeves, H.L., and Anstee, Q.M. (2014). Carriage of the PNPLA3 rs738409 C >G polymorphism confers an increased risk of non-alcoholic fatty liver disease associated hepatocellular carcinoma. J. Hepatol. *61*, 75–81.

Liu, Z., Wang, J., Mao, Y., Zou, B., and Fan, X. (2016b). MicroRNA-101 suppresses migration and invasion via targeting vascular endothelial growth factor-C in hepatocellular carcinoma cells. Oncol. Lett. *11*, 433–438.

Llovet, J.M. (2005). Updated treatment approach to hepatocellular carcinoma. J. Gastroenterol. *40*, 225–235.

Llovet, J.M., and Hernandez-Gea, V. (2014). Hepatocellular carcinoma: reasons for phase III failure and novel perspectives on trial design. Clin. Cancer Res. Off. J. Am. Assoc. Cancer Res. *20*, 2072–2079.

Llovet, J.M., Bustamante, J., Castells, A., Vilana, R., Ayuso, M. del C., Sala, M., Brú, C., Rodés, J., and Bruix, J. (1999a). Natural history of untreated nonsurgical hepatocellular carcinoma: rationale for the design and evaluation of therapeutic trials. Hepatol. Baltim. Md *29*, 62–67.

Llovet, J.M., Brú, C., and Bruix, J. (1999b). Prognosis of hepatocellular carcinoma: the BCLC staging classification. Semin. Liver Dis. *19*, 329–338.

Llovet, J.M., Burroughs, A., and Bruix, J. (2003). Hepatocellular carcinoma. Lancet Lond. Engl. *362*, 1907–1917.

Llovet, J.M., Ricci, S., Mazzaferro, V., Hilgard, P., Gane, E., Blanc, J.-F., de Oliveira, A.C., Santoro, A., Raoul, J.-L., Forner, A., et al. (2008). Sorafenib in advanced hepatocellular carcinoma. N. Engl. J. Med. *359*, 378–390.

Lowes, K.N., Brennan, B.A., Yeoh, G.C., and Olynyk, J.K. (1999). Oval cell numbers in human chronic liver diseases are directly related to disease severity. Am. J. Pathol. *154*, 537–541.

Lu, S.C. (2000). Regulation of glutathione synthesis. Curr. Top. Cell. Regul. *36*, 95–116.

Luangsay, S., Gruffaz, M., Isorce, N., Testoni, B., Michelet, M., Faure-Dupuy, S., Maadadi, S., Ait-Goughoulte, M., Parent, R., Rivoire, M., et al. (2015). Early inhibition of hepatocyte innate responses by hepatitis B virus. J. Hepatol. *63*, 1314–1322.

Lucena-Araujo, A.R., Kim, H.T., Thomé, C., Jacomo, R.H., Melo, R.A., Bittencourt, R., Pasquini, R., Pagnano, K., Glória, A.B.F., Chauffaille, M. de L., et al. (2015). High ΔNp73/TAp73 ratio is associated with poor prognosis in acute promyelocytic leukemia. Blood *126*, 2302–2306.

Lucifora, J., Durantel, D., Belloni, L., Barraud, L., Villet, S., Vincent, I.E., Margeridon-Thermet, S., Hantz, O., Kay, A., Levrero, M., et al. (2008). Initiation of hepatitis B virus genome replication and production of infectious virus following delivery in HepG2 cells by novel recombinant baculovirus vector. J. Gen. Virol. *89*, 1819–1828.

Lunghi, P., Costanzo, A., Levrero, M., and Bonati, A. (2004). Treatment with arsenic trioxide (ATO) and MEK1 inhibitor activates the p73-p53AIP1 apoptotic pathway in leukemia cells. Blood *104*, 519–525.

Lunghi, P., Costanzo, A., Salvatore, L., Noguera, N., Mazzera, L., Tabilio, A., Lo-Coco, F., Levrero, M., and Bonati, A. (2006). MEK1 inhibition sensitizes primary acute myelogenous leukemia to arsenic trioxide-induced apoptosis. Blood *107*, 4549–4553.

Lunghi, P., Giuliani, N., Mazzera, L., Lombardi, G., Ricca, M., Corradi, A., Cantoni, A.M., Salvatore, L., Riccioni, R., Costanzo, A., et al. (2008). Targeting MEK/MAPK signal transduction module potentiates ATO-induced apoptosis in multiple myeloma cells through multiple signaling pathways. Blood *112*, 2450–2462.

Lv, Y., Zhao, S., Han, J., Zheng, L., Yang, Z., and Zhao, L. (2015). Hypoxia-inducible factor-1α induces multidrug resistance protein in colon cancer. OncoTargets Ther. *8*, 1941–1948.

Ma, S., Chan, K.-W., Hu, L., Lee, T.K.-W., Wo, J.Y.-H., Ng, I.O.-L., Zheng, B.-J., and Guan, X.-Y. (2007). Identification and characterization of tumorigenic liver cancer stem/progenitor cells. Gastroenterology *132*, 2542–2556.

Ma, Y., Liang, D., Liu, J., Axcrona, K., Kvalheim, G., Stokke, T., Nesland, J.M., and Suo, Z. (2011). Prostate cancer cell lines under hypoxia exhibit greater stem-like properties. PloS One *6*, e29170.

Ma, Y., Galluzzi, L., Zitvogel, L., and Kroemer, G. (2013). Autophagy and Cellular Immune Responses. Immunity *39*, 211–227.

Machida, K., Cheng, K.T.-N., Sung, V.M.-H., Shimodaira, S., Lindsay, K.L., Levine, A.M., Lai, M.-Y., and Lai, M.M.C. (2004). Hepatitis C virus induces a mutator phenotype: enhanced mutations of immunoglobulin and protooncogenes. Proc. Natl. Acad. Sci. U. S. A. *101*, 4262–4267.

Maclean, K.H., Dorsey, F.C., Cleveland, J.L., and Kastan, M.B. (2008). Targeting lysosomal degradation induces p53-dependent cell death and prevents cancer in mouse models of lymphomagenesis. J. Clin. Invest. *118*, 79–88.

Maddodi, N., Huang, W., Havighurst, T., Kim, K., Longley, B.J., and Setaluri, V. (2010). Induction of autophagy and inhibition of melanoma growth in vitro and in vivo by hyperactivation of oncogenic BRAF. J. Invest. Dermatol. *130*, 1657–1667.

Magerl, C., Ellinger, J., Braunschweig, T., Kremmer, E., Koch, L.K., Höller, T., Büttner, R., Lüscher, B., and Gütgemann, I. (2010). H3K4 dimethylation in hepatocellular carcinoma is rare compared with other hepatobiliary and gastrointestinal carcinomas and correlates with expression of the methylase Ash2 and the demethylase LSD1. Hum. Pathol. *41*, 181–189.

Makowska, Z., Boldanova, T., Adametz, D., Quagliata, L., Vogt, J.E., Dill, M.T., Matter, M.S., Roth, V., Terracciano, L., and Heim, M.H. (2016). Gene expression analysis of biopsy samples reveals critical limitations of transcriptome-based molecular classifications of hepatocellular carcinoma. J. Pathol. Clin. Res. *2*, 80–92.

Makowski, M.M., Willems, E., Fang, J., Choi, J., Zhang, T., Jansen, P.W.T.C., Brown, K.M., and Vermeulen, M. (2016). An interaction proteomics survey of transcription factor binding at recurrent TERT promoter mutations. Proteomics *16*, 417–426.

Mantovani, F., Piazza, S., Gostissa, M., Strano, S., Zacchi, P., Mantovani, R., Blandino, G., and Del Sal, G. (2004). Pin1 links the activities of c-Abl and p300 in regulating p73 function. Mol. Cell *14*, 625–636.

Marabese, M., Vikhanskaya, F., and Broggini, M. (2007). p73: a chiaroscuro gene in cancer. Eur. J. Cancer Oxf. Engl. 1990 *43*, 1361–1372.

Marangoni, E., Vincent-Salomon, A., Auger, N., Degeorges, A., Assayag, F., de Cremoux, P., de Plater, L., Guyader, C., De Pinieux, G., Judde, J.-G., et al. (2007). A new model of patient tumor-derived breast cancer xenografts for preclinical assays. Clin. Cancer Res. Off. J. Am. Assoc. Cancer Res. *13*, 3989–3998.

Marqués-García, F., Ferrandiz, N., Fernández-Alonso, R., González-Cano, L., Herreros-Villanueva, M., Rosa-Garrido, M., Fernández-García, B., Vaque, J.P., Marqués, M.M., Alonso, M.E., et al. (2009). p73 plays a role in erythroid differentiation through GATA1 induction. J. Biol. Chem. *284*, 21139–21156.

Martin, P., Stewart, E., Pham, N.-A., Mascaux, C., Panchal, D., Li, M., Kim, L., Sakashita, S., Wang, D., Sykes, J., et al. (2016). Cetuximab Inhibits T790M-Mediated Resistance to Epidermal Growth Factor Receptor Tyrosine Kinase Inhibitor in a Lung Adenocarcinoma Patient-Derived Xenograft Mouse Model. Clin. Lung Cancer *17*, 375–383.e2.

Martin, S.A., Hewish, M., Lord, C.J., and Ashworth, A. (2010). Genomic instability and the selection of treatments for cancer. J. Pathol. *220*, 281–289.

Marusyk, A., Tabassum, D.P., Altrock, P.M., Almendro, V., Michor, F., and Polyak, K. (2014). Non-cell-autonomous driving of tumour growth supports sub-clonal heterogeneity. Nature *514*, 54–58.

Mathew, R., Karp, C.M., Beaudoin, B., Vuong, N., Chen, G., Chen, H.-Y., Bray, K., Reddy, A., Bhanot, G., Gelinas, C., et al. (2009). Autophagy suppresses tumorigenesis through elimination of p62. Cell *137*, 1062–1075.

Mathieu, J., Zhang, Z., Zhou, W., Wang, A.J., Heddleston, J.M., Pinna, C.M.A., Hubaud, A., Stadler, B., Choi, M., Bar, M., et al. (2011). HIF induces human embryonic stem cell markers in cancer cells. Cancer Res. *71*, 4640–4652.

Matter, M.S., Decaens, T., Andersen, J.B., and Thorgeirsson, S.S. (2014). Targeting the mTOR pathway in hepatocellular carcinoma: current state and future trends. J. Hepatol. *60*, 855–865.

McCormick, J.J., and Maher, V.M. (1988). Towards an understanding of the malignant transformation of diploid human fibroblasts. Mutat. Res. *199*, 273–291.

McGivern, D.R., and Lemon, S.M. (2011). Virus-specific mechanisms of carcinogenesis in hepatitis C virus associated liver cancer. Oncogene *30*, 1969–1983.

McGlynn, K.A., Hunter, K., LeVoyer, T., Roush, J., Wise, P., Michielli, R.A., Shen, F.-M., Evans, A.A., London, W.T., and Buetow, K.H. (2003). Susceptibility to aflatoxin B1-related primary hepatocellular carcinoma in mice and humans. Cancer Res. *63*, 4594–4601.

McGranahan, N., Burrell, R.A., Endesfelder, D., Novelli, M.R., and Swanton, C. (2012). Cancer chromosomal instability: therapeutic and diagnostic challenges. EMBO Rep. *13*, 528–538.

McKillop, I.H., and Schrum, L.W. (2005). Alcohol and liver cancer. Alcohol Fayettev. N *35*, 195–203.

Meier, C., Hardtstock, P., Joost, S., Alla, V., and Pützer, B.M. (2016). p73 and IGF1R Regulate Emergence of Aggressive Cancer Stem-like Features via miR-885-5p Control. Cancer Res. *76*, 197–205.

Melino, G., De Laurenzi, V., and Vousden, K.H. (2002). p73: Friend or foe in tumorigenesis. Nat. Rev. Cancer *2*, 605–615.

Melino, G., Bernassola, F., Ranalli, M., Yee, K., Zong, W.X., Corazzari, M., Knight, R.A., Green, D.R., Thompson, C., and Vousden, K.H. (2004). p73 Induces apoptosis via PUMA transactivation and Bax mitochondrial translocation. J. Biol. Chem. *279*, 8076–8083.

Mercer, D.F., Schiller, D.E., Elliott, J.F., Douglas, D.N., Hao, C., Rinfret, A., Addison, W.R., Fischer, K.P., Churchill, T.A., Lakey, J.R., et al. (2001). Hepatitis C virus replication in mice with chimeric human livers. Nat. Med. *7*, 927–933.

Merle, P., and Trepo, C. (2009). Molecular Mechanisms Underlying Hepatocellular Carcinoma. Viruses *1*, 852–872.

Merle, P., Kim, M., Herrmann, M., Gupte, A., Lefrançois, L., Califano, S., Trépo, C., Tanaka, S., Vitvitski, L., de la Monte, S., et al. (2005). Oncogenic role of the frizzled-7/beta-catenin pathway in hepatocellular carcinoma. J. Hepatol. *43*, 854–862.

Merlo, P., Fulco, M., Costanzo, A., Mangiacasale, R., Strano, S., Blandino, G., Taya, Y., Lavia, P., and Levrero, M. (2005). A role of p73 in mitotic exit. J. Biol. Chem. *280*, 30354–30360.

Michelhaugh, S.K., Guastella, A.R., Varadarajan, K., Klinger, N.V., Parajuli, P., Ahmad, A., Sethi, S., Aboukameel, A., Kiousis, S., Zitron, I.M., et al. (2015). Development of patient-derived xenograft models from a spontaneously immortal low-grade meningioma cell line, KCI-MENG1. J. Transl. Med. *13*, 227.

Midorikawa, Y., Ishikawa, S., Iwanari, H., Imamura, T., Sakamoto, H., Miyazono, K., Kodama, T., Makuuchi, M., and Aburatani, H. (2003). Glypican-3, overexpressed in hepatocellular carcinoma, modulates FGF2 and BMP-7 signaling. Int. J. Cancer *103*, 455–465.

Midorikawa, Y., Yamamoto, S., Tsuji, S., Kamimura, N., Ishikawa, S., Igarashi, H., Makuuchi, M., Kokudo, N., Sugimura, H., and Aburatani, H. (2009). Allelic imbalances and homozygous deletion on 8p23.2 for stepwise progression of hepatocarcinogenesis. Hepatol. Baltim. Md *49*, 513–522.

Migliardi, G., Sassi, F., Torti, D., Galimi, F., Zanella, E.R., Buscarino, M., Ribero, D., Muratore, A., Massucco, P., Pisacane, A., et al. (2012). Inhibition of MEK and PI3K/mTOR suppresses tumor growth but does not cause tumor regression in patient-derived xenografts of RAS-mutant colorectal carcinomas. Clin. Cancer Res. Off. J. Am. Assoc. Cancer Res. *18*, 2515–2525.

Mihara, M., Erster, S., Zaika, A., Petrenko, O., Chittenden, T., Pancoska, P., and Moll, U.M. (2003). p53 has a direct apoptogenic role at the mitochondria. Mol. Cell *11*, 577–590.

Mihaylova, M.M., and Shaw, R.J. (2011). The AMPK signalling pathway coordinates cell growth, autophagy and metabolism. Nat. Cell Biol. *13*, 1016–1023.

Mikhaylova, O., Stratton, Y., Hall, D., Kellner, E., Ehmer, B., Drew, A.F., Gallo, C.A., Plas, D.R., Biesiada, J., Meller, J., et al. (2012). VHL-regulated MiR-204 suppresses tumor growth through inhibition of LC3B-mediated autophagy in renal clear cell carcinoma. Cancer Cell *21*, 532–546.

Mills, A.A., Zheng, B., Wang, X.J., Vogel, H., Roop, D.R., and Bradley, A. (1999). p63 is a p53 homologue required for limb and epidermal morphogenesis. Nature *398*, 708–713.

Mínguez, B., Tovar, V., Chiang, D., Villanueva, A., and Llovet, J.M. (2009). Pathogenesis of hepatocellular carcinoma and molecular therapies. Curr. Opin. Gastroenterol. *25*, 186–194.

Mizushima, N. (2007). Autophagy: process and function. Genes Dev. *21*, 2861–2873.

Moinzadeh, P., Breuhahn, K., Stützer, H., and Schirmacher, P. (2005). Chromosome alterations in human hepatocellular carcinomas correlate with aetiology and histological grade--results of an explorative CGH meta-analysis. Br. J. Cancer *92*, 935–941.

Monzani, E., Facchetti, F., Galmozzi, E., Corsini, E., Benetti, A., Cavazzin, C., Gritti, A., Piccinini, A., Porro, D., Santinami, M., et al. (2007). Melanoma contains CD133 and ABCG2 positive cells with enhanced tumourigenic potential. Eur. J. Cancer Oxf. Engl. 1990 *43*, 935–946.

Moreira, R.K. (2007). Hepatic stellate cells and liver fibrosis. Arch. Pathol. Lab. Med. *131*, 1728–1734.

Moriya, K., Fujie, H., Shintani, Y., Yotsuyanagi, H., Tsutsumi, T., Ishibashi, K., Matsuura, Y., Kimura, S., Miyamura, T., and Koike, K. (1998). The core protein of hepatitis C virus induces hepatocellular carcinoma in transgenic mice. Nat. Med. *4*, 1065–1067.

Moriya, K., Nakagawa, K., Santa, T., Shintani, Y., Fujie, H., Miyoshi, H., Tsutsumi, T., Miyazawa, T., Ishibashi, K., Horie, T., et al. (2001). Oxidative stress in the absence of inflammation in a mouse model for hepatitis C virus-associated hepatocarcinogenesis. Cancer Res. *61*, 4365–4370.

Morselli, E., Galluzzi, L., Kepp, O., Mariño, G., Michaud, M., Vitale, I., Maiuri, M.C., and Kroemer, G. (2011). Oncosuppressive functions of autophagy. Antioxid. Redox Signal. *14*, 2251–2269.

Morton, C.L., and Houghton, P.J. (2007). Establishment of human tumor xenografts in immunodeficient mice. Nat. Protoc. *2*, 247–250.

Mueller, M.M., and Fusenig, N.E. (2004). Friends or foes - bipolar effects of the tumour stroma in cancer. Nat. Rev. Cancer *4*, 839–849.

Müller, M., Schilling, T., Sayan, A.E., Kairat, A., Lorenz, K., Schulze-Bergkamen, H., Oren, M., Koch, A., Tannapfel, A., Stremmel, W., et al. (2005). TAp73/Delta Np73 influences apoptotic response, chemosensitivity and prognosis in hepatocellular carcinoma. Cell Death Differ. *12*, 1564–1577.

Munakata, T., Nakamura, M., Liang, Y., Li, K., and Lemon, S.M. (2005). Down-regulation of the retinoblastoma tumor suppressor by the hepatitis C virus NS5B RNA-dependent RNA polymerase. Proc. Natl. Acad. Sci. U. S. A. *102*, 18159–18164.

Murakami, H., Sanderson, N.D., Nagy, P., Marino, P.A., Merlino, G., and Thorgeirsson, S.S. (1993). Transgenic mouse model for synergistic effects of nuclear oncogenes and growth factors in tumorigenesis: interaction of c-myc and transforming growth factor alpha in hepatic oncogenesis. Cancer Res. *53*, 1719–1723.

Nagasue, N., Inokuchi, K., Kobayashi, M., and Saku, M. (1977). Serum alpha-fetoprotein levels after hepatic artery ligation and postoperative chemotherapy: correlation with clinical status in patients with hepatocellular carcinoma. Cancer *40*, 615–618.

Nahor, I., Abramovitch, S., Engeland, K., and Werner, H. (2005). The p53-family members p63 and p73 inhibit insulin-like growth factor-I receptor gene expression in colon cancer cells. Growth Horm. IGF Res. Off. J. Growth Horm. Res. Soc. Int. IGF Res. Soc. *15*, 388–396.

Nakatsura, T., Yoshitake, Y., Senju, S., Monji, M., Komori, H., Motomura, Y., Hosaka, S., Beppu, T., Ishiko, T., Kamohara, H., et al. (2003). Glypican-3, overexpressed specifically in human hepatocellular carcinoma, is a novel tumor marker. Biochem. Biophys. Res. Commun. *306*, 16–25.

Nam, S.W., Park, J.Y., Ramasamy, A., Shevade, S., Islam, A., Long, P.M., Park, C.K., Park, S.E., Kim, S.Y., Lee, S.H., et al. (2005). Molecular changes from dysplastic nodule to hepatocellular carcinoma through gene expression profiling. Hepatol. Baltim. Md *42*, 809–818.

Namba, M., Mihara, K., and Fushimi, K. (1996). Immortalization of human cells and its mechanisms. Crit. Rev. Oncog. *7*, 19–31.

Nassirpour, R., Mehta, P.P., and Yin, M.-J. (2013). miR-122 regulates tumorigenesis in hepatocellular carcinoma by targeting AKT3. PloS One *8*, e79655.

Nault, J.-C., and Zucman-Rossi, J. (2014). Genetics of hepatocellular carcinoma: the next generation. J. Hepatol. *60*, 224–226.

Nault, J.C., Mallet, M., Pilati, C., Calderaro, J., Bioulac-Sage, P., Laurent, C., Laurent, A., Cherqui, D., Balabaud, C., Zucman-Rossi, J., et al. (2013). High frequency of telomerase reverse-transcriptase promoter somatic mutations in hepatocellular carcinoma and preneoplastic lesions. Nat. Commun. *4*, 2218.

Nault, J.C., Calderaro, J., Di Tommaso, L., Balabaud, C., Zafrani, E.S., Bioulac-Sage, P., Roncalli, M., and Zucman-Rossi, J. (2014). Telomerase reverse transcriptase promoter mutation is an early somatic genetic alteration in the transformation of premalignant nodules in hepatocellular carcinoma on cirrhosis. Hepatol. Baltim. Md *60*, 1983–1992.

Ng, S.-A., and Lee, C. (2011). Hepatitis B virus X gene and hepatocarcinogenesis. J. Gastroenterol. *46*, 974–990.

Ning, L., Wentworth, L., Chen, H., and Weber, S.M. (2009). Down-regulation of Notch1 signaling inhibits tumor growth in human hepatocellular carcinoma. Am. J. Transl. Res. *1*, 358–366.

Nishida, N., and Goel, A. (2011). Genetic and epigenetic signatures in human hepatocellular carcinoma: a systematic review. Curr. Genomics *12*, 130–137.

Nishida, N., and Kudo, M. (2013). Oxidative stress and epigenetic instability in human hepatocarcinogenesis. Dig. Dis. Basel Switz. *31*, 447–453.

Nishida, N., Kudo, M., Nishimura, T., Arizumi, T., Takita, M., Kitai, S., Yada, N., Hagiwara, S., Inoue, T., Minami, Y., et al. (2013a). Unique association between global DNA hypomethylation and chromosomal alterations in human hepatocellular carcinoma. PloS One *8*, e72312.

Nishida, N., Arizumi, T., Takita, M., Kitai, S., Yada, N., Hagiwara, S., Inoue, T., Minami, Y., Ueshima, K., Sakurai, T., et al. (2013b). Reactive oxygen species induce epigenetic instability through the formation of 8-hydroxydeoxyguanosine in human hepatocarcinogenesis. Dig. Dis. Basel Switz. *31*, 459–466.

Nomura-Takigawa, Y., Nagano-Fujii, M., Deng, L., Kitazawa, S., Ishido, S., Sada, K., and Hotta, H. (2006). Non-structural protein 4A of Hepatitis C virus accumulates on mitochondria and renders the cells prone to undergoing mitochondria-mediated apoptosis. J. Gen. Virol. *87*, 1935–1945.

Noureddin, M., Mato, J.M., and Lu, S.C. (2015). Nonalcoholic fatty liver disease: update on pathogenesis, diagnosis, treatment and the role of S-adenosylmethionine. Exp. Biol. Med. Maywood NJ *240*, 809–820.

Nowell, P.C. (1976). The clonal evolution of tumor cell populations. Science *194*, 23–28.

O'Brien, C.A., Pollett, A., Gallinger, S., and Dick, J.E. (2007). A human colon cancer cell capable of initiating tumour growth in immunodeficient mice. Nature *445*, 106–110.

Ochiya, T., Tsurimoto, T., Ueda, K., Okubo, K., Shiozawa, M., and Matsubara, K. (1989). An in vitro system for infection with hepatitis B virus that uses primary human fetal hepatocytes. Proc. Natl. Acad. Sci. U. S. A. *86*, 1875–1879.

Oda, K., Uto, H., Mawatari, S., and Ido, A. (2015). Clinical features of hepatocellular carcinoma associated with nonalcoholic fatty liver disease: a review of human studies. Clin. J. Gastroenterol. *8*, 1–9.

Oishi, N., and Wang, X.W. (2011). Novel therapeutic strategies for targeting liver cancer stem cells. Int. J. Biol. Sci. *7*, 517–535.

Okabe, H., Satoh, S., Kato, T., Kitahara, O., Yanagawa, R., Yamaoka, Y., Tsunoda, T., Furukawa, Y., and Nakamura, Y. (2001). Genome-wide analysis of gene expression in human hepatocellular carcinomas using cDNA microarray: identification of genes involved in viral carcinogenesis and tumor progression. Cancer Res. *61*, 2129–2137.

Okuda, M., Li, K., Beard, M.R., Showalter, L.A., Scholle, F., Lemon, S.M., and Weinman, S.A. (2002). Mitochondrial injury, oxidative stress, and antioxidant gene expression are induced by hepatitis C virus core protein. Gastroenterology *122*, 366–375.

Okuno, T., Ueda, M., Tsuruyama, T., Haga, H., Takada, Y., Maetani, Y., Tamaki, K., Manabe, T., Tanaka, K., and Uemoto, S. (2009). Loss of heterozygosity on 10q23 is involved in metastatic recurrence of hepatocellular carcinoma. Cancer Sci. *100*, 520–528.

Orito, E., and Mizokami, M. (2003). Hepatitis B virus genotypes and hepatocellular carcinoma in Japan. Intervirology *46*, 408–412.

Ozaki, T., and Nakagawara, A. (2005). p73, a sophisticated p53 family member in the cancer world. Cancer Sci. *96*, 729–737.

Ozaki, T., Hosoda, M., Miyazaki, K., Hayashi, S., Watanabe, K.-I., Nakagawa, T., and Nakagawara, A. (2005). Functional implication of p73 protein stability in neuronal cell survival and death. Cancer Lett. *228*, 29–35.

Pang, T.C., and Lam, V.W. (2015). Surgical management of hepatocellular carcinoma. World J. Hepatol. *7*, 245–252.

Parent, R., Marion, M.-J., Furio, L., Trépo, C., and Petit, M.-A. (2004). Origin and characterization of a human bipotent liver progenitor cell line. Gastroenterology *126*, 1147–1156.

Park, I.Y., Sohn, B.H., Yu, E., Suh, D.J., Chung, Y.-H., Lee, J.-H., Surzycki, S.J., and Lee, Y.I. (2007). Aberrant epigenetic modifications in hepatocarcinogenesis induced by hepatitis B virus X protein. Gastroenterology *132*, 1476–1494.

Parrales, A., and Iwakuma, T. (2015). Targeting Oncogenic Mutant p53 for Cancer Therapy. Front. Oncol. *5*, 288.

Peng, S.-Y., Chen, W.J., Lai, P.-L., Jeng, Y.-M., Sheu, J.-C., and Hsu, H.-C. (2004). High alpha-fetoprotein level correlates with high stage, early recurrence and poor prognosis of hepatocellular carcinoma: significance of hepatitis virus infection, age, p53 and beta-catenin mutations. Int. J. Cancer *112*, 44–50.

Peng, X.-H., Karna, P., Cao, Z., Jiang, B.-H., Zhou, M., and Yang, L. (2006). Cross-talk between epidermal growth factor receptor and hypoxia-inducible factor-1alpha signal pathways increases resistance to apoptosis by up-regulating survivin gene expression. J. Biol. Chem. *281*, 25903–25914.

Peraino, C., Staffeldt, E.F., Carnes, B.A., Ludeman, V.A., Blomquist, J.A., and Vesselinovitch, S.D. (1984). Characterization of histochemically detectable altered hepatocyte foci and their relationship to hepatic tumorigenesis in rats treated once with diethylnitrosamine or benzo(a)pyrene within one day after birth. Cancer Res. *44*, 3340–3347.

Petherick, K.J., Williams, A.C., Lane, J.D., Ordóñez-Morán, P., Huelsken, J., Collard, T.J., Smartt, H.J.M., Batson, J., Malik, K., Paraskeva, C., et al. (2013). Autolysosomal β-catenin degradation regulates Wnt-autophagy-p62 crosstalk. EMBO J. *32*, 1903–1916.

Petrenko, O., Zaika, A., and Moll, U.M. (2003). deltaNp73 facilitates cell immortalization and cooperates with oncogenic Ras in cellular transformation in vivo. Mol. Cell. Biol. *23*, 5540–5555.

Pez, F., Lopez, A., Kim, M., Wands, J.R., Caron de Fromentel, C., and Merle, P. (2013). Wnt signaling and hepatocarcinogenesis: molecular targets for the development of innovative anticancer drugs. J. Hepatol. *59*, 1107–1117.

Pezzuto, F., Izzo, F., Buonaguro, L., Annunziata, C., Tatangelo, F., Botti, G., Buonaguro, F.M., and Tornesello, M.L. (2016). Tumor specific mutations in TERT promoter and CTNNB1 gene in hepatitis B and hepatitis C related hepatocellular carcinoma. Oncotarget *7*, 54253–54262.

Phadwal, K., Watson, A.S., and Simon, A.K. (2013). Tightrope act: autophagy in stem cell renewal, differentiation, proliferation, and aging. Cell. Mol. Life Sci. CMLS *70*, 89–103.

Piccinin, S., Tonin, E., Sessa, S., Demontis, S., Rossi, S., Pecciarini, L., Zanatta, L., Pivetta, F., Grizzo, A., Sonego, M., et al. (2012). A “twist box” code of p53 inactivation: twist box: p53 interaction promotes p53 degradation. Cancer Cell *22*, 404–415.

Pietsch, E.C., Sykes, S.M., McMahon, S.B., and Murphy, M.E. (2008). The p53 family and programmed cell death. Oncogene *27*, 6507–6521.

Pinkel, D., and Albertson, D.G. (2005). Array comparative genomic hybridization and its applications in cancer. Nat. Genet. *37 Suppl*, S11-17.

Pozniak, C.D., Radinovic, S., Yang, A., McKeon, F., Kaplan, D.R., and Miller, F.D. (2000). An anti-apoptotic role for the p53 family member, p73, during developmental neuron death. Science *289*, 304–306.

Prabhu, V.V., Hong, B., Allen, J.E., Zhang, S., Lulla, A.R., Dicker, D.T., and El-Deiry, W.S. (2016). Small-Molecule Prodigiosin Restores p53 Tumor Suppressor Activity in Chemoresistant Colorectal Cancer Stem Cells via c-Jun-Mediated ΔNp73 Inhibition and p73 Activation. Cancer Res. *76*, 1989–1999.

Prahallad, A., Sun, C., Huang, S., Di Nicolantonio, F., Salazar, R., Zecchin, D., Beijersbergen, R.L., Bardelli, A., and Bernards, R. (2012). Unresponsiveness of colon cancer to BRAF(V600E) inhibition through feedback activation of EGFR. Nature *483*, 100–103.

Puisieux, A., Lim, S., Groopman, J., and Ozturk, M. (1991). Selective targeting of p53 gene mutational hotspots in human cancers by etiologically defined carcinogens. Cancer Res. *51*, 6185–6189.

Pützer, B.M., Tuve, S., Tannapfel, A., and Stiewe, T. (2003). Increased DeltaN-p73 expression in tumors by upregulation of the E2F1-regulated, TA-promoter-derived DeltaN'-p73 transcript. Cell Death Differ. *10*, 612–614.

Qadri, I., Iwahashi, M., Capasso, J.M., Hopken, M.W., Flores, S., Schaack, J., and Simon, F.R. (2004). Induced oxidative stress and activated expression of manganese superoxide dismutase during hepatitis C virus replication: role of JNK, p38 MAPK and AP-1. Biochem. J. *378*, 919–928.

Qiang, L., Wu, T., Zhang, H.-W., Lu, N., Hu, R., Wang, Y.-J., Zhao, L., Chen, F.-H., Wang, X.-T., You, Q.-D., et al. (2012). HIF-1α is critical for hypoxia-mediated maintenance of glioblastoma stem cells by activating Notch signaling pathway. Cell Death Differ. *19*, 284–294.

Qiu, D.-M., Wang, G.-L., Chen, L., Xu, Y.-Y., He, S., Cao, X.-L., Qin, J., Zhou, J.-M., Zhang, Y.-X., and E, Q. (2014). The expression of beclin-1, an autophagic gene, in hepatocellular carcinoma associated with clinical pathological and prognostic significance. BMC Cancer *14*, 327.

Qu, X., Yu, J., Bhagat, G., Furuya, N., Hibshoosh, H., Troxel, A., Rosen, J., Eskelinen, E.-L., Mizushima, N., Ohsumi, Y., et al. (2003). Promotion of tumorigenesis by heterozygous disruption of the beclin 1 autophagy gene. J. Clin. Invest. *112*, 1809–1820.

Quaas, A., Oldopp, T., Tharun, L., Klingenfeld, C., Krech, T., Sauter, G., and Grob, T.J. (2014). Frequency of TERT promoter mutations in primary tumors of the liver. Virchows Arch. Int. J. Pathol. *465*, 673–677.

Racek, T., Mise, N., Li, Z., Stoll, A., and Pützer, B.M. (2005). C-terminal p73 isoforms repress transcriptional activity of the human telomerase reverse transcriptase (hTERT) promoter. J. Biol. Chem. *280*, 40402–40405.

Raimondi, S., Bruno, S., Mondelli, M.U., and Maisonneuve, P. (2009). Hepatitis C virus genotype 1b as a risk factor for hepatocellular carcinoma development: a meta-analysis. J. Hepatol. *50*, 1142–1154.

Raimondo, G., Burk, R.D., Lieberman, H.M., Muschel, J., Hadziyannis, S.J., Will, H., Kew, M.C., Dusheiko, G.M., and Shafritz, D.A. (1988). Interrupted replication of hepatitis B virus in liver tissue of HBsAg carriers with hepatocellular carcinoma. Virology *166*, 103–112.

Ramboer, E., De Craene, B., De Kock, J., Vanhaecke, T., Berx, G., Rogiers, V., and Vinken, M. (2014). Strategies for immortalization of primary hepatocytes. J. Hepatol. *61*, 925–943.

Ramesh, H. (2014). Resection for hepatocellular carcinoma. J. Clin. Exp. Hepatol. *4*, S90-96.

Rao, R., Balusu, R., Fiskus, W., Mudunuru, U., Venkannagari, S., Chauhan, L., Smith, J.E., Hembruff, S.L., Ha, K., Atadja, P., et al. (2012). Combination of pan-histone deacetylase inhibitor and autophagy inhibitor exerts superior efficacy against triple-negative human breast cancer cells. Mol. Cancer Ther. *11*, 973–983.

Rausch, V., Liu, L., Apel, A., Rettig, T., Gladkich, J., Labsch, S., Kallifatidis, G., Kaczorowski, A., Groth, A., Gross, W., et al. (2012). Autophagy mediates survival of pancreatic tumour-initiating cells in a hypoxic microenvironment. J. Pathol. *227*, 325–335.

Recknagel, R.O. (1967). Carbon tetrachloride hepatotoxicity. Pharmacol. Rev. *19*, 145–208.

Rehermann, B., and Nascimbeni, M. (2005). Immunology of hepatitis B virus and hepatitis C virus infection. Nat. Rev. Immunol. *5*, 215–229.

Reiberger, T., Chen, Y., Ramjiawan, R.R., Hato, T., Fan, C., Samuel, R., Roberge, S., Huang, P., Lauwers, G.Y., Zhu, A.X., et al. (2015). An orthotopic mouse model of hepatocellular carcinoma with underlying liver cirrhosis. Nat. Protoc. *10*, 1264–1274.

Reid, Y., Gaddipati, J.P., Yadav, D., and Kantor, J. (2009). Establishment of a human neonatal hepatocyte cell line. In Vitro Cell. Dev. Biol. Anim. *45*, 535–542.

Reya, T., Morrison, S.J., Clarke, M.F., and Weissman, I.L. (2001). Stem cells, cancer, and cancer stem cells. Nature *414*, 105–111.

Roayaie, S., Blume, I.N., Thung, S.N., Guido, M., Fiel, M.-I., Hiotis, S., Labow, D.M., Llovet, J.M., and Schwartz, M.E. (2009). A system of classifying microvascular invasion to predict outcome after resection in patients with hepatocellular carcinoma. Gastroenterology *137*, 850–855.

Rocco, J.W., Leong, C.-O., Kuperwasser, N., DeYoung, M.P., and Ellisen, L.W. (2006). p63 mediates survival in squamous cell carcinoma by suppression of p73-dependent apoptosis. Cancer Cell *9*, 45–56.

Rodriguez, O.C., Choudhury, S., Kolukula, V., Vietsch, E.E., Catania, J., Preet, A., Reynoso, K., Bargonetti, J., Wellstein, A., Albanese, C., et al. (2012). Dietary downregulation of mutant p53 levels via glucose restriction: mechanisms and implications for tumor therapy. Cell Cycle Georget. Tex *11*, 4436–4446.

Roessler, S., Long, E.L., Budhu, A., Chen, Y., Zhao, X., Ji, J., Walker, R., Jia, H.-L., Ye, Q.-H., Qin, L.-X., et al. (2012). Integrative genomic identification of genes on 8p associated with

hepatocellular carcinoma progression and patient survival. Gastroenterology *142*, 957–966.e12.

Roskams, T. (2006). Liver stem cells and their implication in hepatocellular and cholangiocarcinoma. Oncogene *25*, 3818–3822.

Roskams, T., and Desmet, V. (1998). Ductular reaction and its diagnostic significance. Semin. Diagn. Pathol. *15*, 259–269.

Rossi, M., De Laurenzi, V., Munarriz, E., Green, D.R., Liu, Y.-C., Vousden, K.H., Cesareni, G., and Melino, G. (2005). The ubiquitin-protein ligase Itch regulates p73 stability. EMBO J. *24*, 836–848.

Rothe, K., Lin, H., Lin, K.B.L., Leung, A., Wang, H.M., Malekesmaeili, M., Brinkman, R.R., Forrest, D.L., Gorski, S.M., and Jiang, X. (2014). The core autophagy protein ATG4B is a potential biomarker and therapeutic target in CML stem/progenitor cells. Blood *123*, 3622–3634.

Rozman, D. (2014). From nonalcoholic Fatty liver disease to hepatocellular carcinoma: a systems understanding. Dig. Dis. Sci. *59*, 238–241.

Rubio-Viqueira, B., Jimeno, A., Cusatis, G., Zhang, X., Iacobuzio-Donahue, C., Karikari, C., Shi, C., Danenberg, K., Danenberg, P.V., Kuramochi, H., et al. (2006). An in vivo platform for translational drug development in pancreatic cancer. Clin. Cancer Res. Off. J. Am. Assoc. Cancer Res. *12*, 4652–4661.

Rufini, A., Agostini, M., Grespi, F., Tomasini, R., Sayan, B.S., Niklison-Chirou, M.V., Conforti, F., Velletri, T., Mastino, A., Mak, T.W., et al. (2011). p73 in Cancer. Genes Cancer *2*, 491–502.

Rufini, A., Niklison-Chirou, M.V., Inoue, S., Tomasini, R., Harris, I.S., Marino, A., Federici, M., Dinsdale, D., Knight, R.A., Melino, G., et al. (2012). TAp73 depletion accelerates aging through metabolic dysregulation. Genes Dev. *26*, 2009–2014.

Saifudeen, Z., Diavolitsis, V., Stefkova, J., Dipp, S., Fan, H., and El-Dahr, S.S. (2005). Spatiotemporal Switch from ΔNp73 to TAp73 Isoforms during Nephrogenesis IMPACT ON DIFFERENTIATION GENE EXPRESSION. J. Biol. Chem. *280*, 23094–23102.

Santoni-Rugiu, E., Nagy, P., Jensen, M.R., Factor, V.M., and Thorgeirsson, S.S. (1996). Evolution of neoplastic development in the liver of transgenic mice co-expressing c-myc and transforming growth factor-alpha. Am. J. Pathol. *149*, 407–428.

Sasaki, Y., Naishiro, Y., Oshima, Y., Imai, K., Nakamura, Y., and Tokino, T. (2005). Identification of pigment epithelium-derived factor as a direct target of the p53 family member genes. Oncogene *24*, 5131–5136.

Sayan, A.E., Sayan, B.S., Findikli, N., and Ozturk, M. (2001). Acquired expression of transcriptionally active p73 in hepatocellular carcinoma cells. Oncogene *20*, 5111–5117.

Sayan, A.E., Sayan, B.S., Gogvadze, V., Dinsdale, D., Nyman, U., Hansen, T.M., Zhivotovsky, B., Cohen, G.M., Knight, R.A., and Melino, G. (2008). P73 and caspase-cleaved p73 fragments localize to mitochondria and augment TRAIL-induced apoptosis. Oncogene *27*, 4363–4372.

Scherer, E., Hoffmann, M., Emmelot, P., and Friedrich-Freksa, M. (1972). Quantitative study on foci of altered liver cells induced in the rat by a single dose of diethylnitrosamine and partial hepatectomy. J. Natl. Cancer Inst. *49*, 93–106.

Schippers, I.J., Moshage, H., Roelofsen, H., Müller, M., Heymans, H.S., Ruiters, M., and Kuipers, F. (1997). Immortalized human hepatocytes as a tool for the study of hepatocytic (de-)differentiation. Cell Biol. Toxicol. *13*, 375–386.

Schlageter, M., Terracciano, L.M., D'Angelo, S., and Sorrentino, P. (2014). Histopathology of hepatocellular carcinoma. World J. Gastroenterol. *20*, 15955–15964.

Schmale, H., and Bamberger, C. (1997). A novel protein with strong homology to the tumor suppressor p53. Oncogene *15*, 1363–1367.

Schulze, K., Imbeaud, S., Letouzé, E., Alexandrov, L.B., Calderaro, J., Rebouissou, S., Couchy, G., Meiller, C., Shinde, J., Soysouvanh, F., et al. (2015). Exome sequencing of hepatocellular carcinomas identifies new mutational signatures and potential therapeutic targets. Nat. Genet. *47*, 505–511.

Schuster, A., Schilling, T., De Laurenzi, V., Koch, A.F., Seitz, S., Staib, F., Teufel, A., Thorgeirsson, S.S., Galle, P., Melino, G., et al. (2010). ΔNp73β is oncogenic in hepatocellular carcinoma by blocking apoptosis signaling via death receptors and mitochondria. Cell Cycle Georget. Tex *9*, 2629–2639.

Schwartz, M., Roayaie, S., and Konstadoulakis, M. (2007). Strategies for the management of hepatocellular carcinoma. Nat. Clin. Pract. Oncol. *4*, 424–432.

Shafman, T., Khanna, K.K., Kedar, P., Spring, K., Kozlov, S., Yen, T., Hobson, K., Gatei, M., Zhang, N., Watters, D., et al. (1997). Interaction between ATM protein and c-Abl in response to DNA damage. Nature *387*, 520–523.

Shimizu, S., Takehara, T., Hikita, H., Kodama, T., Tsunematsu, H., Miyagi, T., Hosui, A., Ishida, H., Tatsumi, T., Kanto, T., et al. (2012). Inhibition of autophagy potentiates the antitumor effect of the multikinase inhibitor sorafenib in hepatocellular carcinoma. Int. J. Cancer *131*, 548–557.

Shin, J.W., and Chung, Y.-H. (2013). Molecular targeted therapy for hepatocellular carcinoma: current and future. World J. Gastroenterol. *19*, 6144–6155.

Shlomai, A., de Jong, Y.P., and Rice, C.M. (2014). Virus associated malignancies: the role of viral hepatitis in hepatocellular carcinoma. Semin. Cancer Biol. *26*, 78–88.

Shon, J.K., Shon, B.H., Park, I.Y., Lee, S.U., Fa, L., Chang, K.Y., Shin, J.H., and Lee, Y.I. (2009). Hepatitis B virus-X protein recruits histone deacetylase 1 to repress insulin-like growth factor binding protein 3 transcription. Virus Res. *139*, 14–21.

Shultz, L.D., Lyons, B.L., Burzenski, L.M., Gott, B., Chen, X., Chaleff, S., Kotb, M., Gillies, S.D., King, M., Mangada, J., et al. (2005). Human lymphoid and myeloid cell development in NOD/LtSz-scid IL2R gamma null mice engrafted with mobilized human hemopoietic stem cells. J. Immunol. Baltim. Md 1950 *174*, 6477–6489.

Sicklick, J.K., Li, Y.-X., Jayaraman, A., Kannangai, R., Qi, Y., Vivekanandan, P., Ludlow, J.W., Owzar, K., Chen, W., Torbenson, M.S., et al. (2006). Dysregulation of the Hedgehog pathway in human hepatocarcinogenesis. Carcinogenesis *27*, 748–757.

Simões-Wüst, A.P., Sigrist, B., Belyanskaya, L., Hopkins Donaldson, S., Stahel, R.A., and Zangemeister-Wittke, U. (2005). DeltaNp73 antisense activates PUMA and induces apoptosis in neuroblastoma cells. J. Neurooncol. *72*, 29–34.

Singal, A., Volk, M.L., Waljee, A., Salgia, R., Higgins, P., Rogers, M. a. M., and Marrero, J.A. (2009). Meta-analysis: surveillance with ultrasound for early-stage hepatocellular carcinoma in patients with cirrhosis. Aliment. Pharmacol. Ther. *30*, 37–47.

Singh, S.K., Hawkins, C., Clarke, I.D., Squire, J.A., Bayani, J., Hide, T., Henkelman, R.M., Cusimano, M.D., and Dirks, P.B. (2004). Identification of human brain tumour initiating cells. Nature *432*, 396–401.

Siolas, D., and Hannon, G.J. (2013). Patient-derived tumor xenografts: transforming clinical samples into mouse models. Cancer Res. *73*, 5315–5319.

Siu, I.-M., Ruzevick, J., Zhao, Q., Connis, N., Jiao, Y., Bettegowda, C., Xia, X., Burger, P.C., Hann, C.L., and Gallia, G.L. (2013). Erlotinib inhibits growth of a patient-derived chordoma xenograft. PloS One *8*, e78895.

Sivanand, S., Peña-Llopis, S., Zhao, H., Kucejova, B., Spence, P., Pavia-Jimenez, A., Yamasaki, T., McBride, D.J., Gillen, J., Wolff, N.C., et al. (2012). A validated tumorgraft model reveals activity of dovitinib against renal cell carcinoma. Sci. Transl. Med. *4*, 137ra75.

Smedile, A., and Bugianesi, E. (2005). Steatosis and hepatocellular carcinoma risk. Eur. Rev. Med. Pharmacol. Sci. *9*, 291–293.

Smela, M.E., Currier, S.S., Bailey, E.A., and Essigmann, J.M. (2001). The chemistry and biology of aflatoxin B(1): from mutational spectrometry to carcinogenesis. Carcinogenesis *22*, 535–545.

Sobesky, R., Feray, C., Rimlinger, F., Derian, N., Dos Santos, A., Roque-Afonso, A.-M., Samuel, D., Bréchot, C., and Thiers, V. (2007). Distinct hepatitis C virus core and F protein quasispecies in tumoral and nontumoral hepatocytes isolated via microdissection. Hepatol. Baltim. Md *46*, 1704–1712.

Song, J., Qu, Z., Guo, X., Zhao, Q., Zhao, X., Gao, L., Sun, K., Shen, F., Wu, M., and Wei, L. (2009). Hypoxia-induced autophagy contributes to the chemoresistance of hepatocellular carcinoma cells. Autophagy *5*, 1131–1144.

Song, Y.-J., Zhang, S.-S., Guo, X.-L., Sun, K., Han, Z.-P., Li, R., Zhao, Q.-D., Deng, W.-J., Xie, X.-Q., Zhang, J.-W., et al. (2013). Autophagy contributes to the survival of CD133+ liver cancer stem cells in the hypoxic and nutrient-deprived tumor microenvironment. Cancer Lett. *339*, 70–81.

Steder, M., Alla, V., Meier, C., Spitschak, A., Pahnke, J., Fürst, K., Kowtharapu, B.S., Engelmann, D., Petigk, J., Egberts, F., et al. (2013). DNp73 exerts function in metastasis initiation by disconnecting the inhibitory role of EPLIN on IGF1R-AKT/STAT3 signaling. Cancer Cell *24*, 512–527.

Stéphenne, X., Najimi, M., and Sokal, E.M. (2010). Hepatocyte cryopreservation: Is it time to change the strategy? World J. Gastroenterol. WJG *16*, 1–14.

Stephens, P.J., Greenman, C.D., Fu, B., Yang, F., Bignell, G.R., Mudie, L.J., Pleasance, E.D., Lau, K.W., Beare, D., Stebbings, L.A., et al. (2011). Massive genomic rearrangement acquired in a single catastrophic event during cancer development. Cell *144*, 27–40.

Stickel, F., Schuppan, D., Hahn, E.G., and Seitz, H.K. (2002). Cocarcinogenic effects of alcohol in hepatocarcinogenesis. Gut *51*, 132–139.

Stiewe, T., and Pützer, B.M. (2000). Role of the p53-homologue p73 in E2F1-induced apoptosis. Nat. Genet. *26*, 464–469.

Stiewe, T., Theseling, C.C., and Pützer, B.M. (2002). Transactivation-deficient Delta TA-p73 inhibits p53 by direct competition for DNA binding: implications for tumorigenesis. J. Biol. Chem. *277*, 14177–14185.

Stiewe, T., Stanelle, J., Theseling, C.C., Pollmeier, B., Beitzinger, M., and Pützer, B.M. (2003). Inactivation of retinoblastoma (RB) tumor suppressor by oncogenic isoforms of the p53 family member p73. J. Biol. Chem. *278*, 14230–14236.

Stiewe, T., Tuve, S., Peter, M., Tannapfel, A., Elmaagacli, A.H., and Pützer, B.M. (2004). Quantitative TP73 transcript analysis in hepatocellular carcinomas. Clin. Cancer Res. Off. J. Am. Assoc. Cancer Res. *10*, 626–633.

Strano, S., Monti, O., Pediconi, N., Baccarini, A., Fontemaggi, G., Lapi, E., Mantovani, F., Damalas, A., Citro, G., Sacchi, A., et al. (2005). The transcriptional coactivator Yes-associated protein drives p73 gene-target specificity in response to DNA Damage. Mol. Cell *18*, 447–459.

Strickler, H.D., Rosenberg, P.S., Devesa, S.S., Hertel, J., Fraumeni, J.F., and Goedert, J.J. (1998). Contamination of poliovirus vaccines with simian virus 40 (1955-1963) and subsequent cancer rates. JAMA *279*, 292–295.

Sumida, Y., Nakashima, T., Yoh, T., Nakajima, Y., Ishikawa, H., Mitsuyoshi, H., Sakamoto, Y., Okanoue, T., Kashima, K., Nakamura, H., et al. (2000). Serum thioredoxin levels as an indicator of oxidative stress in patients with hepatitis C virus infection. J. Hepatol. *33*, 616–622.

Sun, K., Guo, X.-L., Zhao, Q.–., Jing, Y.–., Kou, X.–., Xie, X.–., Zhou, Y., Cai, N., Gao, L., Zhao, X., et al. (2013). Paradoxical role of autophagy in the dysplastic and tumor-forming stages of hepatocarcinoma development in rats. Cell Death Dis. *4*, e501.

Sung, W.-K., Zheng, H., Li, S., Chen, R., Liu, X., Li, Y., Lee, N.P., Lee, W.H., Ariyaratne, P.N., Tennakoon, C., et al. (2012). Genome-wide survey of recurrent HBV integration in hepatocellular carcinoma. Nat. Genet. *44*, 765–769.

Szmuness, W. (1978). Hepatocellular carcinoma and the hepatitis B virus: evidence for a causal association. Prog. Med. Virol. Fortschritte Med. Virusforsch. Progres En Virol. Medicale *24*, 40–69.

Takahashi, Y., Hori, T., Cooper, T.K., Liao, J., Desai, N., Serfass, J.M., Young, M.M., Park, S., Izu, Y., and Wang, H.-G. (2013). Bif-1 haploinsufficiency promotes chromosomal instability and accelerates Myc-driven lymphomagenesis via suppression of mitophagy. Blood *121*, 1622–1632.

Takai, A., Dang, H.T., and Wang, X.W. (2014). Identification of drivers from cancer genome diversity in hepatocellular carcinoma. Int. J. Mol. Sci. *15*, 11142–11160.

Takayama, H., Sato, T., Ikeda, F., and Fujiki, S. (2016). Reactivation of hepatitis B virus during interferon-free therapy with daclatasvir and asunaprevir in patient with hepatitis B virus/hepatitis C virus co-infection. Hepatol. Res. Off. J. Jpn. Soc. Hepatol. *46*, 489–491.

Takigawa, Y., and Brown, A.M.C. (2008). Wnt signaling in liver cancer. Curr. Drug Targets *9*, 1013–1024.

Talos, F., Nemajerova, A., Flores, E.R., Petrenko, O., and Moll, U.M. (2007). p73 suppresses polyploidy and aneuploidy in the absence of functional p53. Mol. Cell *27*, 647–659.

Tan, P.S., Nakagawa, S., Goossens, N., Venkatesh, A., Huang, T., Ward, S.C., Sun, X., Song, W.-M., Koh, A., Canasto-Chibuque, C., et al. (2016). Clinicopathological indices to predict hepatocellular carcinoma molecular classification. Liver Int. Off. J. Int. Assoc. Study Liver *36*, 108–118.

Tang, J.-C., Feng, Y.-L., Guo, T., Xie, A.-Y., and Cai, X.-J. (2016). Circulating tumor DNA in hepatocellular carcinoma: trends and challenges. Cell Biosci. *6*.

Tangkijvanich, P., Anukulkarnkusol, N., Suwangool, P., Lertmaharit, S., Hanvivatvong, O., Kullavanijaya, P., and Poovorawan, Y. (2000). Clinical characteristics and prognosis of hepatocellular carcinoma: analysis based on serum alpha-fetoprotein levels. J. Clin. Gastroenterol. *31*, 302–308.

Tannapfel, A., Wasner, M., Krause, K., Geissler, F., Katalinic, A., Hauss, J., Mössner, J., Engeland, K., and Wittekind, C. (1999). Expression of p73 and its relation to histopathology and prognosis in hepatocellular carcinoma. J. Natl. Cancer Inst. *91*, 1154–1158.

Tannapfel, A., John, K., Mise, N., Schmidt, A., Buhlmann, S., Ibrahim, S.M., and Pützer, B.M. (2008). Autonomous growth and hepatocarcinogenesis in transgenic mice expressing the p53 family inhibitor DNp73. Carcinogenesis *29*, 211–218.

Tao, Y., Ruan, J., Yeh, S.-H., Lu, X., Wang, Y., Zhai, W., Cai, J., Ling, S., Gong, Q., Chong, Z., et al. (2011). Rapid growth of a hepatocellular carcinoma and the driving mutations revealed by cell-population genetic analysis of whole-genome data. Proc. Natl. Acad. Sci. U. S. A. *108*, 12042–12047.

Tarin, D., and Croft, C.B. (1969). Ultrastructural features of wound healing in mouse skin. J. Anat. *105*, 189–190.

Tentler, J.J., Tan, A.C., Weekes, C.D., Jimeno, A., Leong, S., Pitts, T.M., Arcaroli, J.J., Messersmith, W.A., and Eckhardt, S.G. (2012). Patient-derived tumour xenografts as models for oncology drug development. Nat. Rev. Clin. Oncol. *9*, 338–350.

Terrinoni, A., Ranalli, M., Cadot, B., Leta, A., Bagetta, G., Vousden, K.H., and Melino, G. (2004). p73-alpha is capable of inducing scotin and ER stress. Oncogene *23*, 3721–3725.

Terzi, E., Salvatore, V., Negrini, G., and Piscaglia, F. (2016). Ongoing challenges in the diagnosis of hepatocellular carcinoma. Expert Rev. Gastroenterol. Hepatol. *10*, 451–463.

Thiery, J.P., Acloque, H., Huang, R.Y.J., and Nieto, M.A. (2009). Epithelial-mesenchymal transitions in development and disease. Cell *139*, 871–890.

Thorgeirsson, S.S., and Grisham, J.W. (2002). Molecular pathogenesis of human hepatocellular carcinoma. Nat. Genet. *31*, 339–346.

Tian, Y., Kuo, C.-F., Sir, D., Wang, L., Govindarajan, S., Petrovic, L.M., and Ou, J.-H.J. (2015). Autophagy inhibits oxidative stress and tumor suppressors to exert its dual effect on hepatocarcinogenesis. Cell Death Differ. *22*, 1025–1034.

Togni, R., Bagla, N., Muiesan, P., Miquel, R., O'Grady, J., Heaton, N., Knisely, A.S., Portmann, B., and Quaglia, A. (2009). Microsatellite instability in hepatocellular carcinoma in non-cirrhotic liver in patients older than 60 years. Hepatol. Res. Off. J. Jpn. Soc. Hepatol. *39*, 266–273.

Toh, W.H., Nam, S.Y., and Sabapathy, K. (2010). An essential role for p73 in regulating mitotic cell death. Cell Death Differ. *17*, 787–800.

Tomasetti, C., and Vogelstein, B. (2015). Cancer risk: role of environment—response. Science *347*, 729–731.

Tomasini, R., Tsuchihara, K., Wilhelm, M., Fujitani, M., Rufini, A., Cheung, C.C., Khan, F., Itie-Youten, A., Wakeham, A., Tsao, M.-S., et al. (2008). TAp73 knockout shows genomic instability with infertility and tumor suppressor functions. Genes Dev. *22*, 2677–2691.

Tomasini, R., Tsuchihara, K., Tsuda, C., Lau, S.K., Wilhelm, M., Ruffini, A., Tsao, M., Iovanna, J.L., Jurisicova, A., Melino, G., et al. (2009). TAp73 regulates the spindle assembly checkpoint by modulating BubR1 activity. Proc. Natl. Acad. Sci. U. S. A. *106*, 797–802.

Topalian, S.L., Taube, J.M., Anders, R.A., and Pardoll, D.M. (2016). Mechanism-driven biomarkers to guide immune checkpoint blockade in cancer therapy. Nat. Rev. Cancer *16*, 275–287.

Torphy, R.J., Tignanelli, C.J., Kamande, J.W., Moffitt, R.A., Herrera Loeza, S.G., Soper, S.A., and Yeh, J.J. (2014). Circulating tumor cells as a biomarker of response to treatment in patient-derived xenograft mouse models of pancreatic adenocarcinoma. PloS One *9*, e89474.

Totoki, Y., Tatsuno, K., Covington, K.R., Ueda, H., Creighton, C.J., Kato, M., Tsuji, S., Donehower, L.A., Slagle, B.L., Nakamura, H., et al. (2014). Trans-ancestry mutational landscape of hepatocellular carcinoma genomes. Nat. Genet. *46*, 1267–1273.

Towers, C.G., and Thorburn, A. (2016). Therapeutic Targeting of Autophagy. EBioMedicine *14*, 15–23.

Trevisani, F., Santi, V., Gramenzi, A., Di Nolfo, M.A., Del Poggio, P., Benvegnù, L., Rapaccini, G., Farinati, F., Zoli, M., Borzio, F., et al. (2007). Surveillance for early diagnosis of hepatocellular carcinoma: is it effective in intermediate/advanced cirrhosis? Am. J. Gastroenterol. *102*, 2448–2457; quiz 2458.

Tsai, W.-L., and Chung, R.T. (2010). Viral hepatocarcinogenesis. Oncogene *29*, 2309–2324.

Tuve, S., Wagner, S.N., Schittek, B., and Pützer, B.M. (2004). Alterations of DeltaTA-p 73 splice transcripts during melanoma development and progression. Int. J. Cancer *108*, 162–166.

Urist, M., Tanaka, T., Poyurovsky, M.V., and Prives, C. (2004). p73 induction after DNA damage is regulated by checkpoint kinases Chk1 and Chk2. Genes Dev. *18*, 3041–3054.

Vella, V., Puppin, C., Damante, G., Vigneri, R., Sanfilippo, M., Vigneri, P., Tell, G., and Frasca, F. (2009). DeltaNp73alpha inhibits PTEN expression in thyroid cancer cells. Int. J. Cancer *124*, 2539–2548.

Vera, J., Schmitz, U., Lai, X., Engelmann, D., Khan, F.M., Wolkenhauer, O., and Pützer, B.M. (2013). Kinetic modeling-based detection of genetic signatures that provide chemoresistance via the E2F1-p73/DNp73-miR-205 network. Cancer Res. *73*, 3511–3524.

Vessoni, A.T., Muotri, A.R., and Okamoto, O.K. (2012). Autophagy in stem cell maintenance and differentiation. Stem Cells Dev. *21*, 513–520.

Viale, A., Pettazzoni, P., Lyssiotis, C.A., Ying, H., Sánchez, N., Marchesini, M., Carugo, A., Green, T., Seth, S., Giuliani, V., et al. (2014). Oncogene ablation-resistant pancreatic cancer cells depend on mitochondrial function. Nature *514*, 628–632.

Vilgelm, A., Wei, J.X., Piazuelo, M.B., Washington, M.K., Prassolov, V., El-Rifai, W., and Zaika, A. (2008). DeltaNp73alpha regulates MDR1 expression by inhibiting p53 function. Oncogene *27*, 2170–2176.

Villanueva, J., Vultur, A., Lee, J.T., Somasundaram, R., Fukunaga-Kalabis, M., Cipolla, A.K., Wubbenhorst, B., Xu, X., Gimotty, P.A., Kee, D., et al. (2010). Acquired resistance to BRAF inhibitors mediated by a RAF kinase switch in melanoma can be overcome by cotargeting MEK and IGF-1R/PI3K. Cancer Cell *18*, 683–695.

Voigt, M.D. (2005). Alcohol in hepatocellular cancer. Clin. Liver Dis. *9*, 151–169.

Vora, S.R., Juric, D., Kim, N., Mino-Kenudson, M., Huynh, T., Costa, C., Lockerman, E.L., Pollack, S.F., Liu, M., Li, X., et al. (2014). CDK 4/6 inhibitors sensitize PIK3CA mutant breast cancer to PI3K inhibitors. Cancer Cell *26*, 136–149.

Wahid, B., Ali, A., Rafique, S., and Idrees, M. (2017). New Insights into the Epigenetics of Hepatocellular Carcinoma. BioMed Res. Int. *2017*, 1609575.

Waly Raphael, S., Yangde, Z., and Yuxiang, C. (2012). Hepatocellular carcinoma: focus on different aspects of management. ISRN Oncol. *2012*, 421673.

Wang, D., Han, S., Peng, R., Wang, X., Yang, X.-X., Yang, R.-J., Jiao, C.-Y., Ding, D., Ji, G.-W., and Li, X.-C. (2015). FAM83D activates the MEK/ERK signaling pathway and promotes cell proliferation in hepatocellular carcinoma. Biochem. Biophys. Res. Commun. *458*, 313–320.

Wang, H., Pan, K., Zhang, H., Weng, D., Zhou, J., Li, J., Huang, W., Song, H., Chen, M., and Xia, J. (2008). Increased polycomb-group oncogene Bmi-1 expression correlates with poor prognosis in hepatocellular carcinoma. J. Cancer Res. Clin. Oncol. *134*, 535–541.

Wang, J., An, H., Mayo, M.W., Baldwin, A.S., and Yarbrough, W.G. (2007). LZAP, a putative tumor suppressor, selectively inhibits NF-kappaB. Cancer Cell *12*, 239–251.

Wang, K., Lim, H.Y., Shi, S., Lee, J., Deng, S., Xie, T., Zhu, Z., Wang, Y., Pocalyko, D., Yang, W.J., et al. (2013a). Genomic landscape of copy number aberrations enables the identification of oncogenic drivers in hepatocellular carcinoma. Hepatol. Baltim. Md *58*, 706–717.

Wang, Q., Luan, W., Warren, L., Fiel, M.I., Blank, S., Kadri, H., Tuvin, D., and Hiotis, S.P. (2016a). Serum hepatitis B surface antigen correlates with tissue covalently closed circular DNA in patients with hepatitis B-associated hepatocellular carcinoma. J. Med. Virol. *88*, 244–251.

Wang, W.L., London, W.T., and Feitelson, M.A. (1991). Hepatitis B x antigen in hepatitis B virus carrier patients with liver cancer. Cancer Res. *51*, 4971–4977.

Wang, Y., Ding, X., Wang, S., Moser, C.D., Shaleh, H.M., Mohamed, E.A., Chaiteerakij, R., Allotey, L.K., Chen, G., Miyabe, K., et al. (2016b). Antitumor effect of FGFR inhibitors on a novel cholangiocarcinoma patient derived xenograft mouse model endogenously expressing an FGFR2-CCDC6 fusion protein. Cancer Lett. *380*, 163–173.

Wang, Z., Jiang, Y., Guan, D., Li, J., Yin, H., Pan, Y., Xie, D., and Chen, Y. (2013b). Critical roles of p53 in epithelial-mesenchymal transition and metastasis of hepatocellular carcinoma cells. PloS One *8*, e72846.

Waris, G., Turkson, J., Hassanein, T., and Siddiqui, A. (2005). Hepatitis C virus (HCV) constitutively activates STAT-3 via oxidative stress: role of STAT-3 in HCV replication. J. Virol. *79*, 1569–1580.

Watson, I.R., Blanch, A., Lin, D.C.C., Ohh, M., and Irwin, M.S. (2006). Mdm2-mediated NEDD8 modification of TAp73 regulates its transactivation function. J. Biol. Chem. *281*, 34096–34103.

Wei, W., Shin, Y.S., Xue, M., Matsutani, T., Masui, K., Yang, H., Ikegami, S., Gu, Y., Herrmann, K., Johnson, D., et al. (2016). Single-Cell Phosphoproteomics Resolves Adaptive Signaling Dynamics and Informs Targeted Combination Therapy in Glioblastoma. Cancer Cell *29*, 563–573.

Wei, Y., Jiang, Y., Zou, F., Liu, Y., Wang, S., Xu, N., Xu, W., Cui, C., Xing, Y., Liu, Y., et al. (2013). Activation of PI3K/Akt pathway by CD133-p85 interaction promotes tumorigenic capacity of glioma stem cells. Proc. Natl. Acad. Sci. U. S. A. *110*, 6829–6834.

White, E. (2012). Deconvoluting the context-dependent role for autophagy in cancer. Nat. Rev. Cancer *12*, 401–410.

White, E. (2015). The role for autophagy in cancer. J. Clin. Invest. *125*, 42–46.

White, E., and DiPaola, R.S. (2009). The double-edged sword of autophagy modulation in cancer. Clin. Cancer Res. Off. J. Am. Assoc. Cancer Res. *15*, 5308–5316.

White, D.L., Kanwal, F., and El-Serag, H.B. (2012). Association between nonalcoholic fatty liver disease and risk for hepatocellular cancer, based on systematic review. Clin. Gastroenterol. Hepatol. Off. Clin. Pract. J. Am. Gastroenterol. Assoc. *10*, 1342–1359.e2.

Wiemann, S.U., Satyanarayana, A., Tsahuridu, M., Tillmann, H.L., Zender, L., Klempnauer, J., Flemming, P., Franco, S., Blasco, M.A., Manns, M.P., et al. (2002). Hepatocyte telomere shortening and senescence are general markers of human liver cirrhosis. FASEB J. Off. Publ. Fed. Am. Soc. Exp. Biol. *16*, 935–942.

Wilhelm, M.T., Rufini, A., Wetzel, M.K., Tsuchihara, K., Inoue, S., Tomasini, R., Itie-Youten, A., Wakeham, A., Arsenian-Henriksson, M., Melino, G., et al. (2010). Isoform-specific p73 knockout mice reveal a novel role for delta Np73 in the DNA damage response pathway. Genes Dev. *24*, 549–560.

Wilkens, L., Flemming, P., Gebel, M., Bleck, J., Terkamp, C., Wingen, L., Kreipe, H., and Schlegelberger, B. (2004). Induction of aneuploidy by increasing chromosomal instability during dedifferentiation of hepatocellular carcinoma. Proc. Natl. Acad. Sci. U. S. A. *101*, 1309–1314.

Williams, E.S., Rodriguez-Bravo, V., Rodriquez-Bravo, V., Chippada-Venkata, U., De Ia Iglesia-Vicente, J., Gong, Y., Galsky, M., Oh, W., Cordon-Cardo, C., and Domingo-Domenech, J. (2015). Generation of Prostate Cancer Patient Derived Xenograft Models from Circulating Tumor Cells. J. Vis. Exp. JoVE 53182.

Wilson, B.G., and Roberts, C.W.M. (2011). SWI/SNF nucleosome remodellers and cancer. Nat. Rev. Cancer *11*, 481–492.

Wolf, E., Gebhardt, A., Kawauchi, D., Walz, S., Eyss, B. von, Wagner, N., Renninger, C., Krohne, G., Asan, E., Roussel, M.F., et al. (2013). Miz1 is required to maintain autophagic flux. Nat. Commun. *4*, ncomms3535.

Wong, C.-M., Wei, L., Law, C.-T., Ho, D.W.-H., Tsang, F.H.-C., Au, S.L.-K., Sze, K.M.-F., Lee, J.M.-F., Wong, C.C.-L., and Ng, I.O.-L. (2016). Up-regulation of histone methyltransferase SETDB1 by multiple mechanisms in hepatocellular carcinoma promotes cancer metastasis. Hepatol. Baltim. Md *63*, 474–487.

Wong, D.J., Liu, H., Ridky, T.W., Cassarino, D., Segal, E., and Chang, H.Y. (2008). Module map of stem cell genes guides creation of epithelial cancer stem cells. Cell Stem Cell *2*, 333–344.

Wu, B.-H., Chen, H., Cai, C.-M., Fang, J.-Z., Wu, C.-C., Huang, L.-Y., Wang, L., and Han, Z.-G. (2016). Epigenetic silencing of JMJD5 promotes the proliferation of hepatocellular carcinoma cells by down-regulating the transcription of CDKN1A 686. Oncotarget *7*, 6847–6863.

Wu, K., Kryczek, I., Chen, L., Zou, W., and Welling, T.H. (2009). Kupffer cell suppression of CD8+ T cells in human hepatocellular carcinoma is mediated by B7-H1/programmed death-1 interactions. Cancer Res. *69*, 8067–8075.

Wu, P.C., Lai, V.C., Fang, J.W., Gerber, M.A., Lai, C.L., and Lau, J.Y. (1999). Hepatocellular carcinoma expressing both hepatocellular and biliary markers also expresses cytokeratin 14, a marker of bipotential progenitor cells. J. Hepatol. *31*, 965–966.

Wu, S.-D., Ma, Y.-S., Fang, Y., Liu, L.-L., Fu, D., and Shen, X.-Z. (2012). Role of the microenvironment in hepatocellular carcinoma development and progression. Cancer Treat. Rev. *38*, 218–225.

Xie, Y., Kang, R., Sun, X., Zhong, M., Huang, J., Klionsky, D.J., and Tang, D. (2015). Posttranslational modification of autophagy-related proteins in macroautophagy. Autophagy *11*, 28–45.

Xue, F., Hu, L., Ge, R., Yang, L., Liu, K., Li, Y., Sun, Y., and Wang, K. (2016). Autophagy-deficiency in hepatic progenitor cells leads to the defects of stemness and enhances susceptibility to neoplastic transformation. Cancer Lett. *371*, 38–47.

Yamashita, T., Forgues, M., Wang, W., Kim, J.W., Ye, Q., Jia, H., Budhu, A., Zanetti, K.A., Chen, Y., Qin, L.-X., et al. (2008). EpCAM and alpha-fetoprotein expression defines novel prognostic subtypes of hepatocellular carcinoma. Cancer Res. *68*, 1451–1461.

Yamashita, T., Ji, J., Budhu, A., Forgues, M., Yang, W., Wang, H.-Y., Jia, H., Ye, Q., Qin, L.-X., Wauthier, E., et al. (2009). EpCAM-positive hepatocellular carcinoma cells are tumor-initiating cells with stem/progenitor cell features. Gastroenterology *136*, 1012–1024.

Yamazaki, K., Suzuki, K., Ohkoshi, S., Yano, M., Kurita, S., Aoki, Y.-H., Toba, K., Takamura, M.-A., Yamagiwa, S., Matsuda, Y., et al. (2008). Temporal treatment with interferon-beta prevents hepatocellular carcinoma in hepatitis B virus X gene transgenic mice. J. Hepatol. *48*, 255–265.

Yang, A., Schweitzer, R., Sun, D., Kaghad, M., Walker, N., Bronson, R.T., Tabin, C., Sharpe, A., Caput, D., Crum, C., et al. (1999). p63 is essential for regenerative proliferation in limb, craniofacial and epithelial development. Nature *398*, 714–718.

Yang, A., Walker, N., Bronson, R., Kaghad, M., Oosterwegel, M., Bonnin, J., Vagner, C., Bonnet, H., Dikkes, P., Sharpe, A., et al. (2000). p73-deficient mice have neurological, pheromonal and inflammatory defects but lack spontaneous tumours. Nature *404*, 99–103.

Yang, J.D., Nakamura, I., and Roberts, L.R. (2011a). The tumor microenvironment in hepatocellular carcinoma: current status and therapeutic targets. Semin. Cancer Biol. *21*, 35–43.

Yang, J.-Y., Zong, C.S., Xia, W., Yamaguchi, H., Ding, Q., Xie, X., Lang, J.-Y., Lai, C.-C., Chang, C.-J., Huang, W.-C., et al. (2008a). ERK promotes tumorigenesis by inhibiting FOXO3a via MDM2-mediated degradation. Nat. Cell Biol. *10*, 138–148.

Yang, L., Zhang, X., Li, H., and Liu, J. (2016a). The long noncoding RNA HOTAIR activates autophagy by upregulating ATG3 and ATG7 in hepatocellular carcinoma. Mol. Biosyst. *12*, 2605–2612.

Yang, S., Luo, C., Gu, Q., Xu, Q., Wang, G., Sun, H., Qian, Z., Tan, Y., Qin, Y., Shen, Y., et al. (2016b). Activating JAK1 mutation may predict the sensitivity of JAK-STAT inhibition in hepatocellular carcinoma. Oncotarget *7*, 5461–5469.

Yang, W., Yan, H.-X., Chen, L., Liu, Q., He, Y.-Q., Yu, L.-X., Zhang, S.-H., Huang, D.-D., Tang, L., Kong, X.-N., et al. (2008b). Wnt/beta-catenin signaling contributes to activation of normal and tumorigenic liver progenitor cells. Cancer Res. *68*, 4287–4295.

Yang, X., Liang, L., Zhang, X.-F., Jia, H.-L., Qin, Y., Zhu, X.-C., Gao, X.-M., Qiao, P., Zheng, Y., Sheng, Y.-Y., et al. (2013). MicroRNA-26a suppresses tumor growth and metastasis of human hepatocellular carcinoma by targeting interleukin-6-Stat3 pathway. Hepatol. Baltim. Md *58*, 158–170.

Yang, X., Guo, X., Chen, Y., Chen, G., Ma, Y., Huang, K., Zhang, Y., Zhao, Q., Winkler, C.A., An, P., et al. (2016c). Telomerase reverse transcriptase promoter mutations in hepatitis B virus-associated hepatocellular carcinoma. Oncotarget *7*, 27838–27847.

Yang, Z., Zhang, L., Ma, A., Liu, L., Li, J., Gu, J., and Liu, Y. (2011b). Transient mTOR inhibition facilitates continuous growth of liver tumors by modulating the maintenance of CD133+ cell populations. PloS One *6*, e28405.

Yang, Z.F., Ho, D.W., Ng, M.N., Lau, C.K., Yu, W.C., Ngai, P., Chu, P.W.K., Lam, C.T., Poon, R.T.P., and Fan, S.T. (2008c). Significance of CD90+ cancer stem cells in human liver cancer. Cancer Cell *13*, 153–166.

Yaswen, P., Goyette, M., Shank, P.R., and Fausto, N. (1985). Expression of c-Ki-ras, c-Ha-ras, and c-myc in specific cell types during hepatocarcinogenesis. Mol. Cell. Biol. *5*, 780–786.

Ye, Q.-H., Qin, L.-X., Forgues, M., He, P., Kim, J.W., Peng, A.C., Simon, R., Li, Y., Robles, A.I., Chen, Y., et al. (2003). Predicting hepatitis B virus-positive metastatic hepatocellular carcinomas using gene expression profiling and supervised machine learning. Nat. Med. *9*, 416–423.

Yeung, O.W.H., Lo, C.-M., Ling, C.-C., Qi, X., Geng, W., Li, C.-X., Ng, K.T.P., Forbes, S.J., Guan, X.-Y., Poon, R.T.P., et al. (2015). Alternatively activated (M2) macrophages promote tumour growth and invasiveness in hepatocellular carcinoma. J. Hepatol. *62*, 607–616.

Yin, S., Li, J., Hu, C., Chen, X., Yao, M., Yan, M., Jiang, G., Ge, C., Xie, H., Wan, D., et al. (2007). CD133 positive hepatocellular carcinoma cells possess high capacity for tumorigenicity. Int. J. Cancer *120*, 1444–1450.

Yokosuka, O., and Arai, M. (2006). Molecular biology of hepatitis B virus: effect of nucleotide substitutions on the clinical features of chronic hepatitis B. Med. Mol. Morphol. *39*, 113–120.

Yoo, J.E., Kim, Y.-J., Rhee, H., Kim, H., Ahn, E.Y., Choi, J.S., Roncalli, M., and Park, Y.N. (2017). Progressive Enrichment of Stemness Features and Tumor Stromal Alterations in Multistep Hepatocarcinogenesis. PLoS ONE *12*.

Yoon, S., and Seger, R. (2006). The extracellular signal-regulated kinase: multiple substrates regulate diverse cellular functions. Growth Factors Chur Switz. *24*, 21–44.

Yoshida, K., Yamaguchi, T., Natsume, T., Kufe, D., and Miki, Y. (2005). JNK phosphorylation of 14-3-3 proteins regulates nuclear targeting of c-Abl in the apoptotic response to DNA damage. Nat. Cell Biol. *7*, 278–285.

Yoshimoto, S., Loo, T.M., Atarashi, K., Kanda, H., Sato, S., Oyadomari, S., Iwakura, Y., Oshima, K., Morita, H., Hattori, M., et al. (2013). Obesity-induced gut microbial metabolite promotes liver cancer through senescence secretome. Nature *499*, 97–101.

Yuan, H., Li, A.-J., Ma, S.-L., Cui, L.-J., Wu, B., Yin, L., and Wu, M.-C. (2014). Inhibition of autophagy significantly enhances combination therapy with sorafenib and HDAC inhibitors for human hepatoma cells. World J. Gastroenterol. *20*, 4953–4962.

Yue, Z., Jin, S., Yang, C., Levine, A.J., and Heintz, N. (2003). Beclin 1, an autophagy gene essential for early embryonic development, is a haploinsufficient tumor suppressor. Proc. Natl. Acad. Sci. U. S. A. *100*, 15077–15082.

Zaika, A., Irwin, M., Sansome, C., and Moll, U.M. (2001). Oncogenes induce and activate endogenous p73 protein. J. Biol. Chem. *276*, 11310–11316.

Zaika, A.I., Slade, N., Erster, S.H., Sansome, C., Joseph, T.W., Pearl, M., Chalas, E., and Moll, U.M. (2002). DeltaNp73, a dominant-negative inhibitor of wild-type p53 and TAp73, is up-regulated in human tumors. J. Exp. Med. *196*, 765–780.

Zaika, E., Wei, J., Yin, D., Andl, C., Moll, U., El-Rifai, W., and Zaika, A.I. (2011). p73 protein regulates DNA damage repair. FASEB J. Off. Publ. Fed. Am. Soc. Exp. Biol. *25*, 4406–4414.

Zawacka-Pankau, J., Kostecka, A., Sznarkowska, A., Hedström, E., and Kawiak, A. (2010). p73 tumor suppressor protein: a close relative of p53 not only in structure but also in anti-cancer approach? Cell Cycle Georget. Tex *9*, 720–728.

Zhai, B., Hu, F., Jiang, X., Xu, J., Zhao, D., Liu, B., Pan, S., Dong, X., Tan, G., Wei, Z., et al. (2014). Inhibition of Akt reverses the acquired resistance to sorafenib by switching protective autophagy to autophagic cell death in hepatocellular carcinoma. Mol. Cancer Ther. *13*, 1589–1598.

Zhang, Y. (2015). Detection of epigenetic aberrations in the development of hepatocellular carcinoma. Methods Mol. Biol. Clifton NJ *1238*, 709–731.

Zhang, H., Ma, H., Wang, Q., Chen, M., Weng, D., Wang, H., Zhou, J., Li, Y., Sun, J., Chen, Y., et al. (2010). Analysis of loss of heterozygosity on chromosome 4q in hepatocellular carcinoma using high-throughput SNP array. Oncol. Rep. *23*, 445–455.

Zhang, J., Xu, E., and Chen, X. (2013a). TAp73 protein stability is controlled by histone deacetylase 1 via regulation of Hsp90 chaperone function. J. Biol. Chem. *288*, 7727–7737.

Zhang, P., Liu, S.S., and Ngan, H.Y.S. (2012a). TAp73-mediated the activation of c-Jun N-terminal kinase enhances cellular chemosensitivity to cisplatin in ovarian cancer cells. PloS One *7*, e42985.

Zhang, X., Claerhout, S., Prat, A., Dobrolecki, L.E., Petrovic, I., Lai, Q., Landis, M.D., Wiechmann, L., Schiff, R., Giuliano, M., et al. (2013b). A renewable tissue resource of phenotypically stable, biologically and ethnically diverse, patient-derived human breast cancer xenograft models. Cancer Res. *73*, 4885–4897.

Zhang, X., Wu, J., Choiniere, J., Yang, Z., Huang, Y., Bennett, J., and Wang, L. (2016). Arsenic silences hepatic PDK4 expression through activation of histone H3K9 methylatransferase G9a. Toxicol. Appl. Pharmacol. *304*, 42–47.

Zhang, Y., Yan, W., Jung, Y.S., and Chen, X. (2012b). Mammary epithelial cell polarity is regulated differentially by p73 isoforms via epithelial-to-mesenchymal transition. J. Biol. Chem. *287*, 17746–17753.

Zhao, L., and Wang, W. (2015). miR-125b suppresses the proliferation of hepatocellular carcinoma cells by targeting Sirtuin7. Int. J. Clin. Exp. Med. *8*, 18469–18475.

Zhao, M., and Klionsky, D.J. (2011). AMPK-dependent phosphorylation of ULK1 induces autophagy. Cell Metab. *13*, 119–120.

Zhao, X., and Subramanian, S. (2017). Intrinsic Resistance of Solid Tumors to Immune Checkpoint Blockade Therapy. Cancer Res. *77*, 817–822.

Zhao, H., Wang, J., Han, Y., Huang, Z., Ying, J., Bi, X., Zhao, J., Fang, Y., Zhou, H., Zhou, J., et al. (2011). ARID2: a new tumor suppressor gene in hepatocellular carcinoma. Oncotarget *2*, 886–891.

Zhong, J., Dong, X., Xiu, P., Wang, F., Liu, J., Wei, H., Xu, Z., Liu, F., Li, T., and Li, J. (2015). Blocking autophagy enhances meloxicam lethality to hepatocellular carcinoma by promotion of endoplasmic reticulum stress. Cell Prolif. *48*, 691–704.

Zhou, J., Huang, A., and Yang, X.-R. (2016a). Liquid Biopsy and its Potential for Management of Hepatocellular Carcinoma. J. Gastrointest. Cancer *47*, 157–167.

Zhou, L., Huang, Y., Li, J., and Wang, Z. (2010). The mTOR pathway is associated with the poor prognosis of human hepatocellular carcinoma. Med. Oncol. Northwood Lond. Engl. *27*, 255–261.

Zhou, X., Zhu, H.-Q., Ma, C.-Q., Li, H.-G., Liu, F.-F., Chang, H., and Lu, J. (2016b). MiR-1180 promoted the proliferation of hepatocellular carcinoma cells by repressing TNIP2 expression. Biomed. Pharmacother. Biomedecine Pharmacother. *79*, 315–320.

Zhu, A.X., Chen, D., He, W., Kanai, M., Voi, M., Chen, L.-T., Daniele, B., Furuse, J., Kang, Y.-K., Poon, R.T.P., et al. (2016). Integrative biomarker analyses indicate etiological variations in hepatocellular carcinoma. J. Hepatol. *65*, 296–304.

Zhu, H., Wang, D., Liu, Y., Su, Z., Zhang, L., Chen, F., Zhou, Y., Wu, Y., Yu, M., Zhang, Z., et al. (2013). Role of the Hypoxia-inducible factor-1 alpha induced autophagy in the conversion of non-stem pancreatic cancer cells into CD133+ pancreatic cancer stem-like cells. Cancer Cell Int. *13*, 119.

Zhu, H., Wang, D., Zhang, L., Xie, X., Wu, Y., Liu, Y., Shao, G., and Su, Z. (2014a). Upregulation of autophagy by hypoxia-inducible factor-1α promotes EMT and metastatic ability of CD133+ pancreatic cancer stem-like cells during intermittent hypoxia. Oncol. Rep. *32*, 935–942.

Zhu, J., Jiang, J., Zhou, W., and Chen, X. (1998). The potential tumor suppressor p73 differentially regulates cellular p53 target genes. Cancer Res. *58*, 5061–5065.

Zhu, L., Gibson, P., Currle, D.S., Tong, Y., Richardson, R.J., Bayazitov, I.T., Poppleton, H., Zakharenko, S., Ellison, D.W., and Gilbertson, R.J. (2009). Prominin 1 marks intestinal stem cells that are susceptible to neoplastic transformation. Nature *457*, 603–607.

Zhu, S., Rezvani, M., Harbell, J., Mattis, A.N., Wolfe, A.R., Benet, L.Z., Willenbring, H., and Ding, S. (2014b). Mouse liver repopulation with hepatocytes generated from human fibroblasts. Nature *508*, 93–97.

Zhu, Z., Hao, X., Yan, M., Yao, M., Ge, C., Gu, J., and Li, J. (2010). Cancer stem/progenitor cells are highly enriched in CD133+CD44+ population in hepatocellular carcinoma. Int. J. Cancer *126*, 2067–2078.

Zhu, Z.W., Friess, H., Wang, L., Abou-Shady, M., Zimmermann, A., Lander, A.D., Korc, M., Kleeff, J., and Büchler, M.W. (2001). Enhanced glypican-3 expression differentiates the majority of hepatocellular carcinomas from benign hepatic disorders. Gut *48*, 558–564.

Zuo, T.-T., Zheng, R.-S., Zhang, S.-W., Zeng, H.-M., and Chen, W.-Q. (2015). Incidence and mortality of liver cancer in China in 2011. Chin. J. Cancer *34*, 508–513.

(2001). Hepatitis B virus X mutants derived from human hepatocellular carcinoma retain the ability to abrogate p53-induced apoptosis. Publ. Online 20 June 2001 Doi101038sjonc1204495 *20*.

Scientific communications

Patricia Gifu, Sonia Brun, Guanxiong Wang, Jérôme Courcambeck, Philippe Halfon, Philippe Merle, Firas Bassissi and Claude Caron de Fromentel. (September 2017). GNS561: A New First-In-Class SLC Transporter Inhibitor With High Efficacy On Hepatocellular Carcinoma Cancer Stem Cells. 3rd International Symposium of the CRCL, Lyon, France. (poster)

Patricia Gifu, Lei Bian, Guanxiong Wang, Floriane Pez, Lydie Lefrancois, Philippe Merle, Claude Caron de Fromentel. (September 2017). ΔNp73 isoforms are involved in the immature phenotype of liver cancer cells. 3rd International Symposium of the CRCL, Lyon, France. (poster)

Patricia Gifu, Floriane Pez, Davide Degli Esposito, Nadim Fares, Anaïs Lopez, Lydie Lefrancois, Maud MicheIet, Michel Rivoire, Brigitte Bancel, Bakary S. Sylla, Zdenko Herceg, Claude Caron de Fromentel, Philippe Merle. (September 2017). Modelling HCC in primary human hepatocytes. 3rd International Symposium of the CRCL, Lyon, France. (poster)

Patricia Gifu, Sonia Brun, Jérôme Courcambeck, Philippe Halfon, Philippe Merle, Firas Bassissi and Claude Caron de Fromentel. (September 2017). GNS561: A New First-In-Class SLC Transporter Inhibitor With High Efficacy On Hepatocellular Carcinoma Cancer Stem Cells. 11th Annual Conference of the International Liver Cancer Association, Seoul, South Coreea. (e-poster)

Patricia Gifu, Lei Bian, Guanxiong Wang, Floriane Pez, Lydie Lefrancois, Philippe Merle, Claude Caron de Fromentel. (September 2017). ΔNp73 isoforms are involved in the immature phenotype of liver cancer cells. 11th Annual Conference of the International Liver Cancer Association, Seoul, South Coreea. (top scored poster)

Patricia Gifu, Floriane Pez, Davide Degli Esposito, Nadim Fares, Anaïs Lopez, Lydie Lefrancois, Maud MicheIet, Michel Rivoire, Brigitte Bancel, Bakary S. Sylla, Zdenko Herceg, Claude Caron de Fromentel, Philippe Merle. (September 2017). Modelling HCC in primary human hepatocytes. 11th Annual Conference of the International Liver Cancer Association, Seoul, South Coreea. (oral communication)

Floriane Pez, **Patricia Gifu**, Davide Degli Esposito, Nadim Fares, Anaïs Lopez, Lydie Lefrancois, Maud Michelet, Michel Rivoire, Brigitte Bancel, Bakary S. Sylla, Zdenko Herceg, Claude Caron de Fromentel, Philippe Merle. (May 2017). Modéliser le carcinome hépatocellulaire à partir des hépatocytes humains différenciés. 10e rencontres en Oncologie Bayer, Paris, France. (poster)

Patricia Gifu, Sonia Brun, Firas Bassissi,Jerome Courcambeck, Gregory Nicolas, Clarisse Dubray, Antoine Beret, Nolwenn Amrani, Claude Caron de Fromentel, Philippe Merle, Philippe Halfon. (May 2017). GNS561 **:** une nouvelle molécule efficace sur les cellules souches cancéreuses dans le Carcinome Hépatocellulaire. 10^{e} rencontres en Oncologie Bayer, Paris, France. (oral communication)

Patricia Gifu, Lei Bian, Guanxiong Wang, Floriane Pez, Lydie Lefrancois, Philippe Merle, Claude Caron de Fromentel. (May 2017). ΔNp73 isoforms are involved in the immature phenotype of

liver cancer cells. Scientific Day of the Early Career Scientist Association of the IARC, Lyon, France. (poster)

Patricia Gifu, Lei Bian, Floriane Pez, Lydie Lefrancois, Philippe Merle, Claude Caron de Fromentel. (November 2016). ΔNp73 isoforms are involved in the immature phenotype of liver cancer cells. Scientific Day of the Doctoral School BMIC, Lyon, France. (poster)

S. Brun, **P. Gifu**, Z. Macek-Jilkova, J. Courcambeck, J.M. Pascussi, J. Pannequin, E. Raymond, F. Bassissi, P. Halfon, P. Merle, T. Decaensand C. Caron de Fromentel. (March 2016). GNS561: a new quinoline derivative with high efficacy on cancer stem cells in colorectal liver metastases and hepatocellular carcinoma. 38th EORTC-PAMM Winter Meeting, Split, Croatia. (oral communication and poster)

Firas Bassissi, Sonia Brun, **Patricia Gifu**, Jerome Courcambeck, Gregory Nicolas, Clarisse Dubray, Antoine Beret, Nolwenn Amrani, Claude Caron de Fromentel, Philippe Merle, Philippe Halfon. (June 2016). Preclinical characterization of a novel first in class GNS561: autophagy inhibitor targeting cancer stem cells therapeutic candidate for treatment of hepatocellular carcinoma. 2016 ASCO Annual Meeting, Chicago, United States. (poster)

Patricia Gifu, Lei Bian, Floriane Pez, Lydie Lefrancois, Philippe Merle, Claude Caron de Fromentel. (November 2015). ΔNp73 isoforms are involved in the immature phenotype of liver cancer cells 2nd International Conference on Stem Cells and Cancer, Lyon, France. (poster)

Training awards

Institute Curie Fellowship to attend the 7th Cytoskeleton course on Cell Matrix Interactions, April 2015, Paris, France.

EACR-ESMO Meeting Bursary for the 7th EACR-OECI Joint Training Course: Molecular Pathology Approach to Cancer, April 2017, Amsterdam, Netherlands.